THE COMPUTATION OF WAVE-INDUCED CIRCULATIONS WITH WAVE-CURRENT INTERACTION AND REFINED TURBULENCE MODELLING

by

P. DONG, B.Sc. (Eng.)

A thesis submitted for the degree of Doctor of Philosophy of the University of London and for the Diploma of Membership of the Imperial College of Science and Technology.

December, 1987

Hydraulics Section
Department of Civil Engineering
Imperial College
London, S.W.7.

TO MY PARENTS

and

MY WIFE

ABSTRACT

Two finite difference models are presented. The first deals with coastal wave propagations taking into account the combined effects of refraction, diffraction, weak reflection and wave-current interaction; the second solves the time and depth averaged equations of motion for the prediction of wave-induced nearshore circulations.

Using conventional perturbation techniques the validity of the mild-slope equation in the presence of a current having weak vertical vorticity is demonstrated for the first time. Thus the mild-slope equation can be applied to the study of the interactions between waves and wave-induced circulations which are certainly not irrotational.

The single second order mild-slope equation has been recasted into a set of first order transient equations on which the present wave model is based. For engineering applications, where the number of computational grid points in one space dimension is comparable with the total number of time increments in the numerical integration, this method of solution has higher computational efficiency compared with existing alternative methods based on the steady state elliptic equation.

With all the wave-induced driving terms directly provided from the wave propagation model, the circulation model developed in this study is capable of taking into account the effects of interactions between waves and wave-induced currents around coastal structures and on slowly varying bed topographies of arbitrary forms. No previously developed numerical schemes for wave-induced circulation can be applied to such general situations.

Another distinct feature of the present circulation model is that the mixing processes are more realistically described by applying depth-averaged one-equation and two-equation ($k-\epsilon$) turbulence transport models which are developed in this work. The turbulent energy production due to wave breaking has been successfully taken into account by introducing some new source terms in the turbulence transport equations.

Numerical results obtained by both the wave and circulation models are compared with typical analytical solutions. It has been shown that the numerical schemes used are stable and accurate for all the cases studied. Available wave basin

experimental data are used to further verify the models. It is found that the wave-current interaction is well predicted and its effects on the circulation rate and in particular on the circulation pattern are shown to be significant.

The use of refined turbulence models has been justified to a certain extent by the better prediction of longshore current outside the surf zone and quite favourable comparisons with experimental data for some circulation cases in which the effect of turbulence transport is important. In general the circulation results obtained by using the refined turbulence models do not differ as appreciably as it would be expected from those derived from the zero equation model. At the same time it is nevertheless demonstrated in this work that the transport effects of turbulence quantities are not neglegible.

ACKNOWLEDGEMENTS

The research described in this thesis has been carried out under the supervision of Dr. K. Anastasiou to whom I am deeply grateful for his very valuable suggestions, guidance and continuous encouragements provided at every stage of this research study.

I wish to express my gratitude to Professor P. Holmes who encouraged my earlier efforts in this field and gave me every possible opportunity for broadening my knowledge and experience.

I am indebted to many of my colleagues whose kindness and friendship have been invaluable to me. In particular, I would like to acknowledge David Walker who showed great generosity and patience in helping me to familiarise myself with various computers and programming techniques, and with whom I shared an office and had many fruitful discussions. I would also like to thank Messrs. C. C. Li, Y. Q. Yang, R. Shih, A. Toumazis and M. Al-Mashouk who have exposed me to many interesting research topics and with whom I have spent many wonderful times together.

I would like to express my gratitude to Drs. A. Davies and G. Copeland who have shown great interest in this work and have given me a lot of valuable advice.

I wish to express my grateful thanks to Mr. G. Thomas for his careful proof-reading of the manuscripts and Miss. P. O'Connell for her continuous assistance throughout the preparation of this thesis.

The financial support from the Chinese Ministry of Education throughout the entire period of this project is greatly appreciated.

Finally, I wish to express my deepest gratitude to my parents and my wife, Lixiang Zhou, for their understanding and unfailing support over such a prolonged period of my research abroad.

TABLE OF CONTENTS

	Page
ABSTRACT	3
ACKNOWELEDGEMENTS	5
LIST OF FIGURES	10
NOMENCLATURE	14
CHAPTER 1 - INTRODUCTION	17
1.1 The Problem Considered	17
1.2 The Objectives of This Study	18
1.3 Outline of The Thesis	19
CHAPTER 2 - REVIEW OF PREVIOUS WORK	21
2.1 Introduction	21
2.2 Coastal Wave Propagation on Water of Variable Depth	21
2.3 Wave-Current Interaction	26
2.4 Wave-induced Nearshore Circulation	28
2.5 Turbulence Models in Computations of Nearshore Circulation	33
CHAPTER 3 - A WAVE PROPAGATION MODEL	36
3.1 Introduction	36
3.2 Mild-Slope Equation for Waves Only	37
3.2.1 Main results for linear waves	37
3.2.2 Derivation of a set of first order model equations	38
3.2.3 Boundary conditions	41
3.3 The Mild-Slope Equation for Waves on Large-Scale Currents	45
3.3.1 Assumptions and boundary conditions	45
3.3.2 Derivation of the mild-slope equation with wave-current interaction	48

3.3.3 Derivation of the model equations 49

3.4 Numerical Scheme 51

3.4.1 Grid arrangement and discretization 51
3.4.2 Initial and boundary conditions 53
3.4.3 Determination of the wave height and wave angle 53
3.4.4 Breaking criteria 55

CHAPTER 4 - THE GOVERNING EQUATIONS OF CIRCULATION 60

4.1 Introduction 60
4.2 Governing Equations 60
4.3 Bottom Friction 63

4.3.1 Formulation 63
4.4.2 Friction factor C_f 65

4.4 Horizontal Turbulence Stresses 66
4.5 Radiation Stresses 69

4.5.1 Non-breaking waves 69
4.5.2 Broken waves 71

CHAPTER 5 – THE MODELLING OF TURBULENT MIXING 73

5.1 Introduction 73
5.2 Energy Equations for Fluctuating Motions 73
5.3 One-Equation Model 76

5.3.1 Conventional turbulent energy equation and its model form 76
5.3.2 Depth-averaged model equation of turbulent energy inside the surf zone 77
5.3.3 The length scale L_m and coefficients $c_{\mu 1}$, c_D 78

5.4 Two-Equation Model 80

5.4.1 The model equations 80
5.4.2 Determination of P_ϵ and $c_{\mu 2}$ 81

5.5 Determination of Turbulence Production by Breaking Waves 85

5.5.1 General expression for F (F_x, F_y) 85
5.5.2 Determination of D_w inside the surf zone 89

5.6 Numerical Formulation 91

5.6.1 Numerical scheme 91
5.6.2 Boundary conditions for κ and ε 92

CHAPTER 6 – THE NUMERICAL SOLUTION OF THE TIME MEAN EQUATIONS 94

6.1 Introduction 94
6.2 Grid Arrangement and General Considerations 95
6.3 Basic Finite Difference Schemes 96

6.3.1 Two-point Leap frog scheme 96
6.3.2 Angled derivative explicite (ADE) scheme 98

6.4 Discretization of the Governing Equations 100

6.4.1 Discretization of the Linear terms 100
6.4.2 Convective accelerations 103

6.5 Turbulence equation 106
6.6 Initial Conditions, Boundary conditions and Computational Procedure 108

CHAPTER 7 - APPLICATION AND VERIFICATION OF THE WAVE MODEL 114

7.1 Introduction 114
7.2 Wave Refraction By A Shear Current 115
7.3 Interaction Between Waves and Analytical Rip-Currents 116
7.4 Waves Around A Semi-Infinite Breakwater in the Presence of A Shear Current 118

CHAPTER 8 - COMPUTATION OF NEARSHORE CIRCULATIONS 131

8.1 Introduction 131

8.2 Longshore Currents On A Plane Beach 132
8.3 Noda's Sinusoidal beach 134
8.4 Circulations Behind A Detached Breakwater 136
8.5 da Silva Lima's Beach in an Enclosed Wave Basin 137

CHAPTER 9 - THE VERTICAL DISTRIBUTION OF LONGSHORE CURRENTS ON A PLANE BEACH 166

9.1 Introduction 166
9.2 Theoretical Formulation 167

9.2.1 Derivation of governing equations 167
9.2.2 Formulation for longshore currents 168
9.2.3 Form of eddy viscosity 170

9.3 Boundary Conditions 171
9.4 Solution Method 172

9.4.1 Transformation of coordinates 173
9.4.2 Application of Galerkin technique 173
9.4.3 Choice of basic functions 175
9.4.4 Discretization in horizontal space 176

9.5 Computational Results And Discussion 177

CHAPTER 10 - CONCLUSIONS AND RECOMMENDATIONS 187

10.1 Conclusions 187
10.2 Recommendations 189

REFERENCES 191

LIST OF FIGURES

		Page
Fig. 3.1	Definition of Vector Variables	57
Fig. 3.2	Finite Difference Grid System for the Wave Model	57
Fig. 3.3	Flow Chart for the Program MSWAVE	58
Fig. 6.1	Angled Derivative Scheme for One Dimensionl Case	111
Fig. 6.2	Finite Difference Grid System for the Circulation Model, U and V are Defined at Grid Edges and all the Scalar Quantities (ζ, h, κ, ε) at Grid Centers	111
Fig. 6.3	Flow Chart for the Program CIRCU	112
Fig. 7.1	The Waveheight and Wave Front Behind a Rigid Semi-Infinite Breakwater from Penney and Price (1952)	120
Fig. 7.2	Waveheight Contours around a Rigid Breakwater Computed by the Wave Model Without the Effects of Current	120
Fig. 7.3	Experimental Set-Up of a Wave Basin from Berkhoff (1976)	121
Fig. 7.4	Relative Wave Height Contour, Measured Results from Berkhoff (1976)	121
Fig. 7.5	Relative Wave Height Contours, Computational Results with a Maximum Run Time of 7 Periods	122
Fig. 7.6	Relative Wave Height Contours, Computational Results with a Maximum Run Time of 14 Periods	122
Fig. 7.7	Shear Current Distribution	123
Fig. 7.8	Calculated Wave Heights for Wave Refraction by a Shear Current with Triangular Distribution	124
Fig. 7.9	Calculated Wave Angles for Wave Refraction by a Shear Current with Triangular Distribution	124
Fig. 7.10	Calculated Wave Heights for Wave Propagation in the Water of Uniform Depth	125
Fig. 7.11	Calculated Wave Heights for Wave Refraction on a Plane Beach	125
Fig. 7.12	Typical Velocity Profiles, a) U and V along x = 150ft, b) U along the Center Line y = 300ft.	126
Fig. 7.13	Wave Ray Patern from Arthur (1950)	126
Fig. 7.14	Wave Height along the Centerline of the Currents, y = 300ft, a Comparison with Liu's Parabolic Solution and the Pure Shoaling Results	127

Fig. 7.15	Wave Height Contours, k is Calculated with the Effects of Current	127
Fig. 7.16	Wave Height Distribution at Various Cross-Sections.	128
Fig. 7.17	Wave Heights along the Centerline of the Currents, y = 300ft Calculated with and without the Effect of Currents in Calculating the Wave Number k	129
Fig. 7.18	The Wave Height Contours, k is Calculated Without the Effect of Currents	129
Fig. 7.19	A Detailed View of the Wave Height Contour behind a Rigid Breakwater without the Effects of Current	130
Fig. 7.20	A Detailed View of the Wave Height Contour behind a Rigid Breakwater with the Effects of Current	130
Fig. 8.1	Geometry of the Plane Beach and the Incident Wave Conditions	140
Fig. 8.2	Numerical and Analytical Longshore Current Profile.	140
Fig. 8.3	The Longshore Current Profile Calculated by Using Zero, One and Two Equation Turbulence Models, $c_{\mu 1} = c_{\mu 2} = 10.0$.	141
Fig. 8.4	The Longshore Current Profile Calculated by Using Zero, One and Two Equation Turbulence Models, $c_{\mu 1} = c_{\mu 2} = 3.0$	141
Fig. 8.5	Sea Bed Contours of Noda's Sinusoidal Beach	142
Fig. 8.6	Predicted Current Vectors for Noda's Beach, Using Zero Equation Turbulence Model and No Wave Current Interaction	143
Fig. 8.7	Predicted Current Vectors for Noda's Beach, Using One Equation Turbulence Model and No Wave Current Interaction	144
Fig. 8.8	Predicted Current Vectors for Noda's Beach, Using Two Equation Turbulence Model and No Wave Current Interaction	145
Fig. 8.9	Predicted Current Vectors for Noda's Beach, Using Zero Equation Turbulence Model and with Wave Current Interaction	146
Fig. 8.10	Predicted Current Vectors for the Breakwater Case, Using Zero Equation Turbulence Model and No Wave Current Interaction.	147
Fig. 8.11	Predicted Current Vectors for the Breakwater Case, Using Two Equation Turbulence Model and No Wave Current Interaction.	148

Fig. 8.12	Predicted Current Vectors for the Breakwater Case, Using Two Equation Turbulence Model and No Wave Current Interaction.	149
Fig. 8.13	Predicted Current Vectors for the Breakwater Case, Using Two Equation Turbulence Model and with Wave Current Interaction.	150
Fig. 8.14	Sea Bed Contours and Grid System Used for da Silva Lima's Experimental Set-Up	151
Fig. 8.15	The Measured Velocity Vectors for Experiment Run 2 from da Silva Lima (1981)	152
Fig. 8.16	The Predicted Velocity Vectors for Experiment Run 2 Using Zero Equation Turbulence Model and No Wave Current Interaction	153
Fig. 8.17	The Predicted Velocity Vectors for Experiment Run 2 Using Two Equation Turbulence Model and No Wave Current Interaction	154
Fig. 8.18	Predicted Velocity Vectors for Experiment Run 2 Using Two Equation Turbulence Model and with Wave Current Interaction. Five Alternative Runs of the Wave and Circulation Models are Presented.	155
Fig. 8.19	Comparison between Predicted Longshore Current for Rows from 2 to 3	159
Fig. 8.20	Comparison between Predicted Longshore Current for Rows from 4 to 5	160
Fig. 8.21	Comparison between Predicted Longshore Current for Rows from 6 to 7	161
Fig. 8.22	Comparison between Predicted Longshore and Rip Currents for the Rows 8 and 2, Respectively	162
Fig. 8.23	Comparison between Predicted Rip Current for Rows from 3 to 4	163
Fig. 8.24	Comparison between Predicted Rip Current for Rows from 5 to 6	164
Fig. 8.25	Comparison between Predicted Rip Current for Rows from 7 to 8	165
Fig. 9.1	Beach Form and Wave Condition	180
Fig. 9.2	Grid Arrangement for Numerical Solution	180
Fig. 9.3	Beach and Wave Field Properties and Quantities; for exps.1 to 7 from Visser (1984)	181
Fig. 9.4	Alongshore Averaged Vertical Velocity Profiles for exp.4	182

Fig. 9.5	Alongshore Averaged Vertical Velocity Profiles for exp.6	182
Fig. 9.6	Computed Longshore Current Profiles across the Surf Zone at Three Locations over the Water Column Using the Linear Expression for ν_z with Input Data from Visser's exp.6	183
Fig. 9.7	Computed Longshore Current Profiles across the Surf Zone at Three Locations over the Water Column Using the Quadratic Expression for ν_z, with Input Data from Visser's exp.6.	183
Fig. 9.8	Comparison between Computed and Measured Velocity Profiles for exp.6	184
Fig. 9.9	Computed Longshore Current Velocity with Input Data from Visser's exp.6 and $\nu_z = 1.0$	185
Fig. 9.10	Computed Longshore Current Profiles across the Surf Zone at Three Locations over the Water Column Using the Linear Expression for ν_z with Input Data from Visser's exp.4	185
Fig. 9.11	Comparison between Computed and Measured Velocity Profiles for exp.4	186

NOMENCLATURE

a	wave amplitude
$B_i(x,y)$	variables representing the horizontal structure of the longshore current
C	wave celeraty
	Courant number
C_g	group velocity
C_f	bottom friction factor
C'_f	bottom friction factor in the longshore current model
$c_{1\epsilon}$	constant in k-ϵ model
$c_{2\epsilon}$	constant in k-ϵ model
c_b	constant in the expresion of P_ϵ
c_D	constant in the one equation model
$d(x,y)$	steady water depth
D	total differencial operator
D_w	the depth integrated wave energy dissipation
D_t	the depth integrated turbulent energy dissipation
e	a subscript denoting any quantity at the local equilibrium state
E	the depth integrated wave energy
E_t	the depth integrated turbulent energy
f	= cosh k(z-h)/coshkh
(F_x, F_y)	the wave energy flux components
(F_{tx}, F_{ty})	the turbulent energy flux components
g	the acceleration of gravity
$h(x,y)$	total water depth
h_{max}	the maximum water depth in the computational domain
H	wave height
H_{max}	maximum wave height in in a model area
i	imaginary unit, $\sqrt{-1}$
i	incremental grid index in the x-direction
j	incremental grid index in the y-direction
k	the wave number of propagating waves
$\mathbf{k}$	the wave number vector directed along the wave orthogonals
$\bar{k}$	depth-averaged turbulent kinetic energy
L	wave length
L_m	the characteristic length scale of turbulent motion

M	the total number of increments in x-direction
n	the time increments
N	the total number of increments in y-direction
N	the dimensionless mixing coefficient in Longuet-Higgins' model
p	the total presure
p	the dimensionless ratio of turbulent mixing to bottom friction
P_k	turbulence production in the k equation
P_ϵ	turbulence production in the $\bar{\epsilon}$ equation
P_w	the depth-averaged wave energy dissipation
Q (Q_x , Q_y)	the unknown vector variable in the wave model
r	the wave reflection coefficient
r	a dimensionless mixing coefficient (= $2N/\gamma$)
s	sea bottom slope
S_{xx}, S_{xy}, S_{yy}	radiation stress components
t	time
T	wave period
T_{xx}, T_{xy}, T_{yy}	effective turbulent stress components
u(u,v,w)	the velocity vector of organized fluid motion, wave and currents
u'(u',v',w')	the turbulent velocity vector
$\tilde{u}_{max}$	the maximum wave orbital velocity at the sea bed
U(U,V)	the time mean velocity vector
W	the vertical component of the mean velocity
x	the horizontal coordinate in the offshore direction
y	the horizontal coordinate in the longshore direction
z	the vertical coordinate directed positive upwards
$\alpha = (i-1)\pi$	parameter in the cosine form function
γ	breaking index
Δ	finite difference increament
∇	horizontal gradient operator
$\bar{\epsilon}$	depth-averaged dissipation rate of turbulent kinetic energy
ζ	surface elevation
$\bar{\zeta}$	time mean surface elevation i.e. set-up or set-down
θ	wave angle
θ_i	incident wave angle
θ_r	angle reflected waves
$\kappa = \lvert\kappa\rvert$	modeling parameter in the wave model

π	3.1415926.....
ρ	density of water
τ	a time delay used in f.d. calculation of transmissive boundary values
$\tau_b(\tau_{bx},\tau_{by})$	bottom frictional stress vector
ν	kinematic viscosity
ν_t	eddy viscosity
Φ	instantaneous wave potential at the water surface
φ	steady part of the wave potential
ω	absolute wave frequency
σ	relative wave frequency
σ_k,σ_ϵ	constants in the one and/or two equation models
λ_1,λ_2	coefficents in the longshore current model
$\sum$	the sum sign

CHAPTER 1
INTRODUCTION

1.1 The Problem Considered

Proper design and maintenance of coastal structures and effective management of activities along coastlines require a good quantitative understanding of the water and sediment motions in the nearshore area. Among all these water motions coastal waves and wave-induced currents are of primary concern since they, together with tides, are responsible for transporting nearshore sediment and pollutants. An accurate and efficient prediction of wave and wave-induced current motions constitutes the first important step towards better understanding of the more complicated tranport processes.

Over the last three decades, considerable effort has been devoted to studies of the hydrodynamics of waves and currents.

For the purpose of predicting coastal wave fields a number of well developed methods are available such as the ray method for the calculation of depth-current refraction, the solution of the Helmholtz equation for wave diffraction, and some extended ray methods capable of handling the pure diffraction as well as the combined effects of refraction and diffraction. The latter technique is very useful in dealing with wave propagation around simple coastal configurations such as detached or attached breakwaters.

Due to certain theoretical constraints most of these methods are applicable only for limited types of wave motions. It was only with the development of solutions of the mild-slope equation that the combined effects of refraction, diffraction, reflection and wave current interaction could be treated in a satisfactory way. However, there still remain some problems with the mild-slope equation. For example, it tends to be rather inefficient and expensive to solve it for real engineering cases when a large area usually needs to be treated. Furthermore the extended mild-slope equation which includes the effects of wave current interaction was originally derived with an irrotationality restriction on the current. This restriction is a severe one since currents in coastal areas are seldom irrotational.

With regard to the prediction of wave-induced circulations the numerical modelling approach based on the radiation stress concept together with the time averaged depth integrated equations of motion has become very popular. Quite a

number of models of varying sophistication are available and some of them have been used in engineering applications. This state of affair does not necessarily imply that these models are versatile enough for general wave and current situations or sufficiently accurate and convenient for the computation of real engineering cases. For example, the interaction between the waves and wave-induced currents is not successfully treated in the existing numerical models, and the methods used to calculate the turbulent mixing are still oversimplified and quite arbitrary. Improvements are certainly necessary.

1.2 The Objectives of This Study

The present study is intended to improve the theoretical representation of a number of physical processes concerning both wave propagation and the generation of nearshore circulation. The specific objectives are summarized as follows

(a) to demonstrate the validity of the 'mild slope' equation in analysing the interaction between waves and a steady current having a weak vertical vorticity and to derive a set of first order approximate equations from the mild-slope equation.

(b) to develop a numerical wave model based on these newly derived wave equations so that the effect of steady currents can be analysed for applications where wave shoaling, refraction, diffraction and reflection may all be present.

(c) to extend and apply a depth averaged two equation turbulence model to the calculation of the lateral mixing due to wave breaking induced turbulence.

(d) to develop an efficient and accurate numerical model for the computation of wave-induced nearshore circulation based on the time averaged, depth integrated equations of motion and using this circulation model combined with the wave and turbulent models to predict current patterns over arbitray coastal configurations.

(e) to assess the mathematical accuracy and physical realism of the numerical models by comparing the predictions with available analytical solutions, published data.

(f) to make a first attempt at analysing the vertical structure of longshore currents on a plane beach.

1.3 Outline of The Thesis

The main body of the thesis consists of ten chapters. Each of the chapters is quite self-contained for ease of reference and every effort was made to ensure clarity of presentation and consistency with regard to both the symbols used and the assumptions made.

Chapter 2 contains a review of the previous work on the subjects of coastal wave propagation, wave-current interaction, wave-induced circulation and turbulence modelling as well as a brief account of existing finite difference schemes used in circulation models. The emphasis has been placed upon the theoretical aspects of the various approaches and a number of well documented experimental investigations are also cited for the purpose of demonstrating the applicability and limitations of currently available theories.

In Chapter 3 the original mild-slope equation for pure waves and its modified version are first discussed. The driving boundary conditions required for solving the equations are derived. As the main part of the chapter, the extended mild-slope equation that includes the effect of wave-current interaction is analysed in detail. Its applicability in a steady current with weak vorticity on the horizontal plane is rigorously proved, which makes it suitable for studying the interaction between coastal waves and wave-induced circulation which is not irrotational. The original equation is then split into a set of first order equations in a way consistent with the method used for estimating the wave number. The resulting equation sets are solved efficiently and conveniently for engineering applications involving large computational areas.

The nearshore circulation generated by breaking waves is then studied using the depth-integrated and time-averaged equations of motion. The theoretical formulation is presented in Chapter 4. The various forcing terms involved such as radiation stress, bottom shear stress and horizontal mixing are examined in detail.

In order to determine the effect of turbulent mixing more accurately the higher order turbulence models are adapted and extended to take into account turbulence production by the wave breaking process. In Chapter 5 the model transport equations in depth integrated and time averaged form are given and possible ways of modelling turbulence production by breaking are put forward and discussed. In addition, an expression is derived for the energy flux of composite waves in terms of the calculated variables of the present wave model.

The numerical scheme and solution procedure are detailed in Chapter 6. Since

the governing equations for the circulation and the turbulence tranport are similar in form and must be solved consecutively for each time step they have been grouped in the same chapter. The stability and accuracy of the numerical scheme are confirmed by a number of computational experiments.

Chapter 7 and 8 contain applications of the present wave and circulation models to some typical coastal situations. Chapter 7 is devoted to the study of wave-current interaction. The cases considered include waves refracted by a shear current, the interaction of waves and an analytical rip current and wave diffraction around a detached breakwater. The computational results are verified by analytical solutions when possible and compared with the available numerical solutions for the same problems. In Chapter 8 wave-induced circulations are computed for a number of sea bottom configurations. Numerical accuracy, performance of the turbulence models and the effect of wave current interaction are all examined. Comparisons with laboratory and field data are also presented.

In order to gain more insight into the structure of the wave-induced currents, the vertical distribution of these currents is also considered. A numerical method is developed to deal with a simple case involving the calculation of the vertical profile of longshore currents on a plane beach. The detailed formulations and some computational results are presented in Chapter 9.

Finally, in Chapter 10, the conclusions from this study are drawn together with some discussions of the approaches used. Some suggestions for future work are also given.

CHAPTER 2
REVIEW OF PREVIOUS WORK

2.1 Introduction

This chapter aims at reviewing the development of studies on coastal wave propagation over uneven sea bed topographies, wave–current interaction and wave–induced nearshore circulations. To limit the scope of coverage only works on deterministic waves are included. Theoretical developments will receive primary consideration with experimental aspects of reviewed works being selected and discussed with a view to demonstrating the applicability and limitations of the theoretical models.

Emphasis has been placed upon the important physical mechanisms involved so as to establish the best possible modelling approaches for predicting wave and current fields in coastal areas. The reference list is by no means exhaustive but nevertheless sufficient to reveal the state of the art and point to possible directions for future developments.

2.2 Coastal Wave Propagation on Water of Variable Depth

As surface waves approach coastal areas with uneven bottom topography they undergo various changes due to the effects of refraction, diffraction, reflection and dissipation. In some situations their shapes may change dramatically. Although these motions can, in principle, be described by conservation laws for mass and momentum, the solution of the exact hydrodynamic equations is, except for some simple cases, very difficult. Even for infinitesimal waves in water of arbitrarily varying depth no exact solution has been found.

Traditional approaches involved developing perturbation approximations based on some physical parameters characterising the relative importance of the dominant mechanisms, so that theoretical models of linear and nonlinear initial boundary value problems could be formulated for particular flows.

The earliest theoretical study on waves was due to Poisson (1818) and Cauchy (1827) who formulated a model of two dimentional wave propagation, and tried to study the variation of the resulting free surface form with time, but did not obtain a final and concrete result. Airy (1845) and Stokes (1849) are probably the first to establish rigorous mathematical models for water waves. By assuming the ratio

between water depth and wave length to be small, Airy derived the well known shallow water equations which are particularly suited to the study of tidal waves and tsunamis. Detailed expositions of these equations can be found in the books by Lamb (1936) and Stoker (1956). Using the ratio of wave height to wavelength as a perturbation parameter Stokes established a third order approximate theory with the solution being expressed as a power series in terms of the wave steepness. The convergence of the method used by Stokes was later proved by Levi-Civita (1924) and Struik (1926). The most impressive modern development on Stokes waves was achieved by Schwartz (1974) and improved for finite water depth by Cokelet (1977). They found a recursive formulation for the coefficients of the power series and with the aid of the computer extended the solution for the Stokes wave to very high orders.

Another important classic theory was originated by Boussinesq (1872). By assuming that the ratio of amplitude to depth (H/d) and the square root of the ratio of depth to wave length $\sqrt{(H/L)}$ are both moderately small and of comparable magnitude, he was able to develop a set of equations which permit wave solutions with permanent form, such as the solitary wave and cnoidal waves (Korteweg-de Vries, 1895). Recent developments in this direction have been reported by Mei and LeMehaute (1966) and Peregrine (1967) who extended Boussinesq's equations to include the effect of slowly varying depth. Numerical solutions and verifications of the Boussinesq equations were reported by Abbott et al (1978) and Larsen and Manson (1982). The results show that these equations are applicable for 'short waves' and have great prospects for becoming the future model for engineering applications in coastal area.

The conditions under which each of the above classic models is valid were firmly established by Ursell (1952) in a fundamental paper. The single important parameter, commonly referred to as the Ursell number, is $Ur = a\lambda^2/h^3(2\pi)^2$ where a is wave amplitude, λ is wave length and h is water depth. The conditions are:

Airy long wave theory	$Ur > 1$
Boussinesq wave theory	$Ur = O(1)$
Stokes wave theory	$Ur < 1$

where O means the same order of magnitude. Therefore in order to use the above nonlinear theories to study wave propagation from deep water to shallow water some sort of matching of more than one theory is necessary. Stiassnie and Peregrine (1980) and Flick et al (1981) partly matched Stokes-type predictions to

those of solitary-cnoidal wave theory in order to describe the shoaling of waves from deep water to shallow water up to the breaking point. James (1974) similarly matches Stokes waves to 'hyperbolic waves' developed by Iwagaki (1968) as the shallow water limit of Cnoidal wave to study set-up and set-down. However because of the rather restricted initial and boundary conditions required for the exact solutions of Boussinesq or K.de.V type equations, it is doubtful whether they are suitable for general shoaling models for surface waves. Also they are definitely of little use in areas with complicated bottom topography or where structures are present in the domain of interest.

Fortunately in most circumstances water waves are surprisingly well described by linear irrotational inviscid flow theory. Over the last thirty years, great progress has been made in this direction. Notably, the ray method as first proposed by Munk and Sverdrup (1944) and later rigorously derived by Keller (1958) from exact linear equations, and has been successfully used in the calculation of wave refraction by slowly varying sea bed. Two distinct numerical solution techniques, one following the ray paths and another solving the equations at fixed grid points have been established, see, for example, Skovgaard and Jonsson (1976) and Noda et al (1972). Both approaches are equally efficient and suitable for waves propagating over large coastal areas. Following the idea of Keller (1962) the ray method may also be extended to study wave diffraction by particular types of breakwater and harbour layout. Details can be found in Larsen (1978) and Southgate (1985). Even though the techniques used are still restricted to some special situations, their high computational efficiency for waves of small periods, typically from 2 seconds to 10 seconds, deserves further study.

With regard to the study of wave diffraction in uniform water depth, Sommerfeld (1896) was the first to give the exact solution for waves diffracted by an impermeable barrier. Penney and Price (1952) gave a solution for waves around a semi-infinite breakwater based on the Fresnel integral method. The similar problem of waves penetrating through a breakwater gap was solved by Blue and Jonsson (1949). The most recent work on the same topic and using the same theory is reported by Sobey (1986) in which the emphasis is on the accuracy of numerical computations.

Although the classic ray method is fairly accurate and efficient for general refraction calculations, it has some severe limitations. It can not handle any partial reflections and also fails whenever there are caustics formed due to particular bottom topographies. To overcome this difficulty uniformly valid assymptotic expansions of one kind or another were proposed and limiting solutions for short

waves were found for particular types of caustics. Chao (1971) was the first to give a solution for a single straight or curved caustic based on Ludwig's anastz (1962). The waves at and away from the caustic were found to be of finite amplitude and did not necessarily break as commonly believed before. A general uniform expansion which included Chao's solution as a special case was then proposed by Shen et al (1975) which takes into account even such effects as surface stress and density stratification. However it is mathematically difficult to extend such an elegant technique to find the solution for the wave field over complicated bottom topographies with caustics of various forms. Also the above uniform expansion is incapable of handling cross waves resulting from structures located on an uneven bottom with total or partial reflective surfaces.

Recently, especially over the last ten years, the mild-slope equation has gained great popularity because of its generality in dealing with complex wave fields and the fact that it showed good agreement with experimental data. Birkhoff (1972) was the first to derive the mild-slope equation from the exact linearized governing equations of irrotational flow in the three dimensional domain under the assumption that the bottom varies very slowly over one wave length. He further demonstrated that it reduces to the Helmholtz diffraction solution for constant depth on the one hand and to the long wave equation for shallow water on the other. Smith and Sprinks (1975), in addition to presenting a formal derivation of the mild-slope equation, examined rigorously the magnitude of error terms involved. The generality of this equation has been further explored by Lozano and Meyer (1976). They showed that it includes 1) all the classical waves over water of uniform depth, 2) linear long waves over water with depth varying slowly with horizontal distance, 3) the first approximation to the exact solution for waves over a plane, gently sloping beach, 4) Keller's geometrical optics approximation for waves of slowly varying depth. They asserted that the 'mild slope' equation contains all the solutions and established approximations for classical, small amplitude surface waves on water of slowly varying depth. However, no work has been done to show the mathematical relation between mild-slope equation and uniform expansion solutions. At present they still remain as quite separate approaches to caustic problems. The satisfactory performance of the mild-slope equation has been reported by Berkhoff (1982) for wave tank data from an ellipsoidal shoal sited on a uniform sloping bed and by Behrendt (1985) for classic rectangular harbour laboratory test performed by Ippen and Goda (1963). Further tests were performed by Copeland (1985) through comparing with the analytical solution for semi-infinite breakwater and other more complicated cases.

Few analytical solutions of the mild-slope equation exist. Jonsson et al (1976)

found the analytical solutions for the wave field around a circular island sited on a paraboloidal shoal. The numerical solutions, in general computation, are obtained using either finite element method (Birkhoff 1976, Mei and Chen 1978) or finite difference method (Williams et al 1980 and Copeland 1985). Since the original equation as presented by Birkhoff is a steady state elliptic equation the computational effort is immense for actual engineering cases when large number of grid points have to be dealt with. Great efforts have, therefore, been made to ease this computational difficulty. This led to the parabolic approximation and the transient wave solution model.

The parabolic equation developed by Radder (1979) is based on the method of Tappert (1977), which includes both refraction and forward scattering but reflection is excluded. It is an initial value problem and according to Booij (1981) requires two orders of magnitude less computer time compared with the original elliptic equation by Birkhoff. But due to the limitation inherent in its derivation it is not suitable for situations where reflected waves are important. A different version of parabolic approximation was proposed by Lozano and Liu (1980). Their work has been extended and tested against experimental data by Tsay and Liu (1982). Further improvement was made by Liu and Tsay (1983) to include both transmitted and weak back scattered wave fields.

An important alternative method was proposed by Copeland (1985). Similar approaches have been reported by Watanabe (1985). By recasting the mild-slope equation into a transient state term a set of first order equations, similar in form to the shallow water equations are derived, which are then solved using finite difference method proposed by Ito and Tanimoto (1972). This method is less efficient than the solution of parabolic equation but, according to the theoretical analysis made by Booij (1981), it is still one order of magnitude quicker than the solution of elliptic equation as long as the number of time steps required for achieving steady state solution is comparable with the number of grid point on a mesh line. More importantly this method does not exclude reflected waves. Therefore it is believed that this method is preferable due to its combination of sufficient accuracy and moderate running cost.

To extend the applicability of mild-slope equation for more realistic coastal situations the bottom friction effect has been taken into account in parabolic method approximation (Liu and Tsay, 1986) and mild-slope equation (Chen, 1986) better agreement with experimental data is achieved in both cases. Also the energy dissipation due to breaking was modelled by Kirby and Dalrymple (1986) and Copeland (1985). Furthermore the nonlinearity was taken into account by Kirby

and Dalrymple (1983) for the parabolic approximation. It must be pointed out here that due to the fact that mild slope equation is a model for irrotational flow, the inclusion of frictional effects or any other form of energy dissipations must be of an empirical nature.

2.3 Wave–Current Interaction

The influence of currents on sea waves has been noted and recorded by navigators for a long time (see Isaacs 1948). The effect is noticeable for instance in entrance channels to estuaries and bays, where ebb flood currents can transform the waves considerably. Another famous example of wave steepening due to an opposing current is found near South Africa, where a sea wave of height 6m meeting the Agulhas current can be tripled in height (Smith, 1976). Extensive damage to a number of ships has been reported in this area. Final example of important wave–current interaction phenomena, as extensively studied in this thesis, occurs inside and close to surf zone where wave induced currents in turn change the driving wave pattern and consequently the breaking line.

Current–wave interaction is a complicated affair to deal with mathematically except in extremely simple cases. Historically, Unna (1942) studied deep water waves meeting a following or opposing current. Later Johnson (1947) presented a method for calculating the refraction of deep water waves by a uniform current meeting the waves at an angle. Arthur (1950) studied the kinematics of shallow water waves moving in currents of given distributions closely resembling rip currents, and noted the importance of distinguishing between wave orthogonals and rays. However, these earlier workers did not realize that there is an exchange of energy between wave and current so that erroneous formulations were used for the prediction of wave height.

The interaction mechanism first became fully understood when Lonquet–Higgins and Steward (1960, 1961) presented an energy equation – correct to second order – for a wave motion superimposed on a large scale slowly varying current field. The same result was also found by Whitham (1962) using the averaged Lagrangian method. The later work demonstrated that wave phase and height are to be determined by eikonal equation and a wave action conservation equation. Important contributions in crystallizing the concept of wave action and generalizing the energy equation have been made by Bretherton and Garret (1969) and Phillips (1977). A general derivation using the WKB perturbation expansion (a multi–scales expansion method) was presented by Mei (1982) which showed clearly that although horizontal velocity should be essentially uniform the vertical vorticity of order h/L is allowed.

Further insight into the wave action concept was gained by Jonsson (1978,1980) who pointed out that the total energy flux with the mean energy level as a datum is conserved. In order to solve the general depth-current refraction problem a general numerical model was presented by Noda et al (1974) using the finite difference method. The solutions were found at fixed nodal points in horizontal space. Recently Christofferson (1982) presented a model to solve the equations by following wave ray-path, in which the dissipation due to bottom friction was also taken into account. Using the method of averaging Lagrangian, finite amplitude water wave interaction with currents was studied by Grapper (1972).

In spite of the great success of the ray method in engineering applications, it has limitations. As pointed out by Hector, Cohen and Bleistein (1972) and by Bretherton and Garrett (1969), this method does not predict any partial reflections as waves advance into regions of varying depth or current. If the reflection is so great that the crests can actually become perpendicular to the current, the waves are reflected back. The standard ray solutions fail at such places which are known as caustics. It also fails whenever there exist cross waves, i.e., a situation where several distinct rays meet due to the presence of coastal structures. Therefore, some alternative methods must be used. Until now the exact methods for dealing with the above situations are yet to be found. There are only a number of solutions which are found for some particular depth and current distribution.

Mckee (1974,1975) adapted the theory of Ludiwig (1966) and presented a single representation which is uniformly valid everywhere in the flow situation considered to calculate wave field at and away from straight caustics. This work is important because it demonstrated that the wave height is finite at caustics and linear theory is capable of giving good approximations there. However this method is only applicable for broad jet type flows and requires that the bottom contour is uniform in cross flow direction. Some other different caustics have also been studied using the similar method to Mckee's. These two works have been further extended to include nonlinearity by Peregrine and Smith (1979) and Peregrine and Thomas (1979). Detailed reviews of wave current interaction have been presented by Peregrine (1976).

Recently a less rigorous, in essence, modelling approach was developed by Booij (1981). By making an assumption about the vertical structure of wave field analogy to pure wave situation, he derived a version of the 'mild slope' equation in which the effect of wave-current interaction is included. Close examination of his model shows that this method is accurate only when the current is parallel and bottom contours are again uniform in the cross current direction. The superiority of this method over Mckee's is reflected by the facts that it gives continuous

solutions across caustics rather than asymptotic ones, and it offers a way to find approximate solutions even when the assumption about the vertical structure is violated. As correctly pointed out by Smith (1975), the vertical structure is, in general, difficult to represent and when bottom contours or currents exhibit two-dimensionality in horizontal space, the incident and reflected waves do not have the same frequency relative to the moving medium and consequently they do not have the same vertical dependence. Therefore the functional form of the composite vertical structure can not be described by any single function which is precisely what Booij did. The error involved has been discussed by Booij for some simple cases but a formal estimation, like Smith & Sprinks (1976) did in the derivation of the mild-slope equation for pure waves, is yet to be worked out.

After Booij two slightly different versions of the mild-slope equation including the effect of wave current interaction were presented by Liu (1983) and Kirby (1984). Kirby pointed out an error in the surface boundary condition used by Booij and gave a final result which is considered to be correct and consistent with the order of approximation in terms of the perturbation parameters. In all three derivations the current is assumed to be irrotational, which is a severe limitation since the currents occuring in nature are seldom irrotational. The derivation of the wave action conservation law from most general hydrodynamic equations does not require the current to be irrotational (see Mei, 1983).

As already discussed in previous section there exist the numerical difficulties in solving the steady state mild-slope equation. Only limited verifications have been performed by Booij (1981) and Liu (1983). The parabolic approximation is derived and used by them to study the cases in which the reflection is considered unimportant. An extension of the mild-slope equation to include nonlinearity was reported by Kirby and Dalrymple (1983) and again in this work only the parabolic version was used.

2.4 Wave-Induced Nearshore Circulation

In nearshore area there exist currents resulting from various causes like wind, tide and other meterological factors. In addition, the existence of coastal currents directly induced by short surface waves and varying with wave state has long been recognized by fishermen and others living near the coast. The motivation of studying such currents is to understand and predict coastal sediment movements and pollutant processes.

Johnson (1919) was probably the first to study wave-induced currents in a

scientific way and identified the wave as the primary cause for their existence and intensity but no quantitative methods for prediction purposes were given. A most clear and complete field measurement result was later presented by Shepard & Inman (1950) in which full nearshore current circulation including longshore currents and rip currents were identified. Other early extensive field measurements were reported by Sonu (1970) in which apart from extensive data being collected, dominant processes responsible for the circulation patterns observed were described qualitatively.

Theoretical studies posed a far more difficult problem in earlier days. The emphasis has been largely placed upon the analysis of simple longshore currents. Due to the lack of suitable wave theories great efforts were made to relate the wave energy or momentum at the breaking line to the time mean flow rate over the entire surf zone. Putnam et al (1949) pioneered such a kind of study. in which two formulae were derived based on, respectively, the wave energy and momentum. This work inspired more research efforts, and subsequently up 12 different formulae of semi theoretical or pure empirical type were proposed as reviewed by Galvin (1967) and Horikawa (1978). Some experiments were conducted both in the field and in laboratory basins. However due to insufficient theoretical knowledge and poor quality of the data then collected, previous theoretical results were rejected by Galvin (1967) as inadequate and better theoretical description and experimental data were demonstrated to be necessary.

Soon after Galvin's review three independent works by Bowen (1969), Longuet-Higgins (1970) and Thornton (1970) marked a breakthrough in longshore current prediction and also laid the theoretical basis on which more sophisticated numerical models for nearshore circulations were to be built and developed. The key to the formulation in all three works is the use of radiation stress concept as first derived by Longuet-Higgins & Stewart (1961,1964) and the identification of the different factors involved in momentum balance in and outside of the surf zone. Inside the surf zone, it is the balance between three forcing terms, i.e., the radiation stress gradient, bottom friction and horizontal mixing. Outside the surf zone the radiation stress gradient is equal to zero and the balance only involves the later two terms. These three works are different only in the expressions used for the radiation stress, bottom friction stress as well as the horizontal mixing. Among them, Longuet-Higgins' theory is the most popular one because of its simplicity and relatively better representation of both friction stress and mixing term, specifically within the surf zone.

Within the same theoretical framework, certain improvements were made,

including the nonlinear effect of waves (James, 1974), better bottom friction stress formula (Madsen and Grant, 1978) and more advanced turbulence model (Visser, 1984). For the calculation of the longshore current generated by waves breaking obliquely on a plane beach quite satisfactory results were found by using properly calibrated empirical coefficients.

Another theoretical breakthrough was the mechanism found for the generation of the rip currents which remained unsolvable until Bowen (1969) developed the first rip current theory. In this theory the interaction between the incoming waves and the edge waves is considered to be the cause for the formation of rip current on a plane beach. Both current intensity and rip space were estimated using linear and nonlinear shallow water equations. The nonlinear term is found to narrow the rip channel formed. Various other theories were subsequently proposed including those of Hino (1974) and Leblond and Tang's (1974) instability theories, Dalrymples's wave wave interaction theory and the most widely studied wave bottom interaction (including interaction with structures) theory (Noda et al, 1974). Although it is still difficult to identify which particular mechanism is responsible for the formation of rip currents at a specific coastal site it is nevertheless firmly extablished that the formation of rip currents is due to uneven distribution of breaking height in the longshore direction. The most important situations from engineering point of view are the wave–bottom or wave–structure interaction in which case nearshore circulations with complex patterns result.

With the theoretical bases for longshore and rip currents being firmly established the solution of the linearized time–averaged and depth–integrated averaged equations of continuity and momentum was achieved using numerical methods. By using the ray method to obtain the wave field over an undulating bed form Noda et al (1972,1974) solved the linear governing equations of the mean current. In this work partially successful attempts were made to include the effect of wave–current interactions in the calculation of the wave field. Similar models were also produced by Sasaki (1974) and Birkemeier and Dalrymple (1975) with the bottom friction terms being better represented. The first attempt to calculate wave induced nearshore circulation with structures present in the region of interest was made by Liu and Mei (1976) using linear equations. All above works have contributed to the understanding of the effects of various physical processes on the circulation patterns but poor comparisons with experimental data were inevitable due to the omission of some important terms which should be present otherwise in the complete governing equations, such as nonlinear terms, horizontal diffusion and set_up inside the surf zone.

To improve the predictability of the numerical models many more sophisticated

models were developed with varying degree of complexities and numerical techniques. It is necessary to point out here that the verification and calibration of such models with field data is not a simple task and, therefore, a decision about the suitability and merit of a particular numerical model is largely made based on, apart from the comparison with the circulation data from full-scale or physical models, the theoretical representations of the mechanisms involved and the properties of the numerical methods used.

The first nonlinear model based on the general shallow water equations was proposed by Bettess et al (1978) using the finite element method. The circulations around a habour were reasonably reproduced. In this model the wave characteristics were obtained from model tests or from a much simplified topography, therefore, it is not directly suitable for prediction purpose.

A more economic numerical model was developed by Ebersole and Dalrymple (1980) which in effect is an extended version of Birkemeier and Dalrymple (1975) taking into account nonlinear convection, horizontal mixing, set-up, and wave current interaction (only partially successful). In spite of its apparent completeness this model is not considered to be accurate enough for use in engineering applications because of the deficiencies inherent in its numerical scheme. It suffers from the time splitting instability, and the correction method used to suppress the instability reduces the order of accuracy down to (Δx , Δt) in nonlinear terms. Also quite significant numerical diffusion is observed (Basco, 1983).

da Silva Lima (1981) followed Ebersole and Dalrymple's approach but employed a numerical scheme with simple forward time-centre difference in space. Instabilities were encountered when the convection terms were included. With regard to the wave calculations Noda's refraction method was adopted, which is strictly applicable for wave refraction and is not, in theory, suitable for comparison with the experimental data collected from his enclosed wave basin in which reflections from side walls are evident. However his well documented data are very useful for in calibrating and verifying numerical models.

Again using the finite element method Liang (1983) developed a model to calculate nearshore circulation due to a monochromatic harmonic wave field. The mild-slope equation was adopted to give radiation stress components outside breaking zone. Detailed studies of the circulation pattern around a detached breakwater were presented. In spite of its generality and flexibility in handling boundaries with complex geometry, several reservations can be put forward against

its use for engineering purposes. Firstly the penalty method introduced excludes the

set-up which makes it very unlikely to be accurate whenever set-up is important compared with still water depth. Secondly, the finite element method requires to solve large matrices, which is generally time consuming in comparison with finite difference methods, especially as in this model the wave field is to be determined by solving an elliptic equation.

Recently two more models have appeared in the literature. The first one was developed by Copeland (1985) in which the wave field is determined by solving transient mild-slope equation of a hyperbolic form and the nearshore current field is calculated using a finite difference model with all the important terms, except wave current interaction, being modelled in a similar way to Ebersole and Dalrymple's model. From the theoretical point of view this model is clearly the most versatile and economical one to date. Extensive tests were performed and results compared with available analytical solutions and experimental data. On the whole the comparisons are quite good although it is noticed that for some complicated cases the comparisons are not as close as the author claimed. The reason for such discrepancies may be attributed, to a certain extent, to the exclusion of wave current interaction as pointed out by the author himself, but in this particular case, is more likely resulted from the arbitrariness involved in the manipulation of the eddy viscosity coefficient in order to ensure stable solutions. Also the scheme used for the convection terms is not properly space centred, which is proved to be the main reason for the instability encountered.

Another model was developed by Wu and Liu (1985) using the finite element method. Set-up was properly taken into account unlike Liang's model. Only simple wave refraction was considered in the calculation of the wave field and no wave-current interaction was included. This model may well be applicable for open beach cases and weak currents, as demonstrated by subsequent comparisons with experimental data (Wu and Liu, 1986) but is not suitable whenever the wave diffraction and reflection by complicated topography and currents are important.

Before ending this section it is considered useful to give a brief discussion of the possible ways of improving the present numerical models and the limitations of the established theoretical approaches. Basco (1982) has made a most extensive review of wave induced currents after Galvin (1967), in which many useful evaluations and recommendations were made. The references listed in the work are exhaustive. Since general situations are fundamentally different from the simple longshore current on a plane beach case, the theoretical approach established by Longuet-Higgins and others can only be regarded as a suitable starting framework.

All the terms in the governing equations must be calculated. Furthermore, the

computational stability and accuracy, which generally give no problem in linearized equations, may be difficult in nonlinear equations and must be achieved in any sophisticated nearshore circulation model based on the full nonlinear equations of motion. With the aid of the mild slope equation the wave field can be determined more accurately than before. After the work of Liu and Dalrymple (1978) arbitrary incident waves and comparable magnitudes of wave orbital motion and current velocity can be treated properly in the estimation of frictional shear stress. However two more important processes i.e. wave current-interaction and turbulent mixing have been either treated for simple cases such as refraction only, or modelled in an unrealistic way such as using the simple mixing length formula for the eddy viscosity. These two processes are to be treated in more depth in the present thesis

The most severe limitation in the present theoretical framework (which is sound in principle) is the assumption about the proportionality between wave height and water depth inside the surf zone due to the lack of quantitative knowledge of the wave energy dissipation process by wave breaking. Thus the models can be, unrealistically, too sensitive to bed form (Battjes, 1978). Another limitation is the complete lack of information about the vertical structure of the circulation owing to the use of depth averaged governing equations. Controversial experimental observations in this respect have been reported by Suno (1972), Shepard and Inman (1950) and Meadows (1976). The need for such knowledge is evident owing to the fact that suspended sediment is transported by the local velocity rather than the depth-averaged velocities and the research effort in this area is only confined to the study of undertow generated by wave breaking at right angles to a plane beach. In this thesis an attempt is made to study the vertical structure of longshore current of the simplest form.

2.5 Turbulence Models in Computations of Nearshore Circulation

In nearshore circulation models the effect of turbulent mixing is important for two reasons: 1) inside the surf zone it effectively reduces the peak current and results in a realistic distribution of currents, 2) outside the surf zone the observed current can be predicted only by the inclusion of such a diffusion mechanism. Without turbulent mixing, the predicted current distribution would not be very realistic (see, e.g. Longuet-Higgins (1970), Leblond and Tang (1974) and Birkmeier and Dalrymple (1975)). Despite this universally accepted evidence, the turbulent mixing is, among all dominant processes, one of the least understood and probably most unsatisfactorily modelled.

Over the last one and half decades the progress made in both experimental

and theoretical studies of turbulence structure caused by wave breaking has been slow and mainly confined to two dimensional situations. Comprehensive experimental studies on turbulence generated by breaking waves in flumes can be found in Sakai et al (1984), Steve and Wing (1982) and others. The turbulent structure was described both qualitatively and quantitatively. Although the results from these works are extremely useful for the understanding of turbulent motions, the lack of theoretical progresses in quantifying the turbulent structure and kinematics reflects the fact that the modelling techniques, which greatly rely upon the support of some plausible physical reasoning and experimental evidence are still the main routes to understanding and in predicting mixing effect on the time mean physical quantities.

In the context of longshore current theories Bowen (1969) assumed the eddy viscosity to be a constant which, as well known, is too simple to be true even for the description of turbulence generated by spilling breakers on a plane beach. An improved and probably the most widely used eddy viscosity formula was proposed by Longuet-Higgins (1970) based on Prandtl's mixing length concept. The characteristic length and velocity were taken to be proportional to the distance to the shoreline and the wave celerity with a proportionality coefficient being determined by physical reasoning and a wide range of field and laboratory data. This formula can be regarded quite satisfactory inside the surf zone but, as pointed out by James (1974), unacceptable outside it where there is no local breaking and, therefore, the turbulence must be much weaker, originating just from turbulence diffusion. Inman et al (1971) in their physical model experiment actually observed little dye patches outside breaking line, which clearly indicates the turbulence intensities are quite different inside and outside the surf zone. Thornton (1970) and Jonsson et al (1974) suggested that the wave orbital velocity and displacement at the sea bottom be used as two characteristic scales. While the turbulence velocity scale may be intimately related to the orbital motions of breaking waves the length scale can be expected to be, to a great extent, independent of the waves and predominantly controlled by the flow field and its boundaries.

Battjes (1975, 1978) has made an important step forward in the modelling of turbulent mixing inside the breaking zone. By assuming that the production and dissipation of turbulence are locally in balance or being so with the inclusion of diffusive transport of turbulence energy, he proposed a turbulent kinetic energy equation which is solved to estimate the velocity scale. This idea is valuable since the turbulent kinetic energy is the most natural choice for the characteristic velocity in an eddy viscosity model. This kind of approach has long been followed in many other branches of fluid dynamics and and has led to successful prediction of not

only time mean velocities but also actual turbulent correlations (Launder and

Spalding, 1972). As to the length scale, Battjes suggests using local depth modified by an adjustable coefficient. For longshore current calculation this choice may be considered to be of the right order of magnitude. Actually all the above mentioned models fitted with proper coefficients do not differ very much in terms of the calculated longshore currents for a large range of bottom slopes and small angles of incidence. They are different only when general two dimensional situations in horizontal space are considered. In such cases, especially whenever there exist coastal structures or complicated bottom topographies, the length scale can not be expected to be controlled solely by the local depth. The transport effect of turbulent quantities is expected to become equally important.

The more sophisticated turbulence models developed for applications related to the mechanical engineering and aeronautical engineering have been thoroughly reviewed by Launder and Spalding (1972) and Bradshaw et al (1982). The applications of such models in a wide range of hydraulic engineering problems have been extensively reviewed by Rodi (1981). Among all the second order turbulence correlation models the $k-\epsilon$ model is most widely tested and its performance is well demonstrated in large scale hydraulic engineering and coastal flows. Recent application in exact two-dimensional flow calculations can be found in Alfrink & van Rijn (1983). In this work the oringinal $k-\epsilon$ model was used and sensitivity of various parameters in the model to the changes of flow conditions was examined.

Probably the most relevant and promising model suitable for large scale horizontal flow modelling is the one proposed by Rostogi and Rodi (1978). They adopted the original $k-\epsilon$ model for use in depth-averaged calculations with all structures of the equations and the constants unchanged. They suggested a method to model the dispersion terms resulting from the vertical nonuniformity of time-mean velocities by relating them to the bottom friction stress. Even though this approach is certainly of a rather empirical nature, the results from calculations are very encouraging. The need to use more sophisticated turbulence model for realistically simulating nearshore turbulence mixing was also indicated by Basco (1982), although no methods were proposed which might be suitable for such calculations.

CHAPTER 3
A WAVE PROPAGATION MODEL

3.1 Introduction

Since the mild-slope equation was first derived by Berkhoff (1972) it has become possible to study wave propagation in coastal areas where refraction, diffraction and reflection are equally important. The mathematical models based on this equation and its variants have been successfully developed, verified and increasingly used in engineering applications. For the calculation of pure wave propagation it is considered to be the most general linear wave model to date.

However, the situation can be quite different if waves are affected also by a current which can be steady or unsteady. In fact, no exact methods are available even for describing the interaction between small amplitude waves and a steady current of arbitrary form. Some rather strict restrictions have to be impossed upon the current in order to establish appropriate methods for dealing with specific wave-current interaction problems.

One type of interaction, which has recieved the most attention over the last thirty years, is the interaction between waves and a steady-state gradually varying current. If the waves are only refracted by the current and the sea bed the classic ray method is applicable and very efficient numerically. In order to deal with wave-current interaction under a complex wave state Booij (1981), by making some acceptable assumptions and using the variational method, extended the mild-slope equation to include the effect of a steady, slowly varying and irrotational current. Two slightly different versions were reported by Liu (1983) and Kirby (1984). The later author has pointed out some errors in the final equations given by both Booij and Liu (1983)

In this chapter the same problem is treated afresh using the perturbation method. Although the equation finally derived is the same as that by Kirby (1984) the assumption made for the current is different. The strict constraint of irrotationality on the current has been shown to be unnecessary and can be relaxed to allow a weak vertical vorticity. This extension allows the interaction between waves and wave-induced currents to be treated using the mild-slope equation, which are free from horizontal vorticity but have, generally, a weak vertical vorticity.

Also in this chapter it is shown that the 'heuristic' driving boundary condition

proposed by Copeland (1985) can be formally derived for long-crested propagating waves. Its limitations in the case of a complex wave field are discussed and possible remedies are proposed.

Finally the transient version of the mild-slope equation with wave-current interaction is decomposed into a set of first order equations. Based on these equations the wave model is developed. It can then be solved by an efficient explicit finite-difference scheme. When large wave propagation areas are to be analysed, which is quite common in most coastal engineering problems, higher computational efficiency can be achieved by using this model.

3.2 Mild Slope Equation For Waves Only

3.2.1 Main results for linear waves

As it is well known, real waves propagate in a viscous fluid over an irregular bottom of varying permeability. However a remarkable fact is that in most cases the main body of the fluid motion of water waves can be nearly irrotational. As a result, a wave potential is considered to exist which satisfies Laplace's equation

$$\frac{\partial^2 \varphi}{\partial z^2} + \nabla^2 \varphi = 0 \qquad (3.1)$$

where $\varphi = \varphi(x_i, z, t)$ is the velocity potential of waves, ∇ is the two dimentional horizontal gradient operator, $x_i (i = 1,2)$ and z are horizontal and vertical axis, respectively, t is time. An equivalent method which describes the wave field is to use a variational principle. A most general one for irrotational flow is given by Luke (1966) as

$$L = \int_{-h}^{\zeta} \left\{ \frac{\partial \varphi}{\partial t} - \frac{1}{2} (\nabla \varphi)^2 - gz \right\} dz \qquad (3.2)$$

where h is the water depth, g is gravitational acceleration and ζ is instantaneous surface elevation.

The mild-slope equation can be formally derived using either one of the above formulations subject to two basic conditions

1) the waves are small in amplitude so that linearized kinematic and dynamic boundary conditions at the free surface may be applied.
2) bottom variation can be arbitrary in form but is sufficiently small over one wave length.

The papers by Smith & Sprinks (1976) and Lozano & Meyer (1976) contain the full exposition of the above considerations and the detailed derivations.

For simple harmonic waves with frequency ω two versions of the mild-slope equation can be written as

Transient version

$$\nabla (CC_g\nabla\Phi) - \frac{C_g}{C}\frac{\partial^2\Phi}{\partial t^2} = 0 \tag{3.3}$$

Steady state version

$$\nabla (CC_g\nabla\tilde{\Phi}) + k^2CC_g\tilde{\Phi} = 0 \tag{3.4}$$

where k, C and C_g respectively are wave number, wave celerity and group velocity of component waves determined by the exact solutions of eq. (3.1) for constant depth

$$\omega^2 = gk\tanh(gh) \tag{3.5}$$

$$C = \omega/k \tag{3.6}$$

$$C_g = \frac{C}{2}\left(1 + \frac{2kh}{\sinh 2kh}\right) \tag{3.7}$$

φ, Φ and $\tilde{\Phi}$ are defined as

$$\varphi(x_i,z,t) = f(x_i,z)\,\Phi(x_i,0,t) \tag{3.8}$$

$$f(x_i,z) = \frac{\cosh k(h+z)}{\cosh kh} \tag{3.9}$$

$$\Phi(x_i,0,t) = \tilde{\Phi}(x_i)e^{-i\omega t} \tag{3.10}$$

Clearly, eq. (3.4) is a steady state elliptic equation with a complex variable while eq. (3.3) is a hyperbolic equation which can be treated either as a complex equation or as a real equation as appeared in Copeland (1985). Analytically both equations should give the same result for φ but, according to the analysis made by Booij (1981), one order of magnitude less computational time is required by the hyperbolic equation for actual engineering computations.

3.2.2 Derivation of a set of first order model equations

The sole purpose of recasting the single transient equation eq. (3.3) into a set of first order equations is to reduce the amount of computations required. The idea was first proposed by Ito & Tanimoto (1972) for solving their modified shallow water equation. Recently the method was adopted by Copeland (1985) to the mild-slope equation without giving sufficient details of the derivation. It is considered useful here to present a brief account since the recasting of the extended mild-slope equation including wave-current interaction follows almost the same procedure.

We shall start by considering eq. (3.3). Using the linear kinematic boundary condition at the free surface in terms of Φ

$$\frac{\partial \Phi}{\partial t} + g\zeta = 0 \tag{3.11}$$

and the harmonic property of Φ and ζ

$$\frac{\partial \Phi}{\partial t} = i\omega\Phi \tag{3.12}$$

$$\frac{\partial \zeta}{\partial t} = i\omega\zeta \tag{3.13}$$

Eq(3.3) can be written as

$$\nabla (CC_g\nabla\zeta) - \frac{C_g}{C}\frac{\partial^2\zeta}{\partial t^2} = 0 \tag{3.14}$$

then by inserting eq. (3.13) into eq. (3.14) we get

$$\nabla(-\frac{i}{\omega} CC_g\nabla\zeta) + \frac{C_g}{C}\frac{\partial\zeta}{\partial t} = 0 \tag{3.15}$$

Now use $\mathbf{Q} = (Q_x, Q_y)$ to represent the quantity inside the bracket in eq. (3.15) as an unknown variable. The first scalar equation becomes

$$\nabla\mathbf{Q} + \frac{C_g}{C}\frac{\partial\zeta}{\partial t} = 0 \tag{3.16}$$

According to the definition of $\mathbf{Q}$ we have

$$\mathbf{Q} = -\frac{i}{\omega} CC_g\nabla\zeta \tag{3.17}$$

Taking the derivative with respect to t of both sides and then substituting eq. (3.13) finally yields

$$\frac{\partial Q}{\partial t} + CC_g \nabla \zeta = 0 \tag{3.18}$$

or written in terms of components as

$$\frac{\partial Q_x}{\partial t} + CC_g \frac{\partial \zeta}{\partial x} = 0 \tag{3.19a}$$

$$\frac{\partial Q_y}{\partial t} + CC_g \frac{\partial \zeta}{\partial y} = 0 \tag{3.19b}$$

Apparently, **Q** is introduced just as a dummy variable without any clear physical meaning. In fact it is closely related to the flow rate of waves, i.e., the wave particle velocity integrated over the entire water depth. By using the relation

$$\zeta = i\frac{\omega}{g} \Phi \tag{3.20}$$

Q can be written as

$$\mathbf{Q} = CC_g/g \ \nabla\Phi = CC_g \ /g \ \mathbf{V}\Big|_{z=0} \tag{3.21}$$

where $V|_{z=0}$ is the wave particle velocity at the still water level. Remembering that the particle velocity is defined as the gradient of φ

$$\mathbf{V} = \nabla\varphi \cong f\nabla\Phi \tag{3.22}$$

where f is determined by eq. (3.9), and that the flow rate over the entire depth denoted by **R** is

$$\mathbf{R} = \int_{-h}^{0} \mathbf{V}\, dz = C^2/g \ \nabla\varphi \tag{3.23}$$

it is now clear that **Q** and **R** are related by

$$\mathbf{Q} = \frac{C_g}{C} \mathbf{R} \tag{3.24}$$

In very shallow water $C_g = C = \sqrt{(gh)}$ so that **Q** and **R** become identical.

In fact the way of recasting eq. (3.15) is not unique. By using eq. (3.24) an alternative set of equations in terms of **R** and ζ can be easily derived (Watanabe, 1985) as

$$\nabla(n\mathbf{R}) + n \frac{\partial \zeta}{\partial t} = 0 \tag{3.25}$$

$$\frac{\partial \mathbf{R}}{\partial t} + C^2 \nabla \zeta = 0 \tag{3.26}$$

where n = C_g/C, being 1/2 and 1 in deep water and shallow water, respectively. Although the flow rate R is physically a better defined quantity than Q, the equations proposed by Copeland are numerically slightly simpler as far as the surface elevation prediction is concerned.

3.2.3 Boundary conditions

As it is well known for problems of the type studied here the boundary conditions are crucial to the accurate solution of the governing equations. There are two kinds of boundary conditions which are to be specified. One corresponds to boundaries from where the waves propagate into the calculation domain, commonly called driving boundary conditions. Another corresponds to the internal boundaries formed by coastal structures and at side boundaries through which waves leave the calculation domain. Copeland (1985) proposed a heuristic driving boundary condition and an analytical internal boundary condition taking account of partial reflectivity, respectively. However, the lack of sufficient physical and mathematical arguments in supporting these boundary conditions have prevented the much needed assessment of their general usefulness and limitations. The following is an attempt to clarify and derive formally the driving boundary conditions.

Driving Boundary

Considering the two dimentional case where axes x and y are in onshore–offshore and alongshore directions, respectively, and taking the x driving boundary as an example, Copeland originally proposed two difference relations which can be written equivalently as following

$$\frac{\partial Q_x}{\partial x} - \frac{\cos\theta}{C}\frac{\partial Q_x}{\partial t} = 0 \qquad \text{at} \quad x=0 \tag{3.27}$$

and also

$$\frac{\partial q_x}{\partial x} - \frac{\cos\theta}{C}\frac{\partial q_x}{\partial t} = 0 \qquad \text{at} \quad x=0 \tag{3.28}$$

where, as shown in Fig. 3.1, Q_x is the x–component of total calculated wave disturbance being the sum of the incoming wave and reflected wave at the boundary, x = 0, q_x is the x–component of the incoming wave only, while the definition of the angle θ was unclear in the original paper. In fact, whenever there exists a reflected wave eqs. (3.27) and (3.28) can not both hold true. If θ is the angle of the incoming long crested wave eq. (3.28) is satisfied but eq. (3.27) does not hold to be true, while if θ is the angle of the resultant velocity vector of the

composite waves none of them is correct. Therefore it is not possible to derive an appropriate boundary condition directly from eqs. (3.27) and (3.28). A different derivation should be taken which can be done based on the argument put forward by Bettess & Zienkiewitz (1977).

Considering that the scattered waves at a large distance from the surface of the disturbance can be regarded as a local plane wave proceeding in a radial direction, a general wave form for this situation can be written as

$$\varphi_r = F_1(r + Ct) + F_2(r - Ct) \tag{3.29}$$

where φ_r is the scarttered wave potential at the boundary area which is composed of two parts, F_1 representing the wave passing through the boundary and F_2 representing the waves reflected from the boundary.

The condition that there is no reflected wave, $F_2 = 0$, requires

$$\frac{\partial \varphi_r}{\partial r} = F_1' \qquad \frac{\partial \varphi_r}{\partial t} = CF_1' \tag{3.30}$$

this leads to a simple boundary condition

$$\frac{\partial \varphi_r}{\partial r} = \frac{1}{C}\frac{\partial \varphi_r}{\partial t} \tag{3.31}$$

Eq. (3.31) can not be directly used in a normal finite difference model in which the boundaries are not circular but parallel to one of the axes. Therefore it is necessary to determine the equivalent boundary condition using appropriate Cartesian coordinates.

Realising that in the present context scattered waves travel in the positive r direction, i.e., $r = x\cos\theta_r + y\sin\theta_r$ and $\partial r/\partial x = \cos\theta_r$, we have

$$\frac{\partial}{\partial r} = \frac{\partial}{\partial x}\frac{\partial x}{\partial r} = \frac{\partial}{\partial x}\frac{1}{\cos\theta_r} \tag{3.32}$$

therefore, eq. (3.31) can be written as

$$\frac{\partial \varphi_r}{\partial x} = \frac{1}{\cos\theta_r}\frac{\partial \varphi_r}{\partial t} \tag{3.33}$$

It should be pointed out that θ_r is the direction of outgoing waves through driving boundaries and is not necessarily related to the incoming wave angle θ_i in a simple way.

Since eq. (3.33) is applicable at any large distance x from the area of disturbance, to obtain a condition in terms of the corresponding components of Q and q we can multiply (3.33) by CC_g/g and then take derivatives with respect to x, which gives

$$\frac{\partial}{\partial x}\left(\frac{CC_g}{g}\frac{\partial \varphi_r}{\partial x}\right) - \frac{\partial}{\partial x}\left(\frac{CC_g}{g}\frac{\cos\theta_r}{C}\frac{\partial \varphi_r}{\partial t}\right) = 0 \tag{3.34}$$

According to the definition in Fig 3.1 and eq. (3.21), it can be easily found that the relations between the x components of the total waves, incoming waves and scattered waves are

$$\frac{g}{CC_g}(Q_x - q_x) = \frac{\partial \varphi_r}{\partial x}$$

If the driving boundary is so chosen that $\cos\theta_r/C$ is nearly constant or slowly varying in x direction at the boundary eq. (3.34) can then be rewritten conveniently as

$$\frac{\partial}{\partial x}(Q_x - q_x) - \frac{\cos\theta_r}{C}\frac{\partial}{\partial t}(Q_x - q_x) = 0 \tag{3.35}$$

It should be noted that this result is different from that given by Copeland (1985) in that θ_r is introduced which is not the same as the incoming wave angle or the total calculated wave angle θ. A similar condition can be written for the y-component of Q at the y driving boundary as

$$\frac{\partial}{\partial y}(Q_y - q_y) - \frac{\sin\theta_r}{C}\frac{\partial}{\partial t}(Q_y - q_y) = 0 \tag{3.36}$$

Before applying eq. (3.35) or (3.36), the only remaining problem is to determine the angle of scattered waves θ_r. In general situations the propagation of scattered waves is not only related to the incoming waves but more fundamentally affected by the bottom topographies and structures present and can not be known a priori. This is an intrinsic difficulty in any general refraction-diffraction calculations as discussed in detail by Engquist and Majda (1977). Only for some special cases methods are available to estimate θ_r accurately. For example if waves propagate on a plane beach or strike a vertical wall with the surface parallel to x axis, the directions of incidient and scattered waves can be simply written as follows

$$\theta_r = \pi - \theta_i \tag{3.36}$$

in which θ_i is here denoting the angle of local incoming wave component. It is

emphasised that this relation does not hold true for general refraction-diffraction cases, especially near scattering sources. However since the driving boundaries can normally be positioned far away from the area of interest where the scattered waves have diminished in amplitude and tend to behave like plane propagating waves it may be considered as a reasonable approximation to apply eq. (3.36) at the boundaries. In fact this relation has also been assumed by Copeland without attempting to present any justification.

Transmissive Boundary

The transmissive boundaries are defined here as both down-wave imaginary boundaries and those formed by internal structure surfaces with total or partial reflectivity. For the first type a condition similar to the driving boundary condition can be used in which the only difference is that the angle used is the total wave angle instead of the scattered wave angle:

$$\frac{\partial Q_x}{\partial x} + \frac{\cos\theta}{C} \frac{\partial Q_x}{\partial t} = 0 \qquad (3.37)$$

and for y boundary

$$\frac{\partial Q_y}{\partial y} + \frac{\sin\theta}{C} \frac{\partial Q_y}{\partial t} = 0 \qquad (3.38)$$

To deal with partial reflectivity Copeland (1985) has derived, following Ito & Tanimoto (1974), an analytical boundary condition. This condition is exact only for a long-crested propagating wave striking the internal boundary at right angle. Nevertheless it has been demonstrated to be applicable from the engineering point of view. The formulae as originally proposed are in difference form

$$Q_{x_{0,j}}^{t} = AF.\ Q_{x_{1,j}}^{t-\tau} \qquad (3.38)$$

$$AF = (1-r)/((1+r)^2\sin^2(k\Delta x\cos\theta) + (1-r)^2\cos^2(k\Delta x\cos\theta))^{1/2} \qquad (3.39)$$

$$\tan(\omega\tau) = \frac{1+r}{1-r} \tan(k\Delta x\cos\theta) \qquad (3.40)$$

where r denotes the reflectivity index varying from 0 to 1, k is the wave number, ω is absolute frequency, τ is a time interval, subscript 0 denotes points on the x boundary and subscript 1 denotes corresponding adjacent internal points at a distance Δx apart, subscript j denotes the grid points along y direction. The two extreme cases are

Totally reflective boundary, r = 1, so that

$$Q_x{}^t{}_{0,j} = 0 \tag{3.41}$$

Totally transmissive boundary, r=0, so that

$$Q_{x_{0,j}}^{t} = Q_{x_{1,j}}^{t-\tau} \quad \text{with } \tau = \frac{\Delta x}{C}\cos\theta \tag{3.42}$$

Eq. (3.42) should be equivalent to eq. (3.37), which can be shown as follows. Apply eq. (3.42) at the time level $t+\tau$, i.e.

$$Q_{x0,j}^{t+\tau} = Q_{x1,j}^{t}$$

expanding $Q_x{}^{t+\tau}$ at time t and retaining the first order derivative only gives

$$Q_{x0,j}^{t} + \frac{\partial Q_x}{\partial t}\tau = Q_{x1,j}^{t}$$

or inserting the expression of τ from eq. (3.42)

$$(Q_{x0,j}^{t} - Q_{x1,j}^{t})/\Delta x + \frac{\cos\theta}{C}\frac{\partial Q_x}{\partial t} = 0$$

taking the limit as Δx approaches zero yields the same result as eq. (3.37).

3.3 The Mild-Slope Equation for Waves on Large-Scale Currents

3.3.1 Assumptions and boundary conditions

In the following we shall restrict ourselves to the consideration of the interaction between short waves and a large-scale current. The motion due to waves is, as usual, assumed irrotational and linear. The current is steady and slowly varying in space. To be specific in mathematical terms we suppose that U, h, k and L respectively are representative values of the current velocity, the water depth, the wave number of the surface waves and horizontal length scale for the variations in either the current or depth. The assumption of depth and current slowly varying in horizontal coordinate x_i(i=1, 2) means that

$$(kL)^{-1} \sim \frac{h}{L} = O(\mu) \ll 1 \tag{3.43}$$

and for linear waves we shall take u_i and w as being O(kA) where A is the wave

amplitude. Similarly the derivative operators have the scales as

$$\frac{\partial U_i}{\partial x_i} \ , \ \frac{\partial h}{\partial x_i} \ \cdots \sim O(\mu) \tag{3.44}$$

$$\frac{\partial u_i}{\partial x_i} \ , \ \frac{\partial w}{\partial x_i} \ \cdots \sim O(kA) \tag{3.45}$$

As shown by Mei (1982) the only vorticity remaining nonzero under the present approximations is the vertical vorticity, i.e.

$$\frac{\partial U_j}{\partial x_i} - \frac{\partial U_i}{\partial x_j} = O(\mu) \tag{3.46}$$

The properties of the steady current have thus been defined. We shall start examining waves which are assumed small in amplitude, i.e. the terms with order of (kA) or above may be omitted. On the free surface the exact kinematic boundary condition is:

$$\frac{\partial}{\partial t}(\bar{\zeta} + \zeta) + (U_j + u_j)\frac{\partial}{\partial x_j}(\bar{\zeta} + \zeta) = W + w \quad \text{on } z = \bar{\zeta}+\zeta \tag{3.47}$$

where $\bar{\zeta}$ is time mean surface elevation. Upon linearizing and using the kinematic boundary condition of the steady current at the mean suface

$$W = \frac{\partial \bar{\zeta}}{\partial t} + U_j \frac{\partial \bar{\zeta}}{\partial x_j} \qquad \text{on } z = \bar{\zeta} \tag{3.48}$$

we get the the kinematic boundary for unsteady motion as

$$\frac{\partial \zeta}{\partial t} + U_j\frac{\partial \zeta}{\partial x_j} + u_j \frac{\partial \bar{\zeta}}{\partial x_j} = w + \zeta\frac{\partial W}{\partial z} \tag{3.49}$$

If here we assume that the wave motion can be described by a velocity potential the governing equation is Laplace's equation:

$$\frac{\partial^2 \varphi}{\partial z^2} + \nabla^2\varphi = 0 \qquad -h < z < \zeta+\bar{\zeta} \tag{3.50}$$

where φ is the wave velocity potential, ∇ is horizontal gradient operator. In terms of φ the surface kinematic boundary condition eq. (3.49) can be written in vector form as

$$\frac{\partial \varphi}{\partial z} = \frac{D\zeta}{Dt} + \nabla\varphi\cdot\nabla\zeta + \zeta\,\nabla\cdot\mathbf{U} \tag{3.51}$$

where

$$\frac{D}{Dt} = \left[\frac{\partial}{\partial t} + \mathbf{U} \cdot \nabla\right] \tag{3.52}$$

and $\partial W/\partial z$ is replaced by $\nabla.\mathbf{U}$ according to the continuity condition for the stream.

Now we proceed to derive the dynamic boundary condition. According to Peregrine (1976) the linear equation of motion for small waves with the presence of a current is

$$\frac{\partial \mathbf{u}}{\partial t} + (\mathbf{U}.\nabla)\mathbf{u} + (\mathbf{u}.\nabla)\mathbf{U} + \frac{1}{\rho}\nabla p = 0 \tag{3.53}$$

replacing $\mathbf{u}$ by its potential φ gives

$$\nabla\left(\frac{\partial \varphi}{\partial t} + \mathbf{U}.\nabla\varphi + p\right) = 0 \tag{3.54}$$

Since eq. (3.54) is satisfied over the entire wave field the integrant must be equal to zero and therefore, after substitution of $p=\rho g\zeta$ the dynamic boundary condition is found as

$$\frac{\partial \varphi}{\partial t} + \mathbf{U}.\nabla\varphi + g\zeta = 0 \tag{3.55}$$

or

$$\frac{D\varphi}{Dt} = -g\zeta \tag{3.56}$$

which is the same as that derived by Kirby (1984). It should be pointed out that the term $\mathbf{w}.\mathbf{W}$ which is not necesarily small in the formal expansion if water is deep, has been ignored in the present derivation as well as in all the existing alternative derivations using the variational principle. This means that the equation is more accurate in water of moderate depth or in shallow water. Combining eqs. (3.51) and (3.56) gives

$$\frac{\partial \varphi}{\partial z} = -\frac{1}{g}\frac{D^2\varphi}{Dt^2} + \nabla\varphi.\nabla\bar{\zeta} + \zeta\nabla\cdot\mathbf{U} \tag{3.57}$$

It should be realized that the second term on the right hand side is due to the existence of first order mean surface elevation gradient and the third term which has been ignored by Liu (1983) is important in the satisfaction of wave action conservation as demonstrated by Kirby (1984).

3.3.2 Derivation of the mild-slope equation with wave-current interaction

As it is well known, the mild-slope equation for pure waves is a two dimensional equation with a single variable $\varphi(x_i, 0, t)$ or simply $\Phi(x_i, t)$ as defined by eq. (3.8). By assuming the validity of the separation of variables and a vertical structure for the waves the mild slope equation is the result of vertically integrating the weighted Laplace equation or variational principle with the exact surface boundary condition being satisfied as a natural boundary condition. While this attractive approach is intuitively supported by the exact solution of linear waves on a gently sloping plane beach (Lozano & Meyer, 1976) and also formally demonstrated suitable for pure waves by Smith & Sprinks (1976), it is not easy to adopt the same approach to deal with the wave-current system. The main difficulty is that the vertical structure of waves moving on an arbitrary current is virtually unknown. Rather than dealing with this difficulty directly Booij (1981) in effect avoided it by making use of a modelling method in which he proposed the following relations:

$$\varphi(x_i,z,t)= f(x_i,z)\Phi(x_i,\bar{\zeta},t) \text{ on } -d<z<\bar{\zeta} \tag{3.58}$$

$$f(x_i,z)= \frac{\cosh(\kappa(d+z))}{\cosh(\kappa h)} \quad \text{where } h=d+\bar{\zeta} \tag{3.59}$$

$$\sigma^2 = g\kappa\tanh(\kappa h) \tag{3.60}$$

where σ is called relative frequency defined by

$$\sigma = \omega - \kappa.\mathbf{U} \tag{3.61}$$

and the total depth is

$$h = d+\bar{\zeta} \tag{3.62}$$

Before proceeding with the derivation details it is considered necessary to clarify certain points related to Booij's approach some of which, to the best of the author's kmowledge, have not been given sufficient notice in previous works. Firstly the representation of the vertical structure of waves using a single function like eq. (3.59) is certainly not evident on formal mathematical grounds. Secondly the unknown vector $\boldsymbol{\kappa}$ being introduced in the place of $\mathbf{k}$ was said to be related to the direction of wave propagation, which is true only for the simple refraction case. The fact is that for a complex wave field which can be viewed as the superposition of many component waves moving independently on a non-homogeneous current each component of the waves propagates in different direction and consequently

has a different vertical structure determined by not only the local depth but also the angle between the directions of the individual component wave and the current. Therefore, it should be realized that this approach is of a quite modelling nature and can not be justified by rigorous mathematical reasoning. Its usefulness can be judged by comparing the computational results from the model with available analytical solutions and experimental data.

Following the same proceedure as that by Liu but using eq. (3.57) as the surface boundary condition and neglecting the term with $\nabla\bar{\zeta}$ for the sake of simplicity the final model equation for the velocity potential, $\Phi(x_i,\bar{\zeta},t)$, on the mean surface, $z = \bar{\zeta}$, can be written as

$$\frac{D^2\Phi}{Dt^2} + (\nabla\cdot U)\frac{D\Phi}{Dt} - \nabla\cdot(CC_g\nabla\Phi) + (\sigma^2 - k^2CC_g)\Phi = 0 \tag{3.63}$$

Strictly speaking, in order to derive the above equation we need to assume either that the variation of the current over the horizontal space is of the same order of magnitude as that of the steady water depth or that the current is small compared with the wave celerity. Only under those conditions can the neglect of the terms multiplied by ∇h as well as $\nabla\bar{\zeta}$ be justified.

3.3.3 Derivation of the model equations

Solutions of a steady version of eq. (3.63) have been presented by Booij for some simple 2-D and 3-D cases. But solving such an elliptic equation is so time consuming that it becomes virtually impossible to solve it for large computational areas encountered in most coastal engineering applications. To reduce the computational effort Booij (1981) derived a parabolic approximation and used it for a real engineering case. In spite of the great saving in computational time, the fact that such a model is unable to deal with the effect of reflection makes it unsuitable for general situations. Therefore, to derive a set of transient equations similar to those for pure waves as a general wave-current interaction model seems to be useful due to its time saving ability when compared with the original mild-slope equation and its better accuracy compared with the parabolic approximation. In the following we shall show that this can be done with certain assumptions consistent with the methods used for determining the parameter κ for general applications.

By inserting eq. (3.56) into eq. (3.58) we get an equation identical to that derived by Kirby using the variational method:

$$-g(\frac{\partial \zeta}{\partial t} + \nabla\cdot(\mathbf{U}\zeta)) - \nabla(CC_g\nabla\Phi) + (\sigma^2 - k^2CC_g)\Phi = 0 \qquad (3.64)$$

This equation has two variables ζ and Φ, and it would be closer to our objective if we could eliminate Φ. It is not easy to do this in a wave-current system. With the presence of currents the wave potential $\varphi(=\Phi)$ and surface elevation ζ are related by eq. (3.56) which is a differential equation unlike the case of pure harmonic waves in which an exact algebraic relation between the two exists. However, as shown by Phillips (1977), for simple depth-current refraction we have:

$$\varphi = -\frac{ig}{\sigma}\zeta \qquad (3.65)$$

where σ is relative frequency and related to absolute frequency ω and wave number by

$$\sigma^2 = gk\tanh(kd) \qquad (3.66)$$

$$\omega = \sigma + \mathbf{k}.\mathbf{U}\ , \qquad \text{where} \quad k=|\mathbf{k}| \qquad (3.67)$$

To find both the wave number k and the direction of wave number vector $\mathbf{k}$ eq. (3.67) must be solved in conjunction with the kinematical conservation equation of wave number

$$\mathbf{C_g}.\nabla\mathbf{k} + \nabla\sigma + \nabla(\mathbf{k}.\mathbf{U}) = 0 \qquad (3.68)$$

where $\mathbf{C_g}$ is the group velocity vector. While eqs. (3.67) and (3.68) are valid for the refraction of long-crested, slowly modulated waves they can not be used in complicated situations where both diffraction and reflection are important. As correctly pointed out by Booij (1981), in general wave-current interaction situations k should be regarded as a parameter rather than as the wave number in the conventional sense, since there is no way to determine the exact direction of $\mathbf{k}$. In fact for a cross wave field $\mathbf{k}$ loses its meaning of the wave number and simply becomes a modelling parameter. Some sort of approximate approach must be applied to estimate k. Under such conditions, as suggested by Copeland (1986) and Christofferson (1982), eq. (3.65) may be used to represent the governing equation in terms of ζ only. This approach is exact for the pure wave case and accurate for the simple refraction case but is considered as a reasonable approximation to be consistent with the ways by which the parameter k is estimated. Substituting eq. (3.65) into eq. (3.64) and making use of the periodicity of ζ in time to eliminate Φ gives

$$-(\frac{\partial \zeta}{\partial t} + \nabla.(\mathbf{U}\zeta)) - \nabla(-iCC_g\nabla(\frac{\zeta}{\sigma})) + \frac{(\sigma^2 - k^2CCg)}{\omega\,\sigma}\frac{\partial \zeta}{\partial t} = 0 \qquad (3.69)$$

After combining similar terms

$$\nabla(-iCC_g\nabla(\frac{\zeta}{\sigma}) + \mathbf{U}\zeta) + \lambda\frac{\partial\zeta}{\partial t} = 0 \tag{3.70}$$

where

$$\lambda = 1 - \frac{(\sigma^2 - k^2CC_g)}{\omega\,\sigma} \tag{3.71}$$

If we let $\mathbf{Q} = -iCC_g\,\nabla(\zeta/\sigma)$ where $\mathbf{Q} = (Q_x, Q_y)$ eq. (3.70) can be readily separated into a set of equations in terms of $\mathbf{Q}$ and ζ

$$\nabla\mathbf{Q} + \nabla(\mathbf{U}\zeta) + \lambda\frac{\partial\zeta}{\partial t} = 0 \tag{3.72}$$

$$\frac{\partial\mathbf{Q}}{\partial t} + \omega CC_g\,\nabla(\frac{\zeta}{\sigma}) = 0 \tag{3.73}$$

Note that $\mathbf{Q}$ is in fact related to the horizontal components of particle velocity on the mean surface by

$$\mathbf{Q} = -iCC_g\nabla(\frac{\zeta}{\sigma}) = CC_g/g\nabla\Phi \tag{3.74}$$

The equations (3.72) and (3.73) can be solved either as real equations or as complex equations. Since in many cases the important quantity is ζ, it is convenient to solve them as real equations.

3.4 Numerical Scheme

3.4.1 Grid arrangement and discretization

A rectangular grid mesh is established over the area of interest as shown in Fig. 3.2, where x and y denote the onshore-offshore and longshore directions, respectively. The variables are so arranged on the grid that Q_x and Q_y are defined at the grid edges and ζ as well as other scalar quantities at the grid centres. The advantages of using such a staggered grid system have been discussed by Patankar (1984). Therefore we can see that the shoreline and offshore boundaries are on the lines where only Q_x is defined and lateral boundaries should always coincide with lines of Q_y.

With both the grid system and the variables being so defined we can now write down Eqs(3.72) and (3.73) in a finite difference form which is identical to

that used by Ito & Tanimoto (1972) and Copeland (1985) except for some extra terms due to the effect of the current.

$$\zeta_{ij}^{n+1/2}=\zeta_{ij}^{n-1/2}-\frac{1}{\lambda}\left[\left(U_{i+1,j}\zeta^{*}_{i+1/2,j}-U_{i,j}\zeta^{*}_{i-1/2,j}\right)\right.$$

$$+\left(Q_{x}{}^{n}_{i+1,j}-Q_{x}{}^{n}_{ij}\right)\Delta t/\Delta x$$

$$\left.+\left(Q_{y}{}^{n}_{i,j+1}-Q_{y}{}^{n}_{ij}\right)\Delta t/\Delta y\right] \qquad (3.75)$$

$$Q_{x}{}^{n+1}_{ij}=Q_{x}{}^{n}_{ij}-\omega(CC_{g})_{ij}\left(\frac{\zeta^{n+1/2}_{ij}}{\sigma_{ij}}-\frac{\zeta^{n+1/2}_{i-1,j}}{\sigma_{i-1,j}}\right)\Delta t/\Delta x \qquad (3.76)$$

$$Q_{y}{}^{n+1}_{ij}=Q_{y}{}^{n}_{ij}-\omega(CC_{g})_{ij}\left(\frac{\zeta^{n+1/2}_{ij}}{\sigma_{ij}}-\frac{\zeta^{n+1/2}_{i,j-1}}{\sigma_{i,j-1}}\right)\Delta t/\Delta y \qquad (3.77)$$

where subscripts i and j denote the increments in x and y directions, respectively; n indicates the time level. To ensure that all the terms are exactly centred both in space and in time, ζ^{*} should idealy be calculated at time level n. Unfortunately this is not possible if we want the numerical scheme to be explicitly solvable because of the fact that both $\zeta^{n+1/2}$ and ζ^{n} in one equation are unknown. Therefore, the unknown ζ^{*} which appears in the convection term of eq. (3.75) has to be estimated approximately by using the known values of ζ at the previous time level, n−1/2.

To find values for ζ at grid edges the average of ζ at two neighbouring points is used, i.e.

$$\zeta^{*}_{i+1/2,j}=\frac{1}{2}\left(\zeta^{n-1/2}_{i+1,j}+\zeta^{n-1/2}_{ij}\right) \qquad (3.78)$$

$$\zeta^{*}_{i-1/2,j}=\frac{1}{2}\left(\zeta^{n-1/2}_{ij}+\zeta^{n-1/2}_{i-1,j}\right) \qquad (3.79)$$

The solution procedure is just a straightforward successive substitution. Starting from the offshore boundary with the initial conditions being specified, one can first update ζ using eq. (3.75) and then by substituting the newly found ζ into Eqs. (3.76) and (3.77) Q_x and Q_y can be updated. Repeating the same calculations across all the grid points all values at the internal points can thus be determined. The time taken to reach the steady state varies from problem to problem

depending on the complexity of the bottom topographies, the current form and the boundary conditions employed.

3.4.2 Initial and boundary conditions

For open beach cases the initial conditions chosen are those corresponding to the waves propagating on a plane beach. A sinusoidal wave form is used and the wave height and wave angle can be determined by means of the wave energy conservation principle and Snell's law. If there exists a current the wave action conservation must be used instead of the wave energy conservation principle. This type of calculation is standard and references concerning computational details can be found in Jonsson and Skovgaard (1978). However if there are structures present inside the computational domain it is advantageous to set the area behind the structures as calm sea. This helps to achieve a relatively faster convergence of the solution to the steady state and the results are less prone to the errors caused by the inaccurate boundary conditions at outgoing boundaries.

The specification of boundary conditions is more difficult especially if the current is present at the boundary. It is considered convenient to use a boundary condition similar to that for pure waves so that the propagating waves can be transmitted through the boundary without being reflected back. This is achieved by modifying eqs. (3.35), (3.36) and (3.37). The resulting boundary conditions are

Driving Boundary

$$\frac{\partial}{\partial x}(Q_x - q_x) - \frac{\cos\theta_r}{C}\frac{\sigma}{\omega}\frac{\partial}{\partial t}(Q_x - q_x) = 0 \qquad (3.80)$$

$$\frac{\partial}{\partial y}(Q_y - q_y) - \frac{\sin\theta_r}{C}\frac{\sigma}{\omega}\frac{\partial}{\partial t}(Q_y - q_y) = 0 \qquad (3.81)$$

Transmissive Boundary

$$\frac{\partial Q_x}{\partial x} + \frac{\cos\theta}{C}\frac{\sigma}{\omega}\frac{\partial Q_x}{\partial t} = 0 \qquad (3.82)$$

It can be seen that in eqs. (3.75) - (3.77) the effect of current at the boundary is taken into account by the ratio of the intrinsic frequency σ to the absolute frequency ω.

3.4.3 Determination of the wave height and wave angle

The wave height and angle are calculated in the final period of the entire

integration process, when a steady state is reached after several wave periods have elapsed from the start of the run. Information about ζ, Q_x and Q_y over one complete period is needed for these calculations. For unbroken waves the formulae used for the calculations of wave height and wave angle are, respectively:

wave height

$$H = 2(2\overline{\zeta^2})^{1/2} \tag{3.83}$$

wave angle

$$\theta = \arctan\left(\frac{\overline{Q_y^2}}{\overline{Q_x^2}}\right)^{1/2} \tag{3.84}$$

It should be noticed that eq. (3.83) is exact for both progressive and standing waves as long as there are enough values within one wave period available for calculating the time mean of ζ^2. This requirement should not be confused with the need of having sufficient points within one wave length. The later is a criteria for space resolution in order to ensure overall computational accuracy.

Unlike eq. (3.83) eq. (3.84) is only exact for a progressive wave and can be quite erroneous for points where more than one wave is present. When reflection, especially multi-reflections, become evident, partial standing waves and cross waves will form. At the nodal points of a standing wave the angle of wave propagation can not be determined due to the local absence of wave form (amplitude is zero). Also in the cross wave area the component waves with different amplitudes propagate in different directions which makes it dificult even interpreting the calculated value for the angle by using eq. (3.84) which is bound to be very sensitive to the interference of reflected waves. Therefore, it is physically acceptable instead of seeking the exact local values, to define values averaged over some area. This is, in fact, a more realistic approach when we compare the computational results with measured data since the mathematical sensitivity has not been supported by actual observations in the laboratory (Berkhoff, 1976).

In fact the need for sufficient computational values within each period is not an extra constraint but can be automatically satisfied for most cases. In shallow water, the wave length reduces with decreasing water depth, and it is clear that finer grid resolutions must be used and also finer time increments in order to satisfy Courant's stability criteria. While in deep water, the increase in Δx and Δy

can be offset by the increase in the wave celerity and therefore, Δt must still be kept small.

3.4.4 Breaking criteria

The initiation of wave breaking is the result of various causes. In deep water waves break due to dynamic instability (Phillips, 1977) and in shallow water due mainly to the decrease of water depth which is described as kinematic instability (Thornton, 1982). These well understood facts have been quantitatively described by various formulae, commonly referred to as breaking criteria. The most important one for shoaling water waves was theoretically derived by Miche (1944)

$$\frac{H_b}{L_b} = 0.142 \tanh\left(2\pi \frac{h_b}{L_b}\right) \qquad (3.85)$$

where the subscript b denotes the value at breaking point. This formula has been modified by Le Mehaute and Koh (1967) based on the experimental data for waves breaking over horizontal bottom. The resulting equation was used by Noda (1972), Noda et al (1974) and Birkmeier & Dalrymple (1975). For simple shoaling there are other formula available which give relatively better predictions, such as those proposed by Wiegel (1972), Battjes & Jansson (1978) and Gaughan & Komar (1975). A fundamental problem is that all the above studies and consequently the results are limitied to simple shoaling of waves normally incident upon a plane beach and there is no conclusive evidence to suggest that they are decisively better than the most simple breaking index criterion

$$H = \gamma h \qquad (3.86)$$

where γ is a constant normally taken as 0.8–0.9 for spilling breakers. This is because wave breaking is not solely controlled by the water depth and the wave steepness in deep water. If waves undergo strong refraction and diffraction as well as being acted upon by mean currents, they will break due to the combined effect of dynamic and kinematic instabilities. Until now very little work has been done to quantify the breaking process under such complex conditions. Hudspeth (1972) has studied wave breaking in a following current or an opposing current. The importance of the current lies in its effects in reducing and enhancing the breaking tendency depending on whether the current moves in the same direction with the wave or opposses it. This result is yet to be generalized for the case where the current is at an angle to the waves. On the other hand Watanabe (1986) has made an attempt to model wave breaking near a breakwater. The proposed criteria was used in a circulation model. The results seemed to be very encouraging.

With the all the limitations in mind eq. (3.84) is to be used in the present work just for its simplicity. The breaking index γ is chosen to be 0.88 throughout the breaking zone. The same formula was used by most of previous numerical models.

The implementation of eq. (3.86) in the time dependent model can follow that proposed by Copeland (1985), i.e. in each time increment in the calculation surface elevation is checked locally at each grid point by

$$\left|\zeta_{ij}^{n+1/2}\right| \leq \gamma/2 \cdot h_{ij} \qquad (3.87)$$

Although this method of reducing wave height and, therefore, taking part of the wave energy out of the wave system is simple and attractive, it is not free from flaws. First of all, the breaking process is highly nonlinear and the surface elevation is very irregular. Even when eq. (3.86) is, to some extent, applicable for predicting the breaking height which is less sensitive to the instantaneous surface profile and largely associated with certain time averaged integral quantities, there is no sufficient justification for the application of eq. (3.87). Secondly this method only allows one broken wave to be formed from each unbroken wave which is seldom the case in a surf zone created by spilling breakers. If the calculated crest profile of a wave exceeds the limit set by eq. (3.87) not just at one point in space or time this results in distorted or clipped waves with clearly cut crests which are certainly different from the real breaking and broken waves.

To overcome this difficulty we shall simply use eq. (3.86) to determine the wave height at the breaking point and inside the surf zone while regarding eq. (3.85) just as a means for modelling the dissipation of wave energy due to breaking. This is certainly an empirical approach and predictions obtained from the model should depend on how accurate eq. (3.86) is for the particular problem under consideration.

Finally, for open beach cases the calculation using this model should not proceed beyond a certain predetermined water depth near a shoreline if one does not want to work on exceesively large number of computational grid points and yet keep the grid size uniform. This restriction is not just particularly associated with the present way of solution but also applies to the wave models based on steady state solutions of the mild-slope equation as well (Berkhoff, 1976 and Liang, 1983).

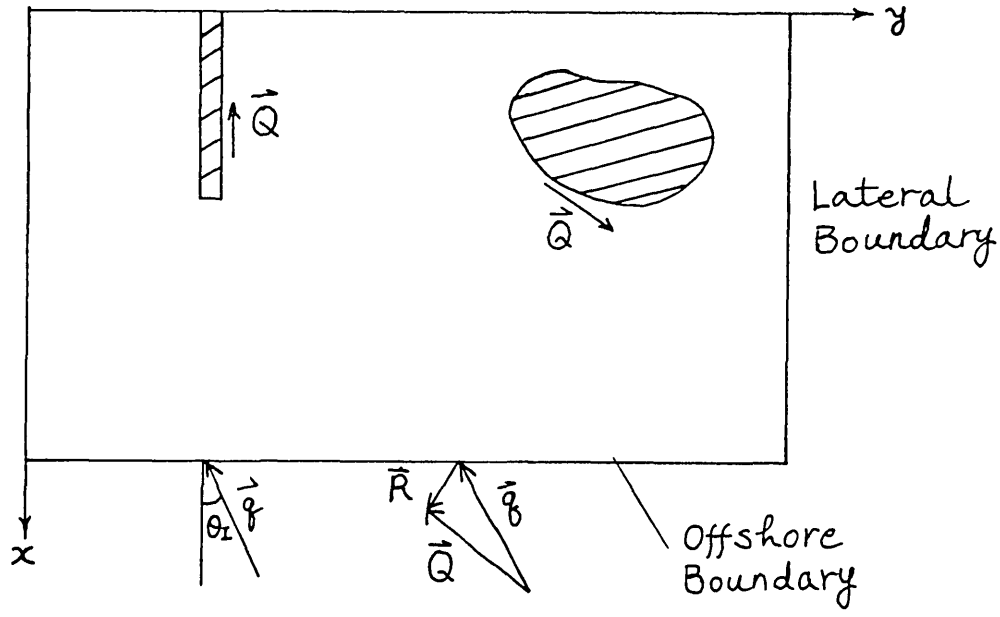


Fig. 3.1 Definition of Vector Variables

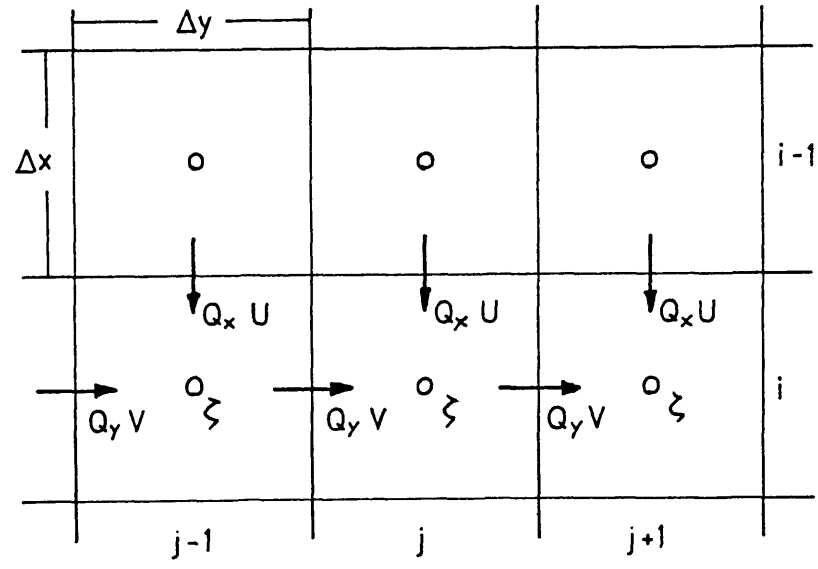


Fig. 3.2 Finite Difference Grid System for the Wave Model

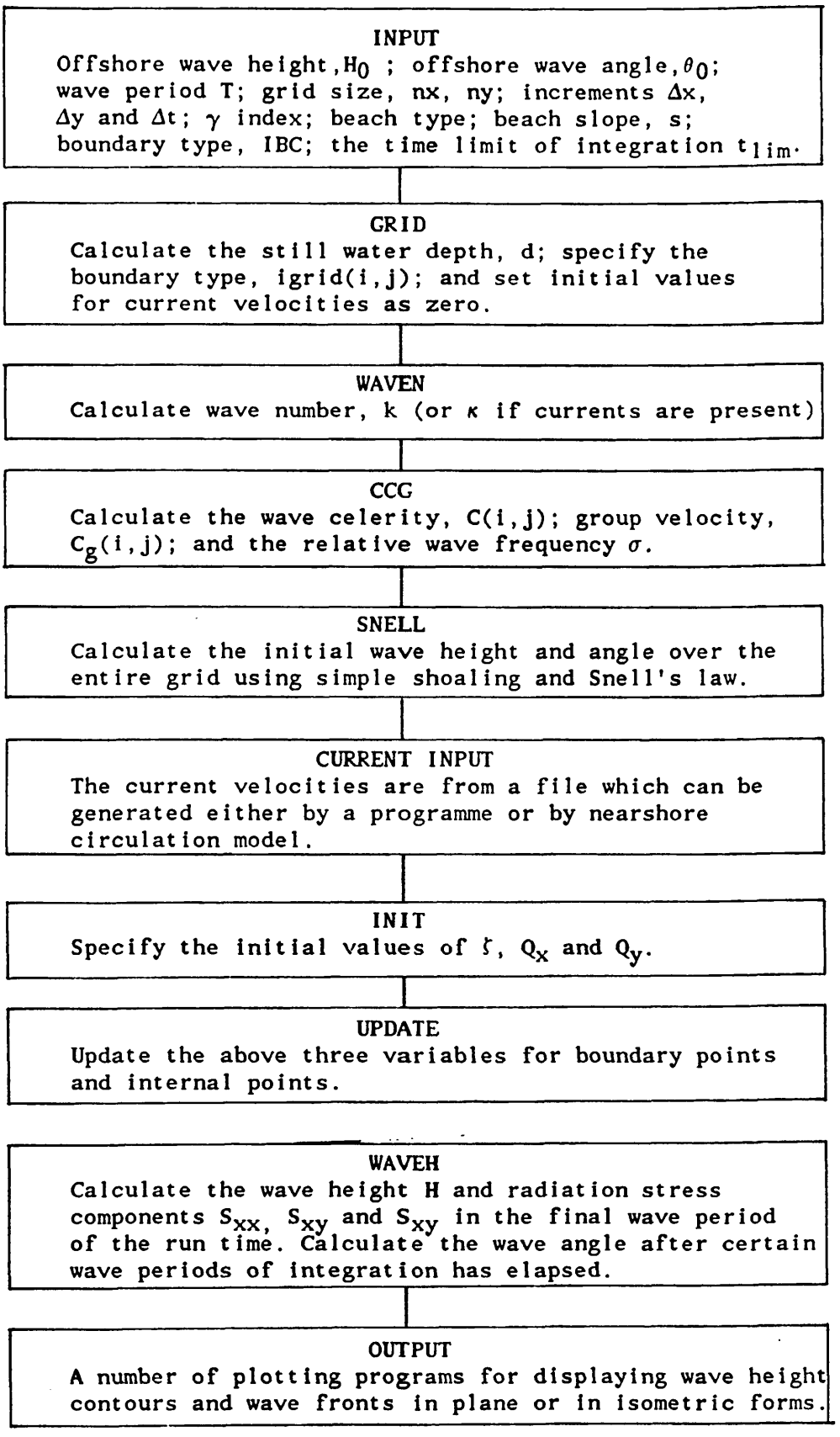


Fig. 3.3 Flow chart for the program MSWAVE

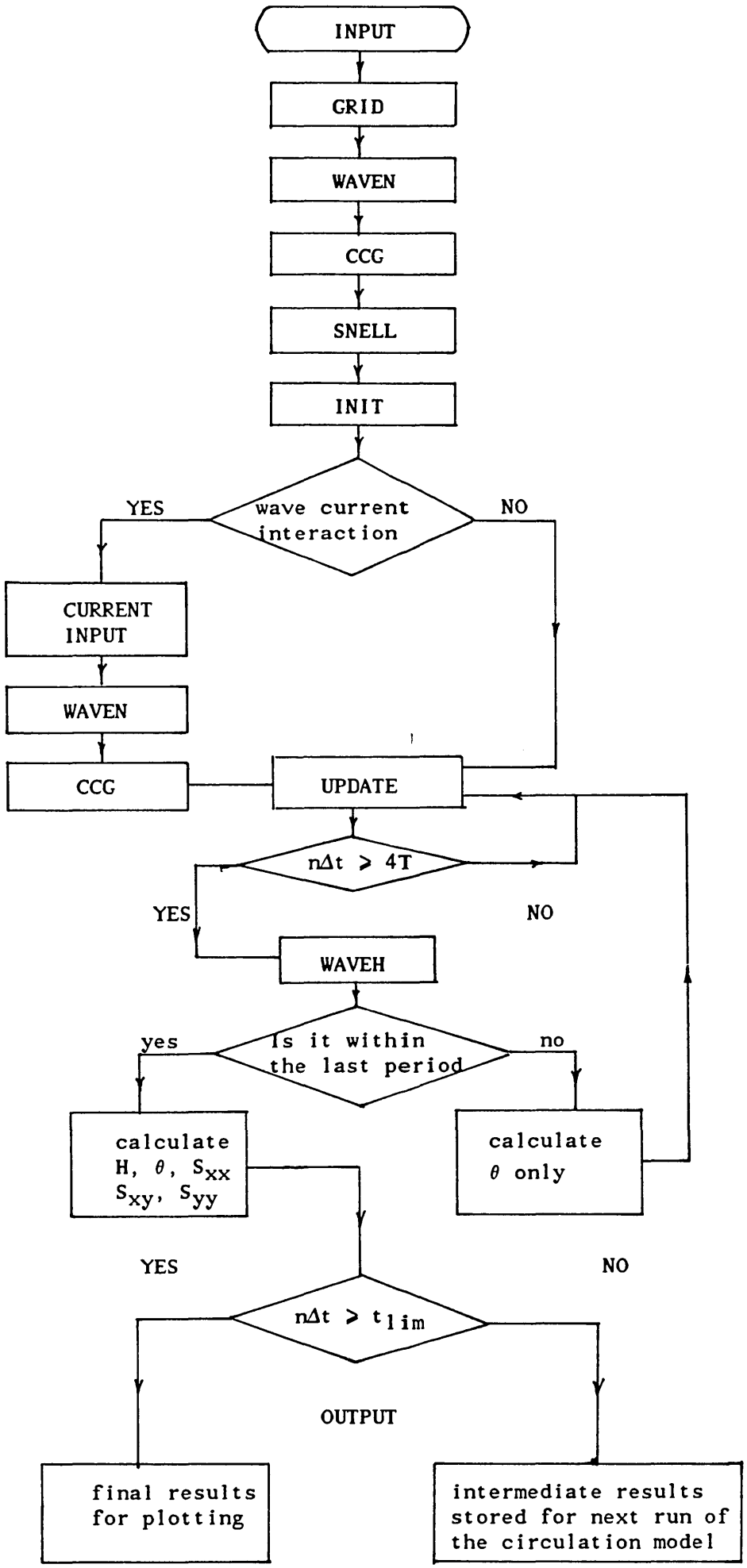


Fig. 3.3 (continued)

CHAPTER. 4
THE GOVERNING EQUATIONS OF CIRCULATION

4.1 Introduction

It has long been recognized that in the nearshore area there exist mean currents which are solely induced by waves. Many laboratory and field measurements have been carried out in order to understand the mechanism of their generation. A number of theories have been proposed for predicting such currents. In this chapter the theoretical aspects of the wave-induced circulation model will be discussed.

The model is based on the time averaged and depth integrated conservation equations of continuity and momentum. The equations are formulated in transient form and solved by integrating in time. The solutions obtained at steady state are the mean velocity and mean surface elevation. Since the detailed derivation of time averaged and depth integrated conservation equations governing wave induced current circulations can be found in numerous references (see, e.g. Phillips, 1977, da Silva Lima, 1981 and Mei, 1982) it is not repeated here. Instead, a discussion of the fundamental assumptions involved in the derivation is presented, some of which have not been fully assessed in many previous works.

The forcing terms found in the governing equations such as radiation stress, bottom friction stress and horizontal mixing are formulated and their roles investigated. Since the circulation model is meant to be applied to most general nearshore situations where complex bottom configuritions may exist, all the wave quantities required will be calculated from the wave model developed in Chapter. 3. The emphasis has been placed on the selection of appropriate formulae which best describe the physical processes involved. The balance between complexity and efficiency is also kept in mind.

The effects of surface stress induced by the wind action and coastal flooding have not been included in order to concentrate on more fundamental processes.

4.2 Governing Equations

The rectangular coordinate system is defined by (x,y,z) which denote the alongshore, inshore-offshore and vertical directions, respectively. Suppose that the instantaneous Eulerian velocity of fluid can be split into the mean velocity vector

(u,v,w) and turbulent velocity (u',v',w') and the mean velocity can once again be split as the time average velocity (U,V,W) which is, as normally assumed, independent of z, and wave obital velocity ($\tilde{u}$,$\tilde{v}$,$\tilde{w}$).

$$\text{total velocity} = (u,v,w) + (u',v',w')$$

$$= (U,V,W) + (\tilde{u},\tilde{v},\tilde{w}) + (u',v',w') \qquad (4.1)$$

The time averaged and depth integrated governing equations are the continuity equation and the momentum equations in the two horizontal directions only which according to Mei (1982), are

continuity equation

$$\frac{\partial \bar{\zeta}}{\partial t} + \frac{\partial}{\partial x}(Uh) + \frac{\partial}{\partial y}(Vh) = 0 \qquad (4.2)$$

x-momemtum equation

$$\frac{\partial}{\partial t}(Uh) + \frac{\partial}{\partial x}(U^2h) + \frac{\partial}{\partial y}(UVh) = -\frac{1}{\rho}\left[\frac{\partial S_{xx}}{\partial x} + \frac{\partial S_{xy}}{\partial y} + \rho g h \frac{\partial \bar{\zeta}}{\partial x}\right] + \frac{1}{\rho}\left[\frac{\partial T_{xx}}{\partial x} + \frac{\partial T_{xy}}{\partial y}\right] - \frac{1}{\rho}\overline{\tau^b_x} \qquad (4.3)$$

y-momentum equation

$$\frac{\partial}{\partial t}(Vh) + \frac{\partial}{\partial x}(VUh) + \frac{\partial}{\partial y}(V^2h) = -\frac{1}{\rho}\left[\frac{\partial S_{xy}}{\partial x} + \frac{\partial S_{yy}}{\partial y} + \rho g h \frac{\partial \bar{\zeta}}{\partial y}\right] + \frac{1}{\rho}\left[\frac{\partial T_{yx}}{\partial x} + \frac{\partial T_{yy}}{\partial y}\right] - \frac{1}{\rho}\overline{\tau^b_y} \qquad (4.4)$$

where h is the mean water depth, (S_{xx}, S_{xy}, S_{yy}) are the radiation stress components, (T_{xx}, T_{xy}, T_{yy}) are the depth integrated Reynolds stress components, τ^b_x and τ^b_y are bottom friction stress components. More explicitly

$$h = d + \bar{\zeta} \qquad (4.5)$$

$$S_{xx} = \overline{\int_{-d}^{\zeta} \{ p + \rho(\tilde{u})^2 \} dz} - \int_{-d}^{\bar{\zeta}} \rho g(\bar{\zeta} - z) dz \qquad (4.6)$$

$$S_{xy} = \overline{\int_{-d}^{\zeta} \rho \tilde{u} \tilde{v} \, dz} \qquad (4.7)$$

$$S_{yy} = \overline{\int_{-d}^{\zeta} (p + \rho(\tilde{v})^2) dz} - \int_{-d}^{\bar{\zeta}} \rho g(\bar{\zeta} - z) dz \qquad (4.8)$$

$$T_{xx} = -\overline{\int_{-d}^{\zeta} \rho(u')^2 dz}, \quad T_{xy} = -\overline{\int_{-d}^{\zeta} \rho(u'v') dz}, \quad T_{yy} = -\overline{\int_{-d}^{\zeta} \rho(v')^2 dz} \qquad (4.9)$$

where d is the steady water depth, p is the pressure and ρ is the density of the water.

In order to derive the governing equations Eqs. (4.2)-(4.4) quite a number of assumptions are made with regard to the flow properties and bottom topography. The most important of these assumptions are

1. wave orbital velocities and turbulent velocities are uncorrelated.
2. the vertical nonuniformity of time mean horizontal velocity is not important.
3. the wave is strictly linear.
4. the water depth varies gradually in the horizontal plane.

The first assumption is fundamental in that it enables treating the radiation stress and turbulent stress separately. If the orbital velocities are large compared with the turbulent velocities Phillips (1977) showed that the interactions between the two motions are extremely weak, which justifies this assumption. However, for waves breaking on beaches some experimental evidence has already suggested that turbulent velocities can be of the same order of magnitude as wave orbital velocities (Sakai et al 1984 and Visser, 1984), therefore, the interaction may not always be negligible. Furthermore, there are practical difficulties in quantifying the possible correlation between wave velocity and current velocity based on experimental data. First of all it is not possible to distinguish the wave motion and turbulent motion accurately. The measured velocities can be very irregular due to wave instability and breaking. Secondly as pointed out by Basco (1983), there is virtually no way to determine the exact temporal averaging time for mean currents. The sensitivity of measured correlations to the averaging interval is not known. Therefore, the currenly adopted theoretical approach to this aspect of nearshore circulation is far from complete.

As it is well known, the non-uniformity of the time averaged horizontal currents over the water depth will lead, in the depth integrated equations, to the dispersion terms which are considered at least as important as the Reynolds stress in

river and tidal flows. Several semi-empirical methods have been proposed to estimate the effect of dispersion terms in numerical models (Kuipers & Vreugdenhil, 1973 and Rastogi & Rodi, 1978). The second assumption has seldom been assessed critically in the context of wave-induced circulation modelling. The reason can be attributed to a generally held belief that the turbulent motion due to wave breaking is so intense that it becomes dominant compared with other diffusive processes and consequently the time averaged current can be regarded as uniform over the water depth to the first order of approximation. The limited field measurements on the vertical distribution of time mean velocities seem not to be conclusive. Meandow (1974) has repored on field measurement of longshore currents which exhibited a fairly uniform distribution from the surface layer to bottom layer. But other meassurements (Shepard & Inman, 1950 and Suno, 1970) have showed that rip currents and general circulations are far from uniform. Based on the present state of knowledge it is difficult to decide conclusively whether or not to include in the depth averaged circulation models the terms due to the vertical nonuniformity of currents. It is, however, quite possible that the dispersion terms become important immediately outside the surfzone where waves do not break and consequently the turbulence is much weaker. Further offshore where the depth increases and the currents become small the effect of nonuniformity is again negligible.

Assumptions 3 and 4 are made specifically for the derivation of Eqs. (4.6)-(4.8). Including higher order terms in wave velocities some extra terms such as mass transport will appear which are not known in general situations. By keeping the bottom slope small the term involving the time mean pressure at the bottom can be neglected. More details can be found in Mei (1982). It should be pointed out here that although the waves are assumed linear they can be quite complex in form.

4.3 Bottom Friction

4.3.1 Formulation

The mean frictional shear stress is commonly defined as the time average of the instantaneous frictional stress at the sea bottom. As first suggested by Longuet-Higgins (1970) it can be related to the instantaneous velocity of flow by a quadratic or Darcy law:

$$(\overline{\tau^b_x}\ ,\ \overline{\tau^b_y}) = \overline{\tau^b} = \rho\, C_f\, \overline{u|u|} \qquad (4.10)$$

where ρ is the fluid density and C_f is the Darcy friction factor. The overbar means

time average. This formula is taken in an analogy to the one found for steady state flows. For the rough boundary layer generated by pure oscillating waves Jonsson (1966) found it performed very well in estimating the maximum shear stress. Writing in terms of component velocities gives

$$(\overline{\tau^b_x} \ , \ \overline{\tau^b_y}) = \rho \ C_f \overline{(U + \tilde{u}) |(U + \tilde{u})|} \tag{4.11}$$

where U is the depth averaged mean velocity vector, $\tilde{u}$ is wave particle velocity vector.

In developing the method for calculating the longshore current Longuet-Higgins (1970a) derived from eq. (4.11) the following expression by making two rather strict assumptions,

(1) the magnitude of the mean current is small in comparison with that of the wave orbital velocity.
(2) the local wave angle normal to the shoreline is very small.

$$\overline{\tau^b_y} = \rho \ C_f \ \overline{|\tilde{u}_b|} V \tag{4.12}$$

where V is depth averaged longshore current, $\tilde{u}_b$ is the wave particle velocity at the bottom. Since $\tilde{u}_b$ is periodic in time it can be shown that

$$\overline{|\tilde{u}_b|} = \frac{2}{\pi} \tilde{u}_{max} \tag{4.13}$$

where $\tilde{u}_{max}$ is the maximum wave particle velocity at bottom. If we are just considering long-crested progressive waves it can then be calculated simply by

$$\tilde{u}_{max} = \frac{\pi H}{T \sinh(kh)} \tag{4.14}$$

wherever there exist reflected waves or cross waves eq. (4.14) is not valid and the more general expression for $\tilde{u}_{max}$ in terms of the variables in the present wave model should be used, see Chaper. 6 for details. Under the same assumptions as those made by Longuet-Higgins but for the two dimensional situation Le Blond & Tang (1974) derived an anisotropic friction stress formula where

$$\tau^b_x = \frac{4\rho C_f}{\pi} \tilde{u}_{max} U \tag{4.15}$$

$$\tau^b_y = \frac{2\rho C_f}{\pi} \tilde{u}_{max} V \tag{4.16}$$

Eqs. (4.15) and (4.16) have been widely used in previous numerical nearshore circulation models such as Noda et al (1974), Birkemeier & Dalrymple (1975) and Sasaki (1975). After showing that most available laboratory and field data rarely satisfy the two assumptions above Liu & Dalrymple (1978) developed an analytical expression for the bottom friction stress which is applicable to any angle of incidence and does not require the mean current being small. Numerical integration is necessary in the calculation. This was incorporated in the models by Ebersole & Dalrymple (1980) and da Silva Lima (1981) and Visser (1984). A relatively simple formulation has been proposed by Sabaton & Hauguel (1979) in which rather than defining the instantaneous bottom shear stress using the instantaneous total velocity the mean shear stress is directly related to mean current velocity and the maximum orbital velocity

$$(\tau^b_x,\ \tau^b_y) = -\frac{\rho g}{C_s^2}(U,\ V)\sqrt{(\overline{U + u_{max}\cos\theta})^2 + (\overline{V + u_{max}\sin\theta})^2}$$

where C_s is taken as a dimensional constant. This method is much easier to use and requires much less time comparing with Liu & Dalrymple's method. The relation between C_f and C_s can be found easily by impossing the two assumptions put forward by Longuet-Higgins (1970) as $Cs = (\pi g/2C_f)^{1/2}$.

The nearshore circulation models presently discussed are two-dimensional. The output of the models is the depth-averaged currents. It is worth pointing out here that there exists an inconsistency due to the use of the depth averaged mean current in eq. (4.11), which has attracted little attention from previous researchers. Since the bottom friction stress is originated from the relative motions between near-bottom flow and the sea bed, it is the wave particle velocities and the mean current velocities at the bottom should be used in eq. (4.11) rather than their depth-averaged values. In general two dimentional situations the depth-averaged velocity can be quite different from the mean velocity near the sea bed both in magnitude and in direction. Even for waves breaking normally on a plane beach when depth averaged velocity is zero the time mean velocity near the bed, so called undertow resulting from wave breaking is not zero and must be locally important in the determination of the frictional stress. This limitation should be borne in mind when deciding which formulae for the bottom friction stress should be used.

4.3.2 Friction factor C_f

The remaining problem is to determine the friction factor C_f to be used in

eq. (4.11). Although extensive studies have led to the standard graph for determining C_f valid for unidirectional steady flow, our knowledge of the boundary layer under the combined action of waves and currents is still quite unsatisfactory and incomplete. Various formulae have been suggested for C_f. Longuet-Higgins (1970) took it as a constant and, after having analyzed the early field and laboratory data, recommended to use a value of the order of 0.01 for longshore current prediction. The same number is used also by Birkemeier & Dalrymple (1976), da Silva Lima (1981) and Copeland (1985).

In fact C_f is not a constant but is dependent upon the flow condition and bed form. The variability of C_f has been reported by Huntley (1976) to be in the range 0.0026–0.0019 much smaller than the standard value 0.01. Indeed Longuet-Higgins later recommended to use 0.005 instead of earlier value 0.01. For a pure wave boundary Jonsson (1966) gave an empirical formulae for the friction factor f_w which is dependent upon the bottom roughness and the boundary layer thickness. It was later recommended by Madsen et al (1978) instead of the constant C_f. However, Grant and Madsen (1978) in a study on the wave-current boundary layer found that the wave friction factor increases with the presence of a mean current. This new insight is very important for any quantitative study of wave-current interaction near a sea bottom boundary but the method itself has yet to be improved so that it may be used in a nearshore circulation model.

Although a number of formulae have been suggested for estimating the friction factor it is still difficult to assess their applicability in general situations. For this reason Liang (1983), Copeland (1985) and Wu & Liu (1985) just used eqs. (4.15) and (4.16) despite the fact that their models were developed for dealing with general situations where the two assumptions put forward by Longuet-Higgins can not hold everywhere.

In this study we shall also use eqs. (4.15) and (4.16) to calculate bottom friction stress and C_f is taken to be 0.005 for most of the cases considered as presented in Chapter 8.

4.4 Horizontal Turbulent Stresses

As shown in Eq (4.9) the integrated Reynolds stress components are expressed in terms of turbulent velocity correlations which are unknown quantities. A hierarchy of turbulence models has been developed so that the stress components can be calculated from known variables. The most commonly used turbulence model is the so called eddy viscosity model proposed originally by Boussinesq (1877) which

assumes that, in analogy to the viscous stresses in laminar flows, the turbulent stresses are proportional to the mean velocity gradient. For general flow situations, this concept may be expressed in a general context as (Rodi, 1980)

$$-\overline{u'_\alpha u'_\beta} = \nu_t \left(\frac{\partial u_\alpha}{\partial x_\beta} + \frac{\partial u_\beta}{\partial x_\alpha} \right) - \frac{2}{3} k\delta_{\alpha\beta} \qquad (4.17)$$

where ν_t is the turbulent or eddy viscosity which, in contrast to the molecular viscosity, is not a fluid property but depends strongly on the state of turbulence; ν_t may significantly vary from one point in the flow to another and also from flow to flow. It is in general also time dependent. u'_α and u_α, as already defined by eq. (4.1), are turbulent velocity and mean unsteady flow velocity tensors in α direction. k is defined as turbulent kinetic energy

$$k = \frac{1}{2}\left[\overline{u'_1}^2 + \overline{u'_2}^2 + \overline{u'_3}^2 \right] \qquad (4.18)$$

and $\delta_{\alpha\beta}$ is the Kroneker delta being 1 for $\alpha=\beta$, and 0 for $\alpha\neq\beta$.

To use eqs. (4.17) and (4.18), which are in three dimensional form, in the present two dimensional problem we can simply substitute $\mathbf{U} + \tilde{\mathbf{u}}$ in place of $\mathbf{u}$ and express T_{xx}, T_{xy} and T_{yy} in terms of the gradients of corresponding components as

$$T_{xx} = 2h\bar{\nu}_t \overline{\left[\frac{\partial(U + \tilde{u})}{\partial x}\right]} - \frac{2}{3} h\bar{k} \qquad (4.19)$$

$$T_{xy} = h\bar{\nu}_t \left\{ \overline{\left[\frac{\partial(U + \tilde{u})}{\partial y}\right]} + \overline{\left[\frac{\partial(V + \tilde{v})}{\partial x}\right]} \right\} \qquad (4.20)$$

$$T_{yy} = 2h\bar{\nu}_t \overline{\left[\frac{\partial(V + \tilde{v})}{\partial y}\right]} - \frac{2}{3} h\bar{k} \qquad (4.21)$$

where $\mathbf{U} = (U,V)$ is depth-averaged mean current velocity, $\bar{\nu}_t$ is time averaged eddy viscosity and $\bar{k}$ is time-depth averaged turbulent kinetic energy. Strictly speaking $\bar{\nu}_t$ is not the same as the time and depth-average of local ν_t values at a particular location in the water column and should be regarded as an equivalent overall modelling parameter.

Since the waves considered are periodic in time and if we assume $\bar{\nu}_t$ is independent of time eqs. (4.19) – (4.21) can be further simplified as

$$T_{xx} = 2h\bar{\nu}_t \frac{\partial U}{\partial x} - \frac{2}{3} h\bar{k} \tag{4.22}$$

$$T_{xy} = h\bar{\nu}_t \left(\frac{\partial U}{\partial y} + \frac{\partial V}{\partial x} \right) \tag{4.23}$$

$$T_{yy} = 2h\bar{\nu}_t \frac{\partial V}{\partial y} - \frac{2}{3} h\bar{k} \tag{4.24}$$

In the case of very simple longshore current patterns, the inshore–offshore component of the depth averaged mean velocity, U, and the gradient of V in the longshore direrction are both zero. The only turbulent stress term remaining is T_{xy} which becomes the same as that used by Longuet-Higgins (1970):

$$T_{xy} = h\bar{\nu}_t \frac{\partial V}{\partial x} \tag{4.25}$$

If a simple algebraic eddy viscosity model is used $\bar{\nu}_t$ is normally parameterized a characteristic length scale l and a by characteristic velocity scale v as

$$\bar{\nu}_t = c_\nu \, l \, v \tag{4.26}$$

in which c_ν is an empirical constant.

Several different closure models for calculating the turbulent mixing can be found in literature. Ebersole & Dalrymple (1980) as well as da Silva Lima (1981) neglected the normal stresses completely and only retained the lateral shear stress in their circulation models. By assuming different eddy viscosities for alongshore and onshore–offshore directions, the following formulae were proposed which, written in terms of the present variables, read

$$T_{xy} = h\nu_x \frac{\partial V}{\partial x} + h\nu_y \frac{\partial U}{\partial y} \tag{4.27}$$

where ν_x and ν_y are the proposed eddy viscosities in x and y directions. ν_x is estimated in a way similar to that by Longuet-Higgins (1970b) but ν_y is assumed to be simply a constant. Eq. (4.27) is slightly different from eq (4.23) in which a single eddy viscosity, $\bar{\nu}_t$, is used for both directions. Clearly the closure employed by them is incomplete since it excludes normal stresses (T_{xx} and T_{yy}) which can be as important as the lateral stress in general circulations. A slightly different closure was used by Copeland (1985) in which separate eddy viscosities were again defined for different directions but included all the stress components:

$$\frac{\partial T_{xx}}{\partial x} = \frac{\partial}{\partial x} \left(h\nu_x \frac{\partial U}{\partial x} \right) \tag{4.28}$$

$$\frac{\partial T_{xy}}{\partial y} = \frac{\partial}{\partial y} \left(h\nu_y \frac{\partial U}{\partial y} \right) \tag{4.29}$$

$$\frac{\partial T_{yx}}{\partial x} = \frac{\partial}{\partial x}\left(h\nu_x \frac{\partial v}{\partial x}\right) \tag{4.30}$$

$$\frac{\partial T_{yy}}{\partial y} = \frac{\partial}{\partial y}\left(h\nu_y \frac{\partial v}{\partial y}\right) \tag{4.31}$$

Comparing with eqs. (4.22) - (4.24), eqs. (4.29) - (4.30) are incomplete due to the neglect of the second order cross-derivatives. This group of expressions is similar to those used by Leendertse et al (1973) for estimating the turbulent mixing in large-scale tidal model except that the eddy viscosity ν_x is used in T_{xx} and T_{xy}, and ν_y in T_{yx} and T_{yy}. Again the arbitrariness is obvious in this type of closure. Since there is no reliable quideline to use for chosing ν_y it was simply taken as a constant being of the order 0.5.

Recently Wu & Liu (1985) presented a finite element model of nearshore circulation in which the turbulent mixing was modelled using eqs. (4.22)-(4.24) without the correction terms involving $\bar{K}$. The eddy viscosity was determined using Longuet-Higgins' expression and the same value was used in both x and y directions. The condition that the turbulence is locally isotropic was implicitly assumed. (Rodi, 1980)

The above discussions have shown the limitations of previous work with regard to the turbulence modelling. Improvements can not be achieved merely by specifying a different algebraic expression for the eddy viscosity. More advanced closure models should be used so that the effect of turbulence transport can be described. For this purpose the standard one equation and two equation models ($k-\epsilon$) have been extended specifically for application inside the breaking zone. Details are presented in Chapter 5.

4.5 Radiation Stresses

4.5.1 Non-breaking waves

The concept of radiation stress was introduced by Longuet-Higgins & Stewart (1960, 1962) in the study of interactions between short waves and long waves and between short waves and steady currents. It is an integral quantity and physically interpreted as the excess momentum flux associated with the wave motion alone. For purely progressive linear waves on uniform depth Longuet-Higgins & Stewart have shown that the forms of radiation stress components as defined by eqs. (4.6)-(4.8) can be simplified to the following expressions

$$S_{xx} = S_{11} \cos^2\theta + S_{22} \sin^2\theta \tag{4.32}$$

$$S_{yy} = S_{11} \sin^2\theta + S_{22} \cos^2\theta \tag{4.33}$$

$$S_{xy} = S_{yx} = S_{11} \sin\theta \cos\theta - S_{22} \cos\theta \sin\theta \tag{4.34}$$

$$S_{ij} = E \begin{vmatrix} \frac{1}{2} + \frac{2kh}{\sinh 2kh} & 0 \\ 0 & \frac{kh}{\sinh 2kh} \end{vmatrix} \tag{4.35}$$

where $E = 1/8\ \rho g H^2$ is the wave energy per unit area, θ is local wave angle, k is the wave number and H is the local wave height. If the water depth is not uniform but slowly varying and waves undergo depth-current refraction only, the waves can be regarded as locally progressive with wave angle θ and wave number being dependent on local depth and current and, therefore, eqs. (4.32)-(4.35) are still applicable. The existence of mean currents does not change the form of radiation stress but its effects are included through the calculation of θ and the new wave number κ.

The radiation stress gradients are commonly referred to as the driving terms in the governing equation of nearshore circulation, eqs. (4.3) and (4.4). But the mere existence of radiation stress gradients does not necessarily result in the net depth-averaged current circulations. If waves only shoal and refract without breaking, the spatial gradients in the radiation stress components are almost exactly balanced by the variation of the mean sea level and no net current can be generated by waves (Longuet-Higgins, 1972). This is because the wave energy (or wave action in the case where a mean current is present) is conserved. However with the inception of breaking this very balance ceases to exist and the resulting differences then act as body forces on the water mass, thus causing the time mean water circulations to occur.

The radiation stress expressions given in eqs. (3.2)-(3.5), although being simple, are limited to refracted waves only and can not be applied to situations where diffraction and reflection are important. General expressions for the radiation stress components have been given in terms of the complex velocity potential present in the steady state version of mild-slope equation by Bettess and Bettess (1982). General radiation stress formulations were also presented by Copeland (1985) in terms of the calculated variables Q_x and Q_y in his transient wave model. His results are also valid for the present case except that the wave number k should be

replaced by κ, which means the current effect can be considered in a way consistent with that followed in solving the wave equations. The expressions to be used are

$$S_{xx} = \overline{Q_x^2}\,\Omega^2 A - \overline{\left[\frac{\partial}{\partial x}(Q_x\Omega) + \frac{\partial}{\partial y}(Q_y\Omega)\right]^2} B$$

$$+ \frac{\partial}{\partial x}\overline{\left\{ Q_x\,\Omega\left[\frac{\partial}{\partial x}(Q_x\Omega) + \frac{\partial}{\partial y}(Q_y\Omega)\right] D\right\}}$$

$$+ \frac{\partial}{\partial y}\overline{\left\{ Q_y\,\Omega\left[\frac{\partial}{\partial x}(Q_x\Omega) + \frac{\partial}{\partial y}(Q_y\Omega)\right] D\right\}} + \frac{1}{2}\rho g\overline{\zeta^2} \qquad (4.36)$$

$$S_{xy} = \overline{Q_x\,Q_y}\,\Omega^2 A \qquad (4.37)$$

where A, B, D and γ are all dependent on k (or κ for the case of wave current interaction) and h only

$$A = \frac{\rho k}{4\sinh^2 kh}(\sin 2kh + 2kh) \qquad (4.38)$$

$$B = \frac{\rho}{4\sinh^2 kh}(\sinh 2kh - 2kh) \qquad (4.39)$$

$$D = \frac{\rho h}{4\sinh^2 kh}\left[\frac{1}{2kh}\sinh 2kh - \cosh 2kh\right] \qquad (4.40)$$

$$\Omega = \frac{C}{C_g} = \frac{2}{1+2kh/\sinh 2kh} \qquad (4.41)$$

a similar expression for Q_{yy} can be easily written down by interchanging x and y everywhere in eq. (4.36). The time average calculation of various terms in eqs. (4.36) and (4.37) follows the same procedure as that used for determining wave height and angle. (see Chapter. 3)

4.5.2 Broken waves

Strictly speaking eqs. (4.36) and (4.37) are only exact for unbroken waves which are harmonic in time. Inside the surf zone the wave forms calculated by imposing breaking criteria may result in unrealistic wave profiles (clipped). This distortion can subsequently cause errors in the calculation of Q_x and Q_y. This is

indeed a severe limitation of the mild–slope equation when applied inside the surf zone, where the radiation stress gradients are the greatest and constitute the main driving force in generating currents. The same limitation is applied to the steady state version of mild–slope equation as well (see, e.g. Liang, 1985).

Therefore, for broken waves an approximate method has to be sought in which the breaking criteria for wave height eq. (3.86) is explicitly used to modify the formulae for radiation stresses. Detailed formulations can be found in Copeland (1986) and are not to be repeated here. It is sufficient to point out here that this approach is based on the assumption that waves retain the form of propagating waves after breaking and therefore, it is accurate for linear progressive broken waves. For general broken waves it can only be regarded as a first order approximation. The reason is simply that the explicit relation between surface elevation ζ and the components of the dummy variable **Q** used in the derivation is exact only for progressive waves on uniform depth and can be a good approximation for the same type of waves propagating over gently sloping bottom when the effects of reflection are absent or negligible. For general broken waves not only the simple relation between **Q** and ζ is invalid the proportionality assumption between the wave height and total water depth is also incorrect, to say the least, the wave height index in eq. (3.86) for progressive waves is very much different from that for standing waves.

CHAPTER. 5
THE MODELLING OF TURBULENT MIXING

5.1 Introduction

As shown in Chapter. 4 in order to describe accurately the effects of turbulent mixing the simple algebraic eddy viscosity approximations, no matter what characteristic length and velocity scales are used, are simply not good enough, since in general circulation cases the diffusion and convection of turbulent quantities can be important, especially in the recirculation area. Some more advanced turbulence models are necessary for this purpose.

This Chapter presents two turbulence transport models, developed specifically for the application inside the breaking zone where turbulent mixing due to breaking is predominant compared with the turbulence generated by the mean velocity shear and the dispersion caused by the nonuniformity of the mean horizontal velocity over the water depth. The first model is commonly called one-equation model in which the kinetic energy of turbulent motion is found by solving a transport equation. In the case of calculating longshore current distribution over a plane beach this model is identical to the one proposed by Battjes (1983). The second model is based on the vertically integrated version of the standard $k-\epsilon$ turbulence model, where k is the kinetic energy and ϵ is the turbulent energy dissipation as shown later on in the text, similar to that proposed by Rastogi and Rodi (1978) except that the role of breaking waves in the production of turbulence is also incorporated as additional model terms.

After the completion of this study an independent work was published by Wind & Vreugdenhil (1986) in which the turbulent mixing effect is also calculated by using the $k-\epsilon$ model and the prediction of rip currents generated by waves in an enclosed wave basin was presented. Although there is agreement between the two models with regard to the general approach to the problem the present study is different in the detailed representation of breaking-induced turbulence production terms in the turbulence transport equations as detailed in Section 5.3.

5.2 Energy Equation for Fluctuating Motions

The exact depth-integrated energy equation for general fluctuating motions including dissipation, has been given by Phillips (1977, p66) which can be applied either to wave motion only, turbulent motion only or the combination of the two.

If it is assumed that $(a/h)^2$ is much smaller than 1, where a is the wave amplitude and h is the mean water depth, and taking also into account the four basic assumptions set forth in Chapter 4, this energy equation can be simplified by separating the contributions from waves and turbulence as

$$\frac{\partial}{\partial t}(E+E_t)+\frac{\partial}{\partial x_i}\{U_i(E+E_t)+(F_i+F_{ti})\}+(S_{ij}+T_{ij})\frac{\partial U_j}{\partial x_i}=-D_t \tag{5.1}$$

where E and E_t are respectively the wave energy and turbulence energy integrated over the entire water depth; F and F_t are the energy fluxes resulting from the wave and turbulent motions, respectively. They are defined in terms of velocity components by

$$E=\rho\int_{-h}^{\zeta}\overline{\frac{1}{2}\{(\tilde{u})^2+(\tilde{v})^2\}}\,dz \tag{5.2}$$

$$E_t=\rho\int_{-h}^{\zeta}\overline{\frac{1}{2}\{(u')^2+(v')^2\}}\,dz \tag{5.3}$$

$$(F_x,\ F_y)=\int_{-h}^{\zeta}\overline{(\tilde{u},\ \tilde{v})\left\{\frac{1}{2}\rho(\tilde{u})^2+\frac{1}{2}\rho(\tilde{v})^2+\rho gz+p\right\}}dz \tag{5.4}$$

$$(F_{tx},\ F_{ty})=\int_{-h}^{\zeta}\overline{(u',\ v')\left\{\frac{1}{2}\rho(u')^2+\frac{1}{2}\rho(v')^2+p'\right\}}dz \tag{5.5}$$

where S_{ij} is the radiation stress tensor and T_{ij} is the Reynolds stress tensor as discussed in Chapter 4. Subscripts i and j take the values of 1 or 2 corresponding to x (offshore) and y (alongshore) components, respectively. D_t is the depth-integrated turbulence energy dissipation of the system. The dissipation due to the bottom shear stress has been neglected since it is considered insignificant outside the surf zone and much smaller than the dissipation due to wave breaking inside the surf zone (Iwata & Sarahawa (1974) and Thornton & Guza, 1986).

Following Visser (1984) we shall introduce a term D_w which denotes the wave energy dissipation due to breaking. Eq. (5.1) can then be separated into two equations which describe the wave motion and turbulent motion, respectively:

energy equation for waves

$$\frac{\partial E}{\partial t} + \frac{\partial}{\partial x_i}\{EU_i+F_i\} + S_{ij}\frac{\partial U_j}{\partial x_i} = -D_w \qquad (5.6)$$

energy equation for turbulence

$$\frac{\partial E_t}{\partial t} + \frac{\partial}{\partial x_i}\{E_tU_i+F_{ti}\} + T_{ij}\frac{\partial U_j}{\partial x_i} = D_w - D_t \qquad (5.7)$$

Clearly, the term D_w in eq. (5.7) acts as an extra turbulence production term originated from wave breaking. It has different values depending on the conditions of breaking. Outside the surf zone waves do not break and the dissipation due to other reasons can be regarded negligible, therefore, D_w must be zero. Inside the surf zone due to wave breaking part of the wave energy will be transfered to irregular turbulent motions and ultimately dissipate into heat, which results in a non-zero D_w. Consequently, eqs. (5.6) and (5.7) are, in general, coupled through D_w. This means that in order to calculate the turbulent energy the wave dissipation D_w must be determined beforehand.

Apparently eqs. (5.6) and (5.7) are both depth-integrated equations and very similar in form but quite different methods for solving each one are required. Eq. (5.6) is a wave equation in which wave energy and energy flux can be estimated by choosing a suitable wave theory and, therefore, the only unknown variable is the dissipation term D_w. On the contrary in eq. (5.7) none of the terms involved, except D_w which comes from the wave energy equation, can be regarded as known. Consequently a certain closure model should be used in order to calculate E_t. As is shown later, this can actually be done in a number of ways.

Eqs. (5.6) and (5.7) are the most general energy equations since, apart from the small amplitude assumption they do not impose any other restrictions either on the wave form or on the structure of turbulence. In particular, if we are to deal with progressive waves only, a simple relation exists between wave energy and energy flux (Phillips, 1977)

$$(F_x, F_y) = E(C_{gx}, C_{gy}) \qquad (5.8)$$

where $(C_{gx}, C_{gy}) = (C_g\cos\theta, C_g\sin\theta)$ and E and C_g are defined by eqs. (4.35) and (3.7). Substituting eq. (5.8) into eq. (5.6) gives

$$\frac{\partial E}{\partial t} + \frac{\partial}{\partial x_i}\{E(U_i+C_{gi})\} + S_{ij}\frac{\partial U_j}{\partial x_i} = -D_w \qquad (5.9)$$

which is equivalent to the wave action conservation equation when applied to

nonbreaking waves when D_w is zero (Bretherton and Garrett, 1968). Eq. (5.9) was used by Visser (1984) in his longshore current model and by Wind & Vreugdenhil (1986) for the calculation of wave-induced circulation in a physical model basin. It should be pointed out that for the later case eq. (5.9) can only be considered approximately applicable since the waves near the side walls of their experimental basin were not propagating waves but partial standing waves.

In the following sections, a one-equation turbulence model will firstly be presented. Its original form is due to Battjes (1983) except for the convection terms which were not present in the original formulation have also been included in this model. A two equation turbulence model which forms the essential part of this chapter is then presented. Different ways to construct the model form of dissipation equation are discussed. With regard to the calculation of the wave dissipation D_w the general expressions for the energy flux components, F_x and F_y in terms of the variables in the present wave model are derived so that the method is suitable for both propagating wave and standing wave fields. Finally the boundary conditions which are required for solving turbulent equations are summarized and discussed.

5.3 One-Equation Model

5.3.1 Conventional turbulent energy equation and its model form

In order to overcome the limitations associated with the simple algebraic eddy viscosity model, more general turbulence models were developed in many branches of applied fluid mechanics. These turbulence models take into account the transport of turbulence quantities by solving differential transport equations (Launder & Spalding, 1972). It has been argued that if the velocity fluctuations are to be characterized by one scale, the physically most meaningful scale is $\sqrt{k}$, where k is the kinetic energy of turbulent motion per unit mass. The starting point is the exact turbulent energy equation without buoyancy, see e.g. Rodi(1980)

$$\frac{\partial k}{\partial t} + U_\alpha \frac{\partial k}{\partial x_\alpha} = \frac{\partial}{\partial x_\alpha} u'_\alpha \left[\frac{u'_\alpha u'_\beta}{2} + \frac{p}{\rho} \right] - u'_\alpha u'_\beta \frac{\partial U_\alpha}{\partial x_\beta} - \nu \frac{\partial u'_\alpha}{\partial x_\beta} \frac{\partial u'_\alpha}{\partial x_\beta} \qquad (5.10)$$

where α and β are 3-D tensor subscripts, ν is molecular viscosity. Eq. (5.10) can not be used to build a turbulence model because the unknown turbulence correlations appear in the first and third terms on its RHS which are commonly called diffusion and dissipation terms. This closure problem can be solved by making some reasonable model assumptions. The commonly used modelling

approaches for the k–equation assume

$$u'_\alpha \left[\frac{u'_\alpha u'_\beta}{2} + \frac{p}{\rho} \right] = \frac{\nu_t}{\sigma_k} \frac{\partial k}{\partial x_\alpha} \tag{5.11}$$

$$\epsilon = - \nu \frac{\partial u'_\alpha}{\partial x_\beta} \frac{\partial u'_\alpha}{\partial x_\beta} = c_D \frac{k^{3/2}}{L} \tag{5.12}$$

where σ_k and c_D are empirical coefficients, L is a characteristic length scale of turbulent motion and normally assumed to be independent of time. Inserting eqs. (5.11) and (5.12) into eq(5.10) together with the definition for shear stress components

$$-u'_\alpha u'_\beta = \nu_t \left[\frac{\partial U_\alpha}{\partial x_\beta} + \frac{\partial U_\beta}{\partial x_\alpha} \right] - \frac{2}{3} k \delta_{\alpha\beta} \tag{5.13}$$

the complete turbulent energy equation of model form can thus be written as

$$\frac{\partial k}{\partial t} + U_\alpha \frac{\partial k}{\partial x_\alpha} = \frac{\partial}{\partial x_\alpha} \left[\frac{\nu_t}{\sigma_k} \frac{\partial k}{\partial x_\alpha} \right] + \nu_t \left[\frac{\partial U_\alpha}{\partial x_\beta} + \frac{\partial U_\beta}{\partial x_\alpha} \right] \frac{\partial U_\alpha}{\partial x_\beta}$$

$$- c_D \frac{k^{3/2}}{L} \tag{5.14}$$

Strictly speaking, the above equation should be applied per unit mass of 3–D or exact 2–D flows since the model assumptions are expected to be valid only locally. However, as demonstrated by Rastogi & Rodi (1978), the same turbulence energy equation can also be used in depth–averaged calculations where the turbulent stress terms appear in the depth–averaged equations of motion. In a river flow case both 3–D and 2–D computations were performed by them and good agreement between the two was found. Therefore it is considered reasonable to follow a similar approach in order to develop a depth–averaged modelled energy equation particularly applicable inside the surf zone where the turbulent energy is not only produced by shear, but also by wave breaking.

5.3.2 Depth–averaged model equation of turbulent energy inside the surf zone

Examining eq. (5.7) let $\bar{k}$ denote the depth–averaged turbulent energy and one has

$$E_t = \rho \bar{k} h \tag{5.15}$$

Assuming that the depth integrated diffusion term F_t and dissipation term D_t can

be modelled in a similar manner as eqs. (5.11) and (5.12)

$$F_{ti} = \rho \frac{\bar{\nu}_t}{\sigma_k} \frac{\partial \bar{k}}{\partial x_i} h \tag{5.16}$$

$$D_t = c_D \rho \frac{\bar{k}^{3/2}}{L_m} h \tag{5.17}$$

in which the overbar denotes the time and depth averaged quantities, L_m is the length scale which is not neccessarily the same as L. For the sake of easy comparison P_w is introduced to denote the depth averaged value of turbulence production by wave breaking per unit mass

$$P_w = \frac{1}{h} \frac{D_w}{\rho} \tag{5.18}$$

Inserting eqs. (5.15)-(5.18) into eq. (5.7) gives the model equation for the depth-integrated turbulence energy transport.

$$\frac{\partial \bar{k}h}{\partial t} + U \frac{\partial \bar{k}h}{\partial x} + V \frac{\partial \bar{k}h}{\partial y} = \frac{\partial}{\partial x}\left[\frac{\bar{\nu}_t}{\sigma_k} h \frac{\partial \bar{k}}{\partial x}\right] + \frac{\partial}{\partial y}\left[\frac{\bar{\nu}_t}{\sigma_k} h \frac{\partial \bar{k}}{\partial y}\right] + (P_h + P_w - c_D \frac{\bar{k}^{3/2}}{L_m})h \tag{5.19}$$

in which the turbulence production by shear, P_h, and eddy viscocity $\bar{\nu}_t$ are represented, respectively, by

$$P_h = \bar{\nu}_t \left[2 \left[\frac{\partial U}{\partial x}\right]^2 + 2 \left[\frac{\partial V}{\partial y}\right]^2 + \left[\frac{\partial U}{\partial y} + \frac{\partial V}{\partial x}\right]^2 \right] \tag{5.20}$$

$$\bar{\nu}_t = c_{\mu 1} \sqrt{(\bar{k})}\, L_m \tag{5.21}$$

All the turbulent velocity correlations have now been related to the turbulent energy and mean velocity gradients. The remaining problems are the determination of the characteristic length scale L_m, constants $c_{\mu 1}$ and c_D as well as D_w. As D_w also appears in the two-equation model it will be discussed later on in Section 5.5.

5.3.3 The length scale L_m and coefficients $c_{\mu 1}$, c_D

In the context of developing simple algebraic eddy viscosity models several length scales have been proposed. Longuet-Higgins (1970), in establishing his longshore current model, postulated that the local length scale should be proportional to the distance to the shoreline. Thornton (1970) used horizontal

distance of wave orbital motion at the bottom instead. Considering the same situation but concentrating on the structure of turbulence Battjes (1975) argued that the development of large turbulent eddies is effectively limited by the vertical distance of flow domain rather than the horizontal distance. The closest possible characteristic length scale was suggested to be proportional to the local water depth, h. This assumption of local dependence, although quite reasonable for simple longshore current situation, may not be equally valid in a more complex flow field. Nevertheless, it is used here and its adequacy will be checked by comparing the results obtained by using the two equation model. The difficulty in determining L_m has been, at least in theory, overcome altogether in the k-ϵ model.
With

$$L_m \propto h \tag{5.22}$$

the eddy viscosity becomes

$$\bar{\nu}_t = c_{\mu 1} \sqrt{(\bar{k})}\, h \tag{5.23}$$

where $c_{\mu 1}$ is a proportional constant. In the case of shear induced turbulence the values recommended for σ_k, $c_{\mu 1}$ and c_D (Launder & Spalding, 1972) are

$$c_{\mu 1}\, c_D \approx 0.08 \qquad\qquad \sigma_k \approx 1 \tag{5.24}$$

which implies that it is not the individual values of the constants $c_{\mu 1}$ and c_D that are important but only their product. Due to the difference in the origin of turbulence between shear flows and breaking waves eq. (5.24) can not be expected to hold true here. In fact by using Battjes' one equation model for turbulence energy in longshore current computation Visser (1984) found that with c_D fixed as 1.0, $c_{\mu 1}$ (his notation is M) in the range 2.5-3.0 gave the best fit with his experimental data on longshore currents, which leads to

$$c_{\mu 1} c_D = 2.5\text{-}3.0 \tag{5.25}$$

The reason for such a large discrepancy in the product of the coefficients from the 'standard values' found elsewhere is not very clear. It may be argued that the turbulent mixing due to wave breaking is much stronger than that originating from conventional shear flows and therefore needs a greater $\bar{\nu}_t$ or $c_{\mu 1}$. But this effect on $\bar{\nu}_t$ would have been implicitly taken into account by a greater value of k. The only explanation is that the length scale should be much greater than water depth h. As it will be shown in Chapter 8 the value of $c_{\mu 1}$ as great as 8.0 is required in order to achieve the mixing level equivalent to P $\approx$ 0.4 in Longuet-Higgins' analytical model. But for laboratory scale the $c_{\mu 1}$ value found by

Visser (1984) is adequate. In the present study the values 2.5, 1.0 and 1.0 will be used for $c_{\mu 1}$, c_D and σ_k, respectively in da Silva Lima's sinusoidal beach case.

5.4 Two-Equation Model

5.4.1 The model equations

It has been the experience of many early modellers who used the one-equation turbulence model that the one-equation model is not much better than a simple algebraic eddy viscosity model in the computation of general turbulent flows with strong recirculations. The same is true for the present application. As long as appropriate coefficients are used, any algebraic eddy viscosity model is as good as a one-equation model as far as the mean velocity prediction is concerned. The difficulty lies with specifying an appropriate length scale. To overcome this difficulty a depth-averaged two-equation model has been developed by the author in which both the turbulence kinetic energy $\bar{k}$ and the rate of dissipation $\bar{\epsilon}$ are found by solving a pair of coupled transport equations. The derivation of depth-averaged equations for $\bar{k}$ and $\bar{\epsilon}$ is similar to that used in the one-equation model except that more terms have to be modelled.

The model turbulence kinetic energy equation reads as

$$\frac{\partial \bar{k}h}{\partial t} + U\frac{\partial \bar{k}h}{\partial x} + V\frac{\partial \bar{k}h}{\partial y} = \frac{\partial}{\partial x}\left[\frac{\bar{\nu}_t}{\sigma_k} h\frac{\partial \bar{k}}{\partial x}\right] + \frac{\partial}{\partial y}\left[\frac{\bar{\nu}_t}{\sigma_k} h\frac{\partial \bar{k}}{\partial y}\right] + (P_h + P_w - \bar{\epsilon})h \qquad (5.26)$$

which is almost the same as eq. (5.18) except that here the dissipation term appears in its original form rather its model form. $\bar{\epsilon}$ is to be determined by adding another equation. The need to determine a length scale using algebraic means is, therefore, eliminated.

The corresponding model dissipation equation is proposed as

$$\frac{\partial \bar{\epsilon}h}{\partial t} + U\frac{\partial \bar{\epsilon}h}{\partial x} + V\frac{\partial \bar{\epsilon}h}{\partial y} = \frac{\partial}{\partial x}\left[\frac{\bar{\nu}_t}{\sigma_\epsilon} h\frac{\partial \bar{\epsilon}}{\partial x}\right] + \frac{\partial}{\partial y}\left[\frac{\bar{\nu}_t}{\sigma_\epsilon} h\frac{\partial \bar{\epsilon}}{\partial y}\right] + \left(c_1\frac{\bar{\epsilon}}{\bar{k}} P_h + P_\epsilon - c_2\frac{\bar{\epsilon}^2}{\bar{k}}\right)h \qquad (5.27)$$

which closely resembles the ϵ-equation given by Rastogi & Rodi (1978) apart from an extra source term P_ϵ which is necessary in order to increase $\bar{\epsilon}$ to balance the

local increase in $\bar{K}$ due to wave breaking.

The eddy viscosity for this model is likewisely defined as

$$\bar{\nu}_t = c_{\mu 2} \frac{\bar{k}^2}{\bar{\epsilon}} \tag{5.28}$$

In eqs. (5.26) - (5.28) $c_{\mu 2}$, σ_k , σ_ϵ , c_1 and c_2 are empirical coefficients. It should be noted that not all the coefficients are independent. One important feature found in many previous studies using the exact k-ϵ equation is that these coefficients are to a certain extent insensitive to the type of turbulent flows examined so long as the turbulent characteristics are similar. The recommended values are (Rodi, 1980)

$c_{\mu 2}$	σ_k	σ_ϵ	c_1	c_2
0.09	1.0	1.3	1.44	1.92

In the present application turbulence is mainly generated by breaking waves, hence it would be reasonable to suggest that it should have different structures compared with that induced by mean shear alone. Also it is the depth averaged turbulence properties that we are concerned with and, therefore, the constants applicable to the 3-D equations, when used in the depth averaged equations, can not be expected to give as accurate results. Nevertheless, this set of constants, except $c_{\mu 2}$ which must be related to $c_{\mu 1}$ as shown later, will be used in this work for the following two reasons:

1) the insufficient quantitative knowledge of turbulence structure in the surf zone makes it difficult to recommend any alterations in the values;

2) Sakai & Battjes (1982) have suggested that the breaking induced turbulence has a structure resembling that of a turbulent wake. Therefore, this set of constants, proved applicable for general turbulent wakes, should be regarded as reasonable estimates in the present case;

5.4.2 Determination of P_ϵ and $c_{\mu 2}$

Unlike P_w which can be calculated by solving the wave energy equation the determination of P_ϵ is not easy. Certainly P_ϵ should somehow depend on P_w but the exact form of dependence is not known. As a start it would be informative

and reasonable to propose a linear relation between P_ϵ and P_w. Since the wave field and topographic features can be characterized to a certain extent by the wave celerity and water depth, the simplest possible expression could be taken as

$$P_\epsilon = c_b P_w \frac{C}{h} \tag{5.29}$$

where c_b is a coefficient and can be determined by analysing certain extreme situations for which the eqs. (5.26) and (5.27) can be greatly simplified due to the absence of a number of terms. Understandably, more elaborate forms of dependence for P_ϵ can be proposed. This will be discussed later with reference to a similar two-equation model by Wind & Vreugdenhil (1986)

To determine c_b, the particular case considered is normally incident waves propagating forwards and eventually breaking on a plane beach. In this situation the convection and diffusion terms as well as the production term by shear in eqs. (5.26) and (5.27) must vanish since the mean velocities are zero. This can be regarded as a local equilibrium condition in a depth averaged sense. The reduced turbulence equations are

$$(P_w)_e - \bar{\epsilon}_e = 0 \tag{5.30}$$

$$(P_\epsilon)_e - c_2 \frac{\bar{\epsilon}_e^2}{\bar{k}_e} = 0 \tag{5.31}$$

in which subscript e denotes the values of turbulence energy and dissipation at equilibrium state. Eq. (5.30) simply states that under local equilibrium condition the turbulent energy production is exactly balanced by the energy dissipation rate. Previously Battjes (1975) assumed this balance in order to derive the expression for eddy viscosity in his zero equation turbulence model for the computation of longshore currents. Inserting eqs. (5.29) and (5.30) into (5.31) gives

$$c_b P_w \frac{C}{h} - c_2 \frac{P_w^2}{\bar{k}_e} = 0 \tag{5.32}$$

or

$$c_b = c_2 \frac{h}{C} \frac{P_w}{\bar{k}_e} \tag{5.33}$$

Under the present local equilibrium condition, the same expression for the dissipation rate $\bar{\epsilon}$, in terms of $\bar{k}$, and the same length scale used in the one

equation model as an approximation for general flow computations can be regarded as exact, i.e.

$$\bar{\epsilon}_e = c_D \frac{\bar{k}_e^{3/2}}{h} \tag{5.34}$$

by taking $c_D = 1$ eq. (5.34) and eq. (5.30) should give

$$\bar{k}_e = ((P_w)_e \; h)^{2/3} \tag{5.35}$$

Substitution of eq. (5.35) into eq. (5.33) gives

$$c_b = c_2 \left(\frac{h}{C}\right)^{1/3} P_w^{1/3} \tag{5.36}$$

For normal incident waves breaking on a plane beach of mild slope Battjes (1975) derived, by using the linear wave expression for the energy flux and the breaking index, the expression for the wave energy dissipation as

$$D_w = \frac{5\gamma^2}{16} \rho \; g^{3/2} \; h^{3/2} \; s \tag{5.37}$$

where γ is the breaking index and s is sea bed slope. Using eqs. (5.31) and (5.18) and the shallow water approximation for wave celerity $C = \sqrt{(gh)}$ we get from eq. (5.36)

$$c_b = c_2 \gamma \left[\frac{5}{16} s\right]^{1/3} \tag{5.38}$$

This completes the derivation of an expression for c_b and the construction of this two equation model. To get some idea about the magnitude of c_b it is assumed that typical values of the input parameters are $\gamma = 0.8$, $s = 0.025$ and $c_2 = 1.92$. The resulting value for c_b from eq. (5.38) is about 0.3.

Different expressions for P_w and P_ϵ have been reported recently by Wind & Vreugdenhil (1986) in their independent study using a similar depth-averaged $k-\epsilon$ turbulence model. Their expressions can be written, with the notations used in this thesis, as

$$P_w = \frac{c_{\mu 2}}{c_{\mu 1}} \left[\frac{D_w}{\rho}\right] \frac{1}{h} \tag{5.39}$$

$$P_\epsilon = c_2 \left[\frac{c_{\mu 2}}{c_{\mu 1}}\right]^2 \left[\frac{D_w}{\rho}\right]^{4/3} \frac{1}{h^2} \tag{5.40}$$

Eq. (5.39) is very similar to eq. (5.18) apart from the eddy viscosity ratio term, which, according to the present derivation, should not present. The expressions of P_ϵ are markedly different in form as inspection of eqs. (5.40) and (5.29) reveals. It is observed that in order to derive eq. (5.40) Wind & Vreugdenhil used the following relations

$$\bar{k} = \left[\frac{D_w}{\rho h}\right]^{2/3} \tag{5.41}$$

and

$$\bar{\nu}_t = c_{\mu 1}\, h \left[\frac{D_w}{\rho}\right]^{1/3} \tag{5.42}$$

It should be realized that the above two expressions are not the generally valid formula but only valid for a local equilibrium situation. The use of these expressions to derive the expression for P_ϵ is, therefore, just another modelling approach. The reason why it is necessary to employ some kind of modelling approach for a term like P_ϵ is simply because there is no generally valid expression for it. The present approach is similar to the method used by Rastogi & Rodi (1978) for finding the expression for the dispersion terms.

To explore the alternative representations further we can choose $(P_w h)^{1/3}$ and h as the velocity and length scales in the dimensional analysis, the appropriate form for P_ϵ taken as

$$P_\epsilon = c_r \frac{(P_w h)^{4/3}}{h^2} = c_r \left[\frac{D_w}{\rho}\right]^{4/3} \frac{1}{h^2} \tag{5.43}$$

where c_r is taken as a proportional constant. To determine c_r we should once again examinine the local equilibrium case. Inserting eq. (5.37), (5.26) and (5.32) into eq. (5.28) yields

$$c_r = c_2 \tag{5.44}$$

so that

$$P_\epsilon = c_2 \frac{P_w^{4/3}}{h^2} \tag{5.45}$$

Interestingly, eq. (5.45) is almost the same as eq. (5.40) which is given by Wind & Vreugdenhil (1986) except for the term involving the ratio between $c_{\mu 1}$ and $c_{\mu 2}$ which has now disappeared. This difference is due to the particular approach used

by Wind & Vreugdenhil. At present without detailed experimental data on turbulent quantities it is still difficult to tell which one of these two models is superior.

Before proceeding into the next section it is necessary to determine the conditions under which the eddy viscosities calculated from the one-equation model, eq. (5.26), and the two equation model, eq. (5.45) are the same in the case of local equilibrium state. As described by Rodi (1980), $c_{\mu 2}$ is conventionally determined by considering the balance between the production by shear and the dissipation in the turbulence equation for the local equilibrium state. Measurements of turbulent energy and velocity correlations are usually needed. Here the problem is somewhat different and the balance is between the production by breaking and dissipation. Inserting eq. (5.35) into eq. (5.23) and eqs. (5.30) and (5.35) into eq. (5.28) gives

$$\bar{\nu}_t = c_{\mu 1}(P_w h)^{1/3} h \tag{5.46}$$

$$\bar{\nu}_t = c_{\mu 2} \frac{(P_w h)^{4/3}}{P_w} \tag{5.47}$$

Clearly to ensure identical $\bar{\nu}_t$ we must have

$$c_{\mu 1} = c_{\mu 2}$$

In all the later computations both $c_{\mu 1}$ and $c_{\mu 2}$ are assumed to be 2.5.

5.5 Determination of Turbulence Production by Breaking Waves

5.5.1 General expression for F (F_x, F_y)

The need for a general expression for F applicable to linear waves with an arbitrary surface form is not just limited to the present problem of calculating the wave energy dissipation in the surf zone, but it is also useful in the study of the mean surface variation related to complex nonbreaking waves.

In order to simplify the expressions in the following derivations the relevant terms in eq. (5.4) are defined as

$$I_u = \overline{\int_{-h}^{\zeta} \rho \tilde{u}^3 \, dz} \tag{5.48}$$

$$I_v = \overline{\int_{-h}^{\zeta} \rho \tilde{v}^3 dz} \tag{5.49}$$

$$I_{uv} = \overline{\int_{-h}^{\zeta} \rho \tilde{u}\tilde{v}^2 dz} \tag{5.50}$$

$$I_{vu} = \overline{\int_{-h}^{\zeta} \rho \tilde{v}\tilde{u}^2 dz} \tag{5.51}$$

$$I_{us} = \overline{\int_{-h}^{\zeta} \tilde{u}\, \rho g z\, dz} \tag{5.52}$$

$$I_{vs} = \overline{\int_{-h}^{\zeta} \tilde{v}\, \rho g z\, dz} \tag{5.53}$$

$$I_{up} = \overline{\int_{-h}^{\zeta} \tilde{u}p\, dz} \tag{5.54}$$

$$I_{vp} = \overline{\int_{-h}^{\zeta} \tilde{v}p\, dz} \tag{5.55}$$

Since the wave is periodic in time, the terms I_u, I_v, I_{us}, I_{vs}, I_{uv} and I_{vu} must be zero, correct to the third order of wave amplitude. The remaining non-zero contributions to F_i come from the correlation between the velocity and presure I_{up} and I_{vp}. The physical meaning is that the part of momentum flux that is associated with the wave particle velocity, when averaged over a full period, should vanish. Only the part that is associated with the wave pressure has a nonzero contribution to F_i.

The velocity components and pressure must be now be represented in terms of the calculated variables of the wave model. The horizontal components can be written down easily using eqs. (3.58) and (3.69)

$$\tilde{u} = \frac{\partial \varphi}{\partial x} = f \frac{\partial \Phi}{\partial x} = \frac{g}{CC_g} fQ_x \tag{5.56}$$

$$\tilde{v} = \frac{\partial \varphi}{\partial y} = f \frac{\partial \Phi}{\partial y} = \frac{g}{CC_g} fQ_y \tag{5.57}$$

In order to find the expression for w the use is made of the continuity equation for the waves which is

$$-\left(\frac{\partial \tilde{u}}{\partial x} + \frac{\partial \tilde{v}}{\partial y}\right) = \frac{\partial \tilde{w}}{\partial z} \tag{5.58}$$

Inserting the new expressions for u and v, eqs. (5.56) and (5.57), into eq. (5.58) and integrating the two sides of the resulting equation over the arbitry vertical interval (−h, z) yields

$$\tilde{w} = -\int_{-h}^{z} f \, dz \, \frac{g}{CC_g} \left(\frac{\partial Q_x}{\partial x} + \frac{\partial Q_y}{\partial y} \right) \tag{5.59}$$

Realizing that with z=0 as the up-limit the integral of f yields tanh(kh) we can write $\hat{w}$ in terms of its value at the surface as

$$\tilde{w} = \int_{-h}^{z} f \, dz \, w\Big|_{z=0} \frac{1}{\tanh(kh)} \tag{5.60}$$

Following Mei (1982) the general expression for the total pressure is

$$p=\rho g(\zeta - z) - \rho\tilde{w}^2 + \frac{\partial}{\partial x}\int_z^0 \rho\tilde{u}\tilde{w}\, dz + \frac{\partial}{\partial y}\int_z^0 \rho\tilde{v}\tilde{w}\, dz + \frac{\partial}{\partial t}\int_z^0 \rho\tilde{w}\, dz \tag{5.61}$$

Again due to the periodicity of the wave velocity some terms in I_{up} will vanish and the expression for F_x becomes

$$F_x = I_{up} = \overline{\int_{-h}^{\zeta} \left[\rho g \tilde{u} (\zeta - z) + \tilde{u} \frac{\partial}{\partial t} \int_z^0 \rho\tilde{w}\, dz \right] dz} \tag{5.62}$$

Consider the first integral which is the part of the energy flux resulting from the free surface elevation of the waves. Making use of eq. (5.56) and the relation

$$\int_{-h}^{\zeta} f \, dz = \frac{C^2}{g} \tag{5.63}$$

it is easily found

$$F_{x1} = \frac{g}{CC_g} \overline{\int_{-h}^{\zeta} f \, (\zeta - z) dz \, \rho g Q_x} = \rho g \, \overline{Q_x \zeta} \, \frac{C}{C_g} \tag{5.64}$$

Considering the second integral denoted by F_{x2}

$$F_{x2} = \overline{\int_{-h}^{\zeta} \tilde{u} \left[\frac{\partial}{\partial t} \int_z^0 \rho\tilde{w}\, dz \right] dz} \tag{5.65}$$

On inserting the expression for $\hat{w}$, eq. (5.60)

$$F_{x2} = \overline{\int_{-h}^{\zeta} \left(\int_z^0 \int_{-h}^{z} f \, dzdz \right) \tilde{u} \frac{\partial}{\partial t} \tilde{w}\Big|_{z=0} dz} \, \frac{1}{\tanh(kh)} \tag{5.66}$$

After performing the two inner integrations and substituting eq. (5.56) for u eq. (5.66) becomes

$$F_{x2} = -\frac{g}{CC_g}\,\overline{Q_x\,\frac{\partial}{\partial t}\,w\Big|_{z=0}\int_{-h}^{\zeta} f\frac{\cosh(kh)-\cosh(k(z+h))}{k^2\cosh(kh)}\,dz}\;\frac{1}{\tanh(kh)}$$

According to the wave kinematic boundary condition on the free surface

$$w\Big|_{z=0} = \frac{\partial \zeta}{\partial t} \tag{5.67}$$

thus

$$\frac{\partial}{\partial t}\,w\Big|_{z=0} = \frac{\partial^2 \zeta}{\partial t^2} = -\omega^2 \zeta \tag{5.68}$$

also

$$\overline{\int_{-h}^{\zeta} f\,\frac{\cosh(kh)-\cosh k(z+h)}{\cosh(kh)}\,dz} = \int_{-h}^{\overline{\zeta}} \frac{\cosh(kh)\cosh(k(z+h))-\cosh^2(k(z+h))}{\cosh^2(kh)}\,dz$$

which on integration gives

$$\frac{\cosh(kh)\sinh(kh) - 0.5(2kh+0.5\sinh(2kh))}{2k\cosh^2(kh)}$$

and therefore

$$F_{x2} = -\frac{\rho g}{CC_g}\,\overline{Q_x\zeta}\,\frac{\omega^2}{k^2}\,\frac{\cosh(kh)\sinh(kh)-0.5(kh+0.5\sinh(2kh))}{k\,\sinh(kh)\,\cosh(kh)} \tag{5.69}$$

On inserting the relation $C=\omega/k$ and again using the relation

$$\sinh(2kh) = 2\,\sinh(kh)\cosh(kh) \tag{5.70}$$

eq. (5.69) yields

$$F_{x2} = \rho g\,\frac{C}{C_g}\,\frac{-0.5\sinh(kh)\cosh(kh)+0.5(kh)}{\sinh(kh)\cosh(kh)}\,\overline{Q_x\zeta}$$

$$= \rho g\,\frac{C}{C_g}\left[\frac{kh}{\sinh(2kh)} - \frac{1}{2}\right]\overline{Q_x\zeta} \tag{5.71}$$

Combining eqs. (5.64) and (5.71) gives

$$F_x = F_{x1} + F_{x2} = \rho\overline{Q_x\zeta}\,\frac{C}{C_g}\left[\frac{1}{2} + \frac{kh}{\sinh(2kh)}\right] \tag{5.72}$$

Recalling the definition for the group velocity

$$C_g = \frac{C}{2}\left[1 + \frac{2kh}{\sinh(2kh)}\right] \tag{5.73}$$

we end up with a very simple relation as

$$F_x = \rho\overline{Q_x\zeta} \tag{5.74}$$

Similarly

$$F_y = \rho\overline{Q_y\zeta} \tag{5.75}$$

Clearly for the two special cases, progressive waves and standing waves, eqs. (5.74) and (5.75) will yield the well known results. For the exact standing waves Q and ζ are out of phase, and so F must be zero which just means no energy propagation in such waves.

5.5.2 Determination of D_w inside surfzone

In order to solve the $\bar{k}$ and $\bar{\epsilon}$ equations it is necessary to determine the wave energy dissipation, D_w. Due to the extremely complex character of breaking waves, no accurate method is currently available for this purpose. There, however, exist two different approximate methods which have been widely used.

The first approach entails formulating a dissipation model in terms of known wave properties, and has been devised mainly for normal incident waves breaking on a plane beach. As it will be shown, even in such a simple case a number of formulae have been proposed. By drawing an analogy between breaking waves and hydraulic jump, a wave energy dissipation model similar to that for a propagating bore was first proposed by Le Mehaute (1962) and advanced later by Divoky et al (1968), a general form of which can be written as

$$D_w \propto \rho g \frac{H^3}{4hT} \tag{5.76}$$

where H is wave height and T is wave period. A slightly modification was proposed by Battjes & Janssen (1978) which reads

$$D_w = 0.2\rho g \frac{H^2}{T} \tag{5.77}$$

Although this model is physically more appealing compared with the propagating bore model, it is by nature only applicable to normally incident waves on a plane beach. Since the proposed analogy between breaking waves and hydraulic jump does not hold true in a 3-D wave field, this type of dissipation model can not be recommended for general use. After pointing out that the energy

dissipation should be related to wave height square rather the cube and on the basis of the experimental evidence of wave height variation on a uniform bottom presented by Horikawa & Kuo (1966), Dally et al (1984) proposed a heuristic expression for the energy dissipation term as

$$D_w = \frac{K}{d} [EC_g - EC_{g_s}] \qquad (5.78)$$

where EC_g is the energy flux for linear progressive waves, d is the steady water depth and the subscript s denotes quantities associated with the so-called stable wave. The stable wave height was proposed, largely based on the experimental finding by Horikawa & Kuo, as $H_s = \Gamma d$, where Γ is a constant that is generally different from γ. The physical interpretation of Eq. (5.78) is that the energy dissipation is proportional to the difference between the energy flux of the wave and a stable flux. Whether this simple hypothesis truely represents the dissipation process of breaking waves is yet to be demonstrated. The two empirical constants K and Γ were determined by the field and laboratory data. This model has recently been incorporated in a parabolic wave model by Kirby & Dalrymple (1986) so that the effect of breaking on the wave field can be more realistically predicted. Some encouraging results were reported.

The second approach assumes that an analytical form for the energy flux is available and that the breaking wave height is related to the water depth by the wave index, γ. In this way, the wave energy dissipation D_w can be estimated from the wave energy equation, which implies that the difficult task of formulating D_w directly is effectively avoided. This approach was first adopted by Battjes (1975) for finding an appropriate turbulent velocity scale and was later on used by Visser (1984) and also Wind & Vreugdenhil (1986) in estimating the actual value of D_w. For propagating waves this method proved quite successful.

Comparing these two approaches it can be said that the first is physically more attractive since it models the actual energy dissipation directly. But given the present quite limited knowledge about breaking waves, D_w can hardly be found except in very simple cases. The modelling approach proposed by Dally et al (1984) does have a prospect of wider application but the general validity of coefficients is yet to be fully tested. On the other hand the second method as outlined in the previous paragraph relies upon the proportionality assumption between wave height and local water depth which is far from exact in general situations. Also in the case of the progressive wave breaking on a beach it has the tendency of over estimating the real turbulence energy since part of the wave energy is transfered to a forward flow which is not, by nature, just a turbulent

motion (Svendsen, 1984). In spite of the above mentioned limitations the second method has some advantages. It is quite general and can be used in relatively broader breaking wave fields. Moreover it requires only one empirical coefficient, which is consistent with the method used in determining broken wave heights when calculating other forcing terms. Therefore this method is to be used in this work.

Theoretically the full wave energy equation eq. (5.6) should be used to determine D_w. However it is considered unnecessary here to include the effect of wave-current interaction for two simple reasons:

1) breaking wave quantities such as F can not be accurately determined and the use of the exact energy equation does not necessarily give a better estimate of D_w but rather makes the computation much more complicated.

2) the two turbulent transport equations for $\bar{\kappa}$ and $\bar{\epsilon}$ are just model equations, the understanding the relative importance of the various terms involved and their effects on the eddy viscosity is, at this early stage, more important than pursuing the accurate estimation of D_w.

Therefore after neglecting mean currents eq. (5.6) becomes

$$\frac{\partial F_x}{\partial x} + \frac{\partial F_y}{\partial y} = - D_w \qquad (5.79)$$

This simplified energy equation will be used for the calculation of D_w.

As to the determination of F_x and F_y, eqs. (5.74) and (5.75) can be used and the effect of wave breaking must be introduced through the calculation of the time average of $Q_x\zeta$ and $Q_y\zeta$ in the original form and the breaking condition must be introduced through the calculation of time averages of $Q_x\zeta$ and $Q_y\zeta$ in a way identical to that used in determining the radiation stresses inside the surf zone.

5.6 Numerical Formulations

5.6.1 Numerical scheme

The finite difference scheme used to discretize the $\bar{k}$ and $\bar{\epsilon}$ equations are very similar to that used for the equations of motion. In order to ensure numerical stability the convection terms are discretized by the ADE method and the rest of the terms are discretized using central difference method. The mean velocities U and V are treated as known. The detailed formulations are presented in Chapter 6.

5.6.2 Boundary conditions for $\bar{k}$ and $\bar{\epsilon}$

At the offshore boundary, wave-induced currents tend to be very small and waves do not break. The appropriate boundary conditions for such situation is

$$\bar{k} = 0 \qquad \text{and} \qquad \bar{\epsilon} = \text{a small value} \tag{5.80}$$

which means that the eddy viscosity is kept as zero there. This is a significant difference from the model used by Longuet-Higgins (1970b) which allows an unrealistic monotonic increase of the eddy viscosity in the offshore direction.

At the inshore boundaries where a finite depth is required by the wave model for computational reasons $\bar{k}$ as well as $\bar{\epsilon}$ must be finite there. The zero eddy viscosity condition employed in the analytical solution can no longer be used now in order to determine $\bar{k}$ and $\bar{\epsilon}$. The simplest alternative boundary conditions which can be reasonably specified are zero gradient conditions (Rodi, 1981), i.e. both $\bar{k}$ and $\bar{\epsilon}$ at the boundary will have values the same as those at the neighbouring points.

$$\bar{k}_{1,j} = \bar{k}_{2,j} \qquad \bar{\epsilon}_{1,j} = \bar{\epsilon}_{2,j} \tag{5.81}$$

where subscripts 1 and 2 denote computational shoreline and a line one grid distance apart, respectively. Obviously these conditions are expected to be more applicable for a long straight shore line than a curved one.

At lateral boundaries the intensity and distribution of turbulence are virtually unknown. General boundary conditions are not available. For the sake of simplicity periodic conditions for both the turbulent energy and energy dissipation are used which are as follows

$$\bar{k}_{i,1} = \bar{k}_{i,N} \qquad \bar{\epsilon}_{i,1} = \bar{\epsilon}_{i,N}$$

$$\bar{k}_{i,2} = \bar{k}_{i,N+1} \qquad \bar{\epsilon}_{i,2} = \bar{\epsilon}_{i,N+1}$$

in which the subscripts are defined as in Fig. 6.2

The inaccuracies so introduced at the lateral boundaries are considered insignificant as long as these boundaries are positioned sufficiently away from the area of interest.

Finally the internal boundaries formed by any obstacles present in the computational domain must be determined. If they are the impermeable walls the standard wall functions described in Rodi (1980) can be used. However, since the grid size used are normally of the order of several meters and the points where k and $\bar{\epsilon}$ are defined are half the grid size from the walls the application of accurate boundary conditions such as wall functions may not be effective or even necessary for such a coarse grid system. Therefore, in this work the $\bar{K}$ and $\bar{\epsilon}$ at those boundaries are specified to be equal to the values at the neighbouring points on the same side of the walls.

CHAPTER 6
THE NUMERICAL SOLUTION OF THE TIME MEAN EQUATIONS

6.1 Introduction

In Chapter 4 the time-averaged and depth-integrated differential equations governing the wave-induced circulation were formulated and discussed. These equations are coupled and nonlinear. Apart from a few simple and idealized nearshore situations these equations are not amenable to analytical solution. Numerical means of solution must be sought. Even in cases where linearized equations may be used numerical methods are still necessary for dealing with realistic bottom contours and coastal planforms with manmade structures.

Basco (1983), after reviewing ten existing numerical models dated up to 1982, concluded that they all had serious limitations and none of them was considered recommendable for engineering purposes. This conclusion, despite being disputed by Kirby & Dalrymple (1984) as an over-statement, is in fact not without factual support. The earlier versions of this type of model tend to omit certain physically important terms in the momentum balance equations and the later models, although quite complete in formulations, did have certain numerical difficulties. Both drawbacks cited above from Basco (1983) have been, to a great extent, overcome by several recently developed models (Liang, 1985, Copeland, 1986 and Wu & Liu, 1986). In these models all the physically important terms except the wave-current interaction have been included and by using the finite element or finite difference method the nonlinear terms are better treated. Stable solutions and much improved predictions have been reported.

However, the need for more efficient and accurate numerical schemes still remains. The finite element method, although having certain merits in resolving nonlinear instability and being flexible in handling complex boundaries, has two severe disadvantadges compared with the finite difference method. Firstly it is generally considered uneconomic in terms of computer time when used for the solution of shallow water equations (Weare, 1976). This drawback becomes even more severe in the present case since, in addition to the three basic equations of motion, two more turbulence equations have to be solved simultaneously in order to determine the eddy viscosity. Secondly, as correctly pointed out by Basco (1983), the accuracy of the finite element method when applied to nonlinear shallow water wave type problems is difficult to assess. The qualitative comparison of predicted current patterns with the limited available experimental data is by no means

sufficient.

Bearing in mind the properties of the two methods briefly summarized above, it was decided to adopt the finite difference method. From the view point of the programming effort involved and also considering the computational efficiency an explicit scheme was chosen instead of an implicit scheme.

In this chapter a finite difference scheme is described which is then used to solve the equations of motion as well as the turbulence equations. All the terms in the equations are exactly centered in space and in time except for the diffusion terms which are discretized using the forward time difference in order to enhance numerical stability. Throughout the numerical tests performed in this work the model has shown to be numerically stable and accurate with all the parameters being determined by using physical reasoning. The overall accuracy of the model is of the order $(\nabla x^2, \nabla t)$.

6.2 Grid Arrangemant and General Considerations

The finite difference grid system is the same as that used for the wave propagation model. As it is shown in Fig. 6.1 the axis x and y denote the inshore–offshore and longshore directions, respectively. The staggered grid system is so arranged that in which the time mean velocity components U and V are defined and stored at the corresponding grid edges and all the scalar variables such as the mean water depth h, turbulent energy $\overline{k}$ and dissipation $\overline{\epsilon}$ are stored at the grid centres. The subscripts i and j will be used to identify discretized variables corresponding in the x and y directions.

It is well established that such a staggered grid system has several advantages. Among them the most important one is that the velocity components are stored at just the points at which they are required for the calculation of the continuity balance over a grid. A detailed exposition on this subject can be found in Partanka (1982). A difficult situation may often occur when a variable is required at points other than those at which it is stored. This can be dealt with by using a certain kind of averaging of neighbouring values. The simple two point averaging method is used here while a more accurate weighted average technique has been employed in the computation of tidal currents as reported by Flather & Heaps (1974).

In order to ensure numerical stability, the present finite difference scheme consists of several sub–schemes which are applied to particular terms in the governing equations. The simplest one is FTCS scheme (Forward Time Central

Space) which was used for all the source terms and the diffusion terms. The standard two-point leap frog scheme was used for the continuity equation and the basic parts of the momentum equations. For the nonlinear convective acceleration terms the ADE (Angled Derivative Explicit) developed by Roberts and Weiss (1966) is adopted in order to ensure numerical stability.

In the following sections the sub-schemes used in this work will firstly be discussed individually and the corresponding stability conditions will be given based mainly on one dimentional forms of the governing equations. The discretization of the full equations of motion will then be given, term by term. Finally the solution procedure and flow chart will be presented.

6.3 Basic Finite Difference Schemes

6.3.1 Two-point leap frog scheme

The two-point leap frog scheme is a quite common explicit finite difference scheme. Its use can be found in many hydraulics problems including the wave equations in Chapter 3. The properties of this scheme can be illustrated conveniently by considering the one dimensional form of the equations of continuity and momentum ignoring, for the time being, the frictional, diffusive, radiation stress and convective acceleration effects. The resulting equations become simply

$$\frac{\partial \zeta}{\partial t} + \frac{\partial (hU)}{\partial x} = 0 \tag{6.1}$$

$$\frac{\partial (hU)}{\partial t} + gh\frac{\partial \zeta}{\partial x} = 0 \tag{6.2}$$

In an explicit method the unknown value is expressed directly in terms of the known values. For the present problem this means that unknown ζ and U at the advanced time level (n+1) Δt can be calculated directly from the known values at the previous and present time levels as well as from values already calculated at (n+1) Δt. This can be done by taking central differences as

$$\frac{1}{\Delta t}\left(\bar{\zeta}_i^{n+1/2} - \bar{\zeta}_i^{n-1/2}\right) + \frac{1}{\Delta x}\left[(Uh)_{i+1}^{n} - (Uh)_i^{n}\right] = 0 \tag{6.3}$$

$$\frac{1}{\Delta t}\left[(Uh)_i^{n+1} - (Uh)_i^{n}\right] + g\frac{h}{\Delta x}\left(\bar{\zeta}_{i+1}^{n+1/2} - \bar{\zeta}_i^{n+1/2}\right) = 0 \tag{6.4}$$

It is evident from eqs. (6.3) and (6.4) that due to the use of the staggered grid system the continuity and x-momentum equations have been discretized at

different points in space. For instance eq. (6.3) is centred at the grid centres (ζ_i defined points) while eq. (6.4) at the grid edges (U_i defined points). In order to ensure that the equations are explicitly solvable, eq. (6.3) is centred at time step n while eq. (6.4) at n+1/2. As a result once the initial values for ζ and U at the time $-1/2\Delta t$ and 0 are given, the values of ζ and U at any new time step can be established easily over the entire solution domain.

The same scheme has been used by Copeland (1985) for both his wave equations and the basic linearized equations of nearshore circulation. A similar scheme which defines ζ at the integer time step n and velocity U at the time step n+1/2 has been outlined by Falconer (1976). The only difference between the two schemes lies in the sequence of solution. The present scheme requires that the continuity equation be solved first and then by substituting the new ζ in the momentum equation U can be up-dated while in the later scheme a reverse sequence of solution is followed.

As already discussed by Falconer (1976), this scheme is exactly centred in space and time and, therefore, possesses second order accuracy. As in many other explicit finite difference schemes the two-time step leap frog scheme is only conditionally stable. If h_i is constant ($h_i = h$) the time and space steps allowed in computations are controlled by Courant stability criteria.

$$\frac{\Delta t}{\Delta x}\sqrt{gh} < 1 \qquad (6.5)$$

If h is not a constant but dependent on locations in space the above criteria should be modified as

$$\frac{\Delta t}{\Delta x}\sqrt{gh_{max}} < 1 \qquad (6.5)$$

where h_{max} is the maximum water depth in the computational domain.

Since in eqs. (6.3) and (6.4) values of the depth are required at the velocity points where they are not defined the simplest way to follow is to use the average of the corresponding values at the neighbouring points. Thus, eqs (6.3) and (6.4) can be written as

$$\bar{\zeta}_i^{n+1/2} = \bar{\zeta}_i^{n-1/2} + \frac{1}{2}\left[(h_{i+1} + h_i)U_{i+1}^n - (h_i + h_{i-1})U_i^n\right]\frac{\Delta t}{\Delta x} \qquad (6.6)$$

$$U_i^{n+1} = U_i^n + g\frac{2}{h_{i+1} + h_i}(\bar{\zeta}_{i+1}^{n+1/2} - \bar{\zeta}_i^{n+1/2})\frac{\Delta t}{\Delta x} \qquad (6.7)$$

6.3.2 Angled derivative explicit (ADE) scheme

The angled derivative explicit scheme with second order accuracy in both space and time was originally proposed by Roberts and Weiss (1966) for the transport of a single scalar quantity on a normal (non-staggered) grid system. In the following an outline of the method is given following Roache (1977). Consider the inviscid one-dimensional convective equation

$$\frac{\partial \xi}{\partial t} = - u_0 \frac{\partial \xi}{\partial x} \tag{6.8}$$

where u_0 is a constant, ξ is a scalar quantity. As shown in Fig. (6.1) ξ is defined at integer time and space steps. Centering time and space at half-steps eq. (6.8) becomes

$$\frac{\xi_i^{n+1} - \xi_i^n}{\Delta t} = - u_0 \frac{\xi_{i+1/2}^{n+1/2} - \xi_{i-1/2}^{n+1/2}}{\Delta x} \tag{6.9}$$

Since ξ is defined only at integer space and time steps the ξ terms on the right hand side of eq. (6.9) must be evaluated from their neighbouring points. Refering to Fig. 6.2 which denotes the computational sweep proceeding in the increasing i direction, we have

for sweeps in increasing i direction

$$\xi_{i+1/2}^{n+1/2} = \frac{1}{2} \left(\xi_i^{n+1} + \xi_{i+1}^n \right) \tag{6.10}$$

$$\xi_{i-1/2}^{n+1/2} = \frac{1}{2} \left(\xi_{i-1}^{n+1} + \xi_i^n \right) \tag{6.11}$$

Substituting these into eq. (6.9) gives

$$\xi_i^{n+1} = \xi_i^n - \mu \left(\xi_{i+1}^n - \xi_{i-1}^{n+1} \right) \tag{6.12}$$

where

$$\mu = \frac{u_0 \Delta t / 2\Delta x}{1 + u_0 \Delta t / 2\Delta x} \tag{6.13}$$

For reasons of symmetry in the actual computations the sweeps should normally proceed alternatively in the increasing i direction and decreasing i direction. The difference equation in decreasing i direction can be similarly

derived as

for sweep in decreasing i direction

$$\xi_i^{n+1} = \xi_i^n - \mu'(\xi_{i+1}^{n+1} - \xi_{i-1}^n) \tag{6.14}$$

where

$$\mu' = \frac{u_0\Delta t/2\Delta x}{1-u_0\Delta t/2\Delta x} \tag{6.15}$$

According to Roberts and Weiss (1966), this ADE method has an amplification factor of unity, which is normally regarded as a condition of unconditional stability. However, based on further theoretical considerations concerning the effect of boundary values on the values subsequently determined at the interior points and some numerical tests, a stability condition was suggested as:

$$-1 \leq \frac{u_0\Delta t}{\Delta x} < 2 \tag{6.16}$$

The ADE scheme has been discussed in detail by Roache (1977). One notable property is that it does not suffer from numerical diffusion as most other explicit finite difference schemes do.

This ADE scheme can now be readily adapted to the present grid system which is staggered in space. Consider again the one dimensional linearized momentum equation

$$\frac{\partial Uh}{\partial t} = - U_0\frac{\partial Uh}{\partial x} + R_{other} \tag{6.17}$$

where U_0 is a constant local value of velocity U, R_{other} represents all the remaining terms whose discretizations are not directly affected by the numerical scheme adopted for the convection terms.

Centering at half steps in time and space for U which is defined at the grid edges and refering to Fig. (6.2) give

$$\frac{(Uh)_i^{n+1} - (Uh)_i^n}{\Delta t} = - U_0\frac{(Uh)_{i+1/2}^{n+1/2} - (Uh)_{i-1/2}^{n+1/2}}{\Delta x} + R_{other} \tag{6.18}$$

where, the subscript i now identifies U-defined points in space. Following the

averaging procedure outlined for ξ in the previous example, the velocities at the grid centres can be determined, as

for increasing i sweeps

$$(Uh)_i^{n+1} = (Uh)_i^n - \mu^+\{[(Uh)_{i+1}^n - (Uh)_{i-1}^{n+1}] + R_{other}\} \tag{6.19}$$

where

$$\mu^+ = \frac{U_0\,\Delta t}{2\Delta x + U_0\Delta t} \tag{6.20}$$

for decreasing i sweeps

$$(Uh)_i^{n+1} = (Uh)_i^n - \mu^-\{[(Uh)_{i+1}^{n+1} - (Uh)_{i-1}^n] + R_{other}\} \tag{6.21}$$

where

$$\mu^- = \frac{U_0\,\Delta t}{2\Delta x - U_0\Delta t} \tag{6.22}$$

Before proceeding to present the discretized depth-integrated and time-averaged governing equations describing wave-induced nearshore circulation, it is considered necessary to make clear some important points regarding the use of eqs. (6.19) and (6.21) in two dimensional non-linear equations.

1) Since the convective acceleration terms in the momentum equations are nonlinear, finite differences can only be taken after local linearization of the equations. Therefore, the correct centering in space and time should be understood refering to the direction terms while the velocity components that act as coefficients may be calculated explicitly using values from previous time steps.

2) In two dimensional situations there are four possible directions in which the numerical computation can proceed and the appropriate ADE formulations can be derived for all four of the directions of computational sweeps. For the sake of simplicity only two alternative directions are considered in this work, which are the positive x and y direction, and negative x and y direction.

6.4 Discretization of the Governing Equations

6.4.1 Discretization of the linear terms

The continuity and momentum equations can be rewritten in the following form

continuity equation

$$\frac{\partial \bar{\zeta}}{\partial t} = - \frac{\partial Uh}{\partial x} - \frac{\partial Vh}{\partial y} \tag{6.23}$$

x-momentum equation

$$\frac{\partial Uh}{\partial t} = - \frac{\partial U^2 h}{\partial x} - \frac{\partial UVh}{\partial y} + R^x_{other} \tag{6.24}$$

y-momentum equation

$$\frac{\partial Vh}{\partial t} = - \frac{\partial UVh}{\partial x} - \frac{\partial V^2 h}{\partial y} + R^y_{other} \tag{6.25}$$

The continuity equation is a linear equation and can be readily written in finite difference form. Applying the two time level leap frog scheme for the derivatives in both x and y directions gives

$$\bar{\zeta}^{n+1/2}_{i,j} = \bar{\zeta}^{n-1/2}_{i,j} - [\frac{h_{i+1,j} + h_{i,j}}{2} U^n_{i+1,j} - \frac{h_{i,j} + h_{i-1,j}}{2} U^n_{i,j}] \frac{\Delta t}{\Delta x}$$

$$- [\frac{h_{i,j} + h_{i,j+1}}{2} V^n_{i,j+1} - \frac{h_{i,j-1} + h_{i,j}}{2} V^n_{i,j}] \frac{\Delta t}{\Delta y} \tag{6.26}$$

The discretization of the two momentum equations is more involved than that related to the continuity equation. All the basic schemes previously discussed were used in order to achieve overall stability and accuracy of the resulting difference equations. Using the two-point leap frog scheme for the linear first order derivative terms and a central difference scheme for the diffusion and source terms, R_{other} in eq. (6.24) can be discretized term by term as follows

$$R^x_{other} = \frac{g}{2} (h_{i,j} + h_{i-1,j}) (\bar{\zeta}^{n+1/2}_{i,j} - \bar{\zeta}^{n+1/2}_{i-1,j}) \frac{\Delta t}{\Delta x}$$

$$- (S_{xx_{i,j}} - S_{xx_{i-1,j}}) \frac{\Delta t}{\rho \Delta x}$$

$$- (S_{xy_{i,j+1}} - S_{xy_{i,j-1}} + S_{xy_{i-1,j+1}} - S_{xy_{i-1,j-1}}) \frac{\Delta t}{2\rho \Delta y}$$

$$+ [h_{i,j} \bar{\nu}_{t_{i,j}} (U^n_{i+1,j} - U^n_{i,j}) - h_{i-1,j} \bar{\nu}_{t_{i-1,j}} (U^n_{i,j} - U^n_{i-1,j})] \frac{2\Delta t}{\Delta x \Delta x}$$

$$+[h_1\,{}^{\nu}t_1(V^n_{i,j+1} - V^n_{i-1,j+1}) - h_2{}^{\nu}t_2(V^n_{i,j} - V^n_{i-1,j})]\frac{\Delta t}{16\Delta x\Delta y}$$

$$+[h_1{}^{\nu}t_1\,(U^n_{i,j+1} - U^n_{i,j}\,) - h_2{}^{\nu}t_2\,(U^n_{i,j} - U^n_{i,j-1})]\frac{\Delta t}{16\Delta x\Delta x}$$

$$-\frac{2C_f}{\pi}\,(\tilde{u}_{max_{i,j}} + \tilde{u}_{max_{i-1,j}})\,U^n_{i,j}\,\frac{\Delta t}{\rho} \qquad (6.27)$$

where

$$h_1 = (h_{i,j} + h_{i-1,j} + h_{i,j+1} + h_{i-1,j+1}) \qquad (6.28)$$

$${}^{\nu}t_1 = (\bar{\nu}t_{i,j} + \bar{\nu}t_{i-1,j} + \bar{\nu}t_{i,j+1} + \bar{\nu}t_{i-1,j+1}) \qquad (6.29)$$

$$h_2 = (h_{i,j} + h_{i-1,j} + h_{i,j-1} + h_{i-1,j-1}) \qquad (6.30)$$

$${}^{\nu}2 = (\bar{\nu}t_{i,j} + \bar{\nu}t_{i-1,j} + \bar{\nu}t_{i,j-1} + \bar{\nu}t_{i-1,j-1}) \qquad (6.31)$$

Similarly for eq. (6.25)

$$R^y_{other} = \frac{1}{2}\,(h_{i,j} + h_{i,j-1})(\bar{\zeta}^{n+1/2}_{i,j} - \bar{\zeta}^{n+1/2}_{i,j-1})\frac{\Delta t}{\Delta y}$$

$$-(Syy_{i,j} - Syy_{i,j-1})\frac{\Delta t}{\rho\Delta y}$$

$$-\,(Sxy_{i+1,j} - Sxy_{i-1,j} + Sxy_{i+1,j-1} - Sxy_{i-1,j-1})\frac{\Delta t}{2\rho\Delta x}$$

$$+[h_{i,j}\bar{\nu}t_{i,j}\,(V^n_{i,j+1} - V^n_{i,j}) - h_{i,j-1}\bar{\nu}t_{i,j-1}\,(V^n_{i,j} - V^n_{i,j-1})]\frac{2\Delta t}{\Delta y\Delta y}$$

$$[h_1\,{}^{\nu}t_1\,\,(V^n_{i+1,j} - V^n_{i,j}\,) - h_2{}^{\nu}t_2(V^n_{i,j} - V^n_{i-1,j})]\frac{\Delta t}{16\Delta x\Delta x}$$

$$+[h_1{}^{\nu}t_1\,(U^n_{i+1,j} - U^n_{i+1,j-1}) - h_2{}^{\nu}t_2\,(U^n_{i,j} - U^n_{i,j-1})]\frac{\Delta t}{16\Delta x\Delta y}$$

$$-\frac{2C_f}{\pi}\,(\tilde{u}_{max_{i,j}} + \tilde{u}_{max_{i-1,j}})\,U^n_{ij}\,\frac{\Delta t}{\rho} \qquad (6.32)$$

where

$$h_3 = (h_{i,j} + h_{i,j-1} + h_{i+1,j} + h_{i+1,j-1}) \qquad (6.33)$$

$${}^{\nu}3 = (\bar{\nu}t_{i,j} + \bar{\nu}t_{i,j-1} + \bar{\nu}t_{i+1,j} + \bar{\nu}t_{i+1,j-1}) \qquad (6.34)$$

$$h_4 = (h_{i,j} + h_{i,j-1} + h_{i-1,j} + h_{i-1,j-1}) \tag{6.35}$$

$$\nu_4 = (\bar{\nu}_{t_{i,j}} + \bar{\nu}_{t_{i,j-1}} + \bar{\nu}_{t_{i-1,j}} + \bar{\nu}_{t_{i-1,j-1}}) \tag{6.36}$$

6.4.2 Convective accelerations

Refering to Fig. (6.3), the ADE formulations for the convective terms in x-momentum equation at half time steps can be written down term by term as

$$Fxt = \frac{\partial Uh}{\partial t} = \frac{1}{\Delta t}\,[(Uh)^{n+1}_{i,j} - (Uh)^{n}_{i,j}] \tag{6.37}$$

$$F_{x1} = \frac{\partial U^2 h}{\partial x} = [(Uh)^{n+1/2}_{i+1/2,j}\, U_1 - (Uh)^{n+1/2}_{i-1/2,j}\, U_2]/\Delta x \tag{6.38}$$

As shown in the previous section the actual neighbouring velocity points used should depend on the direction of the computational sweep. The formulations for the two alternative sweeps can be written as

for increasing i and j *sweep*

$$F_{x1} = \frac{1}{2\Delta x}\{[(Uh)^{n}_{i+1,j} + (Uh)^{n+1}_{i,j}]U_1 - [(Uh)^{n}_{i,j} + (Uh)^{n+1}_{i-1,j}]U_2\} \tag{6.39}$$

in which U_1 and U_2 need not to be calculated at half time steps since it is the derivative only which should be centred at n+1/2. Instead, they are simply evaluated explicitly using values from the previous time step n. However in order to obtain a better estimate values at the new time level n+1 are used in the averaging process whenever they are available. The actual formulae are

$$U_1 = \frac{1}{2}\,(U^{n}_{i+1,j} + U^{n}_{i,j}) \tag{6.40}$$

$$U_2 = \frac{1}{2}\,(U^{n}_{i,j} + U^{n+1}_{i-1,j}) \tag{6.41}$$

Clearly, U_1 is approximated by the values of velocity at the previous time step n while U_2 is calculated exactly at the half time and space steps. This is because the current velocity (at time level n+1/2) at point (i,j) is not yet available but its value at (i-1,j) is known.

for de*creasing i* and j *sweep*

$$F_{x1} = \frac{1}{2\Delta x}\{[(Uh)^{n+1}_{i+1,j} + (Uh)^{n}_{i,j}]U_1 - [(Uh)^{n+1}_{i,j} + (Uh)^{n}_{i-1,j}]U_2\} \tag{6.42}$$

where

$$U_1 = \frac{1}{2}\,(U^{n+1}_{i+1,j} + U^{n}_{i,j}) \tag{6.43}$$

$$U_2 = \frac{1}{2}\,(U^{n}_{i,j} + U^{n}_{i-1,j}) \tag{6.44}$$

For the cross stream convection term the centering is for $U_{i,j}$ and again performed at time level n+1/2

$$F_{x2} = \frac{\partial UVh}{\partial y} = \frac{\partial (Uh)V}{\partial y} = [(Uh)^{n+1/2}_{i,j+1/2}\, V_1 - (Uh)^{n+1/2}_{i,j-1/2}\, V_2]/\Delta y \tag{6.45}$$

for increasing i and j sweeps

$$F_{x2} = \frac{1}{2\Delta y}\{[(Uh)^{n}_{i,j+1} + (\overset{*}{U}h)^{n+1}_{i,j}]V_1 - [(Uh)^{n}_{i,j} + (Uh)^{n+1}_{i,j-1}]V_2\} \tag{6.46}$$

where

$$V_1 = \frac{1}{2}(V^{n}_{i,j+1} + V^{n+1}_{i-1,j+1}) \tag{6.47}$$

$$V_2 = \frac{1}{2}(V^{n}_{i,j} + V^{n+1}_{i-1,j}) \tag{6.48}$$

for decreasing i and j sweeps

$$F_{x2} = \frac{1}{2\Delta y}\{[(Uh)^{n+1}_{i,j+1} + (Uh)^{n}_{i,j}]V_1 - [(\overset{*}{U}h)^{n+1}_{i,j} + (Uh)^{n}_{i,j-1}]V_2\} \tag{6.49}$$

where

$$V_1 = \frac{1}{2}(V^{n+1}_{i,j+1} + V^{n}_{i-1,j+1}) \tag{6.50}$$

$$V_2 = \frac{1}{2}(V^{n+1}_{i,j} + V^{n}_{i-1,j}) \tag{6.51}$$

In eqs. (6.46) and (6.49) the star * sign indicates unknown velocity values at the time of calculation and should be approximated by the corresponding values at the previous time step n.

Now it is possible to combine eqs. (6.27), (6.39), (6.42), (6.46) and (6.49) together to form the complete finite difference equation of eq. (6.24), which can be simply written as

for increasing i and j sweeps

$$(1+\frac{U_1\Delta t}{2\Delta x})(Uh)^{n+1}_{i,j} = (1+\frac{U_2\Delta t}{2\Delta x})(Uh)^{n}_{i,j}$$
$$-\frac{\Delta t}{2\Delta x}[\,U_1(Uh)^{n}_{i+1,j} - U_2(Uh)^{n+1}_{i-1,j}]$$
$$-\frac{\Delta t}{2\Delta y}\{[(Uh)^{n}_{i,j+1} + (Uh)^{n}_{i,j}]V_1$$
$$-[(Uh)^{n}_{i,j} + (Uh)^{n+1}_{i,j-1}]V_2\}$$
$$+R^{x}_{other} \qquad (6.52)$$

for decreasing i and j sweeps

$$(1-\frac{U_1\Delta t}{2\Delta x})(Uh)^{n+1}_{i,j} = (1-\frac{U_2\Delta t}{2\Delta x})(Uh)^{n}_{i,j}$$
$$-\frac{\Delta t}{2\Delta x}[\,U_1(Uh)^{n+1}_{i+1,j} - U_2(Uh)^{n}_{i-1,j}]$$
$$-\frac{\Delta t}{2\Delta y}\{[(Uh)^{n+1}_{i,j+1} + (Uh)^{n}_{i,j}]V_1$$
$$-[(Uh)^{n}_{i,j} + (Uh)^{n}_{i,j-1}]V_2\}$$
$$+R^{x}_{other} \qquad (6.53)$$

Similar formulations can be derived for the convective terms in the y-momentum equation. The final form of the difference equations is as follows

for increasing i and j sweeps

$$(1+\frac{V_1\Delta t}{2\Delta y})(Vh)^{n+1}_{i,j} = (1+\frac{V_2\Delta t}{2\Delta y})(Vh)^{n}_{i,j}$$
$$-\frac{\Delta t}{2\Delta y}[\,V_1(Vh)^{n}_{i,j+1} - V_2(Vh)^{n+1}_{i,j-1}]$$
$$-\frac{\Delta t}{2\Delta x}\{[(Vh)^{n}_{i+1,j} + (Vh)^{n}_{i,j}]U_1$$
$$-[(Vh)^{n}_{i,j} + (Vh)^{n+1}_{i-1,j}]U_2\}$$
$$+R^{y}_{other} \qquad (6.54)$$

where

$$V_1 = \frac{1}{2}(V^{n}_{i,j+1} + V^{n}_{i,j}) \qquad (6.55)$$

$$V_2 = \frac{1}{2}(V^n_{i,j} + V^{n+1}_{i,j-1}) \tag{6.56}$$

$$U_1 = \frac{1}{2}(U^n_{i+1,j} + U^{n+1}_{i+1,j-1}) \tag{6.57}$$

$$U_2 = \frac{1}{2}(U^n_{i,j} + U^{n+1}_{i,j-1}) \tag{6.58}$$

for decreasing i and j sweeps

$$\begin{aligned}(1 - \frac{V_1\Delta t}{2\Delta y})(Vh)^{n+1}_{i,j} = (1 - \frac{V_2\Delta t}{2\Delta y})(Vh)^n_{i,j} \\ - \frac{\Delta t}{2\Delta y}[V_1(Vh)^{n+1}_{i,j+1} - V_2(Vh)^n_{i,j-1}] \\ - \frac{\Delta t}{2\Delta x}\{[(Vh)^{n+1}_{i+1,j} + (Vh)^n_{i,j}]U_1 \\ - [(Vh)^n_{i,j} + (Vh)^n_{i-1,j}]U_2\} \\ + R^y_{other}\end{aligned} \tag{6.59}$$

where

$$V_1 = \frac{1}{2}(V^{n+1}_{i,j+1} + V^n_{i,j}) \tag{6.60}$$

$$V_2 = \frac{1}{2}(V^n_{i,j} + V^n_{i,j-1}) \tag{6.61}$$

$$U_1 = \frac{1}{2}(U^{n+1}_{i+1,j} + U^n_{i+1,j-1}) \tag{6.62}$$

$$U_2 = \frac{1}{2}(U^{n+1}_{i,j} + U^n_{i,j-1}) \tag{6.63}$$

6.5 Turbulence equations

The discretization of the turbulence equations, i.e. turbulent energy and dissipation equations, eqs. (5.26) and (5.27), can be carried out in almost exactly the same way as that for the equations of motion. The only difference is that the unknown variables are scalar quantities and will be discretized at the grid centres rather than at the grid edges. Furthermore, the cross flow convective terms are fully centered in time without introducing approximations. The discretized form of the turbulence energy equation for two alternative sweeps is given below while the discretized $\bar{\epsilon}$ equation can be obtained simply by replacing $\bar{K}$ by $\bar{\epsilon}$ and introducing

the corresponding source terms.

for increasing i and j sweeps

$$\left(1+\frac{\Delta t}{2\Delta x}U^{n}_{i+1,j}+\frac{\Delta t}{2\Delta y}V^{n}_{i,j+1}\right)h_{ij}\bar{k}^{n+1}_{ij}$$

$$=\left(1+\frac{\Delta t}{2\Delta x}U^{n}_{ij}+\frac{\Delta t}{2\Delta y}V^{n}_{i,j}\right)h_{ij}\bar{k}^{n}_{ij}$$

$$-\frac{\Delta t}{2\Delta x}\left(U^{n}_{i+1,j}h_{i+1,j}\bar{k}^{n}_{i+1,j}-U^{n}_{i,j}h_{i-1,j}\bar{k}^{n+1}_{i-1,j}\right)$$

$$-\frac{\Delta t}{2\Delta y}\left(V^{n}_{i,j+1}h_{i,j+1}\bar{k}^{n}_{i,j+1}-V^{n}_{i,j}h_{i,j-1}\bar{k}^{n+1}_{i,j-1}\right)$$

$$+\frac{\Delta t}{2\sigma_k}\frac{1}{2\Delta x^{2}}\left(h_{i+1,j}+h_{i,j}\right)$$

$$\left[\left(\bar{\nu}^{n}_{t\,i+1,j}+\bar{\nu}^{n}_{t\,i,j}\right)\left(\bar{k}^{n}_{i+1}-\bar{k}^{n}_{ij}\right)-\left(\bar{\nu}^{n}_{t\,ij}+\bar{\nu}^{n}_{t\,i-1,j}\right)\left(\bar{k}^{n}_{ij}-\bar{k}^{n}_{i-1,j}\right)\right]$$

$$+\frac{\Delta t}{2\sigma_k}\frac{1}{2\Delta y^{2}}\left(h_{i,j+1}+h_{i,j}\right)$$

$$\left[\left(\bar{\nu}^{n}_{t\,i,j+1}+\bar{\nu}^{n}_{t\,ij}\right)\left(\bar{k}^{n}_{i,j+1}-\bar{k}^{n}_{i,j}\right)-\left(\bar{\nu}^{n}_{t\,ij}+\bar{\nu}^{n}_{t\,i,j-1}\right)\left(\bar{k}^{n}_{ij}-\bar{k}^{n}_{i,j-1}\right)\right]$$

$$+\left(P_{w_{ij}}+P^{n}_{h_{ij}}+\bar{\epsilon}^{n}_{ij}\right)h_{ij}\,\Delta t \qquad (6.64)$$

where

$$P_{h_{ij}}=\bar{\nu}_{t\,ij}\left\{\frac{2\Delta t}{\Delta x}\left(U^{n}_{i+1,j}-U^{n}_{ij}\right)+\frac{2\Delta t}{\Delta y}\left(V^{n}_{i,j+1}-V^{n}_{ij}\right)+\frac{\Delta t}{4\Delta y}\left[\left(U^{n}_{i+1,j+1}+U^{n}_{i,j+1}\right)\right.\right.$$

$$\left.\left.-\left(U^{n}_{i+1,j-1}+U^{n}_{i,j-1}\right)\right]+\frac{\Delta t}{4\Delta x}\left[\left(V^{n}_{i+1,j+1}+V^{n}_{i+1,j}\right)-\left(V^{n}_{i-1,j+1}+V^{n}_{i-1,j}\right)\right]\right\} \qquad (6.65)$$

for decreasing i and j sweeps

$$\left(1-\frac{\Delta t}{2\Delta x}U^{n}_{i+1,j}-\frac{\Delta t}{2\Delta y}V^{n}_{i,j+1}\right)h_{ij}\bar{k}^{n+1}_{ij}$$

$$=\left(1-\frac{\Delta t}{2\Delta x}U^{n}_{ij}-\frac{\Delta t}{2\Delta y}V^{n}_{i,j}\right)h_{ij}\bar{k}^{n}_{ij}$$

$$- \frac{\Delta t}{2\Delta x} (U^n_{i+1,j} h_{i+1,j} \bar{k}^{n+1}_{i+1,j} - U^n_{i,j} h_{i-1,j} \bar{k}^n_{i-1,j})$$

$$- \frac{\Delta t}{2\Delta y} (V^n_{i,j+1} h_{i,j+1} k^{-n+1}_{i,j+1} - V^n_{i,j} h_{i,j-1} \bar{k}^n_{i,j-1})$$

$$+ \frac{\Delta t}{2\sigma_k} \frac{1}{2\Delta x^2} (h_{i+1,j} + h_{i,j})$$

$$[(\bar{\nu}^n_{t\,i+1,j} + \bar{\nu}^n_{t\,i,j})(\bar{k}^n_{i+1} - \bar{k}^n_{ij}) - (\bar{\nu}^n_{t\,ij} + \bar{\nu}^n_{t\,i-1,j})(\bar{k}^n_{ij} - \bar{k}^n_{i-1,j})]$$

$$+ \frac{\Delta t}{2\sigma_k} \frac{1}{2\Delta y^2} (h_{i,j+1} + h_{i,j})$$

$$[(\bar{\nu}^n_{t\,i,j+1} + \bar{\nu}^n_{t\,i,j})(\bar{k}^n_{i,j+1} - \bar{k}^n_{ij}) - (\bar{\nu}^n_{t\,ij} + \bar{\nu}^n_{t\,i,j-1})(\bar{k}^n_{ij} - \bar{k}^n_{i,j-1})]$$

$$+(P_{w_{ij}} + P^n_{h_{ij}} + \bar{\epsilon}^n_{ij})h_{ij} \qquad (6.66)$$

6.6 Initial Conditions, Boundary Conditions and Computational Procedure

It is common knowledge that unique solutions for the finite difference equations as described above can be obtained only after the boundary conditions for a given configuration have been fully specified.

In order to obtain the steady state solutions for the current field, theoretically speaking, any convenient initial conditions are acceptable. Normally computations start from the state of rest. i.e., a calm sea condition. The unknown quantities are either set to be zero such as U, V and $\bar{\zeta}$ or to a small nonzero values such as $\bar{\kappa}$ and $\bar{\epsilon}$ in order to avoid division by zero.

Two types of boundary conditions can be used depending on the situations of beach and waves to be considered. If a beach has a repeatable bottom feature and the width of the computational domain is chosen as a full length of a typical section, denoted here by L_b, a periodic boundary condition can be applied at the lateral boundaries in which all the values on one side of the computation domain are made equal to the corresponding values on the other side of the domain. For some cases, especially for the circulations generated in a wave basin the reflective boundary should be used in which all the scalar quantities at the wall boundary are equal to the corresponding values at the internal points with one computation

space increment Δy apart.

If wave-current interaction is not considered the computation of wave-induced circulation is quite straightforward. Both the wave and circulation models are used only once to get final results. This means that the currents are generated by a fixed wave field which is not to be affected by either the currents or the change in mean surface elevation.

The inclusion of wave-current interaction requires much more computational effort. Generally a number of alternative runs of the wave model and the circulation model are needed in order to arrive at a steady state. One of the iteration procedures that may be used has been described by Walker (1987). The total run time for the wave model consists of several sub-run times any one of which is sufficently long for the wave model to reach a steady state. The first run of the wave model is performed without wave-current interaction and the radiation stress values at the end of first sub-run are used to calculate the wave-induced currents. When the current velocities have been obtained from the circulation model they are then used for the next run of the wave model for another sub-run time. The values from the wave model obtained at the end of this new time level are then used as driving conditions for the next run of circulation model. Repeat this procedure until the steady state is reached for both the wave and circulation models.

This procedure is quite efficient for simple problems since the initial values used in each sub-run can be quite close to the final results and just a few alternative runs are sufficient. But for complicated problems the wave models have to be run for quite a long time and any errors originated from the boundaries will propagate into the entire internal area. The computational results can, therefore, be contaminated.

An alternative approach has been followed in this work, which is considered more flexible and not prone to the accumulative numerical errors generated from the inaccurate representation of the boundary conditions. The idea is that rather than regarding each run as part of the total time sequence, it is considered independent one from the another. Initially the waves are also calculated without the effect of current and quantities such as wave height, wave angle and radiation stresses are determined. With these driving terms being determined the current field is then calculated by running the circulation model. Next, the wave field is recalculated taking into account the effect of currents but the calculations start from the same simple initial state as in the first run. In this way any errors from

earlier run will not accumulate or spread in the following run. The new input for the circulation model is determined as wave model reaches at a nearly steady state. The circulation is recalculated from the state of rest. By repeating this loop a number of times a steady state can be found for both waves and current system.

Theoretically, these two procedures should give the same results for the same problem if the boundary conditions can be described exactly. But in most of the cases the boundary conditions are far from accurate so that proper control of error spreading must be taken into account.

Detailed computational procedures are as shown in the flow charts for the wave and circulation programes which are named, repectively, as MSWAVE and CIRCU.

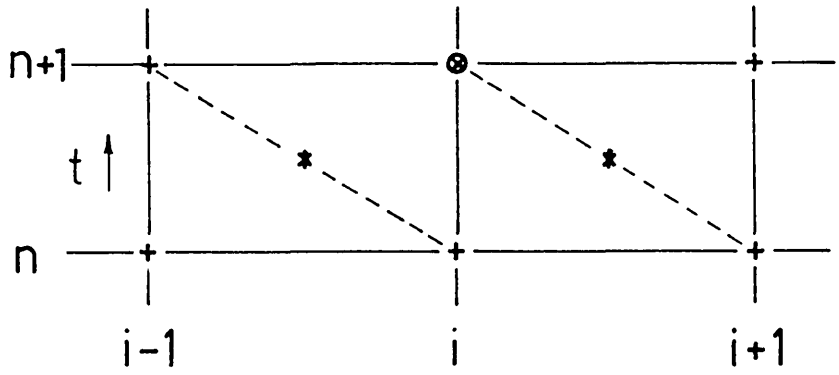


Fig. 6.1 Angled Derivative Scheme for One Dimensional Case

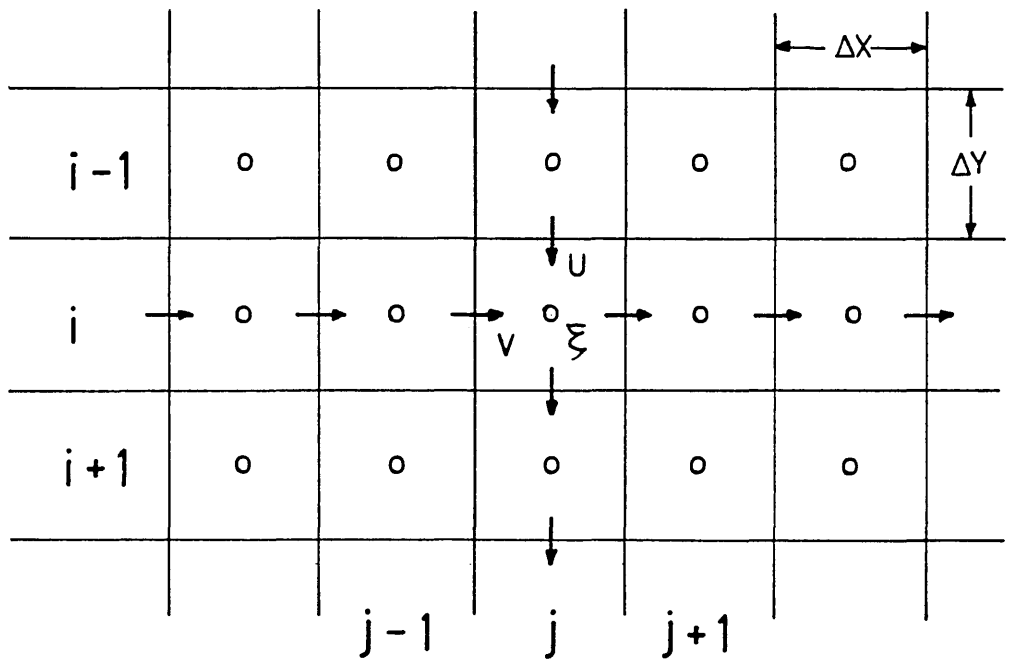


Fig. 6.2 Finite Difference Grid System for the Circulation Model, U and V are Defined at Grid Edges and All the Scalar Quantities (ζ, h, K, τ) at Grid Centers

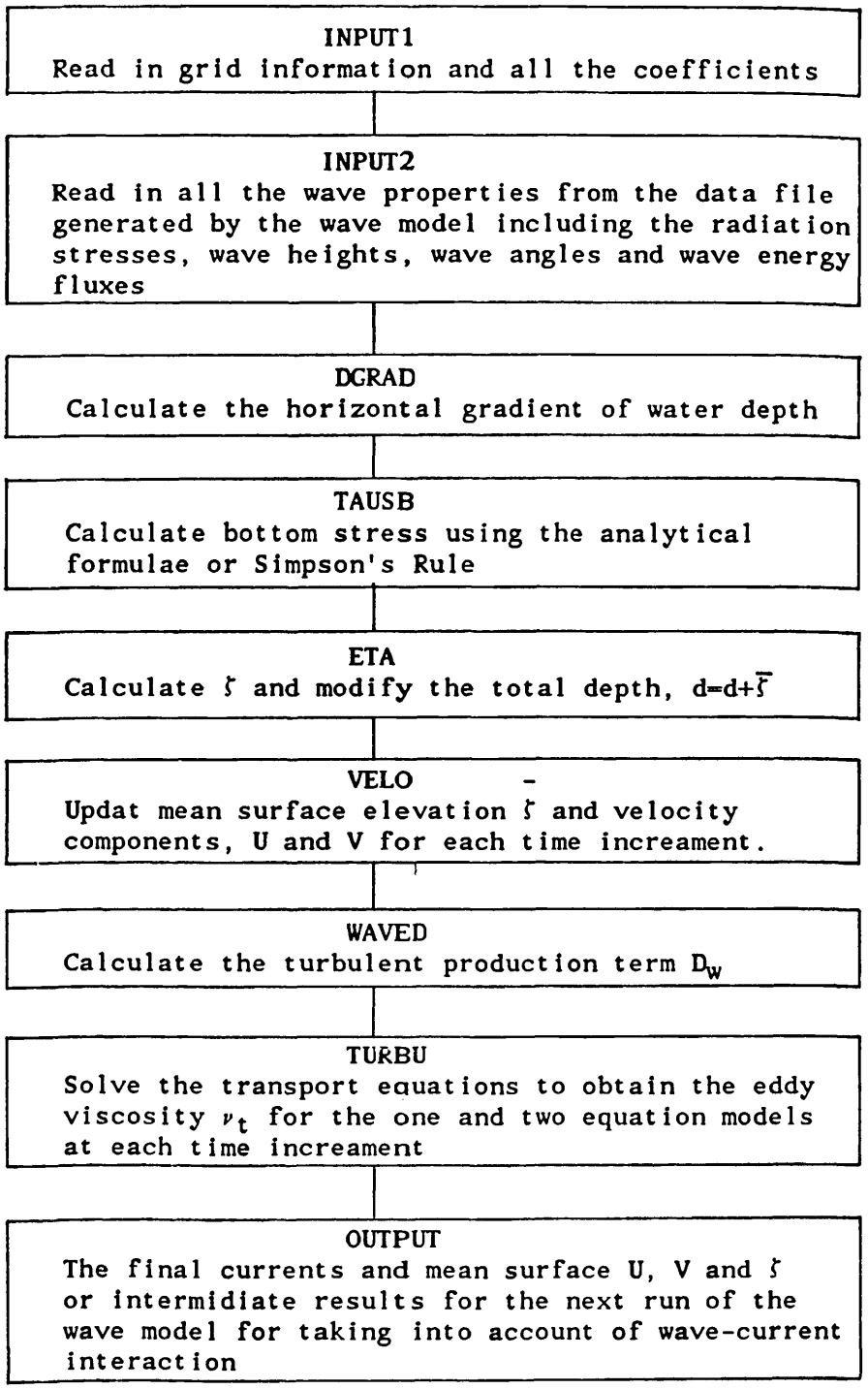


Fig. 6.3 Flow chart for the program CIRCU

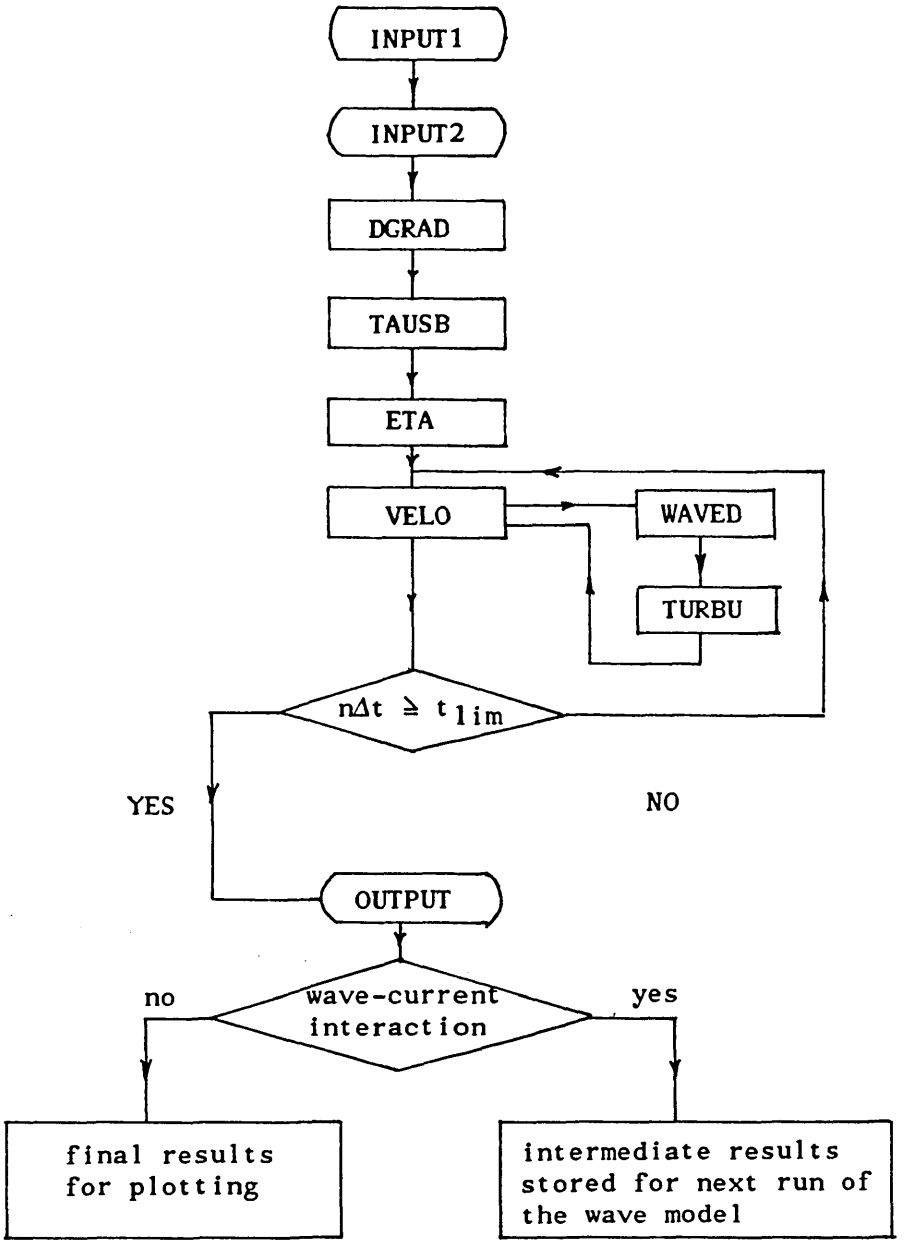


Fig. 6.3 (continued)

CHAPTER. 7
VERIFICATION AND APPLICATIONS OF THE WAVE MODEL

7.1 Introduction

The wave model presented in Chapter 3, applicable for problems of wave propagation without the effect of current, has been extensively verified for typical coastal situations by both Copeland (1985) and Walker (1987). For simple coastal configurations where analytical solutions are available, the comparisons between numerical results and analytical solutions are generally quite satisfactory. The comparisons with experimental data are less satisfactory but still quite reasonable from the engineering point of view.

To demonstrate the performance of the wave model developed based on the transient mild-slope equation discussed in Chapter 3 two typical cases have been computed using the program developed originally by Walker (1987) based on eqs. (3.18), (3.19a) and (3.19b).

The first example is wave diffraction by a semi-infinite breakwater. The analytical solution for this classic case has been given by Penny and Price (1952) which is shown in Fig. 7.1. In order to achieve accurate numerical solutions using this wave model two conditions should be satisfied. One is that the computation domain must be at least several wave lengths in the two directions. This condition ensures that disturbances from the boundaries due to the use of imperfect boundary conditions do not affect the results in the internal area. Thus, a grid area of 8L $\times$ 8L is used in this case, where L is the wave length of the incoming wave. Another condition which needs to be satisfied is that the duration of integration must not be too long since any numerical errors from the boundaries tend to spread into the internal area and affect the accuracy of final results. The longer the run time is, the wider the zone affected by the boundary condition becomes. Therefore, some sensible upper limit of run time must be chosen. According to the experience gained in many numerical experiments a rough criterion is that the integration should be carried for as many wave periods as the approximate number of wave lengths over the entire computational domain.

Fig. 7.2 shows the numerical results after eight periods of computation. It can be seen that the overall agreement between numerical results and analytical solutions is very good except in the area close to the lateral boundaries where the solutions exhibit some oscillation which tend to grow stronger when closer to the

lateral boundaries. This inaccuracy is solely due to the inexact nature of the boundary conditions used.

The second example is concerned with wave propagation into an enclosed wave basin. The geometry of the basin and the input wave condition is as shown in Fig. 7.3. The measured wave height contours inside the basin for $\theta = 67.5^0$ are reproduced from Berkhoff (1976) in Fig. 7.4. Figs. 7.5 and 7.6 show the computed wave contours with the run time being 7 and 14 wave periods, respectively. Comparing with the measured data the computed results can be regarded as fairly good. Both higher and lower wave areas are well reproduced by the numerical model. Local differences may be attributed to the fact that the waves involved here can be quite short-crested due to the cross waves generated by reflective sources and some nonlinearity effects may also be present, which can not be taken into account by this linear wave model. As it is generally the case with this type of problems multi-reflections are always present and the boundary conditions can not be specified accurately. The steady state has already been reached after 7 periods of run and further integration to 14 periods does not change the results appreciably. This is because at the lateral boundary which is, in this case, fully reflective, the no flux boundary condition is used which is an exact boundary condition and does not have the same problem as the transmissive boundary conditions.

In this chapter one aspect of the wave-current interaction will be examined based on the complete model equations developed in Chapter 3. Instead of treating the full process of wave-current interaction the effect of the current on the transformation of waves alone will be treated here. Only non-breaking waves are considered so that the basic wave model can be tested and verified without the effect of any empirical approximations. The full interaction between waves and wave-induced currents including the effect of breaking will be examined in Chapter 8.

The cases that have been studied include

a) wave refraction by a shear current

b) interaction between shoaling waves and Arthur's analytical rip-currents

c) waves around a semi-infinite breakwater with the presence of a shear current

7.2 Wave Refraction By A Shear Current

Studies of wave refraction by a shear current with gradual variation in

amplitude in the cross-flow direction have been very extensive. According to the classic ray theory the waves can be simply refracted, reflected or even trapped depending upon the characteristics of the wave and current as well as the relative directions of these two motions (Peregrine, 1976).

Instead of dealing with the general complex interactions between wave and current involving reflections and caustics, this section is confined to a steady wave train refracted by a shear current in water of uniform depth. Specifically, the aim is to examine the transformation of waves propagating across a shear layer with a triangular velocity distribution, as shown in Fig. 7.7. The input wave height H is 1 m, wave period 8 seconds, maximum shear velocity V_{max} at the centre of the shear layer is 2m/sec and the angle of incidence $\alpha = 210^{\circ}$. The still water depth d is 8 m.

The computed relative wave height and the wave angle together with the analytical solutions obtained using the simple refraction method are as shown in Figs. 7.8 and 7.9. It can be seen that overall agreement for both the wave height and angle is excellent except in the area close to the down wave outgoing boundary where the ten percent errors in calculated wave height and two degrees error in wave angles can be observed. These errors should not be attributed to the presence of the current or to the particular numerical method used. They are actually solely caused by the imperfect transmissive boundary condition.

If the waves are incident at an angle to the boundary, the boundary condition only allows part of the wave energy to go through the boundary and the rest is reflected back into the computational domain. The point made above can be further supported by the results from two simple cases, one is wave propagation in a water of uniform depth and another is wave refraction by a plane beach, with all the other input data being the same. As shown in Figs. 7.10 and 7.11, the wave heights are correctly calculated in most part of the domain but not close to the outgoing boundary. The same degree of error occurs here as in the previous case.

The reason for the slight under-prediction in the wave angle is not obvious. It may be due to the fact that the physically unrealistic change of slope in the current distribution violates locally the slowly varying condition required for the current in the present wave model. Consequently, the numerical model is unable to respond quickly enough to such an abrupt change in the current velocity distribution.

7.3 Interaction Between Waves And Analytical Rip-Currents

The applicability of this wave model is demonstrated for a more general and complicated wave-current interaction situation where the conventional ray method is invalid due to the existence of cusped caustics. An ideal case for such a test concerns the wave interaction with an analytical rip current system, which is a problem originally studied by Arthur (1950) using the ray method and recently by Liu (1983) using a parabolic equation.

The current system exists on a plane beach with a slope s = 0.02. Its velocity components are defined by

$$V = -3.60\left[2-\left[\frac{x}{250}\right]\right]F\left[\frac{x}{250}\right]\int_0^{\frac{-y+300}{25}} F(\alpha)\, d\alpha \qquad (7.1)$$

$$U = 0.1442x\ F\left[\frac{y}{250}\right]F\left[\frac{-y+300}{25}\right] \qquad (7.2)$$

with the function F defined by

$$F(\alpha) = \frac{1}{\sqrt{2\pi}} \exp\ (-\alpha^2/2) \qquad (7.3)$$

where the length and the time units are in feet and seconds, respectively.

The typical velocity profiles along x = 150 ft and along the centre line, y = 300 are shown in Fig. 7.12.

Arthur (1950) constructed a set of wave rays for a train of monochromatic waves with the wave period being 8 seconds as reproduced here in Fig. 7.13. Along the centre line many caustics appear and the classic ray theory fails there since it will give an infinite wave amplitude. Although at or near the ray focusing points the nonlinearity may be important the linear mild-slope equation is expected to be able to give a reasonable first order approximation.

The computation is carried out over an area of 800 x 600 ft^2. Both the offshore and lateral boundaries can be regarded far enough away from the area of interest. Also, since the currents at the boundaries which are either too small to be effective or are parallel to the wave front and therefore, have no effect on the incoming waves, the incoming waves at the offshore boundary as well as the two lateral boundaries are maintained as input sine waves. In order to ensure there are

enough grid points per wave length the space and time increaments are necessarily small. Increaments $\Delta x = \Delta y = 5ft$ and $\Delta t = 0.2sec$ are used in this study. The minimum depth at the outgoing boundary is 0.2ft.

Fig. 7.14 presents the relative wave amplitude along the centre line of the computational domain (y = 300ft). In the same figure the results from pure shoaling and from Liu's parabolic approximation are also shown. It can be seen that the present model, as well as Liu's parabolic equation solution, predicts the wave at caustics to be of finite height but much higher than that due to simple shoaling. The present numerical solution predicts similar trend of variation in wave height at the centerline and almost the same location of maximum height as Liu's model. However, the overall wave height predicted by the present model is smaller than that predicted by Liu's solution. This result suggests that, for this particular case the parabolic equation model may be a reasonable approximation to the full mild-slope equation but even so the difference in predicted results from the two models is quite appreciable. Fig. 7.15 is a wave height contour plot for this case and Fig. 16 presents the relative wave heights along various cross sections (dashed lines). They all show clearly that the waves are greatly enhanced by the presence of such a current system. The high waves are concentrated in a narrow strip along the line of symmetry where the rip current is the strongest and therefore, has the maximum effect on the incoming waves.

As already discussed in Chapter 3, in many real situations the waves can be very complex and it is not always possible to know the wave angle at the start of the computation. The calculation of the wave number k under such a wave-current co-existence situation, therefore, becomes difficult due to the lack of information about the wave angle. In order to avoid this difficulty Booij (1981) has suggested the possibility of estimating k without taking into account the effect of current and include the current effect only in the governing equation. This method needs a quantitative verification.

In the present study the same rip-current problem has been calculated again without including the currents in the calculation of k. The relative wave height along the centre line is plotted agaist the previous result as shown in Figs. 7.17 and the relative wave height contour for this case is as shown in Fig. 7.18. The wave heights along the same cross sections are shown in Fig. 7.16 (continuous lines). It is clear that the wave height is significantly under predicted using the method recommended by Booij. The location of maximum wave height is also not correctly predicted. Therefore, it must be a necessary requirement that in the calculation of k the effect of current should be included whenever it is possible.

7.4 Waves Around A Semi-Infinite Breakwater in the Presence of A Shear Current

The wave propagation around coastal structures with the presence of steady currents such as tidal currents is of great engineering interest. But up until now little theoretical or experimental work has been done, due to the difficulties involved in the analytical formulation and experimental simulation of such complex types of interaction. The extended mild-slope equation developed by Booij (1981) and this work are considered useful for such prediction purposes, at least as a first approximation.

The same offshore semi-infinite breakwater case already discussed in Section 7.1 is considered again but this time a shear current is introduced. The current velocity V is so defined that it is zero at the offshore boundary and increases linearly to the down wave x boundary. The maximum velocity at the outgoing boundary is 2m/sec.

The wave contours behind the breakwater calculated without and with the current are presented in Figs. 7.19 and 7.20. It is clear that marked difference exists between the two results. An obvious effect of the current is, as expected physically, that it refracts the waves behind the breakwater so that the predicted wave height contours are shifted to the right and the contour slopes are also increased. Furthermore, it can be noticed that the results for the case with current become noisier and the quality of the results near the lateral boundaries has deteriorated. This is because the presence of currents at such boundaries results in more reflection being generated by the imperfect boundary conditions used than without the currents.

The above numerical results should naturally indicate that, apart from the need for experimental data to verify the wave model, more work must to be done to improve the boundary conditions at both lateral boundaries and the outgoing down wave boundary.

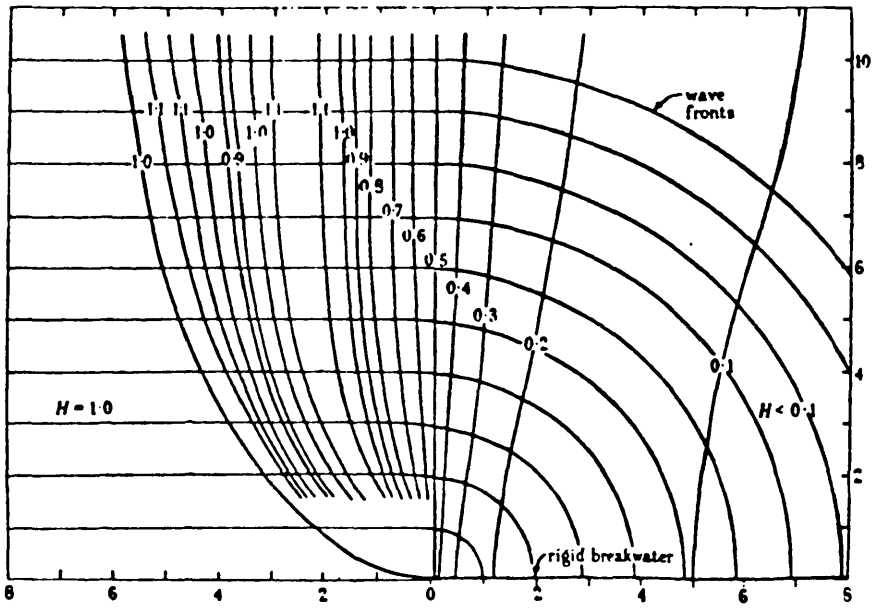


Fig. 7.1 The Waveheight and Wave Front Behind a Rigid Semi-Infinite Breakwater from Penney and Price (1952)

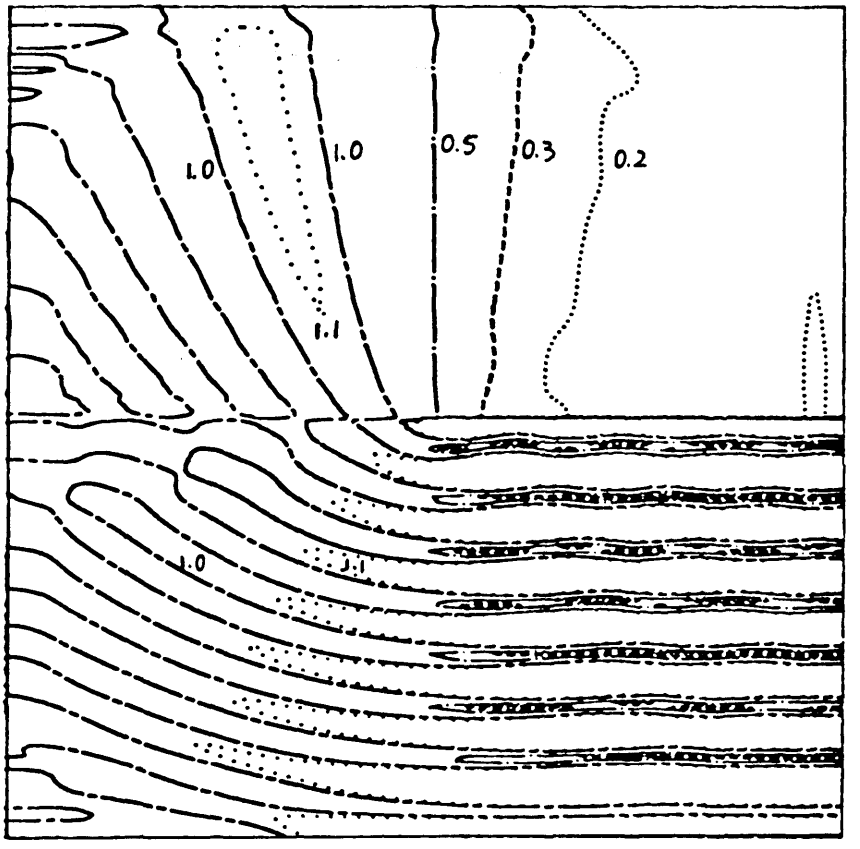


Fig. 7.2 Waveheight Contoursaround a Rigid Breakwater Computed by the Wave Model without the Effects of Current

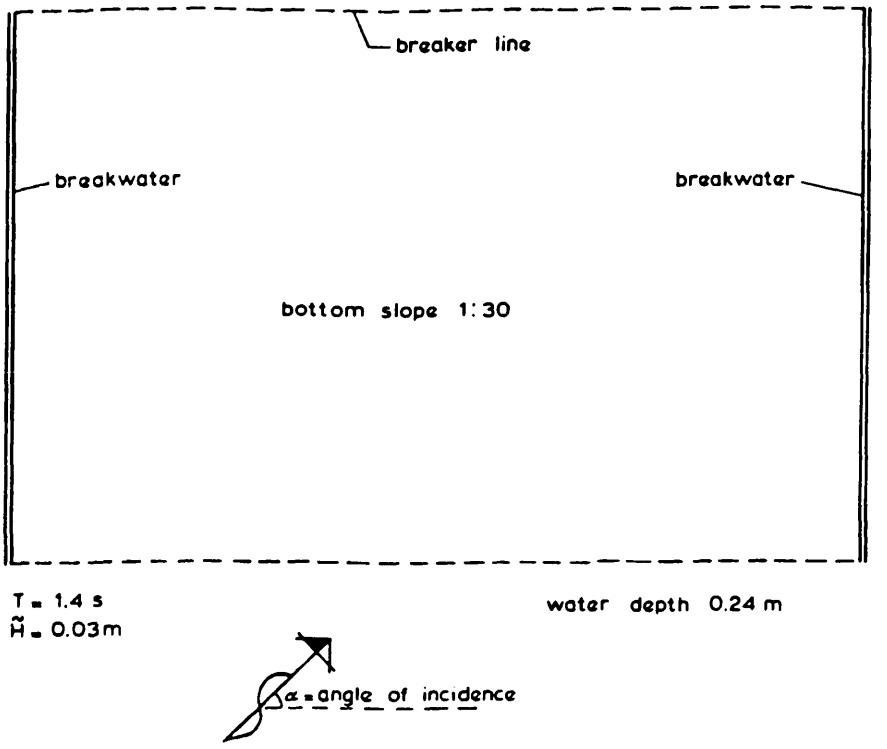


Fig. 7.3 Experimental Set-Up of a Wave Basin from Berkhoff (1976)

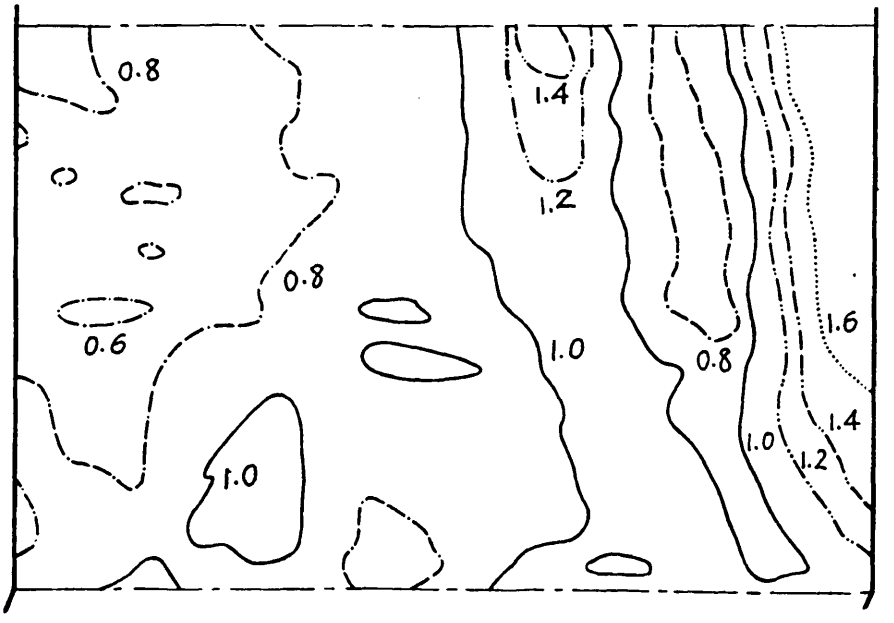


Fig. 7.4 Relative Wave Height Contour, Measured Results from Berkhoff (1976)

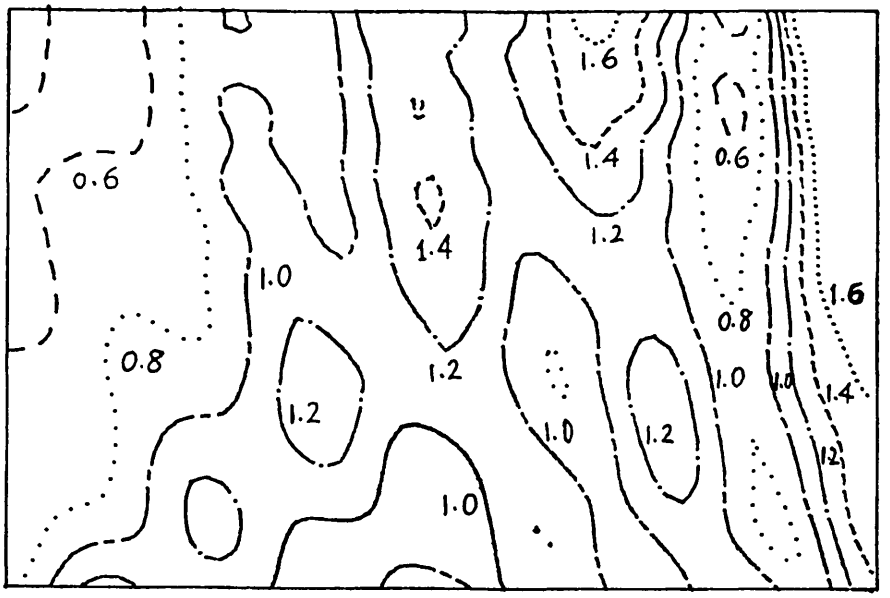


Fig. 7.5 Relative Wave Height Contours, Computational Results with a Maximum Run Time of 7 Periods

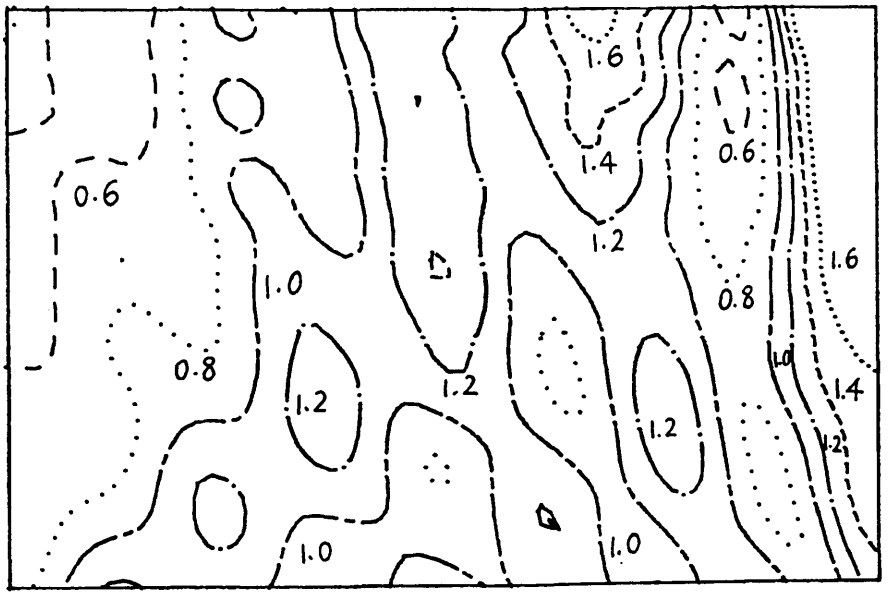


Fig. 7.6 Relative Wave Height Contours, Computational Results with a Maximum Run Time of 14 Periods

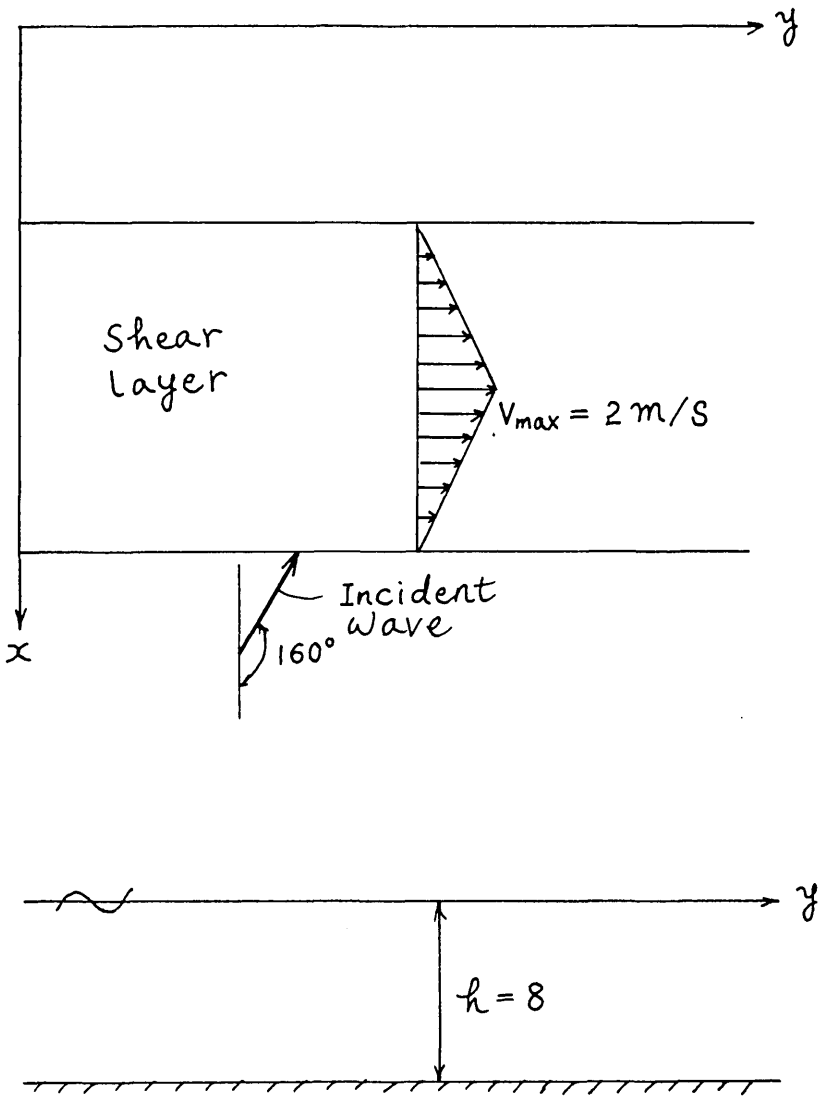


Fig. 7.7 Shear Current Distribution

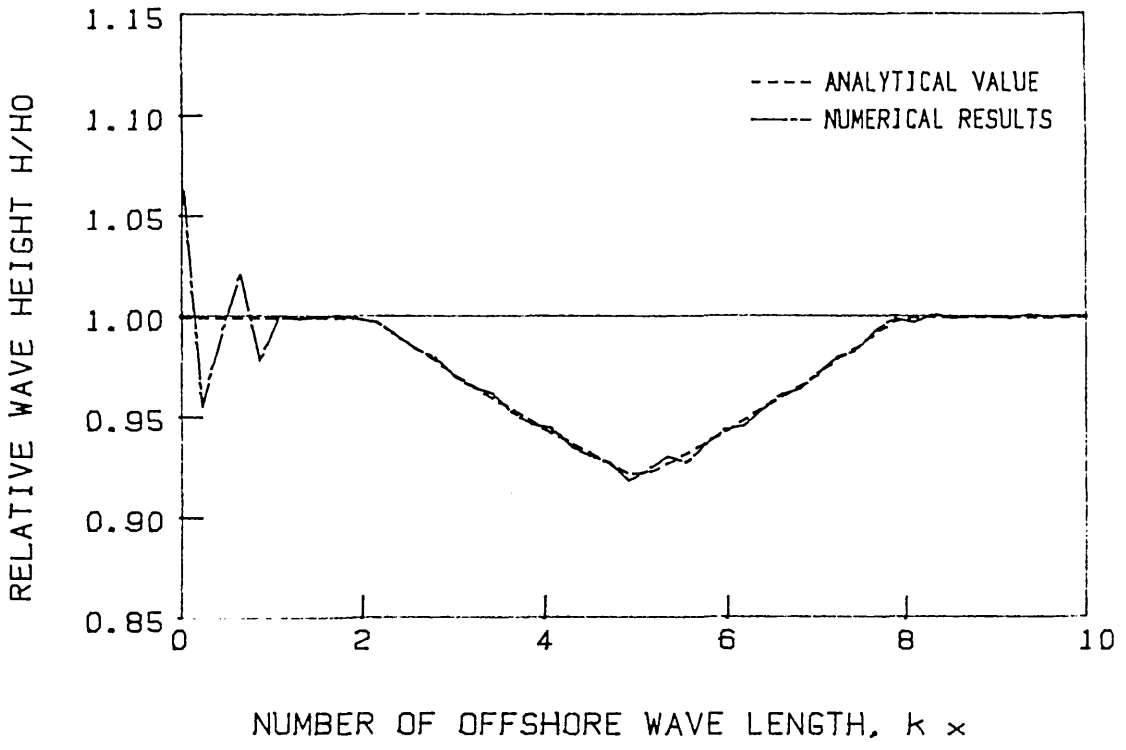


Fig. 7.8 Calculated Wave Heights for Wave Refraction by a Shear Current with Triangular Distribution

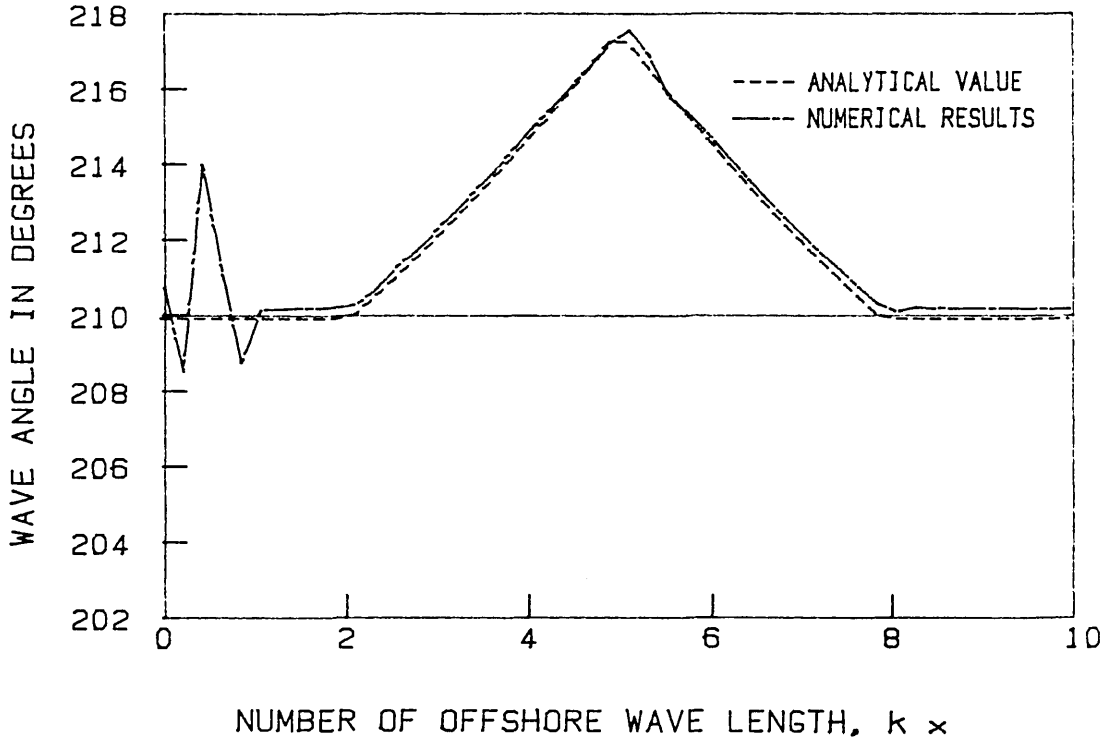


Fig. 7.9 Calculated Wave AngleS for Wave Refraction by a Shear Current with Triangular Distribution

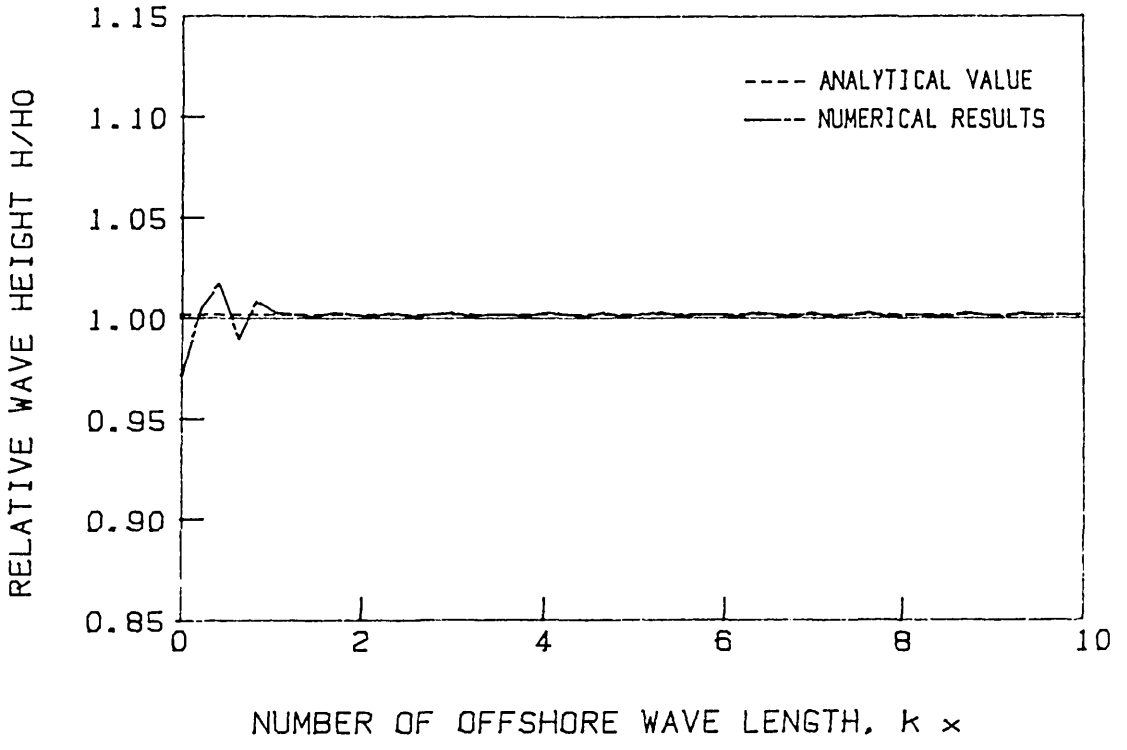


Fig. 7.10 Calculated Wave HeightS for Wave Propagation in Water of Uniform Depth

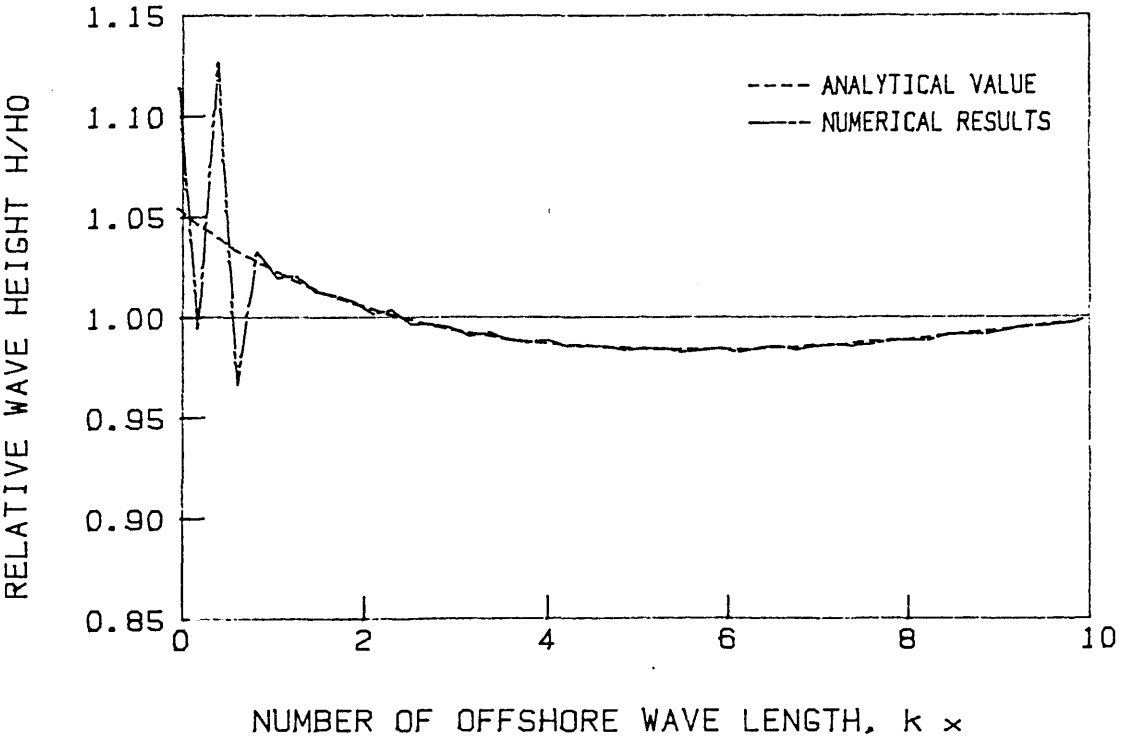


Fig. 7.11 Calculated Wave Heights for Wave Refraction on a Plane Beach

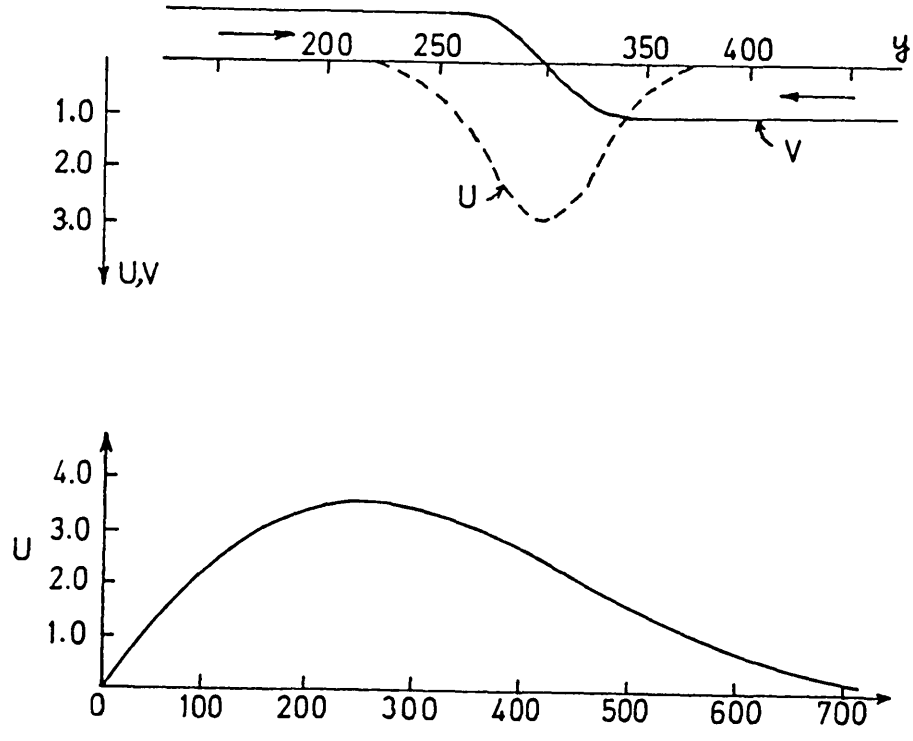


Fig. 7.12 Typical Velocity Profiles, a) U and V along x = 150ft, b) U along the Center Line y = 300ft.

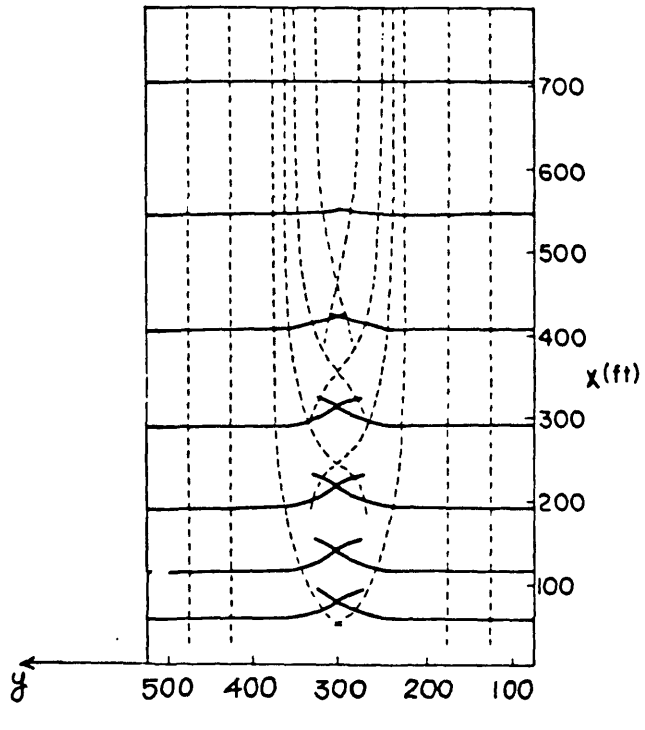


Fig. 7.13 Wave Ray Patern from Arthur (1950)

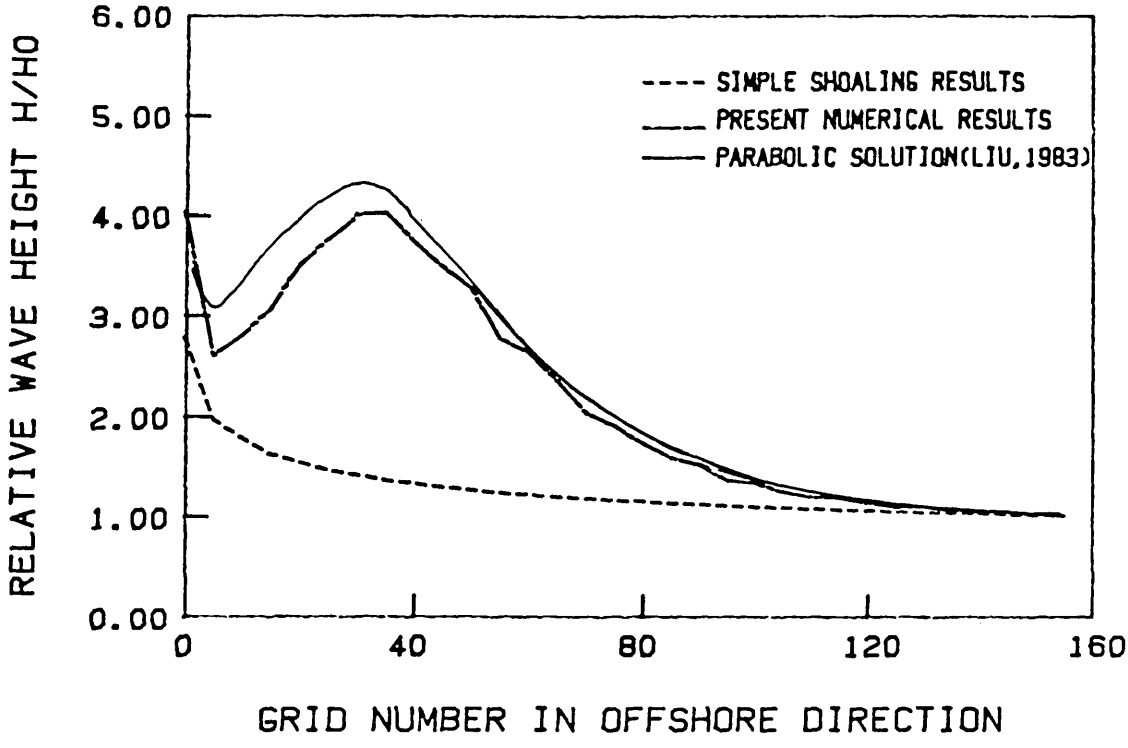


Fig. 7.14 Wave Height along the Centerline of the Currents, y = 300ft, a Comparison with Liu's Parabolic Solution and the Pure Shoaling Results

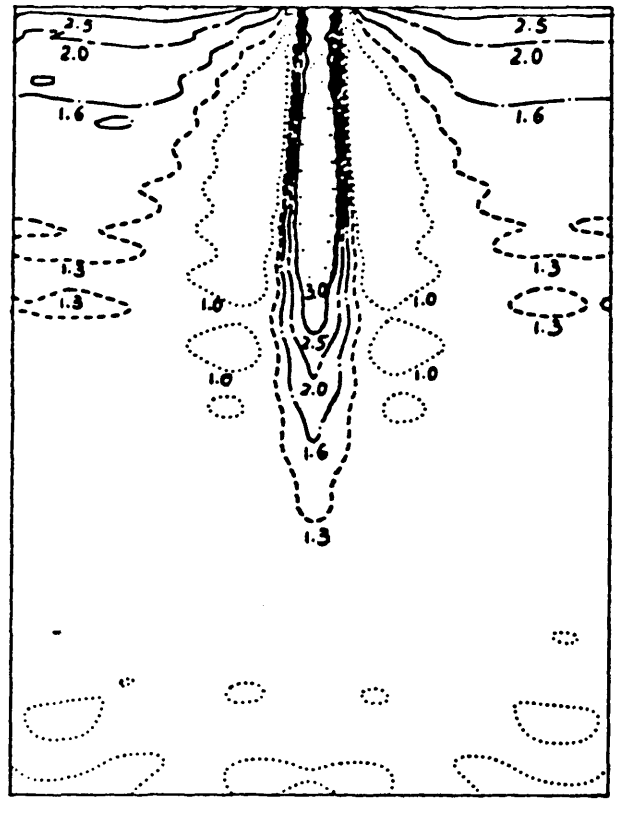


Fig. 7.15 Wave Height Contours, k is Calculated with the Effects of Current

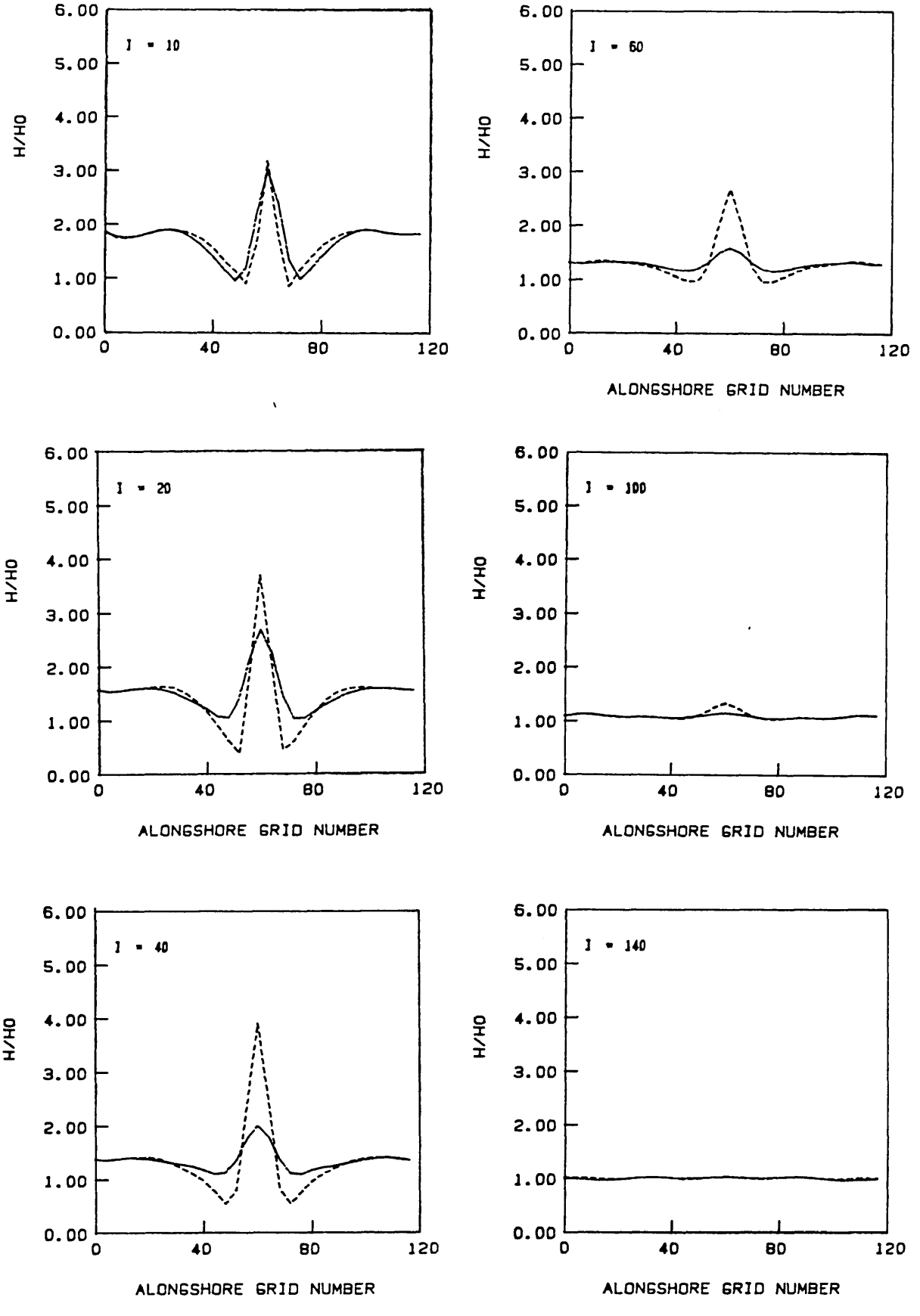


Fig. 7.16 Wave Height Distribution at Various Cross-Sections.

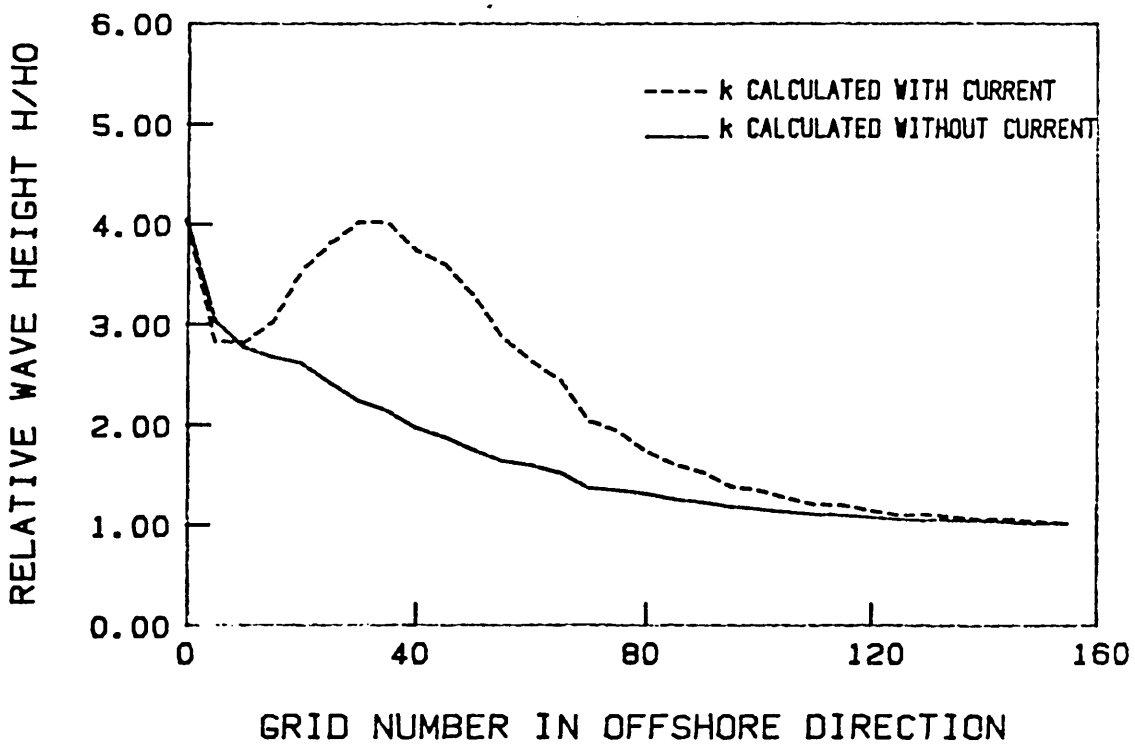


Fig. 7.17 Wave Heights along the Centerline of the Currents, y = 300ft Calculated with and without the Effect of Currents in Calculating the Wave Number k

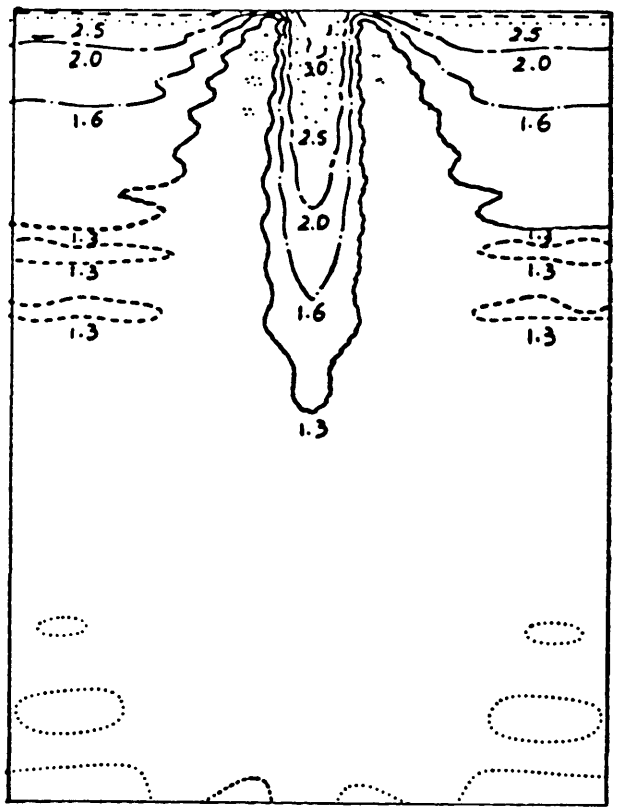


Fig. 7.18 The Wave Height Contours, k is Calculated without the Effect of Currents

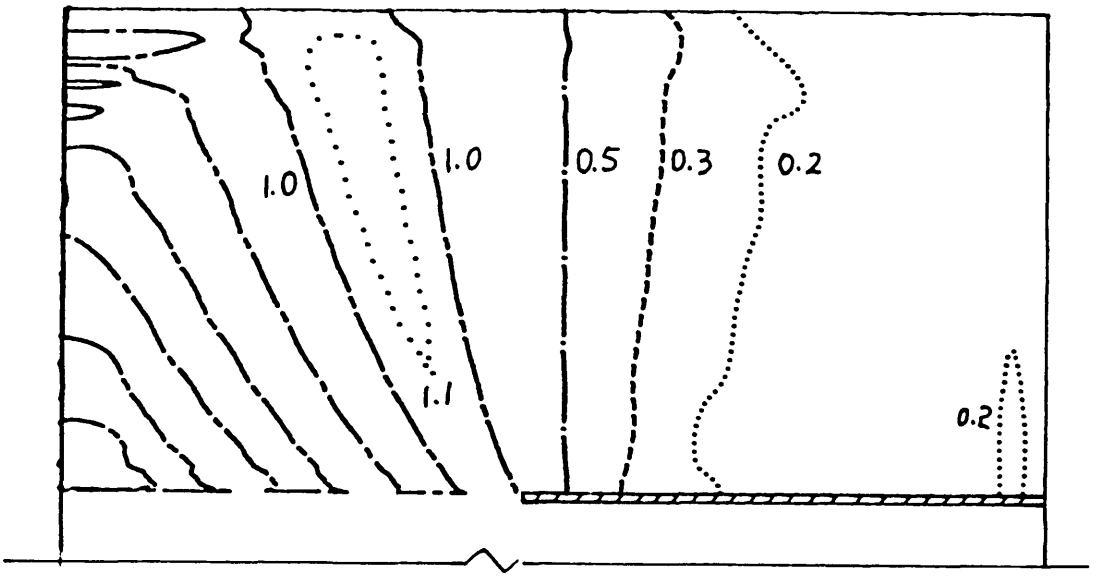


Fig. 7.19 A Detailed View of the Wave Height Contour behind a Rigid Breakwater without the Effects of Current

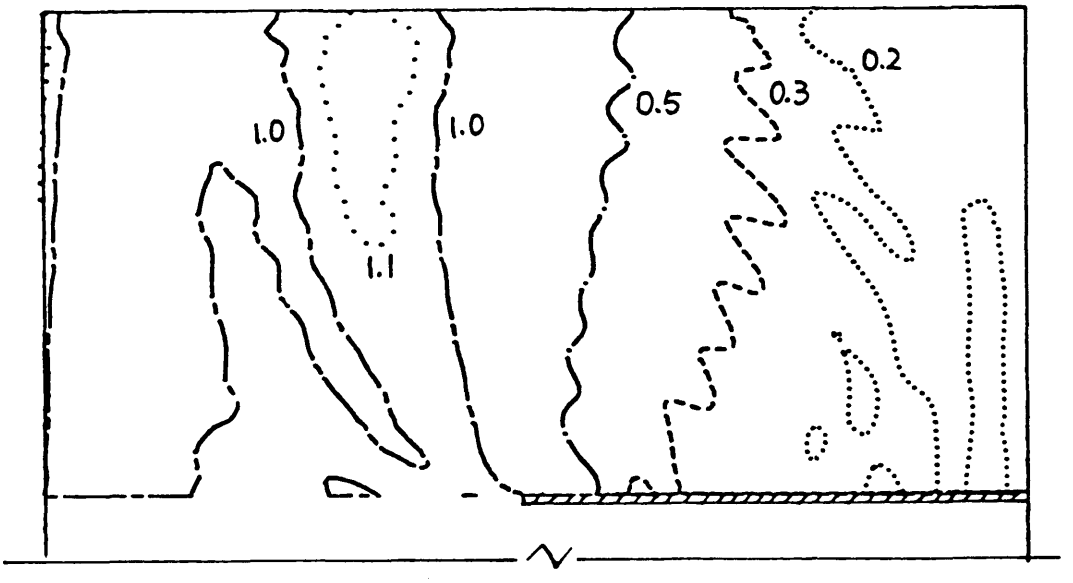


Fig. 7.20 A Detailed View of the Wave Height Contour behind a Rigid Breakwater with the Effects of Current

CHAPTER. 8
THE COMPUTATION OF NEARSHORE CIRCULATIONS

8.1 Introduction

This chapter presents computational results for the wave-induced circulation for a number of coastal configurations. The quantities such as radiation stresses, wave height and wave angle which are required for calculating driving forces for wave-induced circulation are all directly provided by the wave model developed and tested in Chapters 3 and 7, respectively. It is, therefore, hoped that the circulations around coastal structures and in wave basins can be more realistically predicted. Furthermore, by alternatively running the wave and circulation models for a number of times, the full interaction between complex coastal waves and wave-induced circulation has been treated.

Three turbulence models described in Chapter 5 are used for calculating the horizontal mixing due to turbulent motions generated by wave breaking. The advantages and disadvantages in using each of above turbulence models are assessed.

The reliability of the numerical circulation model is verified against available analytical solutions and some published data from physical model tests. The effects of wave-current interaction and different modelling techniques used to describe the turbulence mixing on the computed circulations are analyzed separately for most of the cases considered.

The following cases have been studied:

a) the prediction of longshore currents on a plane beach, which mainly serves the purpose of verifying the numerical accuracy of the model.
b) the circulation pattens on Noda's sinusoidal open beach, where both the effects of wave-current interaction and the use of different turbulence models are examined.
c) the circulation around a breakwater, which is a case suitable for further tests of the proposed turbulence models with turbulence production being controlled not merely by the bottom contours but also by the more complicated wave forms caused by diffraction.
d) da Silva Lima's experimental sinusoidal beach in an enclosed wave basin, which is considered as an ideal case to study the performance of wave and circulation models developed in this work.

8.2 Longshore Currents On A Plane Beach

This section examines the longshore currents generated by a series of long-crested waves breaking on a plane beach at a small angle of incidence to the shore normal. The study of this basic case is intended to serve primarily two purposes,

1) to verify the numerical accuracy of the model by comparing the numerical results with the analytical solutions by Longuet-Higgins (1972a, b).
2) to evaluate the effect of different turbulence modelling techniques on the computed longshore currents.

The geometry of the plane beach and the input incident wave conditions are as shown in Fig. 8.1. The depth increases linearly from a minimum depth 0.5m at the shoreline to 5.5m at the offshore boundary. The input data used are: offshore wave height, H_0 = 3m, wave angle θ_0 = 200°, wave period T = 6 seconds and bottom slope s = 0.02. The wave height and angle at each grid centre have been estimated by using Snell's Law and simple shoaling calculations so that the driving condition is the same as that used in the analytical method. In order to construct a valid comparison with Longuet-Higgins' analytical solution, the wave celerity is calculated by the shallow water approximation, and the still water depth rather than the total water depth is used in the numerical integration.

Two further input quantities needed are C_f and N (see Chapter 4 for definition). By analysing field and laboratory data Longuet-Higgins (1970b) established a single important parameter P defined as

$$P = \pi \frac{s}{C_f} \frac{N}{\gamma} \tag{8.1}$$

where s is the bed slope C_f is the bed friction factor, N is a mixing coefficient and γ is the breaking index. With s = 0.02, C_f = 0.01, γ = 0.88 and P = 0.3 eq. (8.1) gives N = 0.042. This parameter mainly reflects the relative importance of bottom friction and the horizontal mixing and its value should be in the range of 0.2 ~ 0.4.

Finally, following Ebersole and Dalrymple (1981), the deep water wave height was built up gradually in the first 50 secs of integration in order to avoid unrealistic seiching to occur.

The comparison between the analytical solution and the numerical solution

using the zero equation turbulence model is as shown in Fig. 8.2. The agreement is excellent and numerical diffusion which, apparently exists in some other models, is not evident here.

Computations were then carried out for the same case using the one and two equation turbulence models. Before presenting the comparison of the results from these three models some discussion on the determination of $c_{\mu 1}$ and $c_{\mu 2}$ is needed. For the one equation model $c_{\mu 1}$ was suggested by Visser (1984) as 2.5 ~ 3.0 in order to achieve the best fit with his laboratory data. However for the present set of input data $c_{\mu 1}$, as well as $c_{\mu 2}$ in the two equation model, have to be as high as 10.0 in order to achieve a maximum longshore current almost the same as that obtained using the zero equation model of Longuet-Higgins. Here, the calibration of $c_{\mu 1}$ and $c_{\mu 2}$ has been based on the comparison of calculated maximum longshore current using the three turbulence models. This is considered to be a simple as well as reasonable criterion. Other criteria are, of couse, also possible. For example, the total longshore flow rate may be used for such calibration. Whatever criteria are to be used, $c_{\mu 1}$ or $c_{\mu 2}$ can not be regarded as a constant or only varying slightly around 3.0. Battjes (1975, 1978), in formulating his zero and one equation turbulence models, anticipated only that the coefficient M ($c_{\mu 1}$ in present notation) should be of order one but did not expect it to be a constant.

The computed longshore currents are shown in Fig. 8.3. It can be seen that all three models predict the same location and magnitude for peak longshore currents. From the shore line to the peak velocity location the results from the zero, one and two equation models are almost identical while appreciable differences are evident in the section from the peak location to the offshore limit. The one and two equation models give a smoother velocity distribution near the peak and a sharper decrease outside the surf zone than that by the zero equation model. This basic trend in the predicted longshore current distribution is more evident in the results from the two equation model than by the one equation model. This is because the eddy viscosity outside the surf zone, which tends to be grossly over specified in the zero equation model, is more realistically estimated by the one and two equation models.

To further examine the effect of $c_{\mu 1}$ or $c_{\mu 2}$ on the predicted current, the reccomended value $c_{\mu 1} = c_{\mu 2} = 3$ was then used for the same case. The resulting longshore currents, together with the corresponding results obtained using the zero equation model with P = 0.03, are as shown in Fig. 8.4. Comparing with the previous calculations, except for the fact that the predicted velocity is now much greater and the location of maximum velocity shifts more towards the breaking line,

the basic trend of variation in the computed current distribution over the entire cross shore area is similar to that noticed previously. Since the mixing is much smaller in this case the results from the zero, one and two equation models become closer than in the previous case.

8.3 Noda's Sinusoidal Beach

Natural beaches are seldom as simple as plane beaches. They are generally uneven and slowly varying in the horizontal directions. In many cases features of bed form are repeatable in the alongshore direction. Therefore, it is considered practically relevant to test the numerical model using an analytical sinusoidal beach which can be regarded as an idealized natural bed form.

To simulate the meandering currents observed by Sonu (1972) along a skewed rip channel, Noda et al (1974) developed a periodic beach profile whose depth is given by

$$h = 0.025 \times \left[1 + \delta \exp\{-3(x/20)^{1/3}\} \sin^{10}\left[\frac{\pi}{80}(y - x\tan\alpha)\right]\right] \text{ (m)} \qquad (8.2)$$

in which

δ = amplitude of bottom contour, taken to be 20

α = angle of rip channel to the beach normal, being 30°.

and the bottom contour and computational domain are also shown in Fig. 8.5

The input wave conditions for this case are wave height H = 0.5m, wave period T = 4 sec and bottom friction factor C_f = 0.01. The empirical constant N for zero-equation turbulence model is chosen as 0.016 which is a value used in many previous works. All the constants that are needed in the one and two equation turbulence models are the same as those in the previous longshore current computations except $c_{\mu 1}$ and $c_{\mu 2}$. The recommended value $c_{\mu 1} = c_{\mu 2} = 3.0$ which is considered to be closely corresponding to the N in the zero equation model is considered appropriate.

The calculations were first performed without taking into account the effects of wave-current interaction. The computed current velocity vectors from the different turbulence models are presented in Figs. 8.6 to 8.8. It can be seen that generally the three models give quite similar circulation patterns. Two weak current zones, one near the shore line and another behind the bed channel, are identifiable in all three sets of results. Marked differences in the magnitude of the computed current

velocities are evident betweem the zero and two equation model predictions, especially in front of the bed channel. The two equation model predicts much stronger feeding currents to the channel than the zero or one equation models. Also the currents predicted by the two equation model tend to be alongshore across the bed channel rather than forming strong rip current along it. These results indicate that the transport effect of turbulence quantities may be quite important. If a two equation model is used the computed current distribution is not only controlled by the sea bed form but also by the turbulence mixing which is not determined locally.

However, there are only small differences between the results from the zero and one equation model. This should not be surprising since, in fact, it confirms the observation by turbulence modellers in many other branches of fluid mechanics that most of one equation models are not much better than zero equation models for general turbulent flow computations. Finer details in turbulent flows with recirculation can only be predicted by a two equation model or other sophisticated turbulence models involving the solution of more than one transport equation.

Wave–current interactions are then introduced by running the wave model and current model a number of times. The zero equation model is used for this series of runs so that the effects of wave current interaction can be analysed independently. In order to ensure numerical stability the current is incrementally increased to its final value over several wave periods. This procedure effectively avoids the difficulty encountered by the model of Noda et al (1974) where the rip current stops the waves in the bottom channel.

Fig. 8.9 presents the velocity vector after first two alternative runs of wave and circulation models. The computations have been carried out up to 7 alternative runs of the wave and circulation model but no appreciable difference can be identified from the results obtained at the end of the second run, suggesting a steady state having been reached. From Fig. 8.9 it can be seen that the inclusion of wave–current interaction has an appreciable effect on both the distribution and magnitude of the resulting currents. The currents close to the shore line become stronger and the small circulation cell near the shore line, which has been predicted without taking into account wave–current interaction, disappear completely after two runs of the wave and circulation models. Also the predicted currents tend to flow in alongshore direction and do not follow the depth contours as closely as that predicted without the wave–current interaction.

The above results clearly indicate that, for wave–induced currents with strong

circulations such as this case both turbulence transport and wave–current interaction are generally important and needed to be taken into account correctly.

8.4 Circulations Behind A Detached Breakwater

This case concerns the circulation behind a detached breakwater. The plane beach is the same as that in Section. 8.3. The incident waves have a wave height H = 0.8m and wave period T = 10sec and propagate at a normal angle to the shoreline. The breakwater in this numerical test is 90 meters long and 60 meters away from the shoreline. The space and time increaments used are $\Delta x = \Delta y = 3m$ and $\Delta t = 0.3sec$. All the coefficients are kept the same as those used in Section. 8.3. Note that for clarity in presentation the output is given at Dx = 6.0m and Dy = 12.0m in Figs. 8.10 to 8.12.

The circulation patterns computed using zero, one and two equation turbulence models without the effect of wave–current interaction are presented in Figs. 8.10, 8.11 and 8.12. The three models give quite similar overall circulation patterns. They all predict correctly that strong rip currents flowing in offshore direction are generated by the diffracted waves along the centerline. These rip currents are fed by the longshore currents in opposite directions, converging initially and then diverging towards the middle of the breakwater. It has long been realized that such currents are responsible for tranporting large quantities of sediment from the shore and then depositing them behind the breakwater to form a special bed form called tombolo.

The results from the zero and one equation models are close even in details. But the two equation model predicts a much narrower rip channel and slightly stronger current velocity than that predicted by the zero and one equation models. Clearly, the turbulent transport in this case is, although not as significant as it might be expected, certainly not negligible.

The wave–current interaction is taken into account by running alternatively the wave and circulation models for up to 3 times when the steady state is nearly reached in the area of interest. The turbulence model used in this case is the two equation model in order to show the combined effect of refined turbulence modelling and wave–current interaction for such an important case. The computational results for first three runs are shown in Fig. 8.13. It can be seen clearly that the rip currents predicted including the effect of wave–current interaction become stronger and the maximum rip current moves slightly offshore. This is because the rip currents, which move against the diffracted waves behind

the breakwater, result in increasing wave height so that the waves break earlier and the width of the surf zone near the center line becomes greater. Another noticeable feature is that the results obtained with wave-current interaction are generally more noisy that those without wave current interaction, especially in the areas where incoming waves and diffracted waves interact. It should be realized that it is not the finite difference scheme which causes this noice, it is actually due to the uncertainties in the wave angle calculations in the wave model. The inclusion of currents make the problem slightly worse.

8.5 da Silva Lima's Sinusoidal Beach In an Enclosed Wave Basin

da Silva Lima (1981) carried out an experimental investigation on the circulation induced by normal incident waves breaking on a sinusoidal beach in an enclosed wave basin and detailed measurements of the current velocities were undertaken. This is an ideal case for testing the applicability of all the models developed in this project including the wave model, circulation model and the turbulence models, since the waves are not only refracted by curved bottom contours but also reflected by the side walls and both wave-current interaction and turbulence transport are also expected to be important.

The grid scheme and bottom contours are as shown in Fig. 8.14. The beach is defined by the following equation for the still water depth

$$d(x, y) = \begin{cases} sx & \text{for } -0.7 \leq x \leq 0 \text{ (m)}, \\ s\left[x - a \sin\left[\frac{2\pi y}{\lambda}\right]\right] & \text{for } 0 \leq x \leq 4.36 \text{ (m)}. \end{cases} \tag{8.3}$$

where s = bottom slope taken as 0.1

a = amplitude of the periodic contour, given by

$$a = 0.75 \sin\left[\frac{\pi x}{4.36}\right] \text{ (m)} \tag{8.4}$$

λ = the bottom contour wavelength in the longshore direction (i.e. the rip spacing) = 6.0 meter; and

$1.5 \leq y \leq 4.50$m.

In order to ensure there is a reasonable number of grid points per wave

length in the shallow water area the wave model has to be run on a much finer grid system than that actually needed by the circulation model. The grid increments used for the circulation computation are Δx = 0.2m and Δy = 0.375m which correspond to the experimental arrangement but these values are devided by four for the wave computation. This difference in grid size makes it impossible to exchange results at each grid point exactly from one model to another so as to perform alternative runs of the wave and circulation models. To overcome this difficulty approximate methods have to be used. In order to generate the wave input for the circulation model a simple averaging method is used while for generating current input for the wave model linear interpolation is used.

The breaking index γ has been chosen as 0.7, which was recommended by da Silva Lima (1981) based on detailed analysis of measured wave height data. The bottom friction coefficient used is C_f = 0.0075, which is considered appropriate for the smooth bed used in the experiment. For the zero equation turbulence model a mixing coefficient N = 0.0035 is used following da Silva Lima (1981) and Copeland (1986). Since wave properties and bed form used in this experiment are within the same range as those used by Visser (1984) it is expected that the value of 2.5 he has recommended for coefficients $c_{\mu 1}$ and $c_{\mu 2}$ is appropriate, and therefore, it has been employed here for the one and two equation models.

The most reliable data set from Silva Lima's experiment is that corresponding to Run 2. This case involves a relatively high offshore wave steepness, H_0/L = 0.0686 and the type of breaker is identified as spilling breaker. Both turbulence mixing and wave current interaction are expected to be important in this case. The measured current velocity is reproduced in Fig. 8.15 for comparison with numerical results.

The predicted velocity vectors using the zero and two equation turbulence models without wave current interactions are presented in Figs. 8.16 and 8.17. Clearly both calculations predict the center of the large outer circulation cell correctly which is slightly toward the right wall which is evident in the experimental measurements. This has not been previously obtained by either Silva Lima (1981) or Copeland (1985) since it is solely due to the non-linear convective terms in the momentum equations which had not been properly treated in either model mentioned above. Silva Lima's model is based on the linear momentum equations and, therefore, unable to take into account the nonlinearity effect. As to Copeland's model, the numerical manipulation used in the model to suppress instability due to the nonlinear convection terms is quite arbitrary and prone to numerical errors.

The small counter-clockwise inner cell near the shoreline which is evident in the experiment results is reasonably predicted by the zero equation model. It is also visible but much weaker in the results from the two equation model. The magnitudes of velocity vectors change sharply in the results from the zero equation model but they change much more smoothly in the two equation results. In spite of the fact that the detailed velocity distribution and magnitude have not yet been satisfactorily predicted by neither the zero equation nor two equation models, the main features of the circulation have, nonetheless, already been reproduced.

Since the wave-current interaction is expected to be important, up to five alternative runs of wave and circulation models were performed. The velocity vectors after each alternative run are presented in Fig. 8.18. Detailed comparison between calculated longshore and inshore-offshore velocites using both the zero and two equation models at the fifth run and the measured data are shown in Figs. 8.19 to 8.25. The experimental values of the velocities used for comparison come from averaging values at neighbouring points at each side of the row concerned.

Clearly much better agreement between these numerical results and experiment measurements is obtained with the inclusion of wave-current interaction than without it. Generally the predictions for both longshore and inshore-offshor currents along Rows 2 to 4 are better than those along Rows 5 to 8, and the results from the two equation model are marginally better than those from the zero equation model. But large discrepancies occur at several rows such as the longshore currents at Rows 7 and 8, onshore-offshore velocities at Rows 6 and 7. This should not be held as evidence to reject the present approach which incorporates the wave-current interaction and the use of the sophisticated turbulence models. Other factors are also responsible for the discrepancies. The effects of inaccurate breaking criteria and the lack of appropriate theoretical representation of bottom friction terms for general wave fields are both important.

Therefore, it should be concluded that this model, although still unable to predict every detailed variation observed in the experiment, does give reasonable prediction of the overall features of the currents and correct velocity magnitude. In some part of the basin the predictions are in excellent agreement with experimental data. Further improvements can be expected if wave breaking can be described more accurately and bottom frictional stress at the sea bed better modelled.

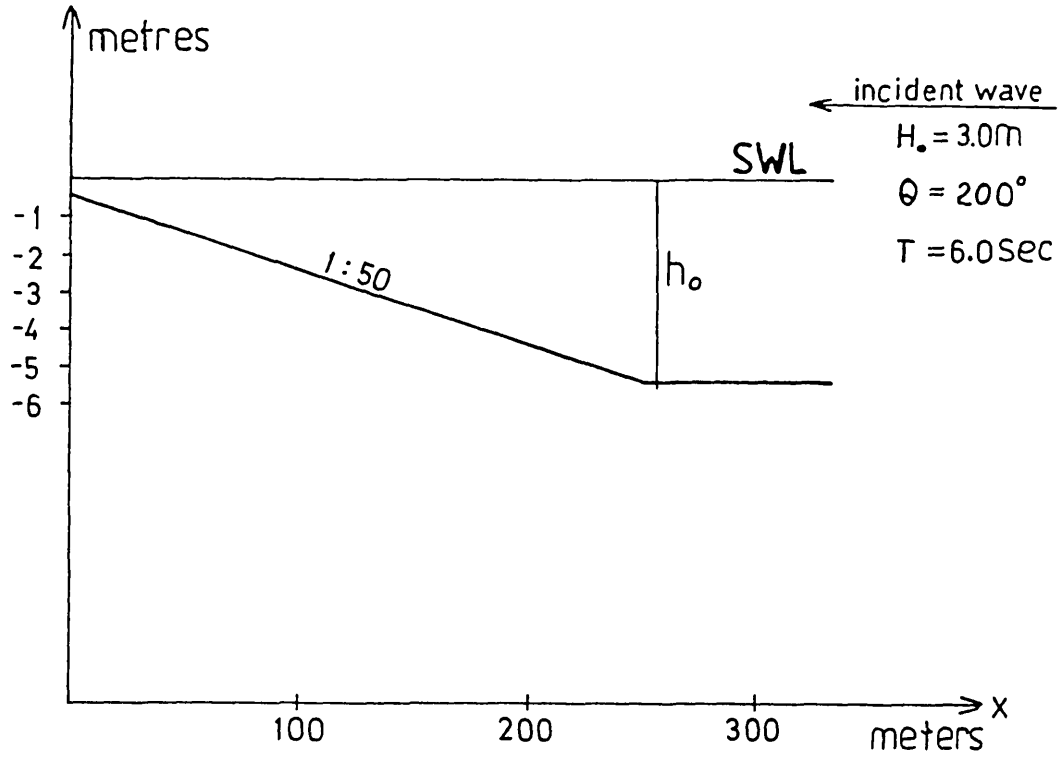


Fig. 8.1 Geometry of the Plane Beach and the Incident Wave Conditions

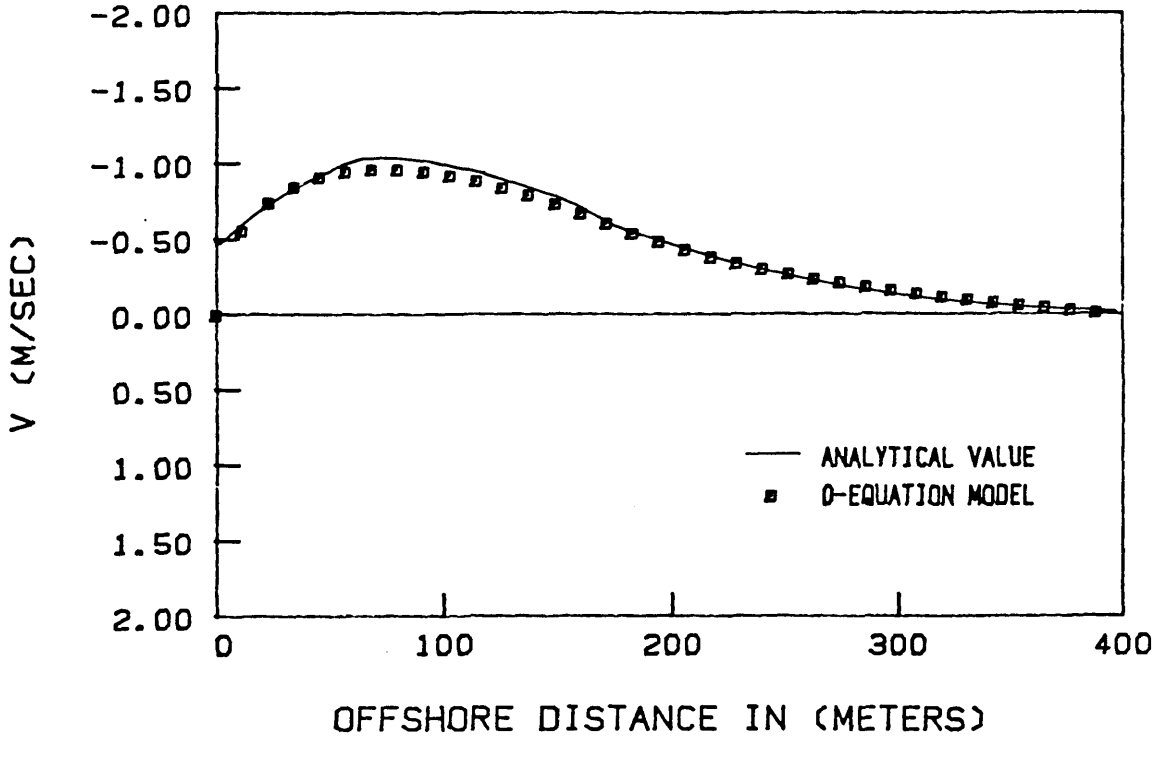


Fig. 8.2 Numerical and Analytical Longshore Current Profile.

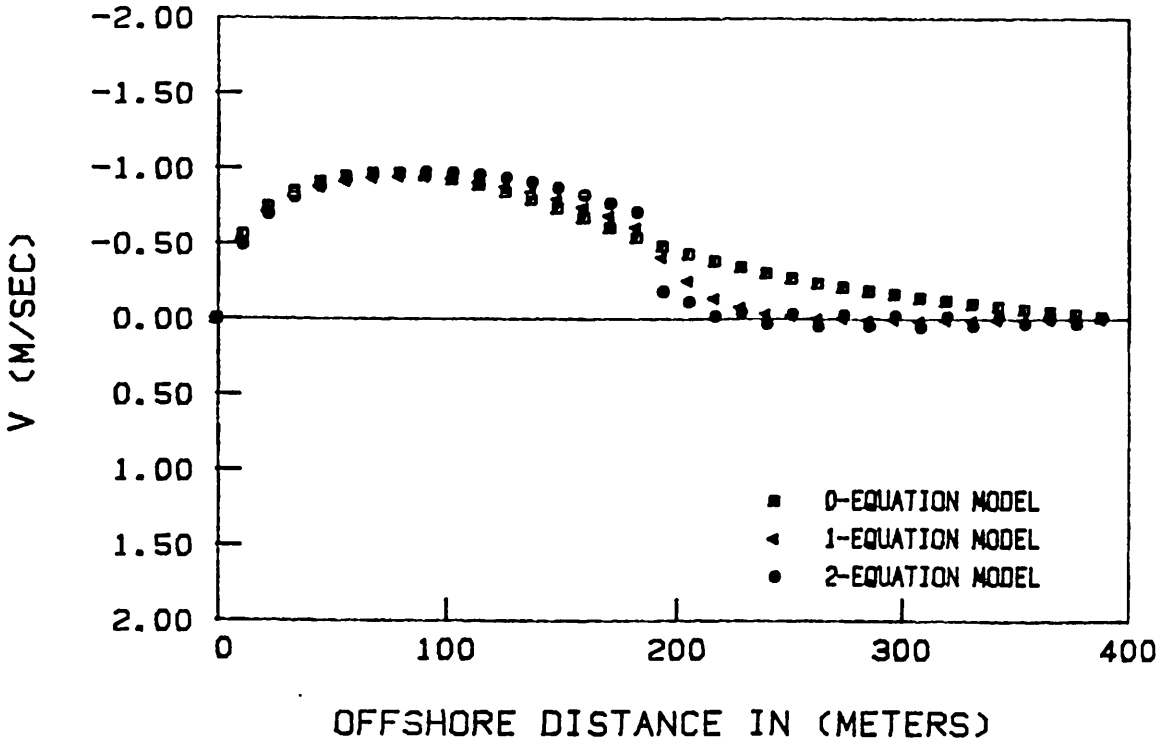


Fig. 8.3 The Longshore Current Profile Calculated by Using Zero, One and Two Equation Turbulence Equation Models, $c_{\mu 1} = c_{\mu 2} = 10.0$.

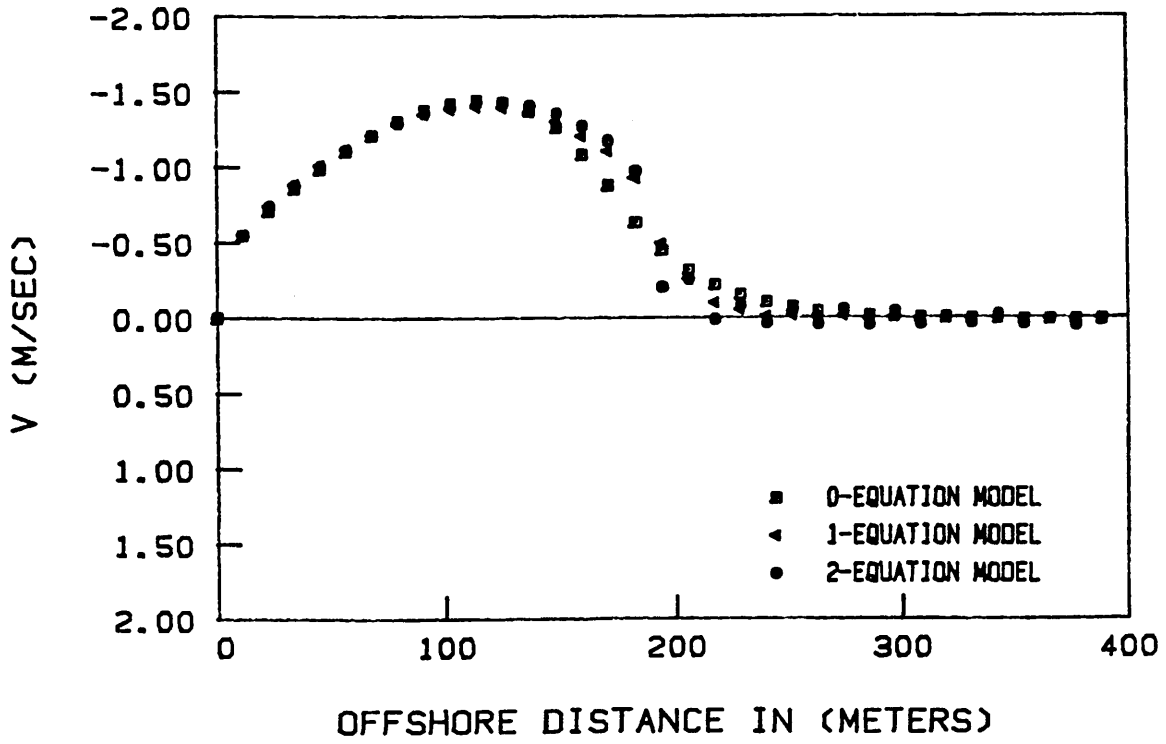


Fig. 8.4 The Longshore Current Profile Calculated by Using Zero, One and Two Equation Turbulence Equation Models, $c_{\mu 1} = c_{\mu 2} = 3.0$

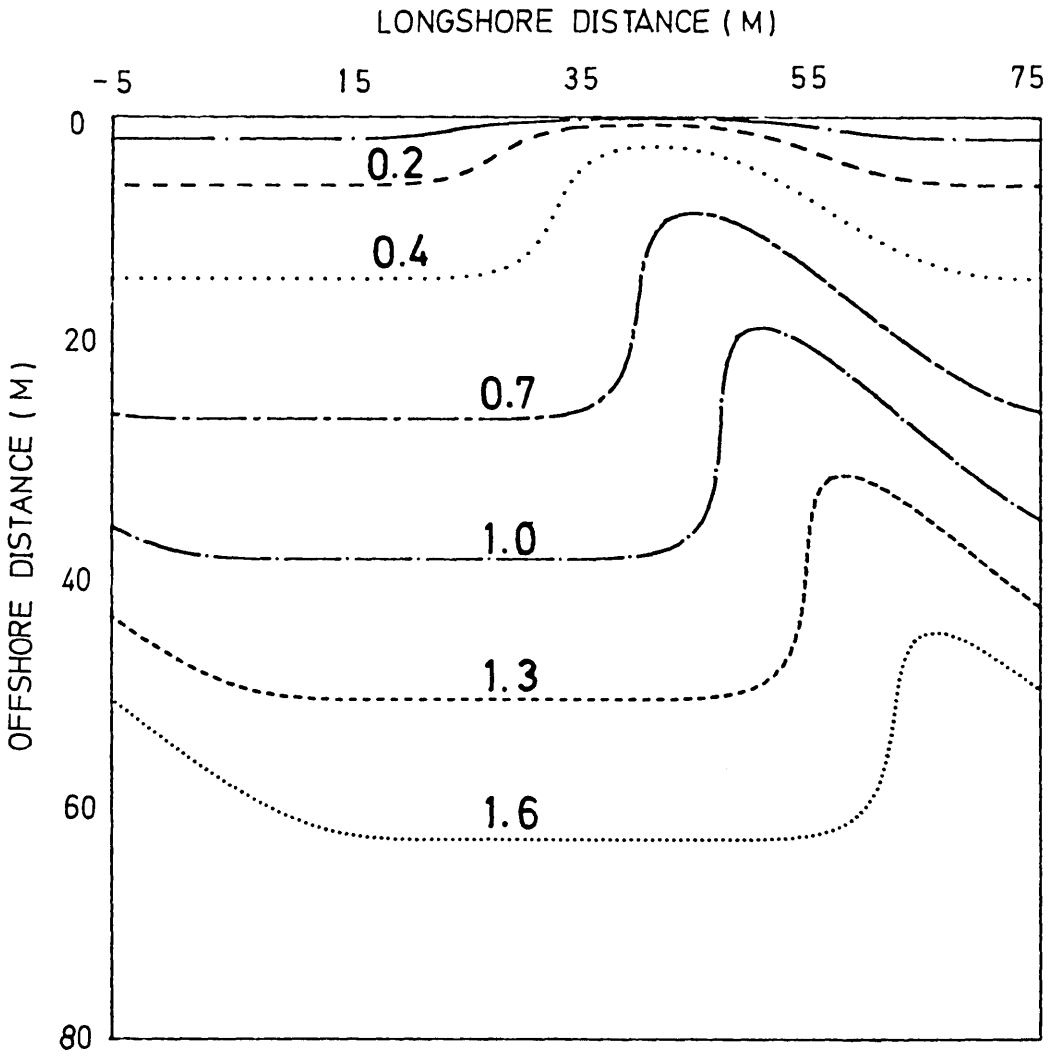


Fig. 8.5 Sea Bed Contours of Noda's Sinusoidal Beach (M)

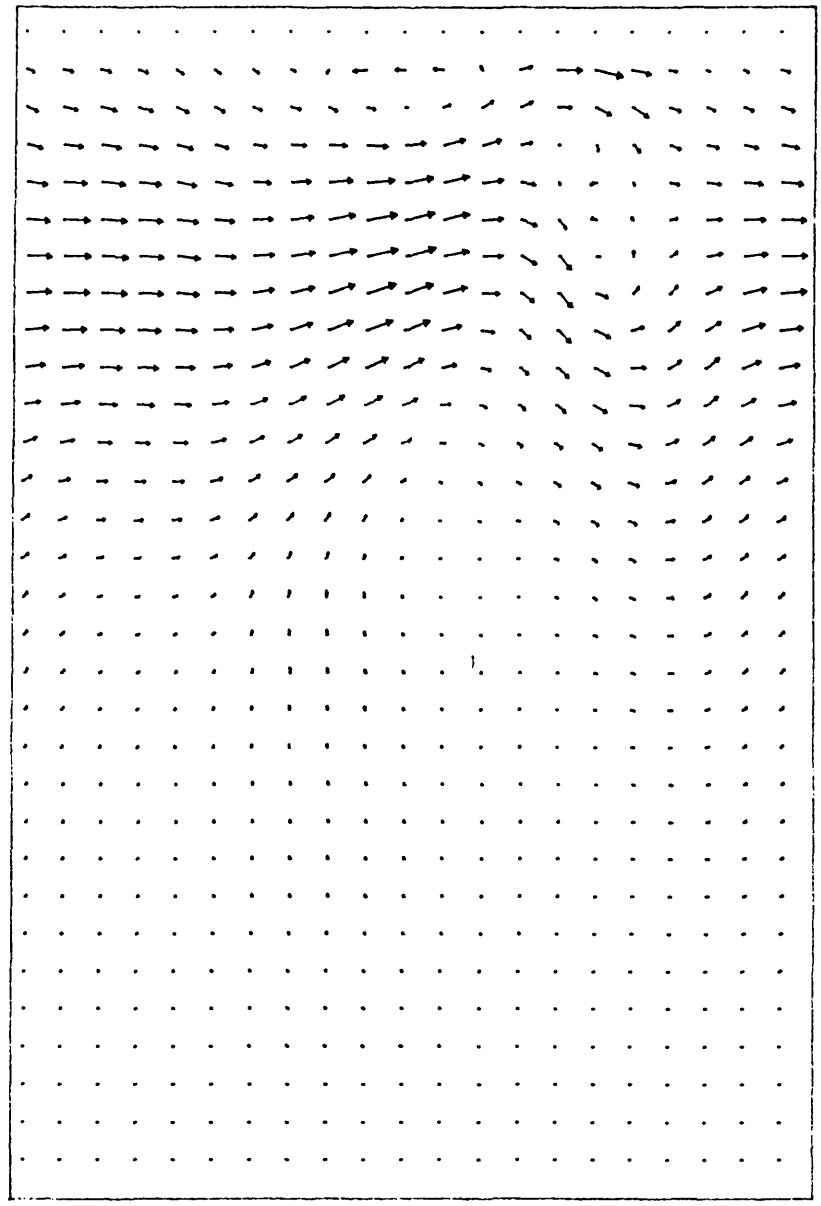


Fig. 8.6 Predicted Current Vectors for Noda's Beach, Using Zero Equation Turbulence Model and No Wave Current Interaction

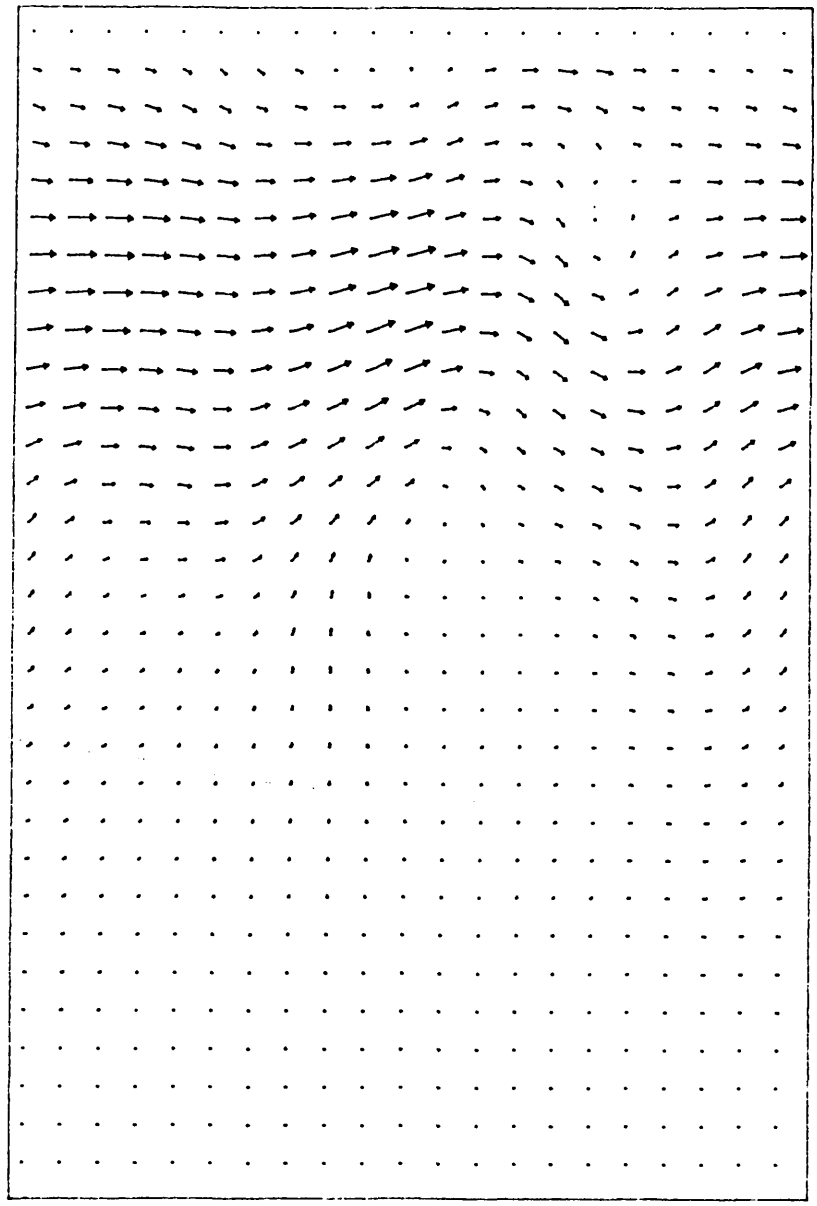


Fig. 8.7 Predicted Current Vectors for Noda's Beach, Using One Equation Turbulence Model and No Wave Current Interaction

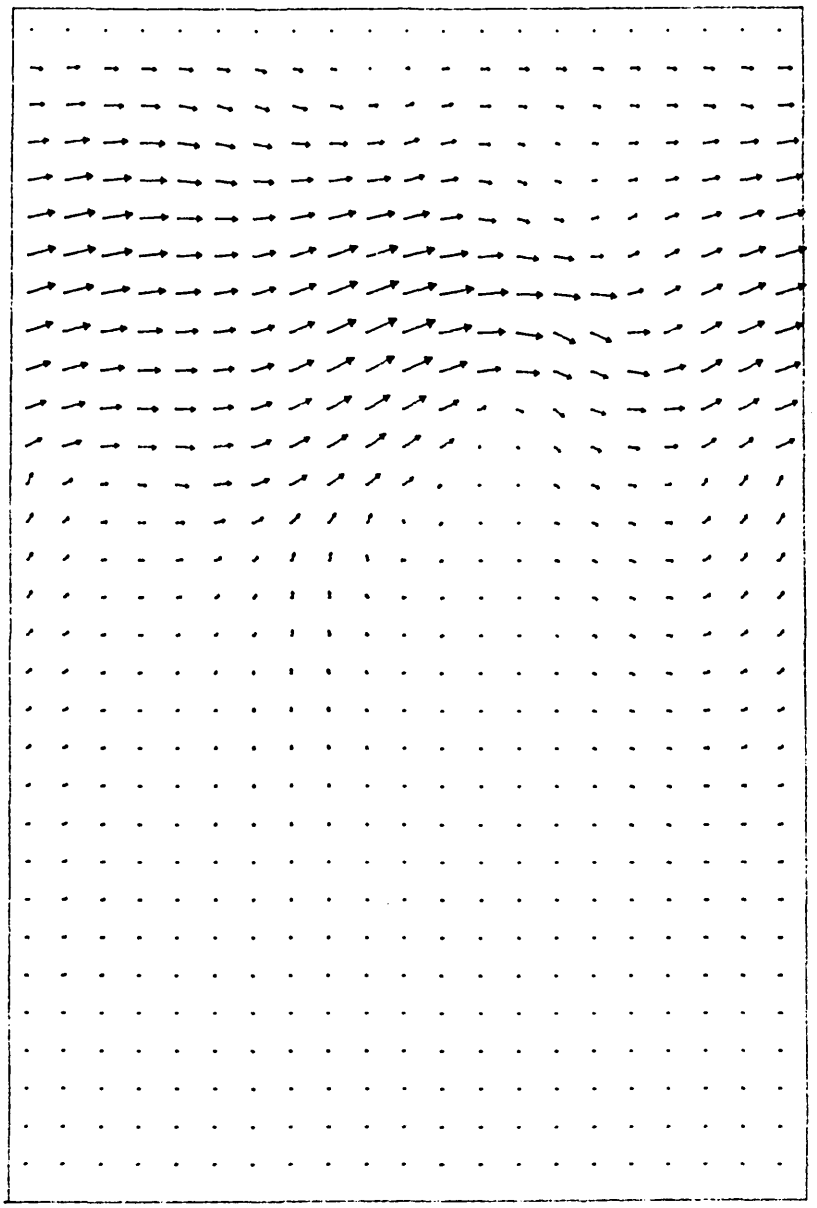


Fig. 8.8 Predicted Current Vectors for Noda's Beach, Using Two Equation Turbulence Model and No Wave Current Interaction

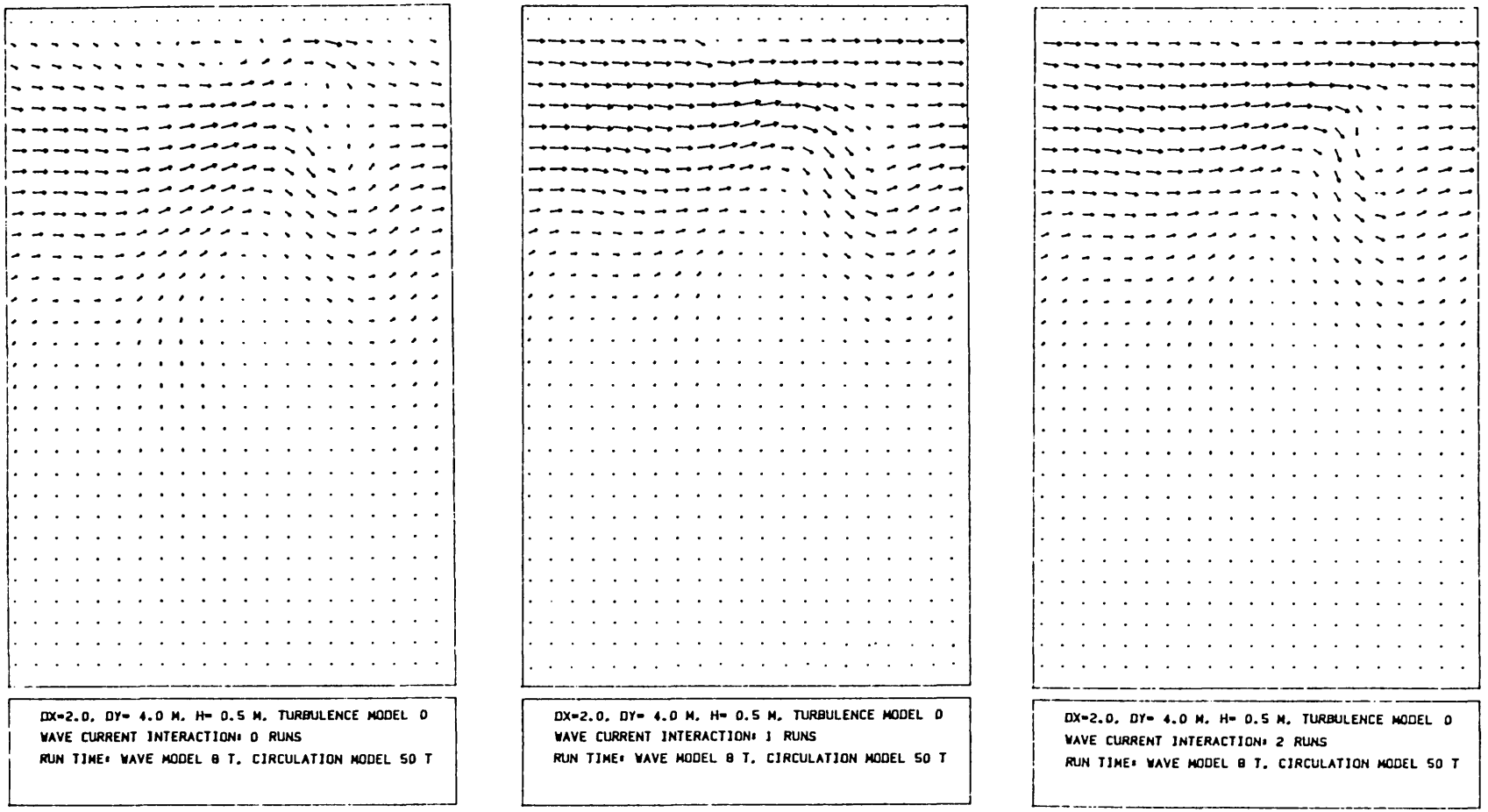


Fig. 8.9 Predicted Current Vectors for Noda's Beach, Using Zero Equation Turbulence Model and with Wave Current Interaction

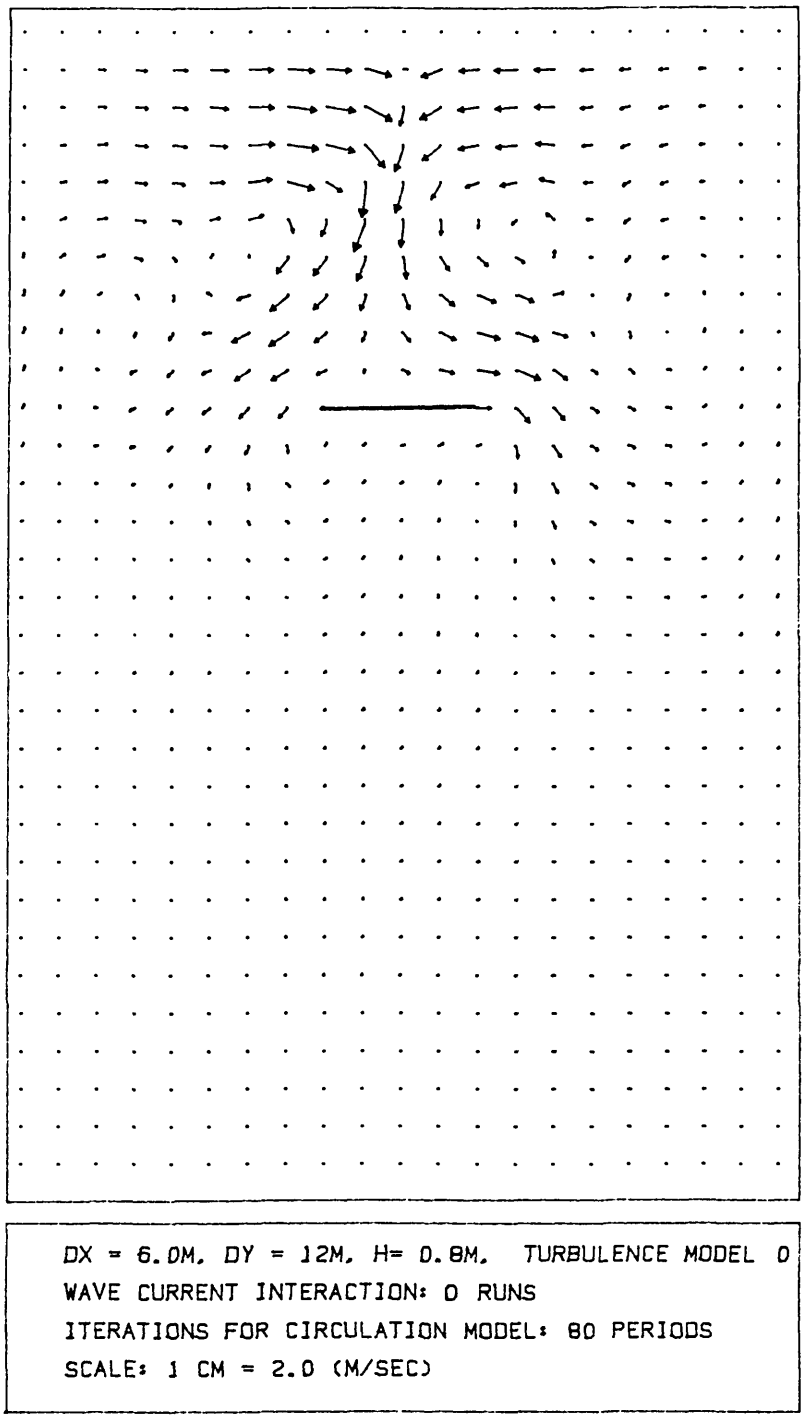


Fig. 8.10 Predicted Current Vectors for the Breakwater Case, Using Zero Equation Turbulence Model and No Wave Current Interaction.

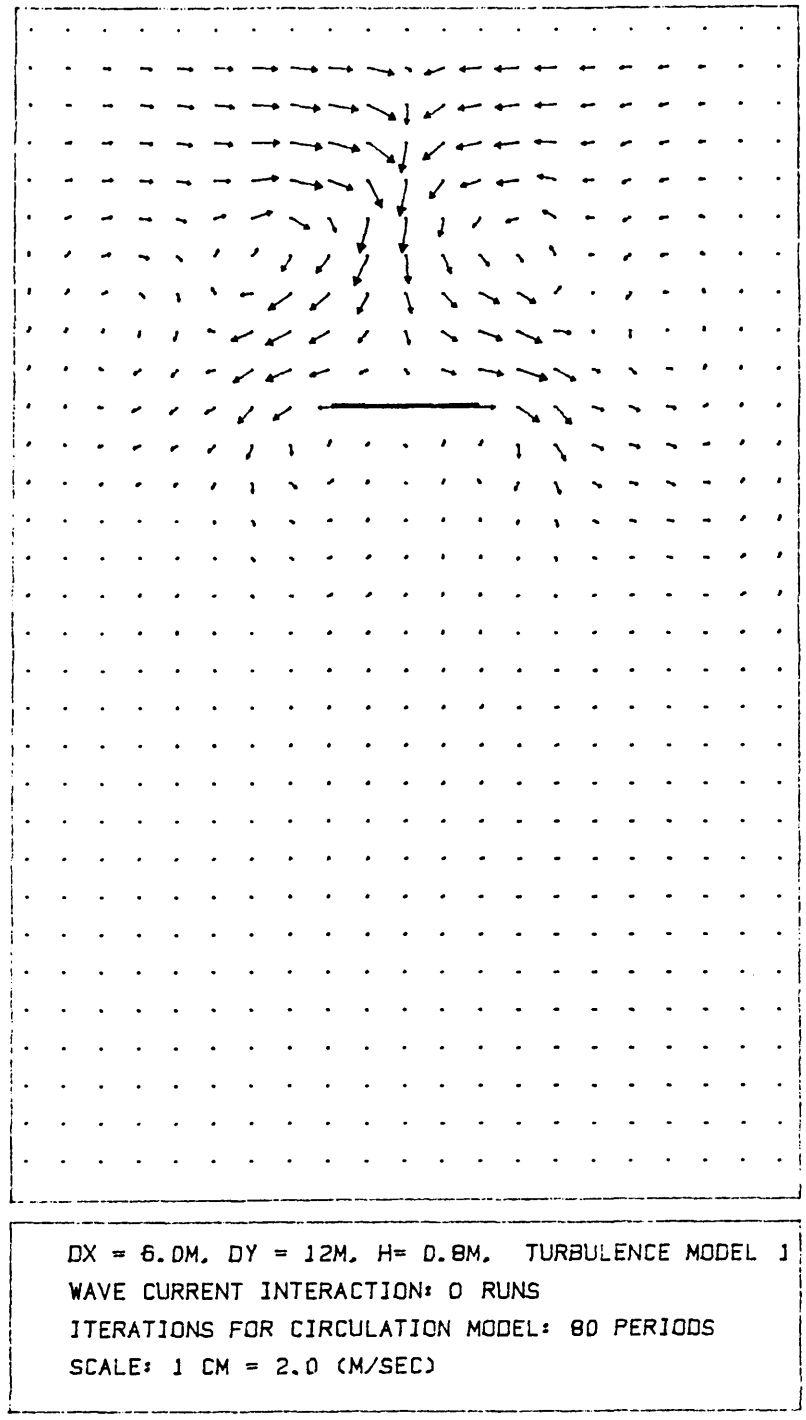


Fig. 8.11 Predicted Current Vectors for the Breakwater Case, Using Two Equation Turbulence Model and No Wave Current Interaction.

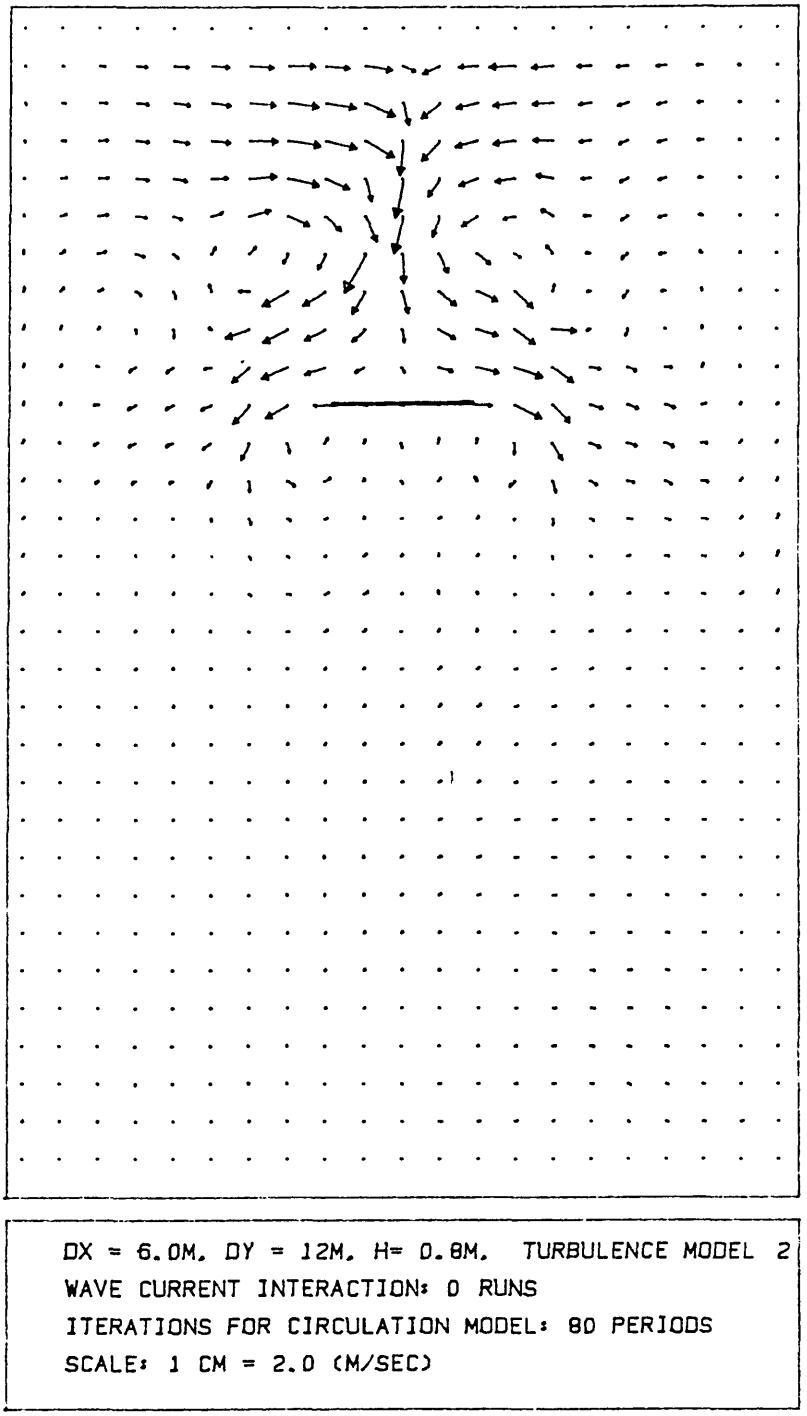


Fig. 8.12 Predicted Current Vectors for the Breakwater Case, Using Two Equation Turbulence Model and No Wave Current Interaction.

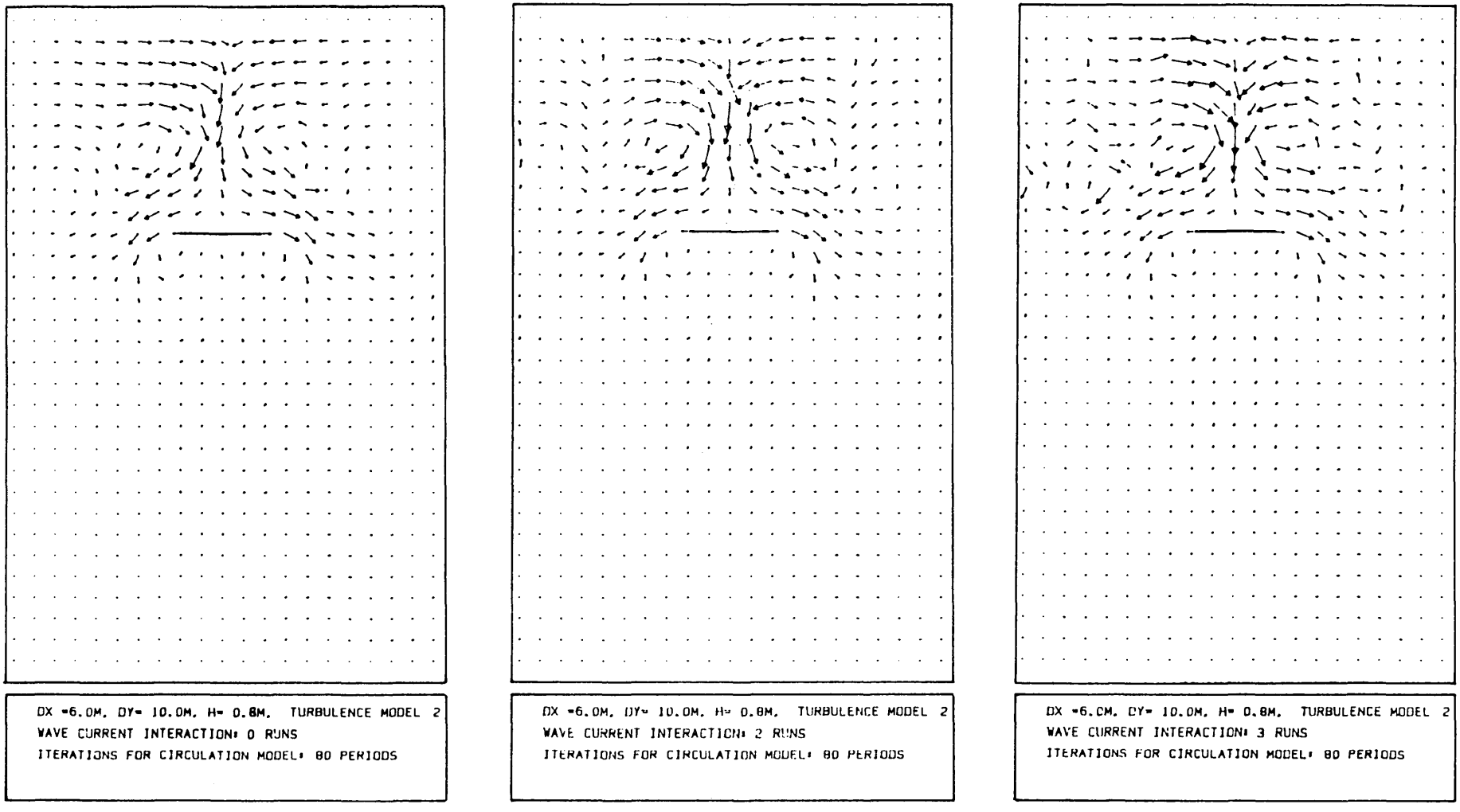


Fig. 8.13 Predicted Current Vectors for the Breakwater Case, Using Two Equation Turbulence Model and with Wave Current Interaction

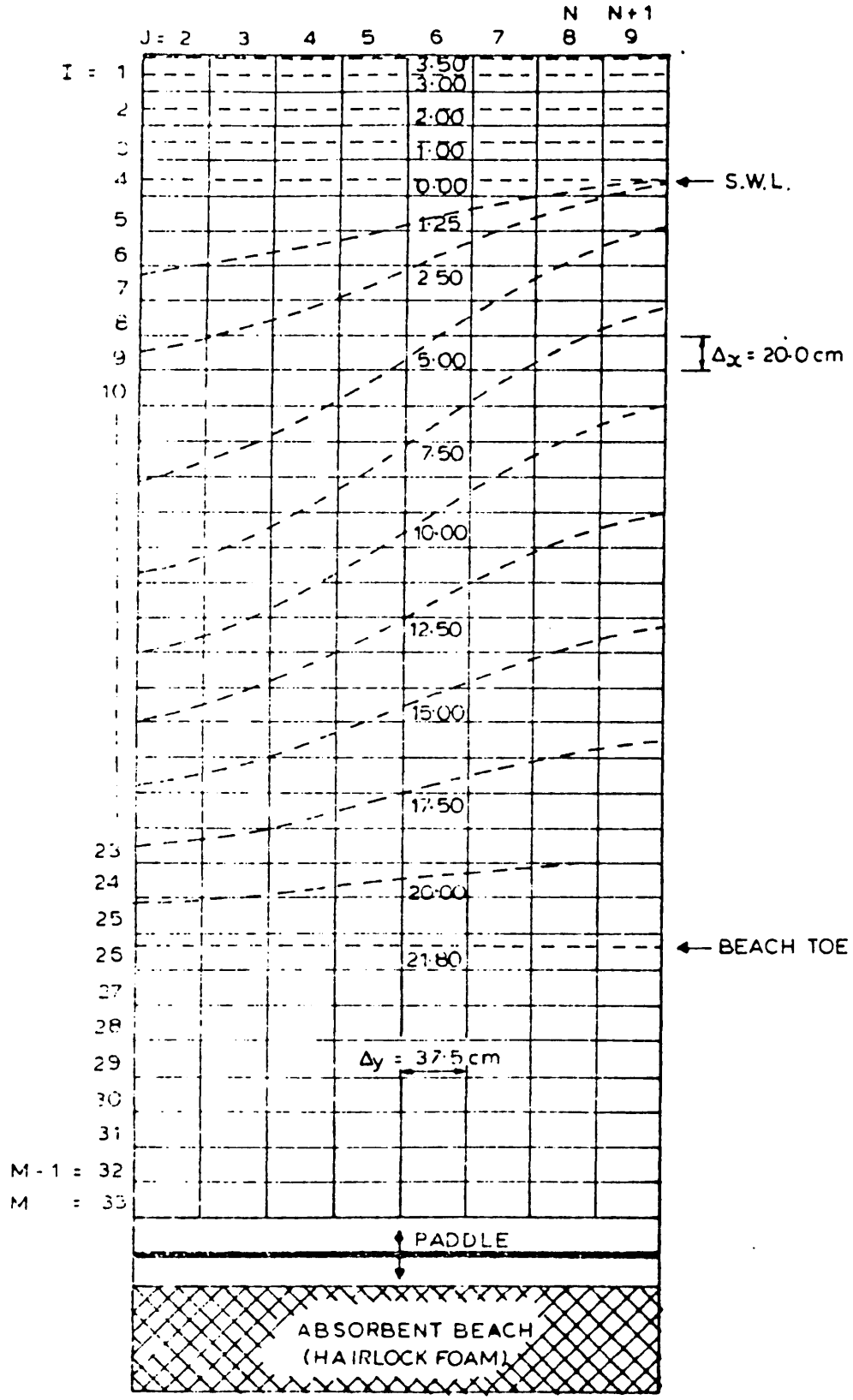


Fig. 8.14 Sea Bed Contours and Grid System Used for da Silva Lima's Experimental Set-Up

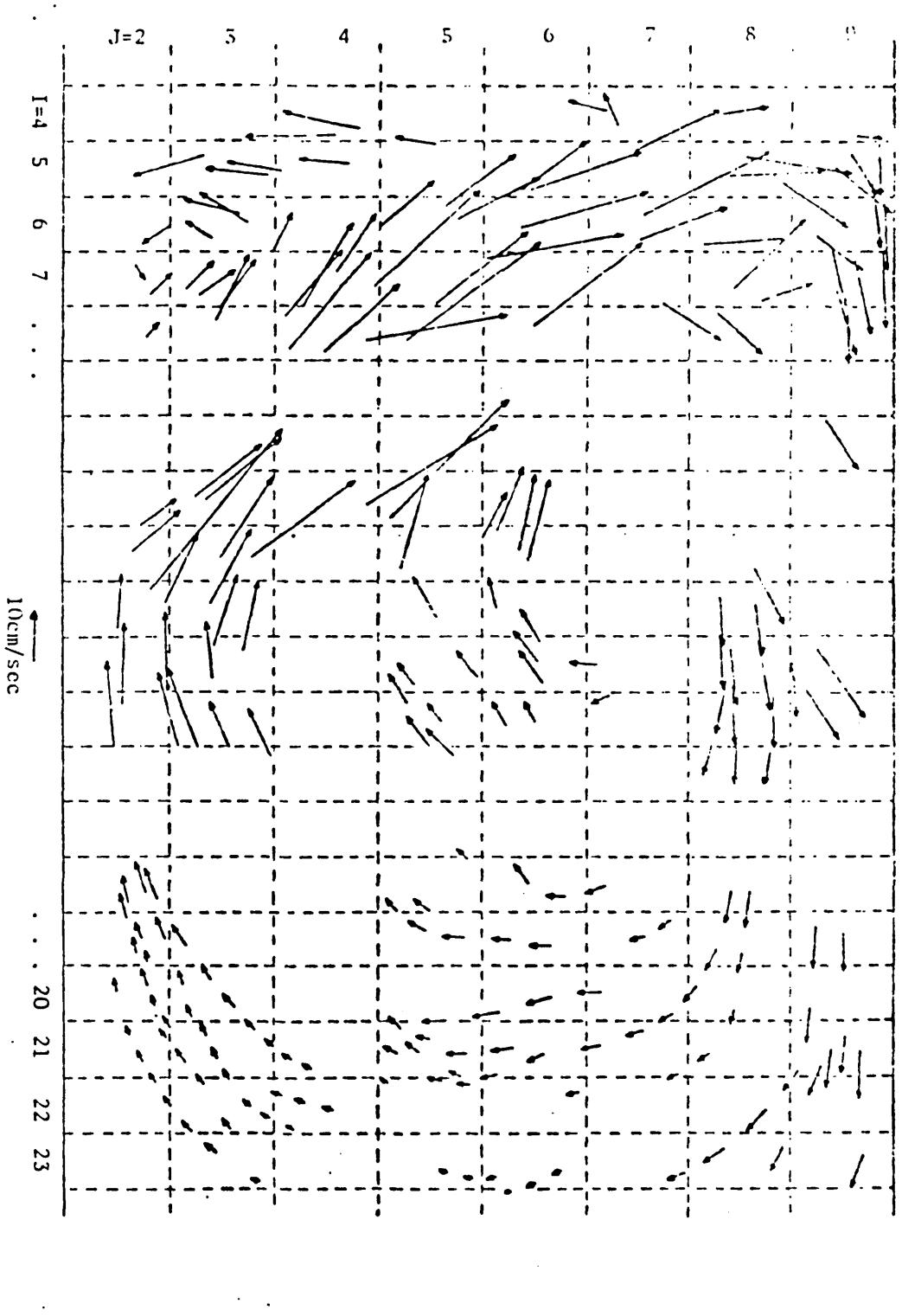


Fig. 8.15 The Measured Velocity Vectors for Experiment Run 2 from da Silva Lima (1981)

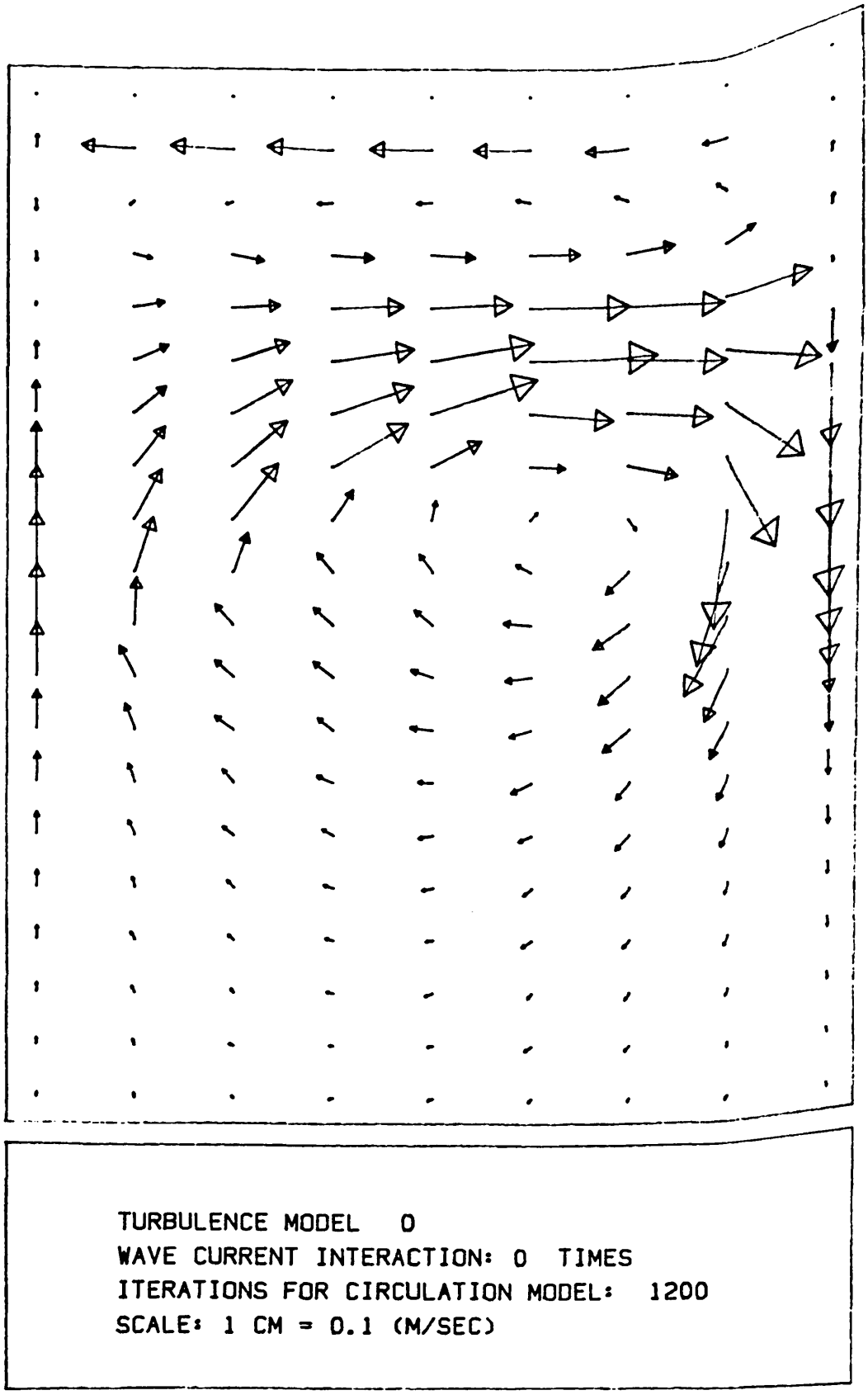


Fig. 8.16 The Predicted Velocity Vectors for Experiment Run 2 Using Zero Equation Turbulence Model and No Wave Current Interaction

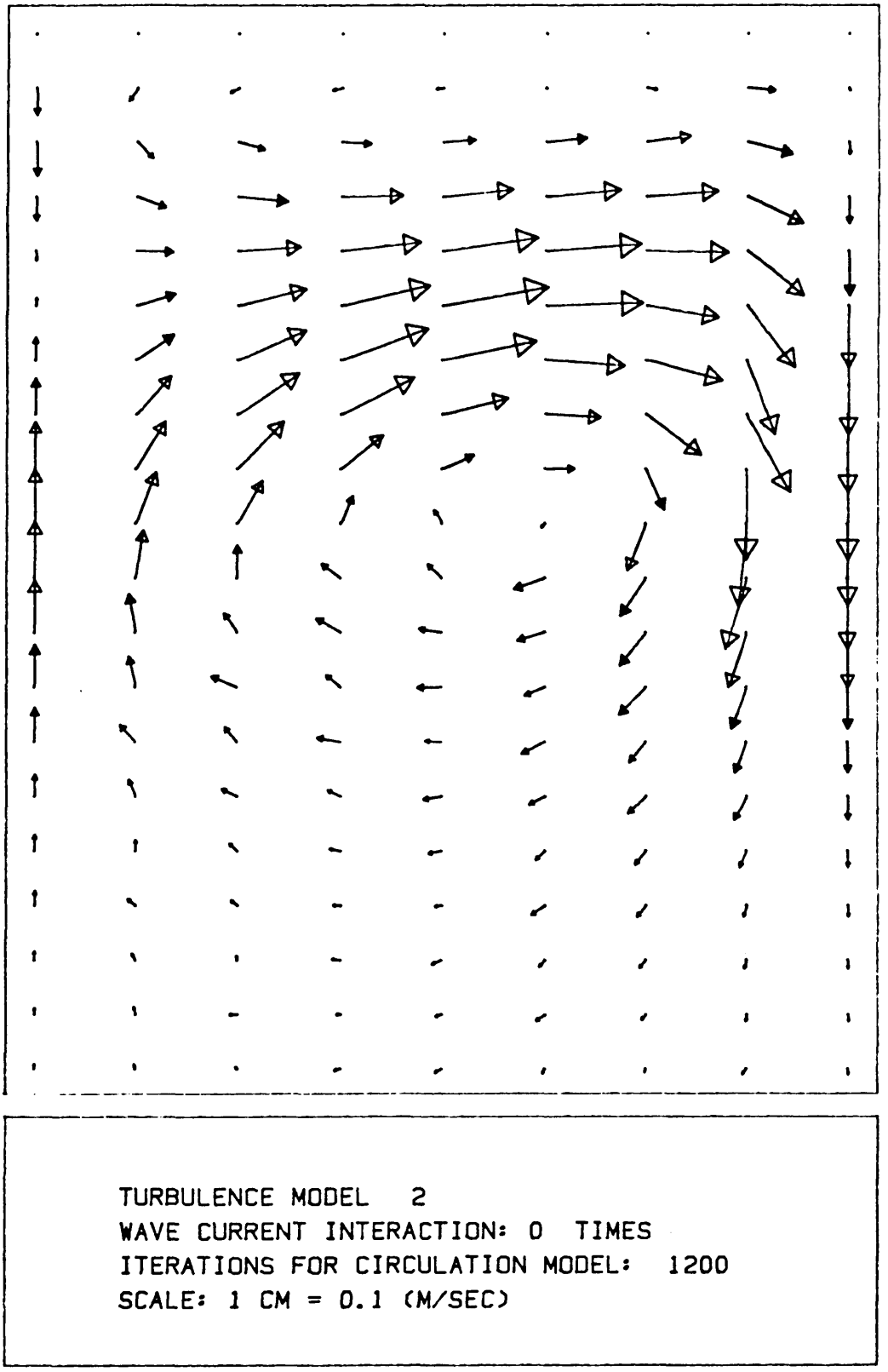
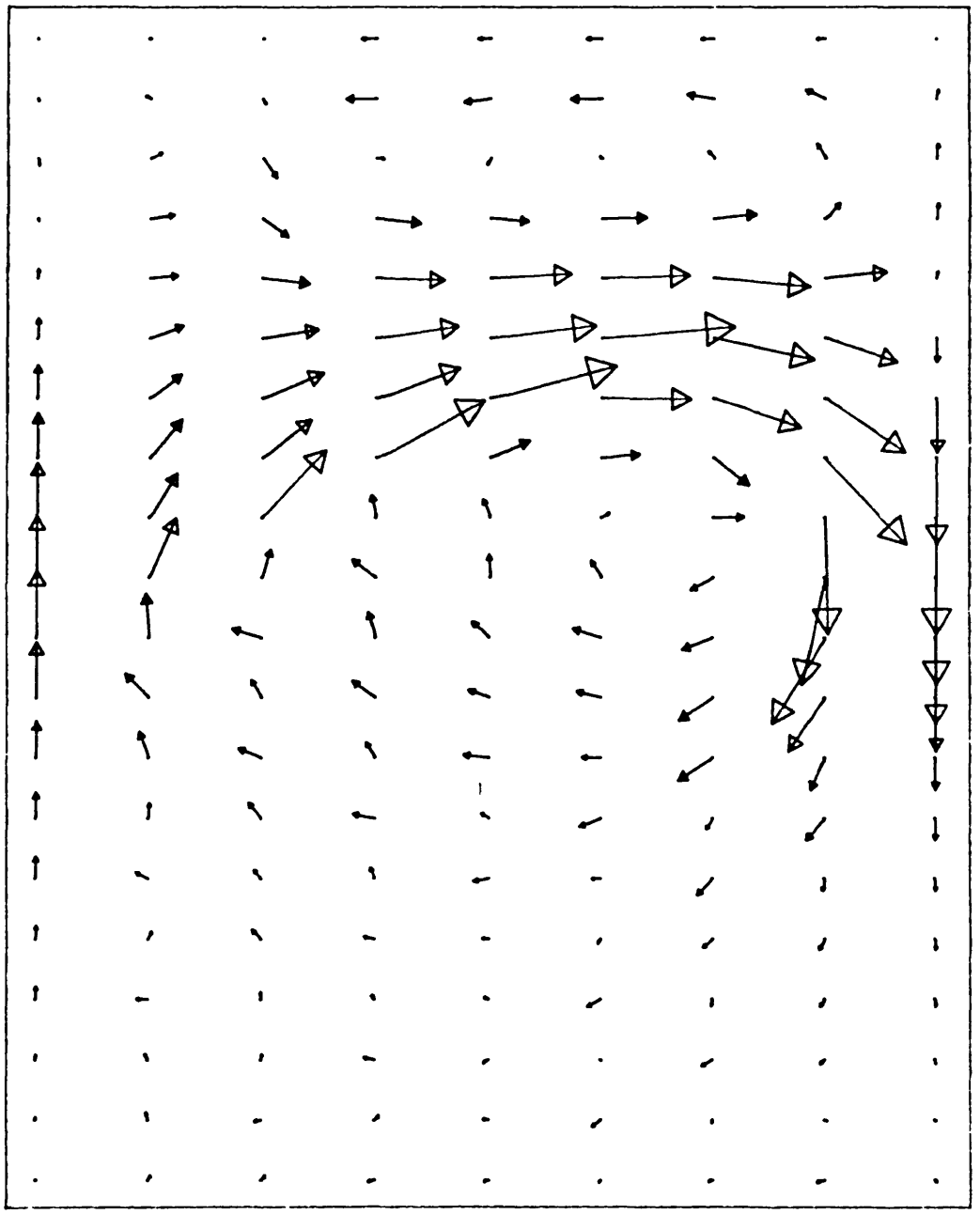
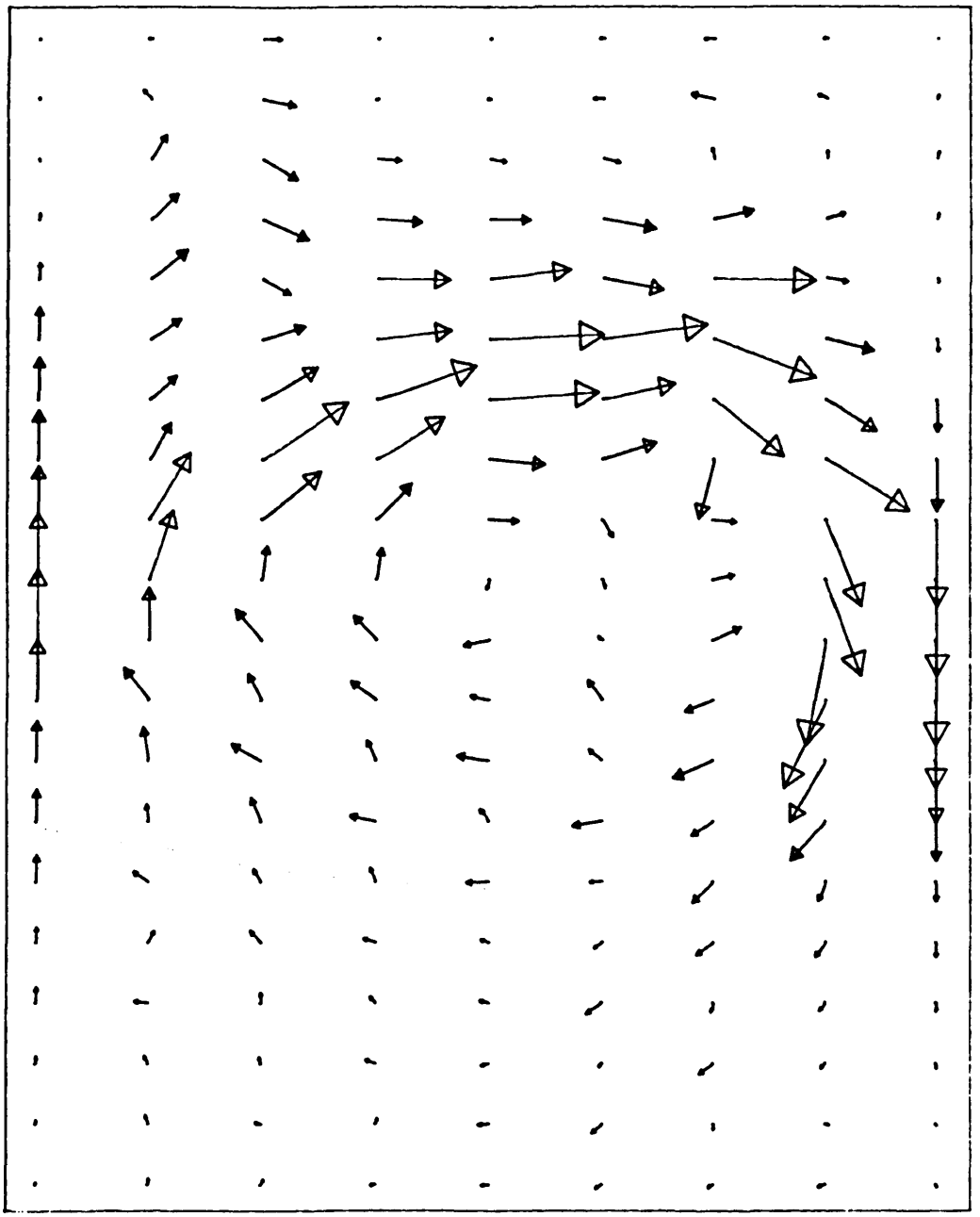


Fig. 8.17 The Predicted Velocity Vectors for Experiment Run 2 Using Two Equation Turbulence Model and No Wave Current Interaction



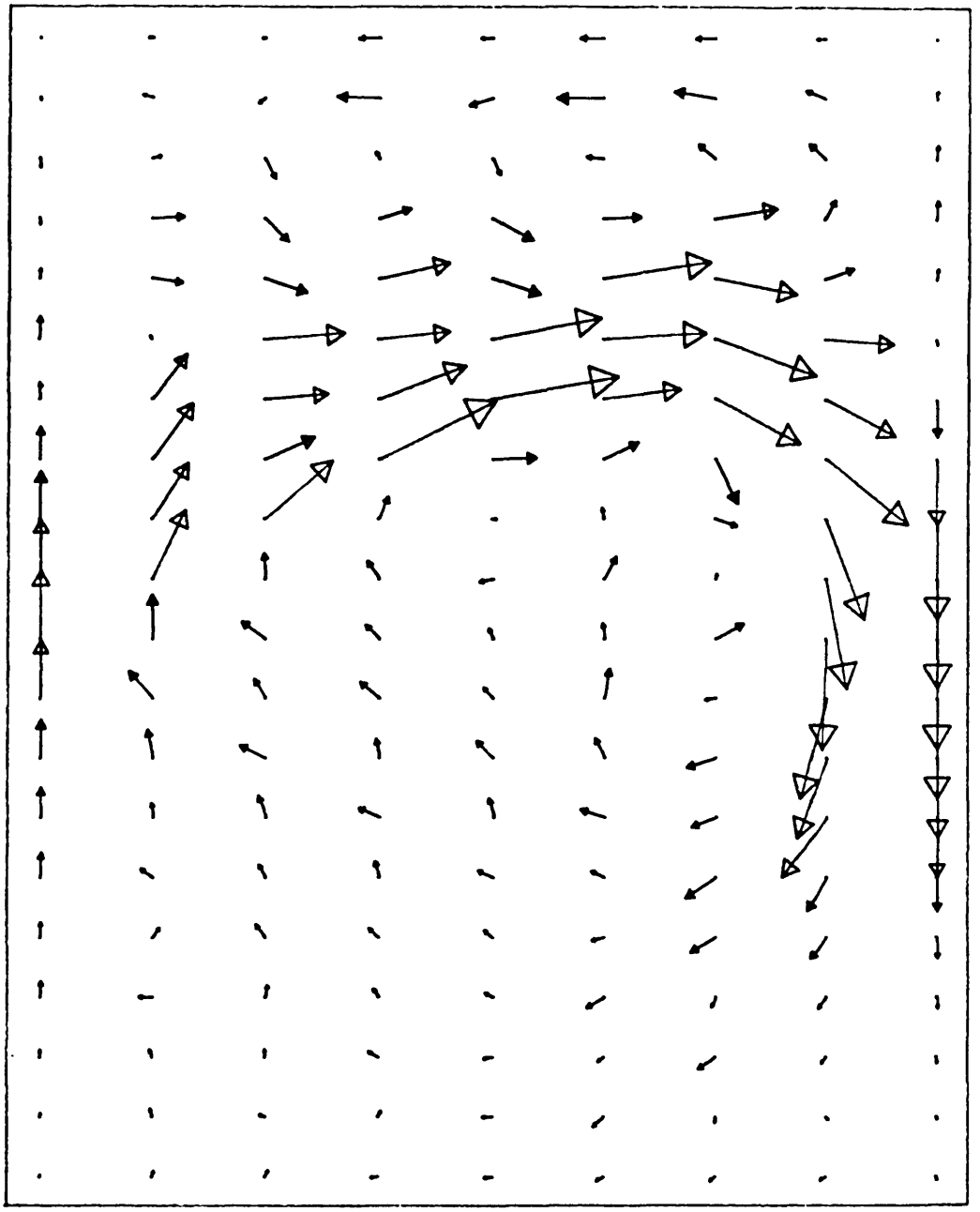
TURBULENCE MODEL 2
WAVE CURRENT INTERACTION: 1 TIMES
ITERATIONS FOR CIRCULATION MODEL: 1200
SCALE: 1 CM = 0.1 (M/SEC)

Fig. 8.18 Predicted Velocity Vectors for Experiment Run 2 Using Two Equation Turbulence Model and with Wave Current Interaction. Five Alternative runs of the Wave and Circulation Models are Carried out.



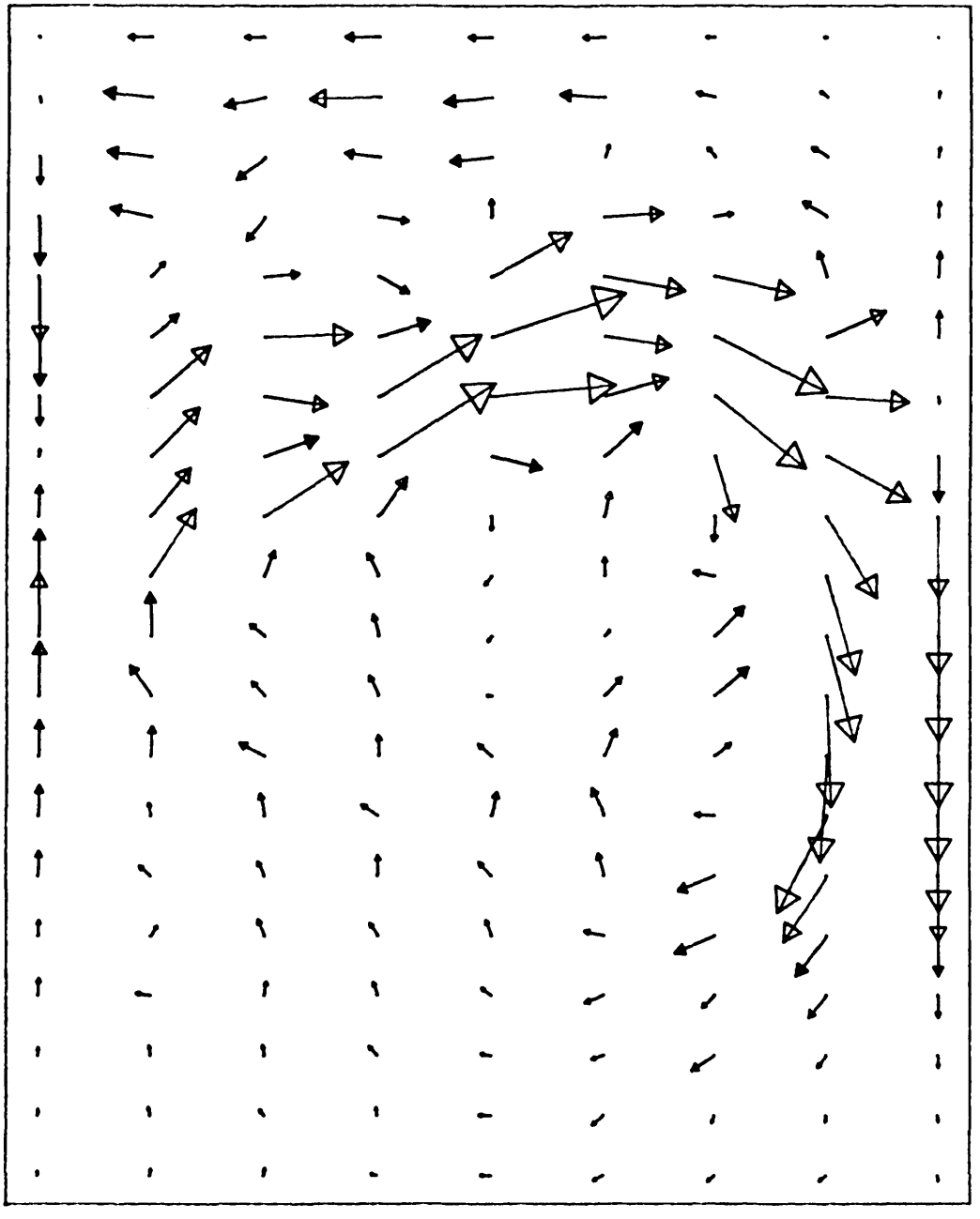
TURBULENCE MODEL 2
WAVE CURRENT INTERACTION: 2 TIMES
ITERATIONS FOR CIRCULATION MODEL: 1200
SCALE: 1 CM = 0.1 (M/SEC)

Fig. 8.18 (continued)



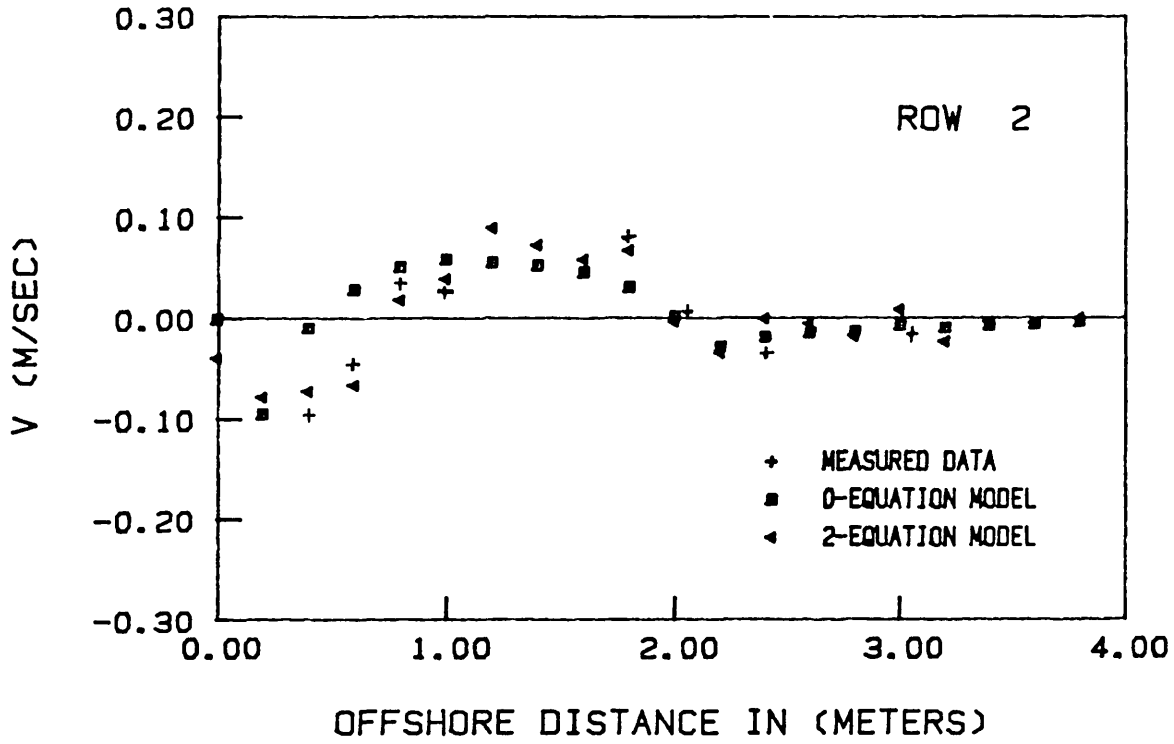
TURBULENCE MODEL 2
WAVE CURRENT INTERACTION: 4 TIMES
ITERATIONS FOR CIRCULATION MODEL: 1200
SCALE: 1 CM = 0.1 (M/SEC)

Fig. 8.18 (continued)



TURBULENCE MODEL 2
WAVE CURRENT INTERACTION: 5 TIMES
ITERATIONS FOR CIRCULATION MODEL: 1200
SCALE: 1 CM = 0.1 (M/SEC)

Fig. 8.18 (continued)



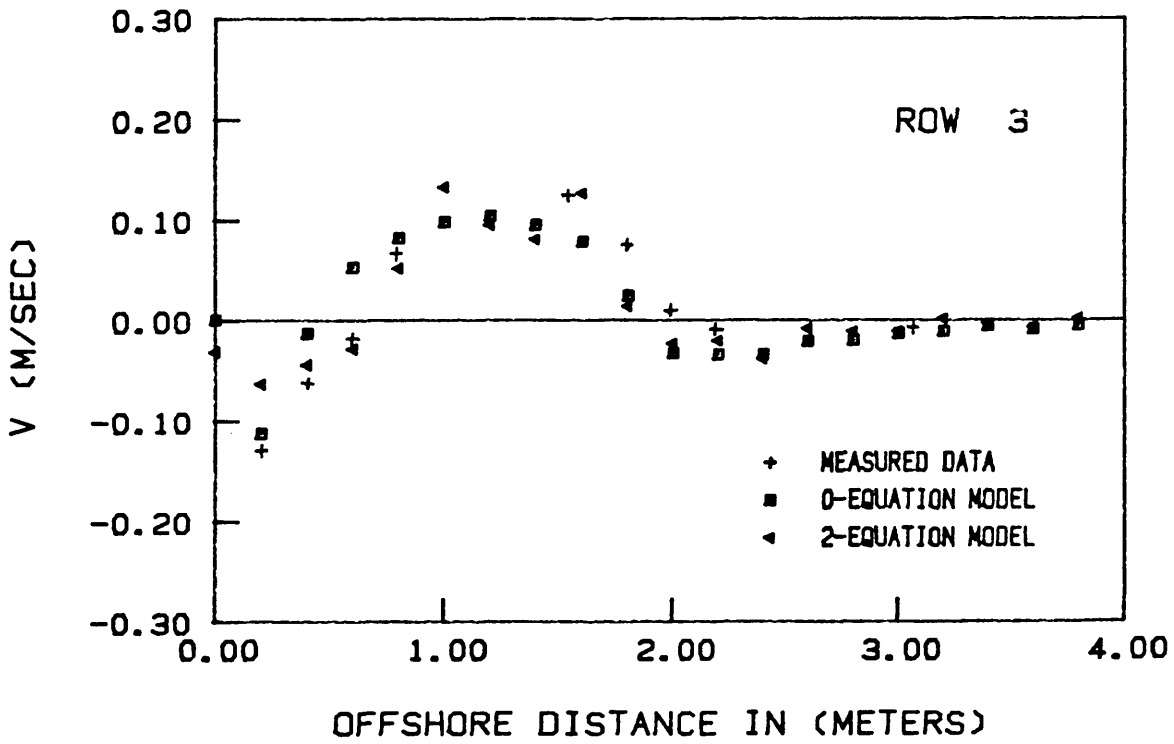
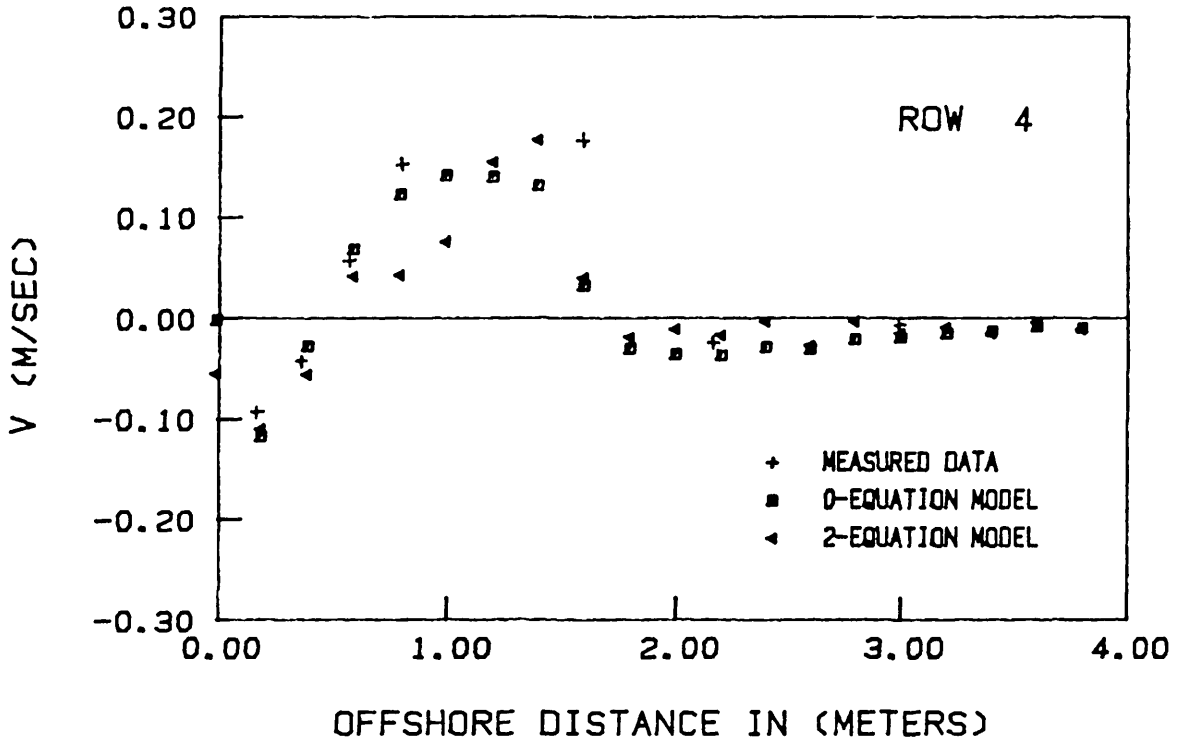


Fig. 8.19 Comparison between Predicted Longshore Current for Rows from 2 to 3



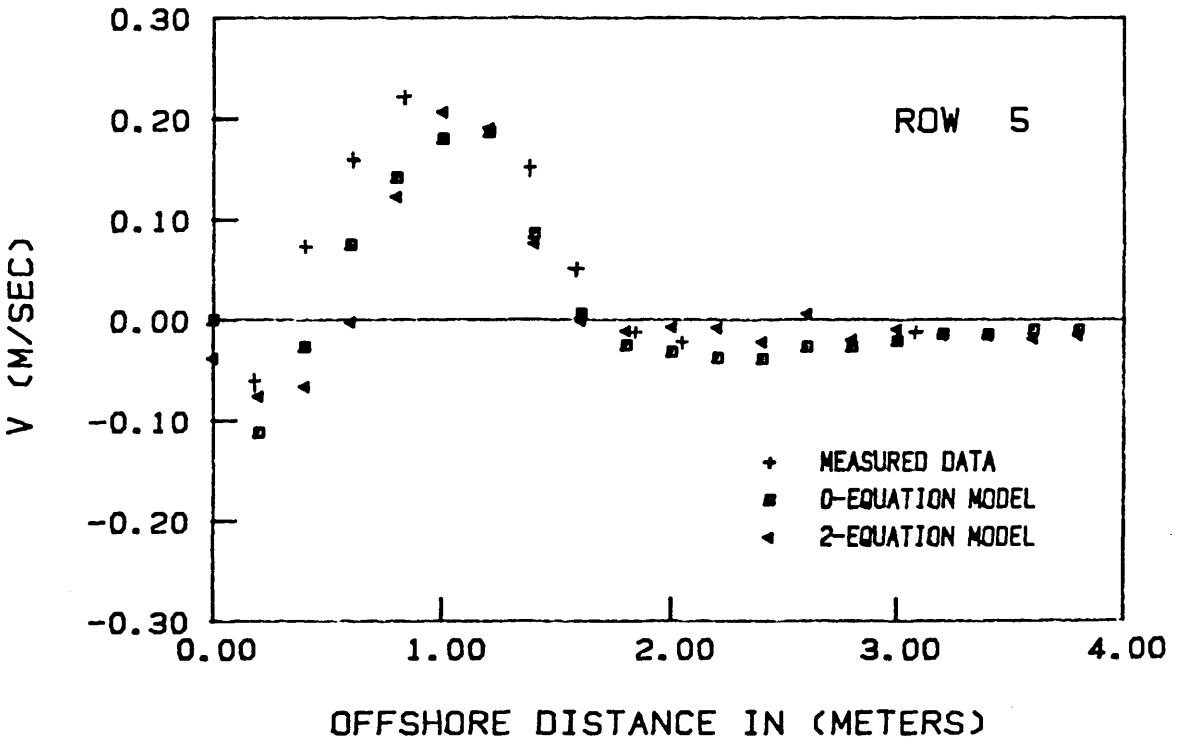
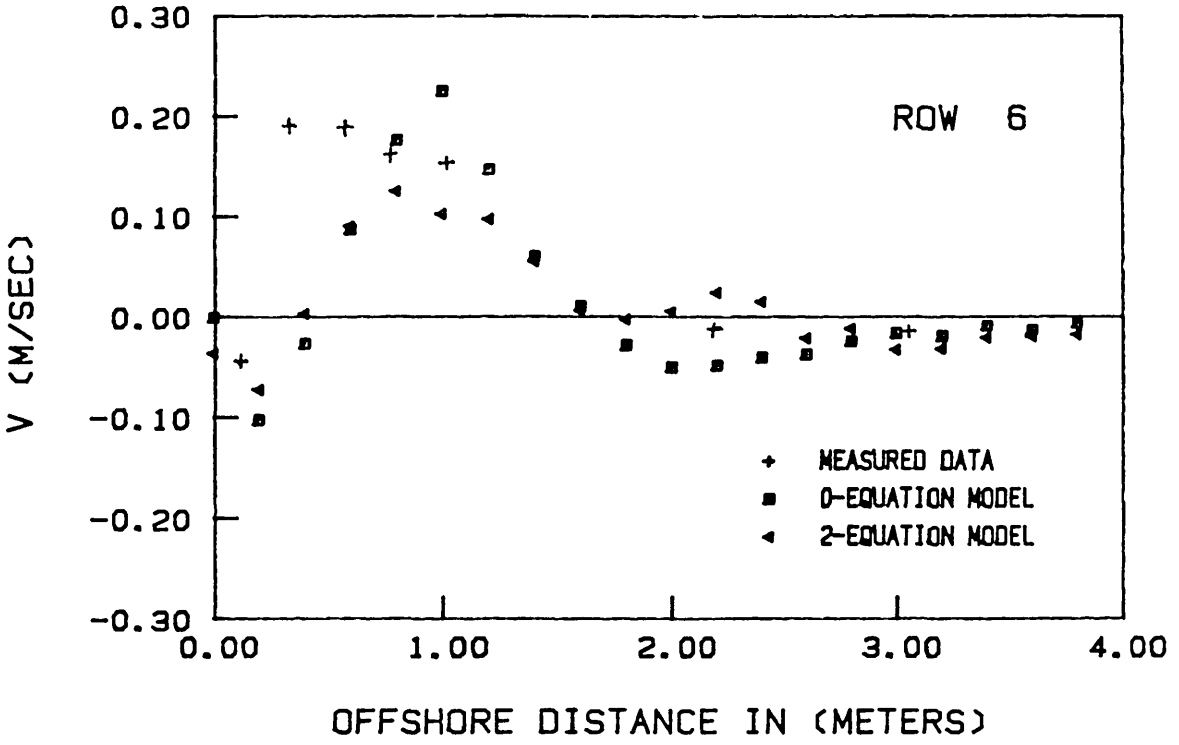


Fig. 8.20 Comparison between Predicted Longshore Current for Rows from 4 to 5



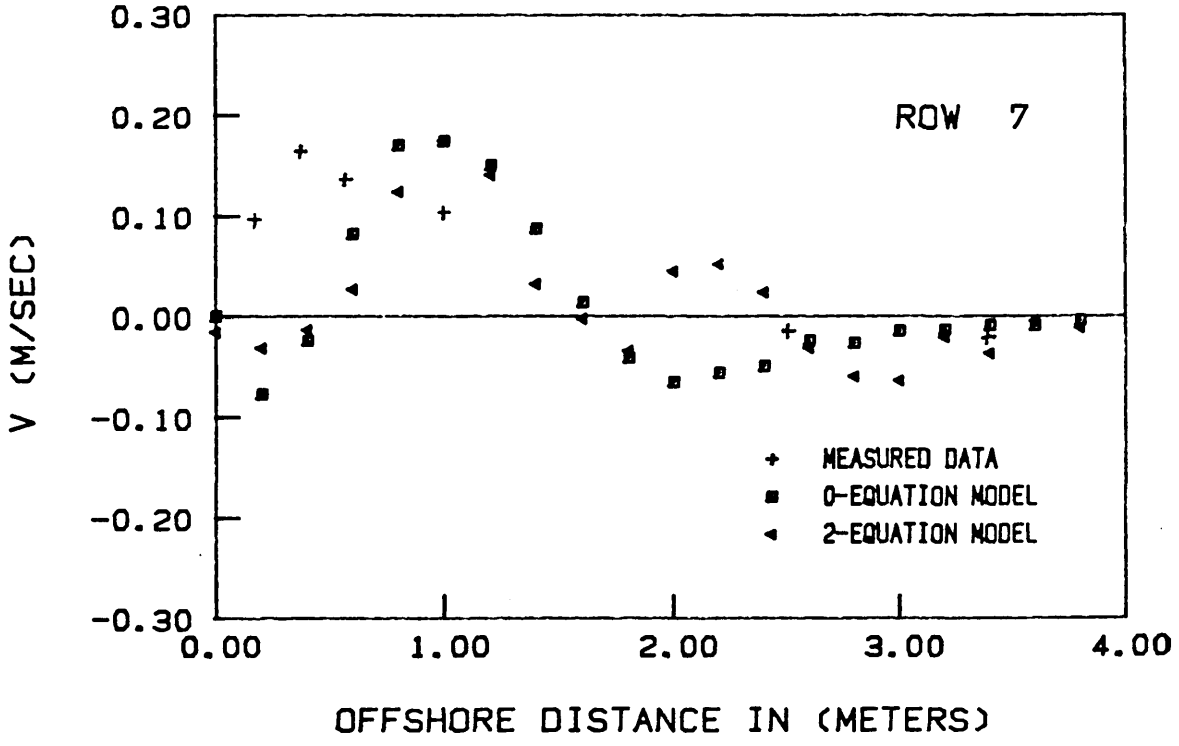
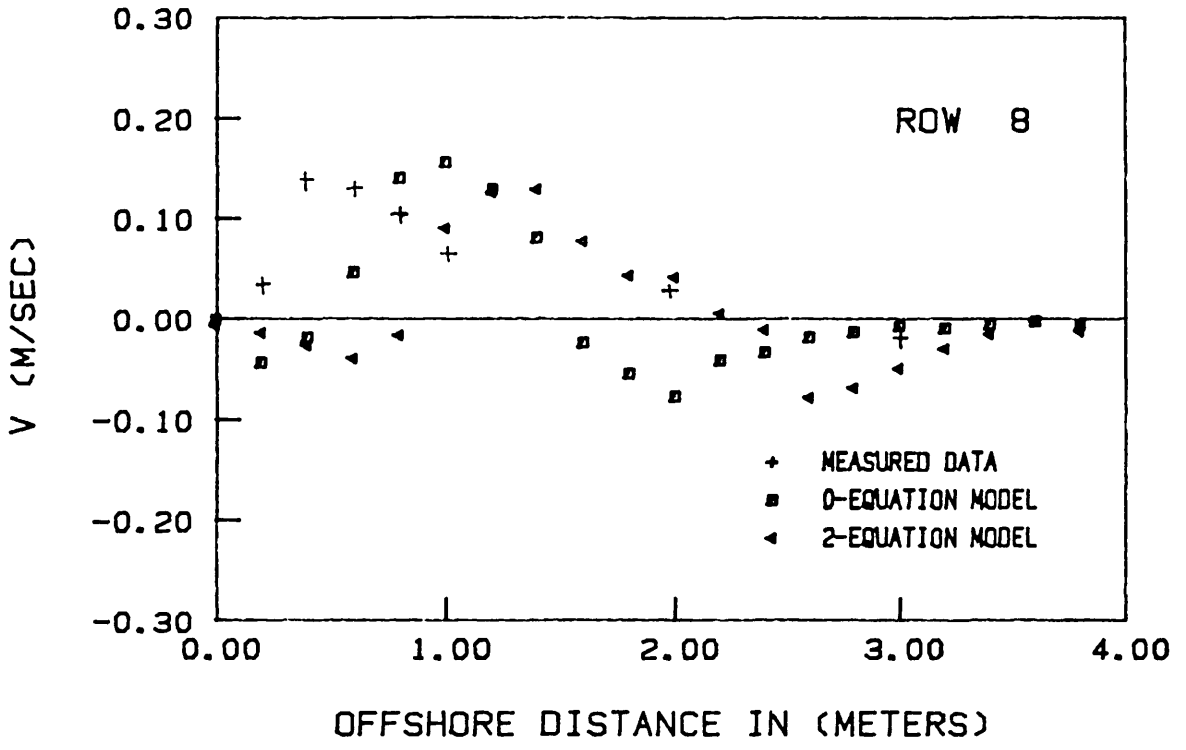


Fig. 8.21 Comparison between Predicted Longshore Current for Rows from 6 to 7



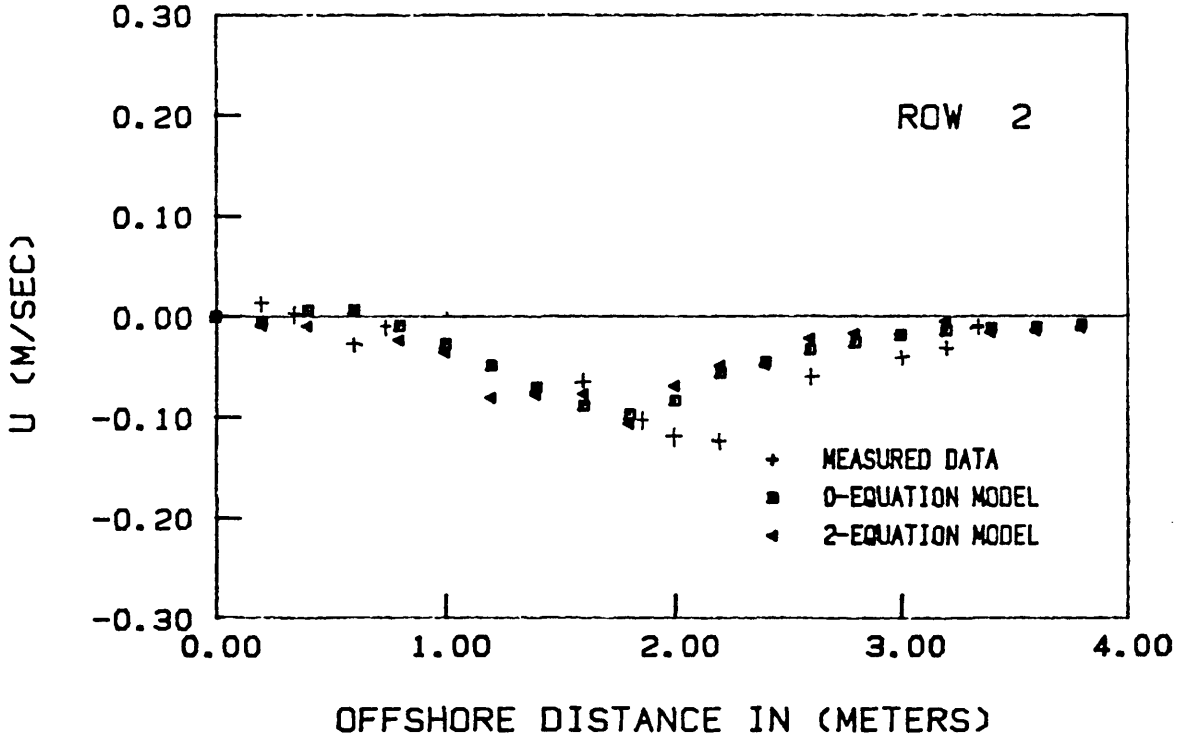
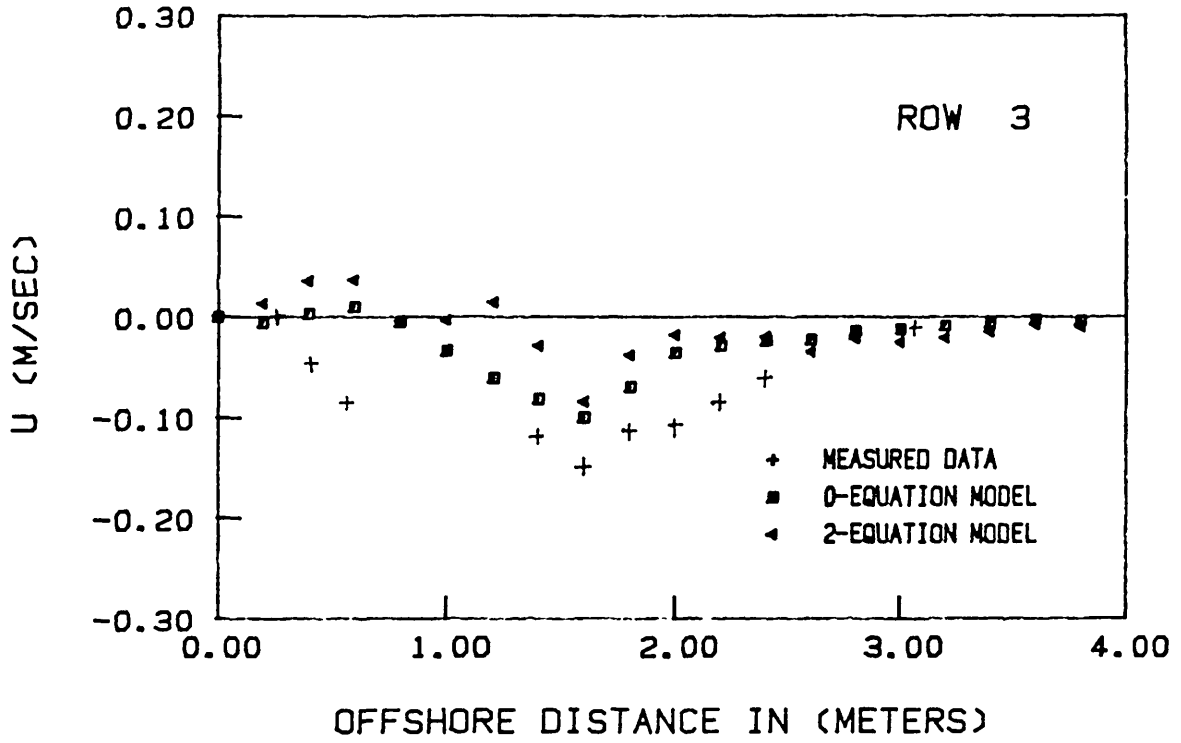


Fig. 8.22 Comparison between Predicted Longshore and Rip Currents for the Rows 8 and 2, respectively



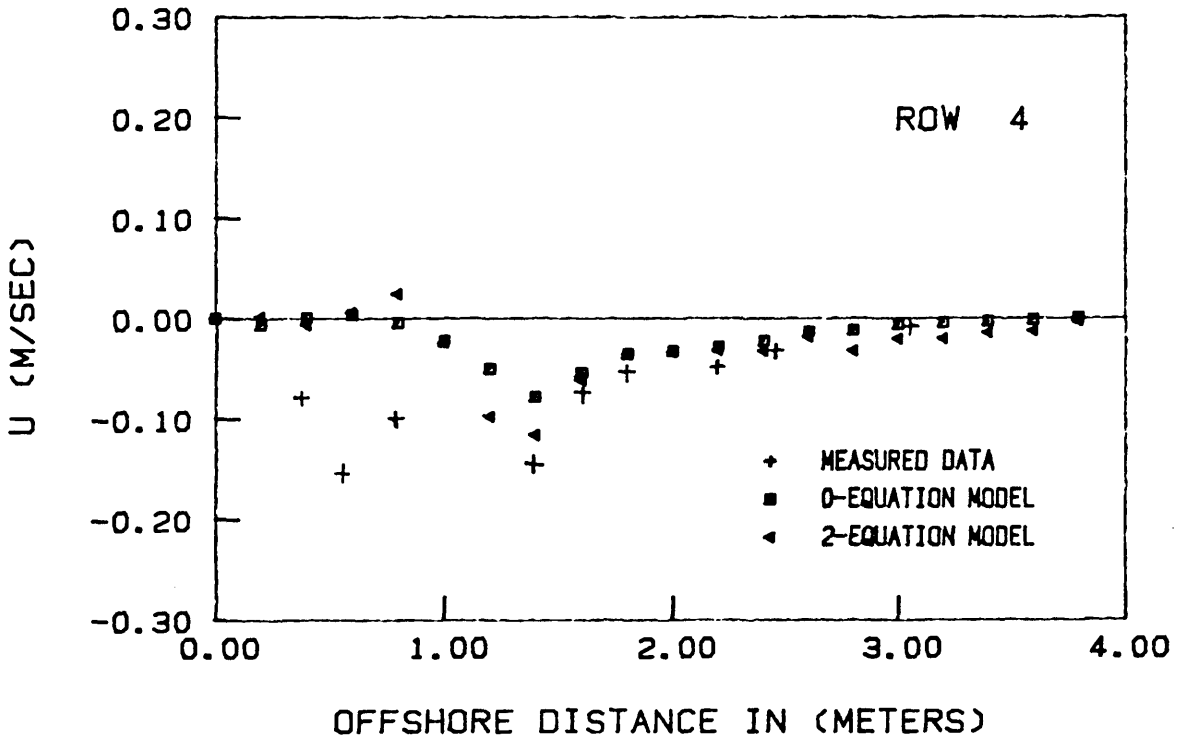
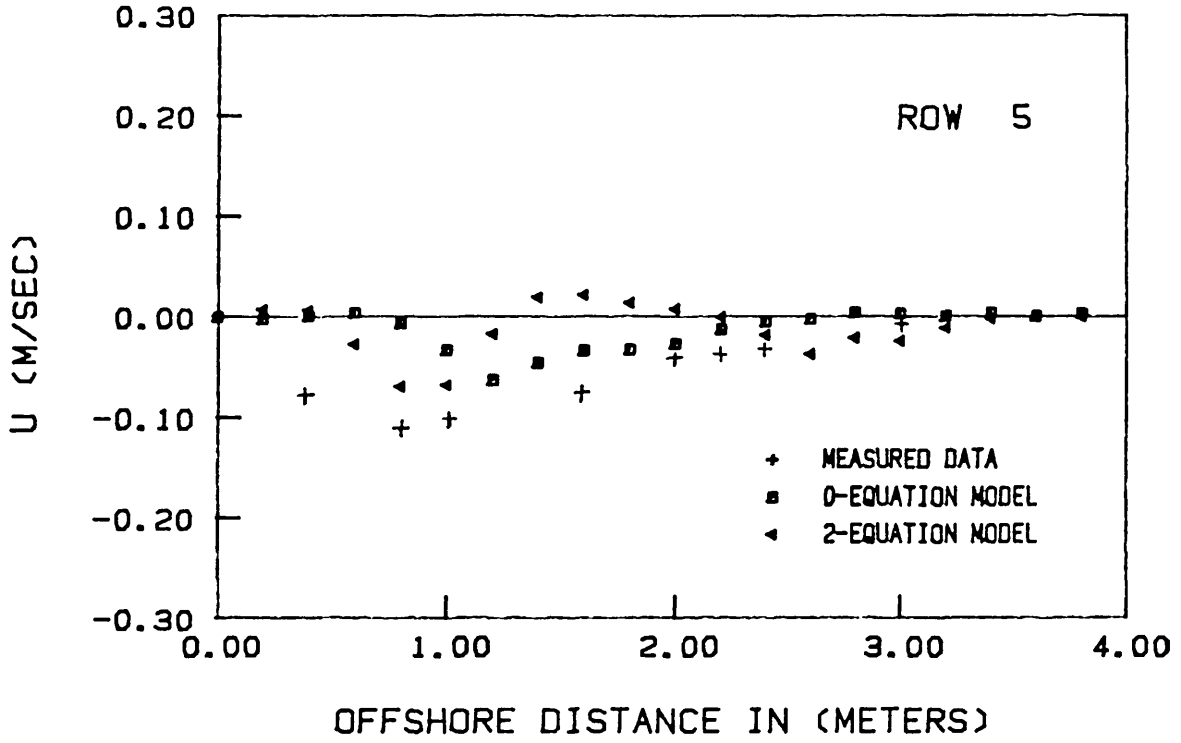


Fig. 8.23 Comparison between Predicted Rip Current for Rows from 3 to 4



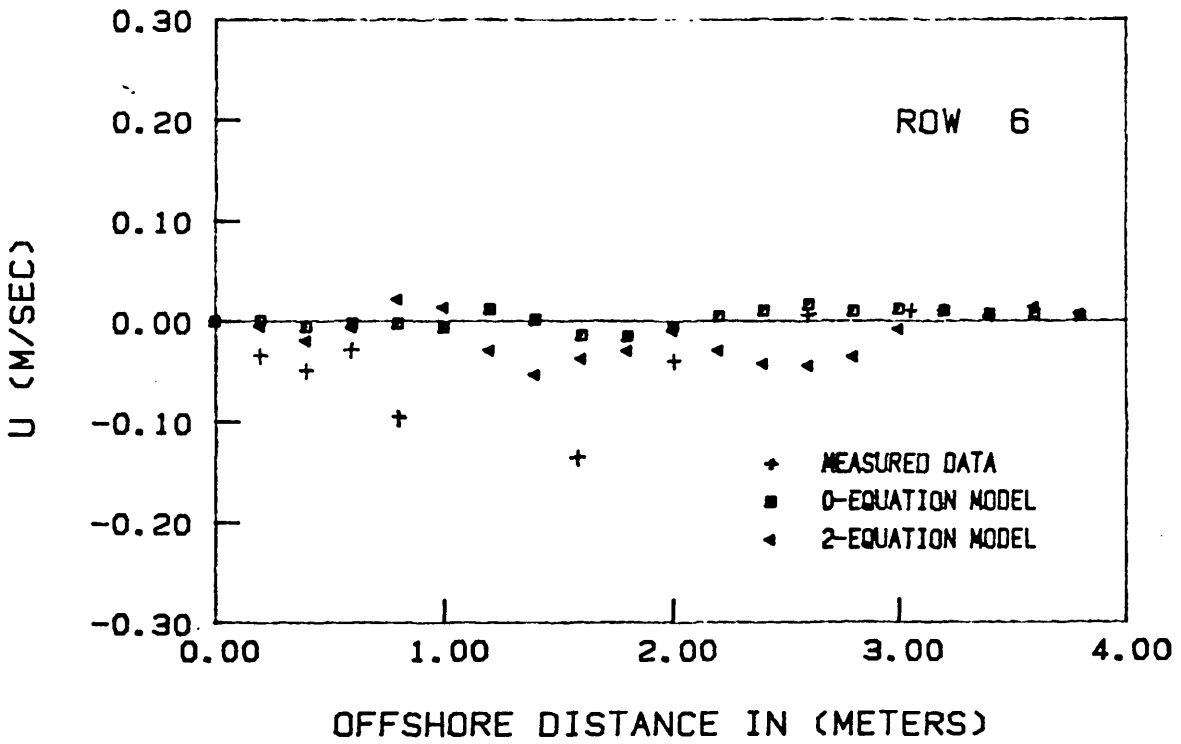
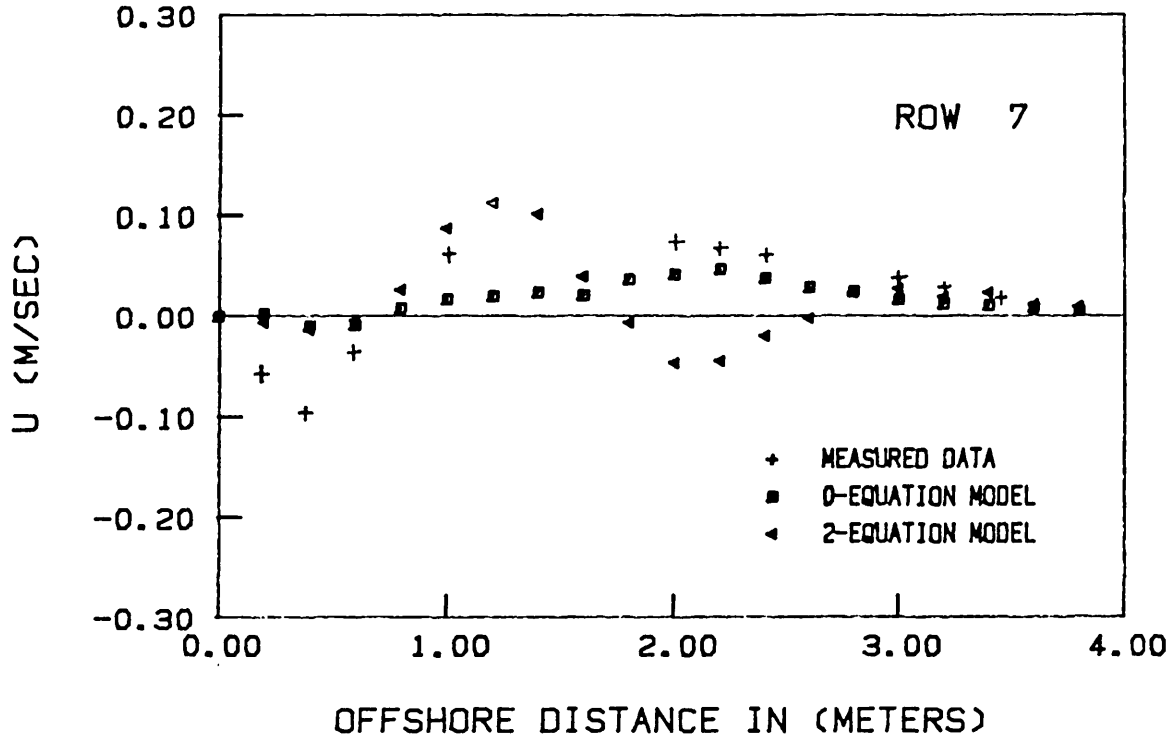


Fig. 8.24 Comparison between Predicted Rip Current for Rows from 5 to 6



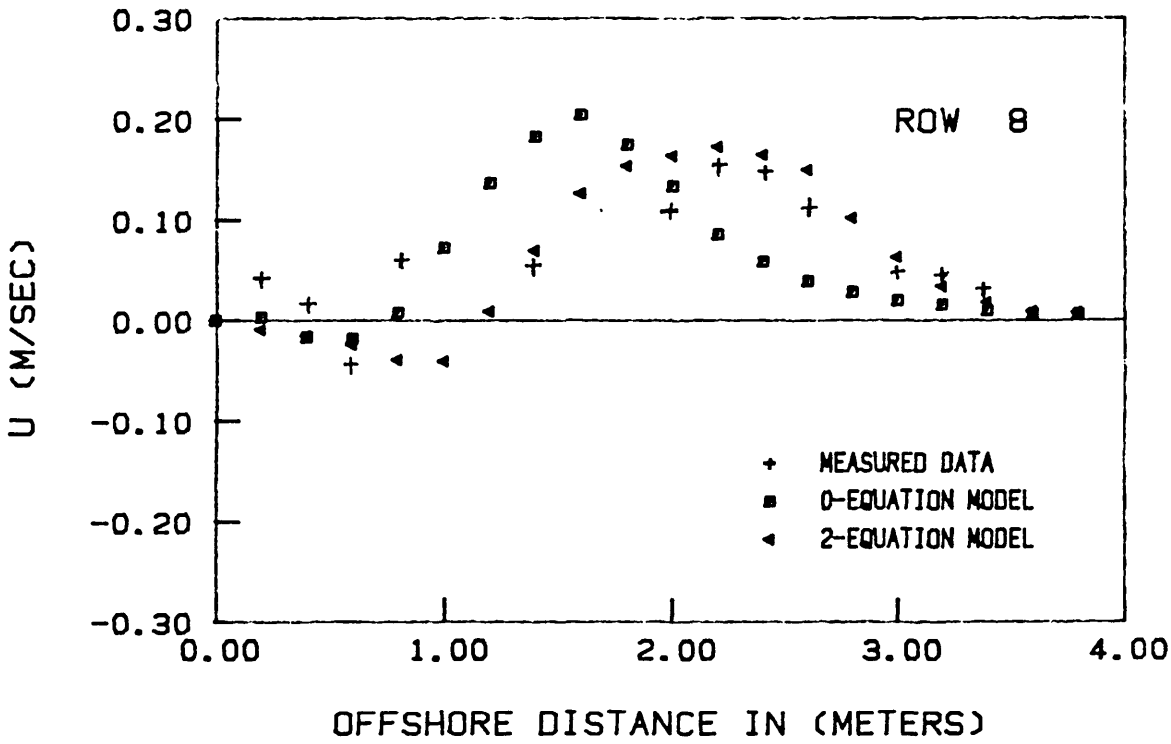


Fig. 8.25 Comparison between Predicted Rip Current for Rows from 7 to 8

CHAPTER. 9
THE VERTICAL DISTRIBUTION OF LONGSHORE CURRENT ON A PLANE BEACH

9.1 Introduction

In coastal areas a significant proportion of the sediment transport along a beach occurs in suspension. This is particularly true with sediment transport inside the surf zone where, as a result of wave breaking, a large amount of sediment which might otherwise remain close to the bottom is brought up into suspension. In some situations the suspended sediment could extend over the entire water column. The transport rate of suspended sediment at a point depends on the local mean flow velocity and mean sediment concentration

$$q = U.\ c \tag{9.1}$$

where q is the local sediment transport rate averaged over one wave period, U is the time averaged velocity of the flow and c is the corresponding time mean sediment concentration. Thus, the total sediment transport rate over the entire water depth d should be

$$Q_s = \int_{-d}^{\bar{\zeta}} U.c\ dz \tag{9.2}$$

In general situations both U and c are dependent on the vertical axis z and could have arbitrary distribution. If, at a particular location in the water column, the concentration is great, even the weakest steady current would carry sizeable amount of sediment alongshore. Therefore, the vertical distribution of U and c must be known in order to be able to calculate the total sediment transport accurately.

However, up until now all the previous studies on wave-induced currents have considered only the depth averaged currents following the theoretical framework established by Bowen (1969), Longuet-Higgins (1970a) and Thornton (1970). Undoubtly such an approach is simpler than a full 3-D modelling and, to a certain extent, the information found this way is useful in estimating roughly the littoral transport and morphological variation of shorelines. But a knowledge of the vertical structure of the longshore currents is essential for further understanding the mechanism of sediment movement and prediction of longshore sediment transport.

In this chapter a method is developed to calculate the vertical profile of the

longshore current velocity generated by monochromatic long-crested waves breaking on a plane beach. Due to the uniformity in the alongshore direction the problem is confined to the vertical plane across the surf zone and can be regarded as a particular case of the general three dimensional wave induced circulation problem. The governing equation is the longshore momentum equation averaged over one wave period but not integrated over the depth. Both the wave and bottom conditions are exactly the same as those considered by Longuet-Higgins (1970) and others for calculating the depth averaged longshore current.

The equation is solved numerically using a Galerkin method with a series of cosine functions and Legendre polynomials as basis functions. The computed current profiles across the surf zone at different vertical locations are presented and analysed with particular regard to the effects of the vertical turbulent stress and bottom boundary conditions on the magnitude and profile of the current velocity. In addition Visser's experimental data are used to compare with the numerical results. With a proper choice of mixing coefficients a reasonable agreement has been achieved. Finally, possible ways to improve the formulations are put forward.

9.2 Theoretical Formulation

9.2.1 Derivation of governing equations

The three-dimensional hydrodynamic processes in the nearshore region are generally fully turbulent and can be described by the basic equations of motion. By separating the instantaneous motions into ordered and turbulent motions and neglecting the viscous stresses which are much smaller compared with the turbulent stresses the equations can be written as

$$\frac{\partial u_\alpha}{\partial x_\alpha} = 0 \tag{9.3}$$

$$\frac{\partial u_\alpha}{\partial t} + u_\beta \frac{\partial u_\alpha}{\partial x_\beta} = - \frac{1}{\rho} \frac{\partial p}{\partial x_\alpha} + g_\alpha - \frac{\partial \overline{u'_\alpha u'_\beta}}{\partial x_\alpha} \tag{9.4}$$

where u_α are the velocity components of ordered motions, u'_α are the turbulent velocities, x_α are the rectangular coordinates, p is the pressure and g_α is the gravitational acceleration tensor. As it was done in the derivation of the time averaged and depth integrated equations in Chapter 4, the ordered motion can be regarded as consisting of a time averaged motion denoted by velocity U_α and a wave motion with a zero time mean value, denoted by $\tilde{u}_\alpha$, i.e:

$$u_\alpha = U_\alpha + \tilde{u}_\alpha \tag{9.5}$$

To simplify the analysis U and $\tilde{u}$ are assumed uncorrelated. It should be pointed out that the time-averaged velocity U here is dependent on the vertical location in the water column while in Chapter 4 it was assumed to be uniform over the entire water column. On substituting eq. (9.5) into eqs. (9.3) and (9.4) and taking time averages, the equations governing the time averaged motions become

$$\frac{\partial U_\alpha}{\partial x_\alpha} = 0 \tag{9.6}$$

$$\frac{\partial U_\alpha}{\partial t} + U_\beta \frac{\partial U_\alpha}{\partial x_\beta} = -\frac{1}{\rho}\frac{\partial p}{\partial x_\alpha} + \bar{g}_\alpha + \frac{\partial \tilde{u}_\alpha \tilde{u}_\beta}{\partial x_\alpha} - \frac{\partial \overline{u'_\alpha u'_\beta}}{\partial x_\alpha} \tag{9.7}$$

Eqs. (9.6) and (9.7) are the most general equations for the time-mean motions. Based on these equations a full three dimentional model for wave-induced circulations can, in principle, be developed. But in practice, this can not be achieved easily since great difficulties exist in determining quantitatively the wave and turbulent motions for general coastal situations.

Therefore, it was decided that instead of dealing with the general equations, a particular situation, i.e. longshore currents induced by monochromatic long-crested progressive waves on a plane beach, will be analysed here. It is hoped that the insight and modelling experience gained in this study should be useful for furture efforts in calculating fully three-dimensional wave-induced circulations.

9.2.2 Formulation for longshore currents

Suppose that a train of long-crested progressive monochromatic waves are obliquely incident onto a plane beach, as shown in Fig. (9.1). Let x and y denote, respectively, the onshore-offshore and longshore directions. Due to the fact that the wave conditions and sea bed topographies are uniform in the alongshore direction all the terms in eqs. (9.6) and (9.7) must be independent of y. Considering steady state and neglecting the nonlinear terms for the sake of simplicity a single governing equation for the longshore current can be derived from the y-momentum equation

$$\frac{\partial \overline{u'v'}}{\partial x} + \frac{\partial \overline{v'w'}}{\partial z} = -\frac{\partial \overline{\tilde{u}\tilde{v}}}{\partial x} - \frac{\partial \overline{\tilde{v}\tilde{w}}}{\partial z} \tag{9.7}$$

If the beach slope is sufficiently small the reflected waves are negligible. As a

result, the long-crested, locally propagating waves can be calculated accurately by refraction theory. According to linear wave theory it is known that for progressive waves

$$\overline{\tilde{u}\tilde{w}} = \overline{\tilde{v}\tilde{w}} = 0 \tag{9.8}$$

and

$$S^z_{xy} = \overline{\tilde{u}\tilde{v}} = \frac{H^2}{4C}\, g\, f^2 \cos\theta \sin\theta \tag{9.9}$$

where, H, θ and C are the wave height, wave angle and wave celerity, respectively, which can be determined from simple refraction calculation. f = f(x) is defined by Fig. (3.9). Here, $S_{xy}(z)$ can be interpreted as the radiation stress or excess momentum flux per unit depth at a particular location in the water column. Thus, eq. (9.7) becomes

$$\frac{\partial \overline{u'v'}}{\partial x} + \frac{\partial \overline{v'w'}}{\partial z} = - \frac{\partial}{\partial x} S^z_{xy} \tag{9.10}$$

It should be realized that the time averaged current velocity U_α is implicitly present in eq. (9.10) through the terms corresponding to the horizontal and vertical turbulent stresses. To represent the turbulent stresses in terms of mean velocity Boussinesq's eddy viscosity concept is used, which gives

$$\rho\overline{u'v'} = \nu_x \frac{\partial V}{\partial x} + \nu_y \frac{\partial U}{\partial y} \tag{9.11}$$

$$\rho\overline{v'w'} = \nu_y \frac{\partial W}{\partial y} + \nu_z \frac{\partial V}{\partial z} \tag{9.12}$$

where ν_x, ν_y and ν_z are the eddy viscosities in the three directions, respectively, assumed to be independent of the time averaged velocity. Because of the uniformity condition in the longshore direction the gradient terms in y should vanish. The single governing equation for V is easily found as

$$\frac{\partial}{\partial x}\left[\nu_x \frac{\partial V}{\partial x}\right] + \frac{\partial}{\partial z}\left[\nu_z \frac{\partial V}{\partial z}\right] = - \rho \frac{\partial}{\partial x} S^z_{xy} \tag{9.13}$$

The solution of this equation depends on the form of ν_x and ν_z which will be discussed in the next section. In the meantime it is considered useful to compare eq. (9.13) with eq. (50) of Longuet-Higgins (1970b) which, written in the

present notation, reads as

$$0 = -\frac{\partial Sxy}{\partial x} + \frac{\partial}{\partial x}(\nu_x d\frac{\partial \langle V \rangle}{\partial x}) - \tau_y \qquad (9.14)$$

where S_{xy} is the radiation stress component, $\langle V \rangle$ is the depth averaged longshore current velocity. Clearly eq. (9.14) can be recovered by integrating eq. (9.13) with two working assumptions:

1) the horizontal mixing is independent of the water depth
2) the bottom frictional stress can be related to the depth-averaged mean velocity and introduced as a stress boundary condition.

It is expected that, with ν_x and ν_z being properly determined, eq. (9.13) will be capable of giving a reasonable estimation of the vertical distribution of longshore currents. In the following section some simple formulae will be proposed for eddy viscosities, ν_x and ν_y.

9.2.3 Form of eddy viscosities

As a first order approximation, it is considered appropriate to represent the eddy viscosities (ν_x and ν_z) by simple algebraic formulae. Such formulae can be constructed by choosing appropriate velocity and length scales characterizing the structures of turbulent motions in both the horizontal and vertical directions.

If there is no wave breaking the turbulence must be confined to the bottom boundary layer while the main part of the flow remains irrotational. But the situation is very different inside the surf zone. As shown by Peregrine and Svendsen (1978), the turbulence generated by the breaking of the wave quickly spreads downwards from the free surface while decaying, and within one wave period it usually covers the whole depth. Based on this observation it is reasonable to assume a continuous function for the eddy viscosity throughout the water depth. In addition, considering the fact that the horizontal dimension of the coastal area normally under consideration far exceeds its vertical dimension, it is decided that different length scales will be specified in determining ν_x and ν_z.

Although the eddy viscosity on the horizontal plane, ν_x, can be assumed to be independent of time, it is generally dependent on z and x. But in order to simplify the formulation, it is further assumed that the horizontal eddy viscosity is independent of z. This means that the horizontal mixing just affects the horizontal distribution of longshore currents across the surf zone as it does in the depth

averaged current model. The simple expression proposed by Longuet-Higgins (1970b) is considered a reasonable algebraic model and adopted here for ν_x

$$\nu_x = N\rho x\ (gd)^{1/2} \tag{9.15}$$

in which it is understood that the wave celerity is determined by the shallow water wave approximation. Eq. (9.15) is certainly not in perfect accordance with the real situation but it is expected not to affect significantly the prediction of the vertical profile which to a great extent, is controlled by the vertical eddy viscosity.

With regard to the form of ν_z the lack of experimental data prevents it from being determined accurately. Heuristic judgement has to be made. One known fact from experiments is that the intensity of turbulent energy generally decreases with the distance from the free surface, which suggests a possible trend for the characteristic velocity scale of the turbulence. Another fact is that the characteristic length scale must be limited by the water depth. Thus the functional form of ν_z over the water column could be reasonably specified as proportional to wave celerity, water depth and a function of z. Two formulae are proposed in this study which have the simplest possible analytical forms, one with a linear variation over the depth and the other with a quadratic variation.

$$\nu_z = \lambda_1\ \rho(gd)^{1/2} d(\alpha - z/d) \tag{9.16}$$

$$\nu_z = \lambda_2\ \rho(gd)^{1/2}\ d(\alpha - (z/d)^2) \tag{9.17}$$

where g is the gravitational acceleration and d is the still water depth. The arbitrary constant α, in principle, should be determined empirically but in this work a value slightly greater than one has been used thereby ensuring that ν_z does not become zero at the bottom (z = d). The coefficents λ_1 and λ_2 are proportionality constants and their exact values can only be obtained by comparing computed longshore currents with experimental data. However, in analogy to the analysis by Longuet-Higgins (1970) the velocity scale should be of the order of 0.1C, where C is wave celerity and the length scale is less than d. Therefore, the values of λ_1 and λ_2 must be less than 0.1 and probabaly around 0.03 ~ 0.06.

9.3 Boundary Condition

In order to solve eq. (9.13) for V, boundary conditions have to be specified. At both the offshore and shoreline boundaries V can be taken as zero. Let x_L be

the location of the offshore boundary. Then

$$V(x_L, z) = V(0, z) = 0 \tag{9.18}$$

Two more boundary conditions are needed at the water surface and the bottom. To avoid the problem of having to describe the thin wave-current boundary layers in detail at two locations, turbulent shear stress conditions, which are much more convenient to deal with, will be specified.

For the sake of convenience in later derivations, the z axis is here taken as positive downward as shown in Fig. 9.1. At the water surface (evaluated at z = 0) the shear stress is taken as zero, which is a so called rigid-lid condition (Davies, 1982)

$$-\rho\left[\nu_z \frac{\partial V}{\partial z}\right]_{z=0} = 0 \tag{9.19}$$

At the sea bed boundary, since the flow is generally fully turbulent the Chezy type stress formula can be specified. It is a slip boundary condition with a quadratic relationship between the shear stress and the flow velocity at the boundary.

$$-\rho\left[\nu_z \frac{\partial V}{\partial z}\right]_{z=d} = \bar{\tau}_b = C' \overline{|u_b| v_b} \tag{9.19b}$$

Clearly eq. (9.19b) is very similar to the bottom friction formula proposed by Longuet-Higgins (1970b). If the wave angle with the normal to the shore is assumed small and the current is also small compared with the orbital motion of the wave, then

$$-\rho\left[\nu_z \frac{\partial V}{\partial z}\right]_{z=d} = \frac{2}{\pi} C' \rho \, \tilde{u}_{max} \, V\Big|_{z=d} \tag{9.20}$$

where C' is a friction factor which is probably still of the order of 0.01 but not necessarily the same as the friction coefficient C_f used in eq. (4.12) and $\tilde{u}_{max}$ is the maximum wave orbital velocity at the bottom and should be calculated by eq. (4.14). It should be noted that the time averaged velocity V used here is no longer substituted by the depth averaged velocity but should be taken as its value at just outside the bottom boundary layer. Since the thickness of the boundary layer is, for the most part of the surf zone, small compared with the water depth both wave and current velocities are specified at the bottom.

9.4 Solution Method

9.4.1 Transformation of coordinates

In order to apply the Galerkin method more conveniently so that different basis functions can be used it is considered advantageous to employ the sigma transformation that maps the interval $0 \leq z \leq d$ which varies with horizontal position x, into the constant interval $b \leq \sigma \leq a$. Following Davies (1982), the sigma transformation is defined as

$$\sigma = (a-b)\ (z/d) + b \tag{9.21}$$

$$x = \tilde{x} \tag{9.22}$$

where a and b are arbitrary constants. For a plane beach the transformation of the differential operators from the physical coordinate system to the new system can be carried out quite easily using the chain rule for multi-variable functions as

$$\frac{\partial}{\partial x} = \frac{\partial}{\partial \tilde{x}} - \frac{\sigma-b}{d}\, m\, \frac{\partial}{\partial \sigma} \tag{9.23}$$

$$\frac{\partial}{\partial z} = \frac{a-b}{d}\, \frac{\partial}{\partial \sigma} \tag{9.24}$$

$$\frac{\partial^2}{\partial x^2} = \frac{\partial^2}{\partial \tilde{x}^2} - 2\frac{\sigma-b}{d}\, m\, \frac{\partial^2}{\partial \sigma \partial \tilde{x}} + \frac{\sigma-b}{d^2}\, m^2\, \frac{\partial}{\partial \sigma} + \left(\frac{\sigma-b}{d}\right)^2 m^2\, \frac{\partial^2}{\partial \sigma^2} \tag{9.25}$$

where m denotes the constant sea bed slope.

9.4.2 Application of Galerkin technique

Following transformation of coordinates from the physical system to the new system and dropping the overstrike from $\hat{x}$ hereafter for the sake of simplicity, the governing equation, eq. (9.13), can be written as

$$D\nu_x \cdot DV + \nu_x D^2V + \frac{a-b}{d}\, \frac{\partial}{\partial \sigma} \left[\nu_z \frac{a-b}{d}\, \frac{\partial V}{\partial \sigma} \right] = - D(S^z_{xy}) \tag{9.26}$$

where

$$D = \frac{\partial}{\partial x} - \frac{\sigma-b}{d}\, m \frac{\partial}{\partial \sigma} \tag{9.27}$$

Expanding the velocity V in terms of the M basis functions $f_i(\sigma)$ and the

coefficients $B_i(x)$ gives

$$V = \sum_{i=1}^{M} B_i(x)\ f_i(\sigma) \tag{9.28}$$

With the basis functions being properly chosen the problem now becomes one of determining the coefficients $B_i(x)$ (i = 1, ..., M). On substitution of eq. (9.28) and multiplication by f_j , eq. (9.26) becomes

$$D\nu_x \sum_{i=1}^{M} \left[\frac{\partial B_i}{\partial x} \int_b^a f_i f_j \, d\sigma - B_i m \int_b^a \frac{\sigma-b}{d} \frac{\partial f_i}{\partial \sigma} f_j \, d\sigma\right]$$

$$+ \nu_x \sum_{i=1}^{M} \left[\frac{\partial^2 B_i}{\partial^2 x} \int_b^a f_i f_j \, d\sigma + B_i m^2 \int_b^a \left(\frac{\sigma-b}{d}\right)^2 \frac{\partial^2 f_i}{\partial \sigma^2} f_j \, d\sigma\right.$$

$$\left. + \frac{2m^2}{d^2} B_i \int_b^a (\sigma-b) \frac{\partial f_i}{\partial \sigma} f_j \, d\sigma - 2m \frac{\partial B_i}{\partial x} \int_b^a \frac{\sigma-b}{d} \frac{\partial f_i}{\partial \sigma} f_j \, d\sigma\right]$$

$$+ \sum_{i=1}^{M} \left\{B_i \left[- C' \frac{a-b}{d} f_i(a) f_j(a) + \left[\frac{a-b}{d}\right]^2 \int_b^a \nu_z \frac{\partial f_i}{\partial \sigma} \frac{\partial f_j}{\partial \sigma} \, d\sigma\right]\right\}$$

$$= \frac{\partial}{\partial x} \left(\int_b^a S_{xy}^z f_j \, d\sigma \right) - m \int_b^a \frac{\sigma-b}{d} \frac{\partial S_{xy}^z}{\partial \sigma} \, d\sigma \tag{9.29}$$

Writing in a more concise form

$$\sum_{i=1}^{M} \left[\frac{\partial^2 B_i}{\partial x^2} R_{ij} + \frac{\partial B_i}{\partial x} P_{ij} + B_i (G_{ij} + S_{ij})\right] = \frac{\partial}{\partial x} F_j + N_j \tag{9.30}$$

where

$$R_{ij} = \nu_x \int_b^a f_i f_j \, d\sigma \tag{9.31}$$

$$P_{ij} = D\nu_x \int_b^a f_i f_j \, d\sigma - 2m\nu_x \int_b^a \frac{\sigma-b}{h} \frac{\partial f_i}{\partial \sigma} f_j \, d\sigma \tag{9.32}$$

$$G_{ij} = -m\, D\nu_x \int_b^a \frac{\sigma-b}{d} \frac{\partial f_i}{\partial \sigma} f_j \, d\sigma + m^2 \nu_x \int_b^a \left[\frac{\sigma-b}{d}\right]^2 \frac{\partial^2 f_i}{\partial \sigma^2} f_j \, d\sigma$$

$$\left. + \left[\frac{a-b}{d}\right]^2 \int_b^a \nu_z \frac{\partial f_i}{\partial \sigma} \frac{\partial f_j}{\partial \sigma} \, d\sigma\right]\Big\} \tag{9.33}$$

$$S_{ij} = - \frac{a-b}{d} C' f_i(a) f_j(a) \tag{9.34}$$

$$F_j = \int_b^a S_{xy}^z \, f_j \, d\sigma \tag{9.35}$$

$$N_j = - m \int_b^a \frac{\sigma - b}{d} \frac{\partial S_{xy}^z}{\partial \sigma} f_j \, d\sigma \tag{9.36}$$

Eqs. (9.30) are linear simultaneous equations with the coefficients B_i as variables. They are also quite general which allows any form of basis functions to be used.

9.4.3 Choice of basic functions

There is no general set of rules to follow in choosing the basis functions except that they must be a complete series. Simplicity in analytical form concerning both the original function and its integrations and good convergence properties seem to be two primary criteria. The first criterion can be met by choosing orthogonal functions and the latter can only be tested by actual computational experiments. In this section we consider the choice of appropriate basis functions f_i, to use in solving eq. (9.30). Two types of function will be used.

a) *Cosine function*

A basis set of triangular functions has been used with the Galerkin method by a number of authors, see, e.g. Orszag (1971) and Davies (1978). With this choice of basis functions, the f_i are generally given by

$$f_i = \cos(\alpha_i \sigma) + \sin(\alpha_i \sigma)$$

Due to the particular surface boundary condition used the sine components should be dropped from f_i since the derivative of the sine function can not be zero at the surface according to eq. (9.19). Therefore, the basis functions become cosine functions only

$$f_i = \cos(\alpha_i \sigma) \tag{9.37}$$

It is convenient to chose a = 0 and b = 1. As shown by Davies (1978) for the case of a slip boundary (a natural boundary condition) it is not necessary to choose α_i such that this condition is satisfied by each basis function (Connor and Brebbia, 1976). A suitable choice of α_i in this case can be

$$\alpha_i = (i-1) \, \pi \tag{9.38}$$

Thus, eq. (9.37) can be written as

$$f_i = \cos\{(i-1)\pi\sigma\} \tag{9.39}$$

b) *Legendre polynomials*

Another set of basis functions used here are Legendre polynomials which are also orthogonal and quite simple in form. These functions, over the interval $-1 \leq \sigma \leq +1$ can be readily generated using the recurrence formulae,

$$f_{i+1}(\sigma) = \frac{2i+1}{i+1}\,\sigma\, f_i(\sigma) - \frac{i}{i+1} f_{i-1}(\sigma) \tag{9.40}$$

$$f'_{i+1} = \sigma\, f'_i + (i+1)\, f_j \tag{9.41}$$

$$f''_{i+1} = \sigma\, f''_i + (i+1)\, f'_j \tag{9.42}$$

with

$$f_0 = 1 \qquad f_1 = \sigma \tag{9.43}$$

$$f'_0 = 1 \qquad f'_1 = \sigma \tag{9.44}$$

$$f''_1 = 1 \qquad f''_1 = \sigma \tag{9.45}$$

It should be noted that the subscript i must start from 1 as required by the summation in eq. (9.28). This can be done simply by actually using f_i of eq. (9.40) as f_{i+1} in eq. (9.28).

9.4.4 Discretization in horizontal space

The computational grid system is as shown in Fig. 9.2 where the x axis across the surf zone is divided into N + 1 nodal points at a distance Δx apart. Using simple forward difference scheme, Eq. (9.30) can be discretized for a typical nodal point k as

$$\sum_{i=1}^{M} \left(\frac{B_{i,k+1} - 2B_{i,k} + B_{i,k-1}}{\Delta x^2} R_{ijk} + \frac{B_{i,k+1} - B_{ik}}{\Delta x} P_{ijk} + B_{ik}\,(G_{ijk} + S_{ijk})\right)$$

$$= \left(\frac{\partial F_{j\,k+1} - F_{jk}}{\Delta x}\right) + N_{jk} \tag{9.50}$$

or written in a more convenient form for solving B_{ik}

$$\sum_{i=1}^{M}(B_{i,k+1}W_{ijk} + B_{ik}X_{ijk} + B_{i,k-1}Y_{ijk}) = A_{jk} \tag{9.51}$$

where

$$W_{ijk} = R_{ijk}/\Delta x^2 + P_{ijk}/\Delta x \tag{9.52}$$

$$X_{ijk} = -2R_{ijk}/\Delta x^2 - P_{ijk}/\Delta x + G_{ijk} + S_{ijk} \tag{9.53}$$

$$Y_{ijk} = R_{ijk}/(\Delta x)^2 \tag{9.54}$$

$$A_{ijk} = -(F_{j,k+1} - F_{jk})/\Delta x + N_{jk} \tag{9.55}$$

9.5 Computational Results and Discussion

In order to verify the predictability of this numerical longshore current model experimental data are necessary for calibrating the coefficients involved in the model such as λ_1 and λ_2. For this purpose Visser's measurements on the longshore currents at several locations over the depth are used. It has been noticed that there exist some obvious differences between wave conditions in the experiments and assumptions made in the theoretical model, for example, the waves in the experiment are plunging waves and incident wave angles are generally not very small. Despite that, Visser's data are used since they are the only reliable systematic experimental data of longshore current distribution over water column. It is initially hoped and later proved by numerical tests that the coefficents are not particularly sensitive to the breaker type and incident wave angles.

For the convenience of comparison the experimental conditions and typical measured longshore velocity profiles for exp.4 and exp.6 have been reproduced from Visser (1984) as shown in Figs. 9.3, 9.4 and 9.5. Since the waves in exp.6 are the mixed plunging/spilling waves, they are the most suitable waves from all the seven experiments for the calibration of the model. The input conditions are, the wave height H = 0.058m, wave period T = 0.7sec, angle of incidence at the breaking point θ_{br} = 14.3° and the breaking index γ = 0.66. The bottom slope is 0.05 with the water depth varying linearly from the shoreline to a depth of 0.35m. Other input coefficients include the friction coefficient C', which is taken as 0.003 according to Visser's reccomendation, and the horizontal mixing coefficient N, which is chosen as 0.04 corresponding to the mixing coefficent M used in Visser's depth averaged one equation turbulence model.

The longshore currents have been calculated using both eqs. (9.16) and (9.17), in which λ_1 and λ_2 are chosen as 0.03 for achieving the best fit with measured data. The cross-shore profiles of the computed longshore velocity at three locations over the water column are presented in Figs. 9.6 and 9.7. The detailed comparison between the computed results and Visser's measurements is presented in Fig. 9.8. It can be seen that the variation of longshore currents over depth is small and quite insignificant over most part of the cross-shore area.

It is also noticed that the results from using eqs. (9.16) and (9.17) are almost identical, which indicates the variation of ν_z over water depth is not important and a constant eddy viscosity ν_z may well be used. In fact, the most important quantity in determining the vertical velocity profile is the values of λ_1 (or λ_2). A large value results in a uniform velocity profile which can be seen clearly in Fig. 9.9 which is obtained by taking λ_1 as 1.0, while unrealistically small values will lead to unrealistcally large differences between calculated velocities at different locations in the water column.

For the verification of this theoretical model Visser's exp.4 is used. Using the same values for λ_1 and λ_2 the cross-shore profiles of the computed longshore velocity at three locations over the water column using eqs. (9.16) is presented in Fig. 9.10. Unlike the previous case, the variation of longshore currents over the water depth in this case is quite appreciable, especially in the region of maximum velocity. As shown by the detailed comparison between computed results and experimental values in Fig. 9.11 the overall agreement at all three locations is quite remarkable except for a small section just outside the breaking line where the currents are overpredicted. An interesting feature in the computed results is that inside the surf zone the computed velocity at the surface is always greater than that at mid-depth or at bottom but outside the surf zone the computed velocity at bottom could exceed that at the surface. This phenomenon is clearly identifiable in the measured velocity profiles.

To summarize this chapter it can be stated that despite the crude nature of this theoretical model with regard to the description of turbulence and wave breaking, the computational results have shown that it is applicable for the prediction of vertical profiles of longshore currents generated by both spilling and plunging waves on a plane beach. The turbulent eddy viscosities have been reasonably modelled by a simple algebraic formula and the key to this model is the coefficient involved in the vertical eddy viscosity which must be specified in accordance with the physical characteristics of wave breaking induced turbulence. The use of the slip boundary condition, which has made the formulation of the

model a lot simpler than in the case of using a non-slip boundary condition, is proved to be appropriate as far as the bottom boundary layer remains thin and is not much disturbed by the turbulent motions originating from the surface. Probably the most important contribution of this study is that, apart from establishing a useful circulation model for a simple two dimensional situation, the basic approach provides a framework based on which a general three-dimensional circulation model can be developed.

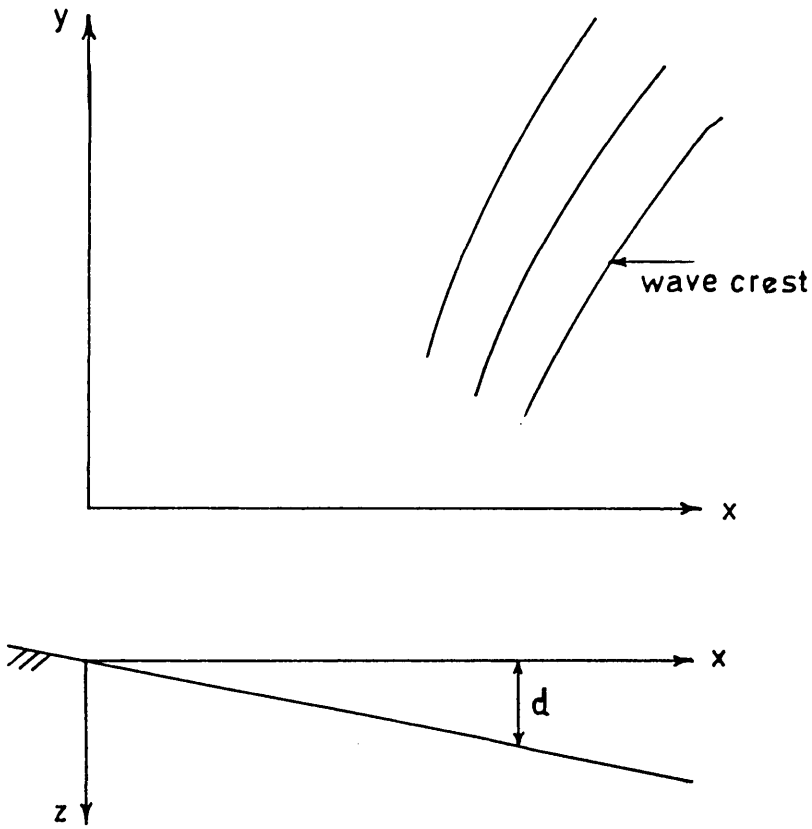


Fig. 9.1 Beach Form and Wave Condition

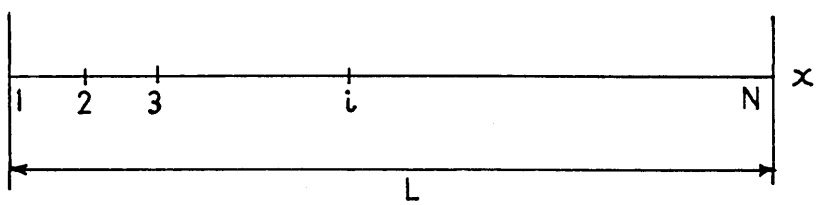


Fig. 9.2 Grid Arrangement for Numerical Solution

exp nr	beach	tgα	T sec	d_1 cm	θ_1 degr	H_1 cm	H_o cm	$\frac{H_o}{\lambda_o}$	θ_o degr	H_{br} cm	d_{br} cm	$\frac{H_{br}}{d_{br}}$	θ_{br} degr	$\bar{\eta}_m$ cm	x_{br} cm	p	R cm	breaker type	$\frac{tg\alpha}{\sqrt{H_o/\lambda_o}}$
1	smooth	0.101	2.01	39.9	31.1	7.2	9.8	0.0155	61.5	10.5	10.4	1.00	20.9	4.20	145	0.59	7.2	pl	0.81
2	smooth	0.101	1.00	39.9	30.5	9.5	10.2	0.0653	32.5	10.0	10.9	0.91	24.0	2.78	136	0.57	4.1	pl	0.39
3	smooth	0.101	1.00	40.1	15.4	8.9	9.6	0.0615	16.4	9.7	11.4	0.85	12.1	2.75	141	0.60	4.1	pl	0.41
4	smooth	0.050	1.02	35.0	15.4	7.8	8.5	0.0523	17.0	9.1	11.0	0.83	12.5	1.64	251	0.76	1.9	pl	0.22
5	smooth	0.050	1.85	34.8	15.4	7.1	7.5	0.0140	26.4	10.8	11.6	0.93	11.5	2.45	279	0.75	3.1	pl	0.42
6	smooth	0.050	0.70	35.0	15.4	5.9	6.0	0.0784	15.5	5.8	8.8	0.66	14.3	1.00	194	0.82	1.1	sp/pl	0.18
7	rough	0.050	1.02	35.0	15.4	7.8	8.5	0.0523	17.0	9.0	12.2	0.74	12.2	1.64	275	0.78		pl	0.22

Fig. 9.3 Beach and Wave Field Properties and Quantities; for exps.1 to 7 from Visser (1984)

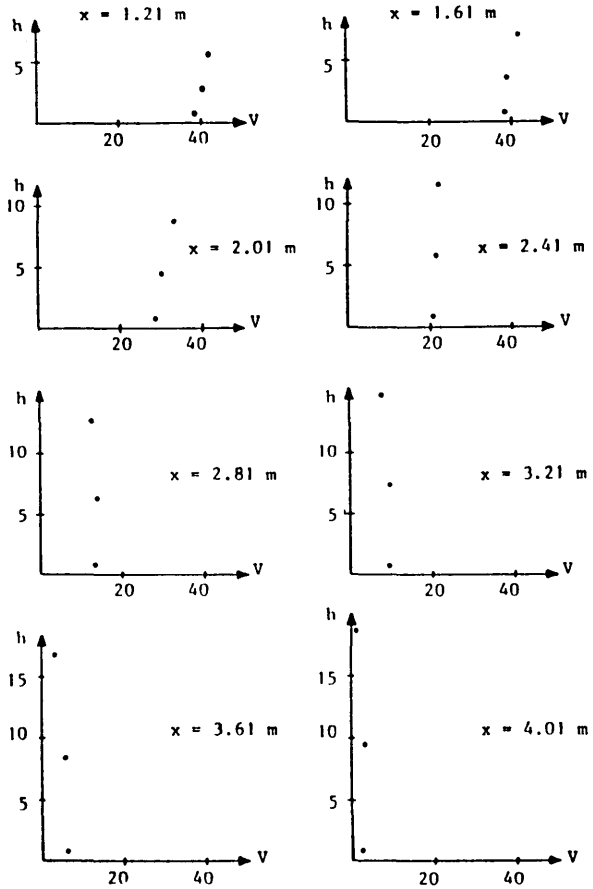


Fig. 9.4 Alongshore Averaged Vertical Velocity Profiles exp.4

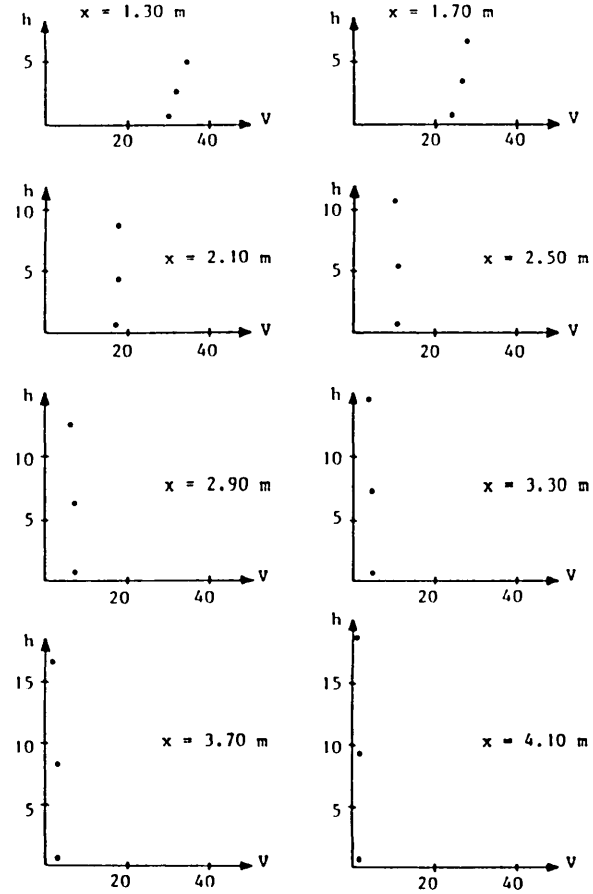


Fig. 9.5 Alongshore Averaged Vertical Velocity Profiles exp.6

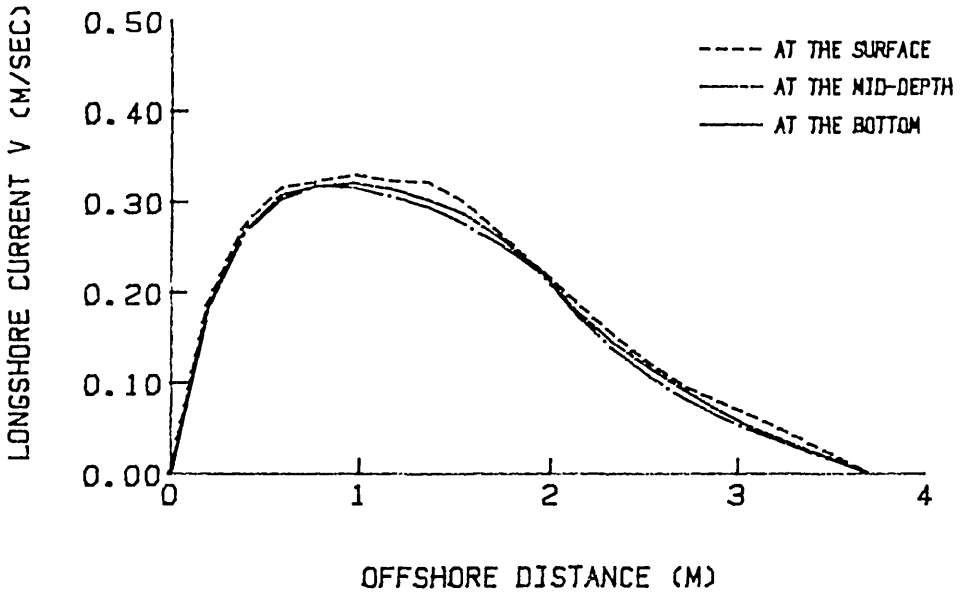


Fig. 9.6 Computed Longshore Current Profiles across the Surf Zone at Three Locations over the Water Column Using the Linear Expression for ν_z with Input Data from Visser's exp.6

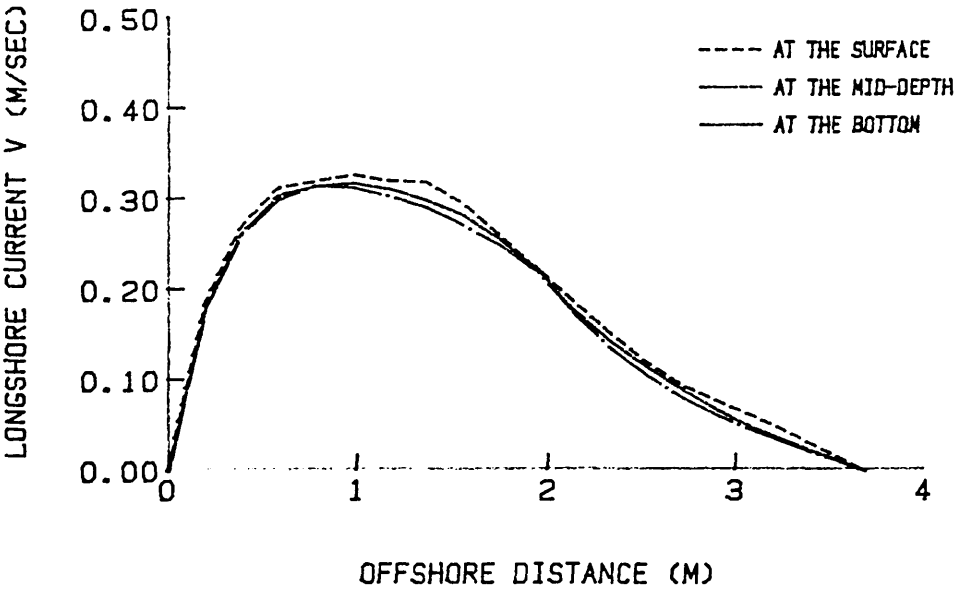


Fig. 9.7 Computed Longshore Current Profiles across the Surf Zone at Three Locations over the Water Column Using the Quadratic Expression for ν_z, with Input Data from Visser's exp.6.

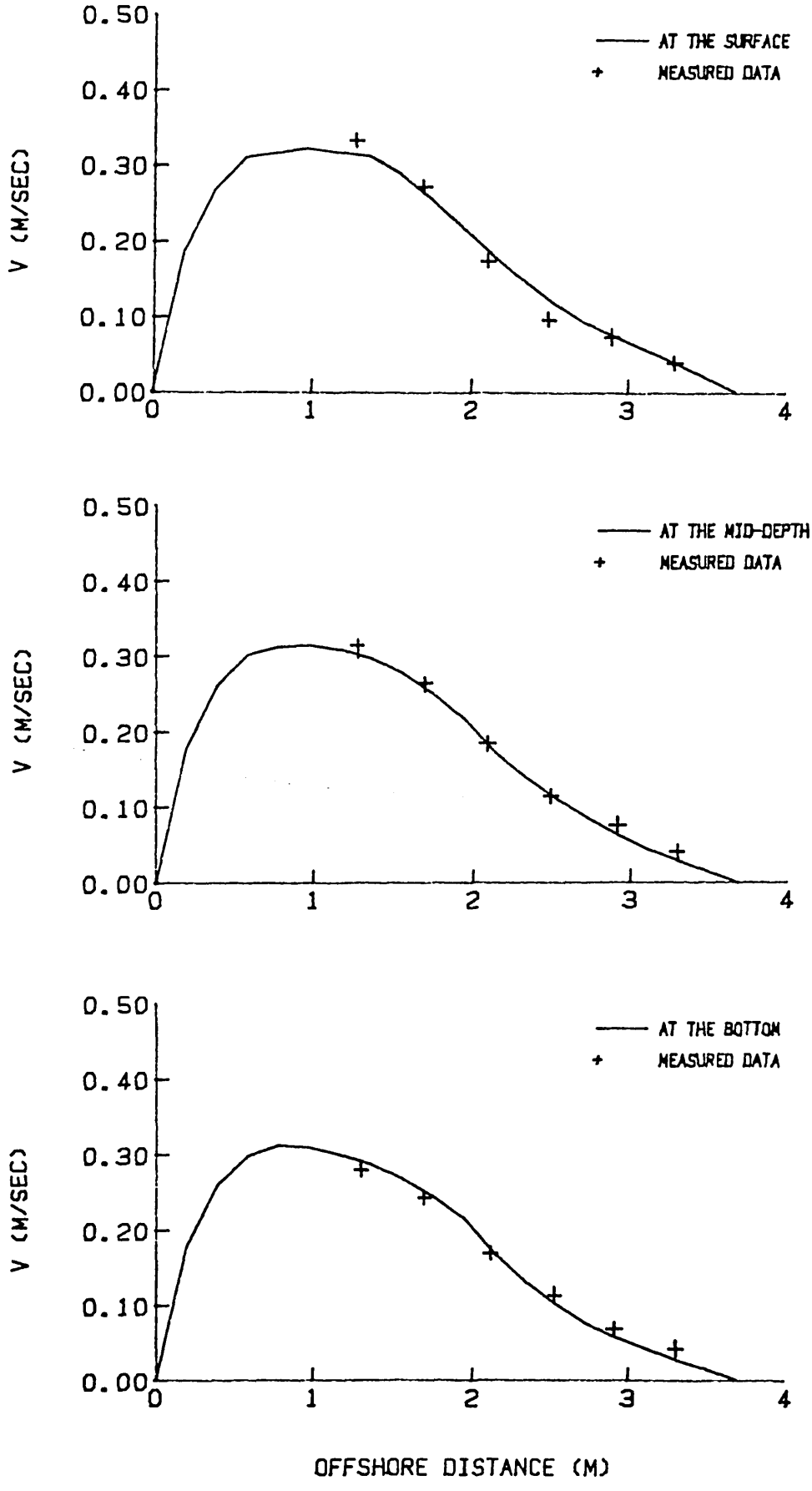


Fig. 9.8 Comparison between Computed and Measured Velocity Profiles for exp.6

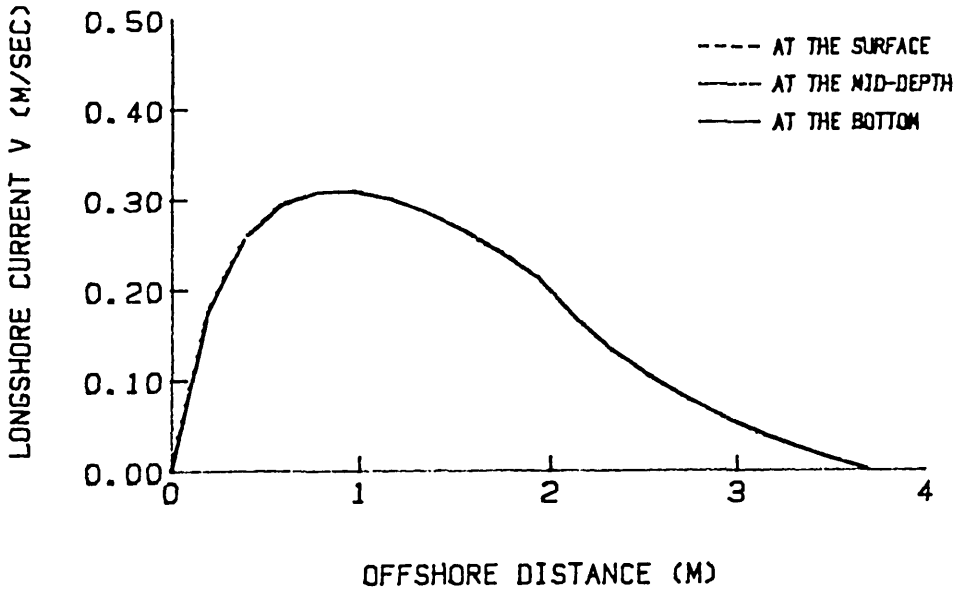


Fig. 9.9 Computed Longshore Current Velocity with Input Data from Visser's exp.6 and $\nu_z = 1.0$

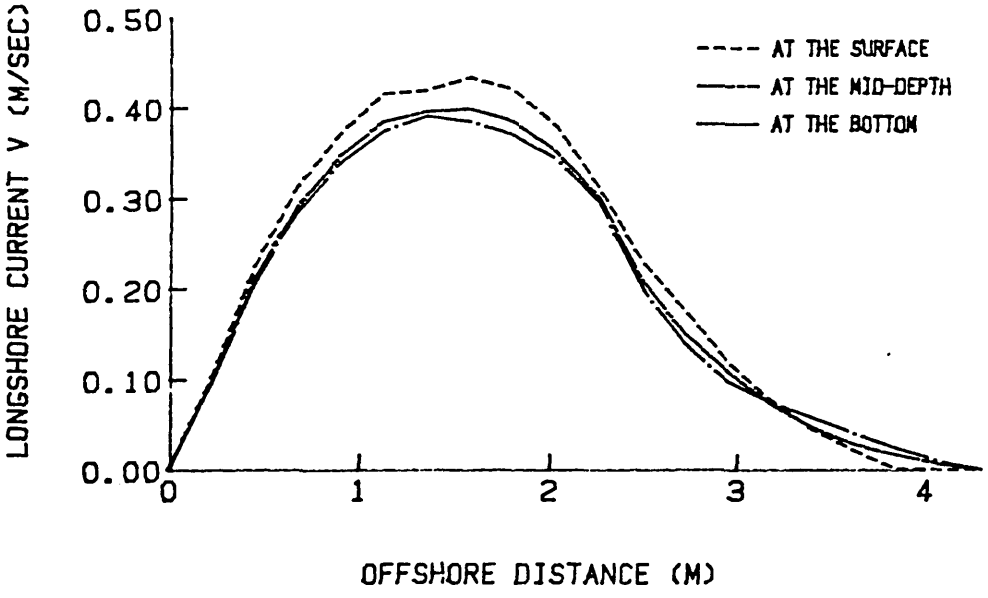


Fig. 9.10 Computed Longshore Current Profiles across the Surf Zone at Three Locations over the Water Column Using the Linear Expression for ν_z with Input Data from Visser's exp.4

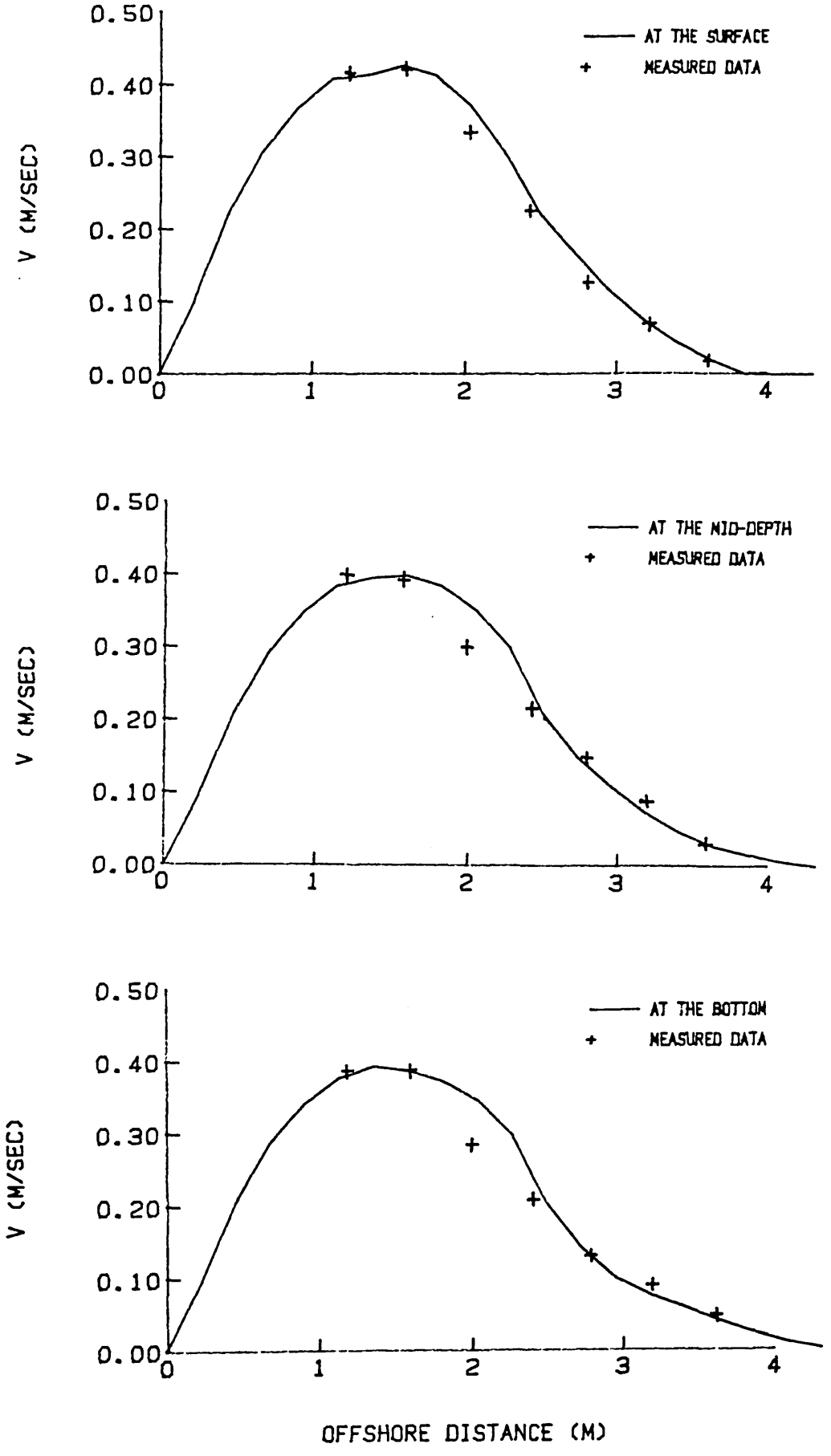


Fig. 9.11 Comparison between Computed and Measured Velocity Profiles for exp.4

CHAPTER. 10
CONCLUSIONS AND RECOMMENDATIONS

10.1 Conclusions

It has been shown that the effects of a large-scale current on linear wave propagation can be described by the wave model which is developed based on the general mild-slope equation originally given by Booij (1981) but, in this work, used in a modified form. The wave induced circulation has been successfully modelled by solving the depth-averaged equations of continuity and motion, in which all the waves quantities are calculated from the wave model. Wave-current interactions are included in both the wave and circulation models. The effects of turbulence transport are also included by developing appropriate one and two equation turbulence models. The resulting numerical model is thus applicable to studies of wave-induced circulation related to more general coastal wave and topographical situations than those achieved by previous numerical models.

With respect to both the theoretical and numerical aspects of the models developed the following conclusions could be drawn

(1) The general mild-slope equation which includes the effects of wave-current interaction is, as it is proved theoretically in this work, applicable to a current system which has a weak vorticity in the horizontal plane. The strict irrotationality constraint required in previous derivations has thus been relaxed. As a result the interaction between waves and wave-induced currents which is generally not irrotational, can be studied using the mild-slope equation.

(2) The transmissive boundary condition commonly used has been shown to be imperfect. Certain amount of wave energy at the boundaries tends to be reflected back into the internal computational domain. Such reflected waves result in errors in computed wave heights which are generally about ten percent of the incident wave height.

(3) The explicit finite difference schemes used for solving the governing equations for the time mean motions and turbulent motions are stable for all cases studied as long as the Courant number is smaller than unity. The convective acceleration terms are properly centered in space and time while the diffusion terms are centered in space only in order to enhance stability. The accuracy of the schemes is estimated to be not less than of the order of $(\Delta t, \Delta x^2)$.

(4) The time step used in the numerical integration must be small in order to ensure the stability of the finite difference equations for the wave and circulation models. Computational experience indicates that, for both models, the Courant number used can only be up to 0.6 rather than 1.0. The number of grid points per wave length needed in the wave model should not be less than 10 when applied to non-breaking waves. For sloping beaches the lower limit should be controlled by the water depth at the breaking line instead of the small depth arbitrarily chosen near the shoreline.

(5) For some cases, in order to ensure the stability of the wave model in the process of alternative intergrations of the wave and the circulation models the currents have to be built up gradually over the first several periods of the integration.

(6) The simple reflective and periodic boundary conditions have been successfully applied in the circulation models, corresponding to the particular cases under consideration. In order to maintain certain level of mixing outside the surf zone, the turbulent energy and dissipation at the offshore boundary are specified as very small values rather than zero.

With respect to the computational results, the following conclusions could be drawn

(7) The wave model developed as an alternative and slightly simplified version of Booij's original mild-slope equation, can be applied to the simple current refraction as well as more complicated current-depth refraction and diffraction where multiple caustics exist.

(8) The wave height and radiation stresses can be calculated accurately in terms of the primary variables in the wave model.

(9) The convective acceleration terms are important in the prediction of wave-induced circulation. In order to treat these terms properly in the numerical model appropriate finite difference schemes are essential, as it has been shown in the case of Silva Lima's experimental beach.

(10) The turbulent mixing terms are important and must be included in every numerical circulation model. However, computational results have shown that the effects of turbulence transport on the computed circulations are not as significant as expected initially but by no means negligible. As far as circulations are concerned

the two equation model generally gives better results than the zero or one equation models.

(11) If wave-induced currents are sufficiently strong the effects of wave current interaction are appreciable and have to be taken into account. The procedure followed in this work involving the combined integration of the wave model and circulation model has been proved to be successful. Generally, for all cases considered the steady solution can be reached or nearly reached in less than 5 alternative runs of the wave and the circulation models.

(12) The wave angles are difficult to determine accurately when waves are short-crested due to cross waves. In such situations some errors could occur in the calculation of the radiation stresses and wave energy fluxes which require knowledge of wave angles.

(13) The longshore current model developed is capable of predicting the vertical profiles of longshore currents in Visser's physical model. It is expected that if the coefficent in the vertical eddy viscosity is further calibrated by adequate field data this model would be prefered rather than the depth-averaged longshore current models used up to now in engineering applications.

10.2 Recommendations for Future Research

Although the main objectives of this research have been satisfactorily accomplished by the numerical models developed (i.e. the numerical modelling of wave propagation and wave induced circulation including the effects of wave current interaction, turbulence transport and the prediction of the vertical profile of longshore velocity on a plane beach) there is further work that can be done to improve these models. The following specific aspects are recommended as suitable topics for further studies.

(1) By dividing the computational domain into several zones according to whether the waves under consideration are propagating or standing or cross waves, different values for the breaking index can be specified for each zone so that wave breaking can be modelled more realistically. Probably an even better way of describing the effect of wave breaking is to calculate directly the wave breaking induced dissipation instead of using a proportionality assumption between the wave height and water depth.

(2) The transmissive boundary condition used in the wave model is far from

satisfactory. Some more sophisticated techniques such as the sponge layer method (Larsen & Warren, 1986) might give better results.

(3) The coefficents $c_{\mu 1}$, $c_{\mu 2}$ and c_D in the one and two equation turbulence models should be calibrated by directly comparing computed turbulence quantities such as $\bar{k}$ and $\bar{\nu}_t$ with corresponding measured values rather than using the mean velocities as means of comparison.

(4) The formula used for the bottom frictional stresses is in fact applicable only when the wave angles are small and current velocities are much smaller than wave particle velocities. For single wave train with arbitrary wave angle and relative magnitude of current and wave velocities the method by Liu and Dalrymple (1978) can be used. However, more realistic formulations should be developed for bottom friction which is applicable not only to propagating waves but also to cross waves.

(5) The model developed for the vertical distribution of the longshore current is only applicable to a plane beach. A natural step forward would be to extend the model to more general two dimensional beaches with particular features like longshore bars. In principle the same approach can also be applied to formulate three dimensional circulation models but in this case the computational penalty in terms of run time would be expected to be much more severe.

(6) Finally and most importantly, with numerical models becoming increasingly sophisticated, more detailed prototype wave and current data are urgently required for proper calibration and verification of the models.

In addition to the above recommendations which refer to specific terms in the models, an even more realistic representation in general terms of the mechanisms related to coastal waves and wave induced circulation would be obtained by the inclusion of

i) Sediment transport which would allow the beach to adjust itself to the wave field.

ii) The randomness of the waves

REFERENCE

Abbott, M. B., Peterson, H. M., Skovgaard, O. (1978)
'On the numerical modelling of short waves in shallow water' J. Hydraulic Res. 16, No. 2, pp. 173-203

Airy, Sir G. B. (1845)
'Tides and Waves', ENCYC. Metrop., Art. 192

Alfrink, B. J. and L. C. van Rijn (1983)
'Two equation turbulence model for flow in trenches', J. of Professional Issues in Eng., Vol. 109, No. 3, pp. 941-957

Arthur, R. S. (1950)
'Refraction of shallow water waves: The combined effects of currents and underwater topography', EOS Trans. AGU, Vol. 31, pp.549-552

Arthur, R. S., Munk, W. H., Isaacs J. D. (1952)
'The direct construction of wave rays', Trans. Am. Geo. Union, Vol. 33, No. 6, pp. 355-865

Arthur, R. S. (1962)
'A note on the dynamics of rip currents' J. Geophys. Res., Vol. 67, No. 7, pp. 2777-2779

Austin, D. J. (1981)
'Longshore boundary conditions for numerical wave models', Int. Jnl. for Num. Method in Fluids, Vol. 2, pp. 263-276

Battjes, J. A. (1975)
'Modelling of turbulence in the surf zone', Proc. Symp. Modelling Techniques ASCE,. pp. 1050-1061

Battjes, J. A. (1983)
'Surf zone turbulence', Proc. Seminar on Hydrodynamics of Waves in Coastal Areas, I. A. H. R., Moscow

Basco, D. R. (1982)
'Surfzone currents', Coastal Engineering 7 (1983), pp. 331-355

Behrendt, L. (1985)
'A finite element model for water wave diffraction including boundary absorption and bottom friction', Series Paper 37, Institute of Hydrodynamics and Hydraulic Engineering, Technical University of Denmark

Berkhoff, J. C. W. (1972)
'Computation of combined refraction and diffraction' , Proc. 14th Coastal Eng. Conf., pp.471-490

Berkhoff, J. C. W., N. Booij, A. C. Radder. (1982)
'Verification of numerical wave propagation models for simple harmonic linear waves', Coast Eng., Vol. 6, pp.255-279

Bettess, P., and O. C Zienkiewicz. (1977)
'Diffraction and refraction of surface waves using finite and infinite elements' , Int. J. Numer. Methods Eng., Vol. 12, pp1271-1290

Bettess, P. and J. A. Bettess (1982)
'A Generalization of the radiation stress tensor', Appl. Math. Modelling, 6 (3), pp. 146–150

Birkemeier, W. A. & Dalrymple, R. A. (1976)
'Numerical models for the prediction of wave sep–up and nearshore circulation', Ocean Eng. Rep. No. 3, Univ. Delaware, Dept. of Civ. Eng.

Blue, F. L. & Johnson, J. W. (1949)
'Diffraction of water waves passing through a breakwater gap', Trans. Am. Geo. Union, Vol. 30, No. 5

Booij, N. (1981)
'Gravity waves on water with non–uniform depth and current' , Ph.D. dissertation, Delft Univ. of Technology, the Netherlands

Booij, N. (1983)
'A note on the accuracy of the mild–slope equation', Coastal Eng., Vol. 7, pp. 191–203.

Boussinesq, J. (1872)
'Theorie des ondes et de remous qui se propagent le long d'un canal rectangulaire horizontale, en communiquant au liquid contenue dans le canal des vitesses sensiblement pareilles de la surface au fond', J. Math. Pures Appliquees, Ser. 2, 17, pp. 55–108

Bowen, A. J., Inman, D. L. & Simmons, V. P. (1968)
'Wave set–up and set–down', J. Geophys. Res., Vol. 73, pp. 2569–2577.

Bowen, A. J. (1969a)
'The generation of longshore currents on a plane beach', Jnl. Marine Res., Vol. 27, No. 2, pp. 206–215

Bowen, A. J. (1969b)
'Rip currents', Jnl. Geophys. Res., Vol. 74, No. 23, pp. 5467–5488

Bowen, A. J. & Inman, D. L. (1969)
'Rip currents – lab and field observations', Jnl. Geophys. Res., Vol. 74, No. 33, pp. 5479–5490

Bowers, E. C. & Southgate, H. N. (1982)
'Wave diffraction, refraction and reflection. A comparison between a physical model and a mathematical ray model'. Report No. IT 240, Nov. Hydraulics Res. Station

Bradshaw, P., Cebeci, T. & Whitelaw. J. H. (1981)
'Engineering Calculation Methods for Turbulent Flow', Academic Press Inc. (London) Ltd

Bretherton, F. P. & C. J. R. Garrett (1969)
'Wave trains in inhomogeneous moving media. Proc. R. Soc. Lond. A302, pp. 529–554

Cokelet, E. D., (1977)
'Steep gravity waves in water of arbitrary uniform depth', Philos. Trans. R. Soc. Lond. A 286, pp. 183–230

Chao, Y. Y. (1971)
'An asymptotic evaluation of the wave field near a smooth caustic', J. Geophy. Res., Vol. 76, pp. 7401–7408

Christoffersen, J. B. (1982)
'Current depthe refraction of dissipative water wave', Series Paper 30, Institute of Hydrodynamics and Hydraulic Engineering, Technical University of Denmark

Copeland, G. J. M. (1985)
'A numerical model for the propagation of short gravity waves and the resulting circulation around nearshore structures', Ph.D Thesis, University of Liverpool

Copeland, G. J. M. (1986)
'Personal communication'

Dally, W. R., Dean. G. and Dalrymple. A. (1984)
'A model for Breaker Decay on Beaches' Proc. 19th Coatal Eng. Conf., Vol. 1, pp. 83-97

Davies, A. M. (1980)
'On formulation of a three-dimensional hydrodynamic sea model with an arbitrary variation of vertical eddy viscosity', Comp. Meth. in Appl. Mech. and Eng., Vol. 22

Ebersole, B. A. & Dalrymple, R. A. (1980)
'Numerical modelling of nearshore circulation', Proc. 17th Conf. Coastal Engrg., Chap. 163

Engquist, B. & Majda, A. (1977)
'Absorbing boundary conditions for the numerical simulation of waves', Math. of Comp., Vol. 31, No. 139, pp. 629-651

Falconer, R. A. (1976)
'Mathematical Modelling of Jet-Forced Circulation In Reservoirs and Harbours', Ph.D thesis, University of London

Flather, R. A. & Heaps, N. S. (1974)
'Tidal computations for Morecambe Bay', Geophy. J. R. astr. Soc, Vol. 42, pp. 489-517

Galvin, C. J. (1967)
'Longshore current velocity: a review of theory and data', Rev. of Geophysics, Vol. 5, No. 3, pp. 287-305

Grant, W. D. & O. S. Madsen (1979)
'Bottom friction under waves in the presence of a weak current', Tech. Mem. ERL-MESA, National Oceanic and Atmospheric Administration

Hales, L. Z. and Herbich, J. B. (1972)
'Tidal inlet current - ocean wave interaction', Proc. 13th Coastal Eng. Conf., Vol. 1, pp. 669-688

Hino, M. (1974)
'Theory on formation of rip-current and cuspidal coast', Coastal Engineering in Japan, Vol. 17, pp. 23-37

Horikawa, K. and Kuo, C. T. (1966)
'A study of wave transformation inside surf zone', Proc. 10th Coastal Eng. Conf., ASCE, Vol. 1, pp. 217-233

Horikawa, K. (1978)
'Coastal engineering - an introduction to ocean engineering', Univ. of Tokyo Press.

Inman, D. L., Tait, R. J. and Nordstrom, C. E. (1971)
'Mixing in the surf zone', J. of Geophy. Res., Vol. 76, No. 15, pp. 3493-3514

Ito, Y. & Tanimoto, K. (1972)
'A method of numerical analysis of wave propagation - application of wave refraction and diffraction', Proc. 13th Conf. Coastal Eng., Chap. 26

Iwagaki, Y. (1968)
'Hyperbolic waves and their shoaling', Proc. 11th Coastal Eng. Conf., Vol. 1, pp. 124-144

James, I. D. (1974)
'A nonlinear theory of longshore currents', Estuary Coastal Marine Sci., Vol. 2, pp. 235-250

Jonsson, I. G., Skovgaad, O. & Brink-Kjaer (1976)
'Diffraction and refraction calculations for waves incident on an island', J. Marine Res., Vol. 34, pp. 469-496

Jonsson, I. G. (1966)
'Wave boundary layers and friction factors', Proc. 10th Conf. Coastal Eng. Chap. 10, pp. 127-148

Johnson, J. W. (1947)
Transactions, American Geophy. Union, Vol. 28, 1947

Jonsson, I. G., O Skovgaard and T. S. Jacobsen (1974)
'Computation of longshore currents', Proc. 12th Conf. Coastal Eng., Vol. 1, pp. 486-501

Keller, J. B. (1958)
'Surface waves on water of non-uniform depth', J. Fluid Mech. 4, pp. 607-614

Keller, J. B. (1962)
'Geometrical theory of diffraction', J. of Optical Soc. of America, Vol. 52, No. 2, pp. 116-129

Kirby, J. T. and Dalrymple, R. A. (1983)
'A parabolic equation for combined refraction-diffraction of Stokes waves by mildly varying topography', J. Fluid Mech., Vol. 136, pp. 453-466

Kirby, J. T. (1984)
'A note on linear surface wave-current interaction over slowly varying topography' ,J. Geophys. Res., Vol. 89, No. C1, pp.745-747.

Kirby, J. T. and Dalrymple, R. A. (1986)
'Modeling waves in surfzones and around islands', J. of Waterway, Port, Coastal and Ocean Engineering, ASCE, Vol. 112, No. 1, pp. 78-93

Korteweg, D. J. & G. de Vries (1895)
'On the change of form of long waves advancing in a rectangular canal and on a new type of long stationary waves', Philos. Mag. Vol. 39, pp. 422-443

Lamb, Sir H. H. (1932)
'Hydrodynamics', Cambridge University Press, and Dover, New York

Larsen, J. (1978)
'A harbour theory for wind generated waves based on ray methods', J. Fluid Mech, 87, pp 143-158

Larsen, J. and Dancy, H. (1983)
'Open boundaries in short wave simulations - a new approach', Coastal Eng., Vol. 7, pp. 285-297

Launder, B. E. and Spalding, D. B. (1974)
'The numerical computation of turbulent flow', Comp. Meth. in Appl. Mech. and Eng., Vol. 3, p. 269

Le Blond, P. H. & Tang C. L. (1974)
'On energy coupling between waves and rip currents', J. Geophy. Res., Vol. 79, No. 6, pp. 811-816

Levi-Civita, T. (1924)
'La determination rigoueuse des ondes permanentes d'ampleur finie', Proc. First Intern. Congr. Appl. Mech., pp. 129-145

Liang, S-C (1983)
'Prediction of wave induced surf zone current adjacent to breakwaters', Ph.D Thesis, U.C. Swansea

Liu, P. L-F. (1983)
'Wave current interactions on a slowly varying topography', J. Geophys. Res., Vol. 88, No. C7, pp. 4421-4426.

Liu, P. L-F., and Dalrymple, R. A. (1978)
'Bottom friction stresses and longshore currents due to waves with large scale of incidence', J. Marine Res., Vol. 36, pp. 357-475

Liu, P. L-F., & Mei, C. C. (1976a, b)
'Water motion on a beach in the presence of a breakwater 1. waves 2. mean currents', J. Geophys. Res., Vol. 81, pp3079-3084 and 3085-3094

Liu, P. L-F. and Tsay, T-K. (1983)
'On weak reflection of water waves', J. Fluid Mech., Vol. 131, pp. 59-71

Longuet-Higgins, M. S.(1970a)
'Longshore currents generated by obliquely incident sea waves', J. Geophys. Res., Vol. 75, pp. 6778-6789

Longuet-Higgins, M. S.(1970b)
'Longshore currents generated by obliquely incident sea waves', J. Geophys. Res., Vol. 75, pp. 6790-6801

Longuet-Higgins, M. S. (1972)
'Recent Progress in the Study of Longshore Currents', in Waves on Beaches, Ed. Meyer, Academic Press, pp. 203-248

Longuet-Higgins, M. S., and Stewart, R. W. (1961)
'The changes in amplitude of short gravity waves on non-uniform currents', J. Fluid Mech., Vol. 10, pp.529-549.

Lozano, C. J. and Meyer, R. E. (1976)
'Leakage and response of waves trapped round islands', Phys. Fluids., Vol. 19, 1075-1088.

Ludwig, D. (1966)
'Uniform asymptotic expansions at a caustic', Comm. Pure Appl. Math., Vol. 19, pp. 215-250

Luke, J. C. (1967)
'A variational principle for fluid with a free surface', J. Fluid Mech., Vol. 27, pp. 395-397.

McKee, W. D. (1974)
'Waves on a shearing current: a uniformly valid asymptotic solution', Proc.

Cambridge Philos. Soc., Vol. 75, pp. 295-301

Mckee, W. D. (1975)
'A two turning point problem in fluid mechanics', Proc. Camb. Phil. Soc., Vol. 77, pp. 581-590

Meadows, G. A. (1976)
'Time dependent fluctuations in longshore currents', Proc. 15th Coastal Eng. Conf. Vol. 1, pp. 661-680

Mei, C. C. (1983)
'The applied dymamics of ocean surface waves', pub. Wiley-Interscience

Mei, C. C. & LeMehaute, B (1966)
'Note on the equations of long waves over an uneven bottom', J. Geophys. Res. Vol. 71, pp. 393-400

Meyer, R. E. (1979)
'Theory of water wave refraction', Adv. in Appl. Mech., Ed. Chia-Shun Yih, Vol. 19, Academic Press, pp. 53-141

Noda, E. K. (1974)
'Wave induced nearshore circulation', Jnl. Geophy. Res., Vol. 79, No. 27, pp. 4097-4106

Noda, E. K., Sonu, C. J. et al (1974)
'Nearshore circulation under sea breeze conditions and wave-current interactions in the surf zone', Tetra Tech. Report, Chapter 3, TC-149-4, Pasadena

Peregrine, D. H. (1967)
'Long waves on a beach', J. Fluid Mech., Vol. 27, pp. 815-827

Peregrine, D. H. (1976)
'Interactions of water waves and currents', Adv. Appl. Mech., vol. 16, pp.9-117.

Peregrine, D. H. and Smith, R (1979)
'Nonlinear effects upon waves near caustics', Phil. Trans. R. Soc. Lond., A292, pp. 341-370

Peregrine, D. H. and Thomas, G. P. (1979)
'Finite-amplitude deep-water waves on currents', Phil. Trans. R. Soc. Lond., A292, pp. 371-390

Peregrine, D. H. and Svendsen, I. A. (1978)
'Spilling breakers, bores and hydraulic jumps', Proc. 16th Coastal Eng. Conf.

Phillips, O. M. (1977)
'The dynamics of the upper ocean', Cambridge University Press, Second Ed., New York.

Poisson, S. D. (1818)
'Memoire sur la theorie des ondes', Mem. Acad. Roy. Sci. Inst., France, [2], Vol. 1, p. 1816

Putnam. J. A., Munk, W. A. & Traylor, M. A. (1949)
'The prediction of longshore currents', Trans, Am. Geophy. Union, Vol. 30, No. 3, pp. 337-345

Radder, A. C. (1979)
'On the parabolic equation method for water wave propagation', J. Fluid. Mech.,

Vol. 95, Part 1, pp. 159-176

Rastogi, A. K. & Rodi, W (1978)
'Predictions of heat and mass transfer in open channels', ASCE, No. HY3, pp. 397-420

Roberts, K. V. & Weiss, N. O. (1966)
'Convective Difference Schemes', Mathematics of Computation XX, Nos. 93-96, Vol. 20, pp. 272-299

Rodi (1980)
'Turbulence models and their applications in Hydraulics', Int. Assoc. for Hyd. Res., Delft, The Netherlands

Sasaki, T. (1975)
'Simulation on shoreline and nearshore current', Civil Engineering in the Oceans, Vol. III, Delaware, pp. 179-196

Schwartz, L. W. (1974)
'Computer extension and analytic continuation of Stokes' expansion for gravity waves', J. Fluid Mech., Vol. 62, pp. 553-578

Shepard, F. P. & Inman, D. L. (1950)
'Nearshore water circulation related to bottom topography and wave refraction',Trans. Am. Geophys. Union, Vol. 31, No. 2, pp. 196-212.

da Silva Lima, S. S. L. (1981)
'Wave Induced Nearshore Currents', Ph.D. Thesis, Department of Civil Engineering, University of Liverpool

Smith, R. (1975)
'The reflection of short gravity waves on a non-uniform current', Proc. Cambridge Philos. Soc., Vol. 78, pp. 517-525

Smith, R. and Sprinks, T. (1975)
'Scattering of surface waves by a conical island' , J. Fluid Mech., Vol. 72, pp.373-384

Sommerfeld, A. (1896)
'OPTICS Lectures on Theoretical Physics Vol. IV', Academic Press. 'The theory of diffraction', pp. 238-267

Sonu, C. J., (1972)
'Field observations of nearshore circulation and meandering currents', Jnl. Geophy. Res., Vol. 79, pp. 4097-4106

Southgate, H. N. (1985)
'A harbour ray model of wave refraction - diffraction', J. of Waterway, Port, Coastal and Ocean Engineering, ASCE, Vol. 111, No. 1, pp. 29-44

Stiasshie, M. & Peregrine, D. H. (1980)
'Shoaling of finite amplitude surface waves and water of slowly varying depth', J. Fluid Mech., 97, pp. 783-806

Stoker, J. J. (1957)
'Water Waves', Interscience, New York.

Stokes, G. G. (1847)
'On the theory of oscillatory waves', Tran. Cambridge Philos. Soc., Vol. 8, pp. 441-455

Struik, D. J. (1926)
'Determination rigoreuse des ondes irrotationelles periodiques dans un canal deprofondeur, finie', Math. Ann., Vol. 95., pp. 595–637

Tappert, F. D., (1977)
'The parabolic approximation method', Ch. V, Lecture Notes in Physics, Springer–Verlag, N.Y.

Thornton, E. B., (1970)
'Variation of longshore current across its surf zone', Proc. of 12th Coastal Engineering Conf, ASCE, pp. 219–308

Tsay, T–K, & Liu, P. L–F. (1982)
'Numerical solution of water wave water refraction–diffraction problems in the parabolic approx', Jnl. of Geophy. Res., Vol. 87, No. C10, pp. 7932–7940

Unna, P. J. H. (1942)
'Waves and tidal streams', Nature, Vol. 149, pp. 219–220

Ursell, F. (1953)
'The long wave paradox in the theory of gravity waves', Proc. Cambridge Phil. Soc., Vol. 49, pp. 685–694

Visser, P. J (1984)
'A mathematical model of uniform longshore currents and the comparison with laboratory data', Report no. 84–2, Communications on Hydraulics, Department of Civil Engineering, Delft University of Technology

Walker, D. J. (1987)
'Nearshore hydrodynamics and the behaviour of groynes on sandy beaches', Ph.D. Thesis, Department of Civil Engineering, Imperial College, University of London, London, U.K.

Watanabe, A. (1985)
'Numerical models of nearshore currents and beach deformation', Coastal Eng. in Japan, Vol. 25, pp. 147–161

Weare, T. J. (1976)
'Finite element or finite difference methods for two–dimensional shallow water equations?', Computer Method in Applied Mechanics and Engineering, Vol. 7, North–Holand Publishing Co., pp. 351–357

Whitham, G. B. (1962)
'Mass, momentum and energy flux in water waves', J. Fluid Mech., vol. 12, pp. 135–147

Williams, R. G., Darbyshire, J. & Holmes, P. (1980)
'Wave refraction and diffraction in a caustic region. Numerical solution and experimental validation', Proc. Inst. Civ. Eng., Part 2, Vol. 69, pp. 635–649

Wind, H. G. & Vreugdenhil, C. B. (1986)
'Rip–current generation near structures', J. Fluid Mech., Vol. 171, pp. 459–476

Wu, C. S. and Philip L.–F. Liu (1985)
'Finite element modelling of nonlinear coastal currents', J. of Waterway, Port, Coastal and Ocean Engineering, Vol. 111, No. 2